

University of Bath



**PHD**

**Hybrid Cooling/Lubricating Strategies for Machining Ti-6Al-4V in CNC End Milling**

Al-Samarrai, Ihsan

*Award date:*  
2018

*Awarding institution:*  
University of Bath

[Link to publication](#)

**General rights**

Copyright and moral rights for the publications made accessible in the public portal are retained by the authors and/or other copyright owners and it is a condition of accessing publications that users recognise and abide by the legal requirements associated with these rights.

- Users may download and print one copy of any publication from the public portal for the purpose of private study or research.
- You may not further distribute the material or use it for any profit-making activity or commercial gain
- You may freely distribute the URL identifying the publication in the public portal ?

**Take down policy**

If you believe that this document breaches copyright please contact us providing details, and we will remove access to the work immediately and investigate your claim.

Download date: 22. May. 2019

# **Hybrid Cooling/Lubricating Strategies for Machining Ti-6Al-4V in CNC End Milling**

Ihsan Ali Al-Samarrai

A thesis submitted for the degree of Doctor of Philosophy

University of Bath

Department of Mechanical Engineering

May 2018

COPYRIGHT

Attention is drawn to the fact that copyright of this thesis rests with its author. A copy of this thesis has been supplied on condition that anyone who consults it is understood to recognise that its copyright rests with the author and they must not copy it or use material from it except as permitted by law or with the consent of the author.

This thesis may be made available for consultation within the University Library and may be photocopied or lent to other libraries for the purposes of consultation.

*Lovingly dedicated to my mother, wife and children*

## **Acknowledgements**

I am sincerely grateful to the almighty God for surrounding me with kindness, favour, and blessing till completing this research.

I would like to express my deepest gratitude to Dr. Alborz Shokrani Shaharsooghi for his kind support. His insightful comments, higher standard supervision, patience, and courage helped me to stay motivated throughout the research. Without his guidance this work would not have been possible.

I would also like to extend my sincere appreciation to my teacher 'Boss', Prof. Stephen Thomas Newman who gave me the opportunity to study at the University of Bath. Kindness, insight, motivation, and professional supervision are all met in this gentleman. His invaluable advice and guidance helped me all the way through this research.

I would also like to express my gratitude to academic and technicians who provided help and support during the experimental part of this research. This includes Dr. Vimal Dhokia, Mr Steve Goguelin, Mr Andrew Green, Mrs Clare Ball, Mr Mathew Ball and Mr David Wood.

I am really grateful to the Iraqi Ministry of Higher Education and Scientific Research who provided me with financial and consulting support throughout the research. Without their help I would not have been studying in this amazing university.

Last but not least, I would like to sincerely thank my wife and children who have never stopped loving and supporting me even, throughout the 4 years of study, I am away from them.

## **Abstract**

Titanium and its alloys are widely used in various engineering applications such as aerospace, biomedical and chemical industries due to their excellent combination of high strength-to-weight ratio and good creep, corrosion and fracture resistance. However, these desirable design properties pose a serious challenge to the manufacturing engineers owing to the high temperatures and stresses generated during the machining of titanium alloys. The extremely low thermal conductivity of titanium alloys results in concentration of high temperature close to the tool cutting edge resulting in accelerated thermochemical and mechanical tool wear.

Many cooling and lubricating techniques such as high pressure cooling (HPC), minimum quantity lubrication (MQL) and cryogenic machining have been proposed for improving the machinability of titanium alloys. In this study, a hybrid combination of MQL and cryogenic cooling using liquid nitrogen (LN<sub>2</sub>) is proposed, designed and manufactured as an innovative cooling/lubricating approach for CNC end milling of Ti-6Al-4V titanium alloy. The machining performance of the new hybrid cooling/lubrication technique is investigated in terms of tool wear and surface finish and compared to that of flood cooling, MQL and cryogenic cooling.

The proposed hybrid cooling/lubrication technique demonstrated the best machining performance among all cooling/lubricating conditions and recorded more the 30 fold increased tool life over conventional flood cooling. In addition, 28% reduction in surface roughness was recorded for hybrid cooling/lubrication method as compared to flood cooling. The improvement in surface roughness was 50% for MQL when compared to flood cooling.

The outstanding improvement in tool life with hybrid cooling/lubricating strategies is encouraging for the wide spread of this cooling/ lubricating technique for industrial adoption.

## Table of Contents

|   |           |
|---|-----------|
| Acknowledgments   | i         |
| Abstract  | ii        |
| Table of contents   | iii       |
| List of figures   | vii       |
| List of tables  | xii       |
| List of Abbreviations   | xiii      |
| <b>1. Introduction</b>  | <b>1</b>  |
| <b>2. Literature review</b>   | <b>4</b>  |
| 2.1 Titanium alloys and their machinability                                       | 4         |
| 2.2 Chip formation in machining titanium alloys                                   | 5         |
| 2.3 Enhancing the machinability of titanium alloys with coolants and lubricants   | 6         |
| 2.4 Cutting fluids (coolants and lubricants)                                      | 7         |
| 2.4.1 Water soluble (water miscible) cutting fluids                               | 8         |
| 2.4.2 Neat cutting oils   | 9         |
| 2.4.3 Gases   | 9         |
| 2.5 Oil/Water-based cooling techniques in machining titanium alloys               | 10        |
| 2.5.1 Flood cooling   | 10        |
| 2.5.2 High pressure (HP) cooling  | 10        |
| 2.6 Sustainable cooling/lubricating techniques in machining titanium alloys       | 13        |
| 2.6.1 Dry machining   | 14        |
| 2.6.2 Minimum quantity lubrication MQL  | 16        |
| 2.6.3 Cryogenic cooling   | 20        |
| 2.6.3.1 Cryogenic cooling of titanium alloys in turning operations                | 22        |
| 2.6.3.2 Cryogenic cooling in milling titanium alloys                              | 32        |
| 2.7 Hybrid sustainable cooling/lubricating techniques in machining titanium alloy | 34        |
| 2.8 Critique  | 39        |
| <b>3. Scope of research and framework</b>   | <b>41</b> |
| 3.1 Introduction  | 41        |
| 3.2 Research gap  | 41        |
| 3.3 Research aims and objectives  | 41        |
| 3.4 Research scope  | 43        |
| 3.4.1 Configuration of hybrid cooling/lubricating technique and strategy          | 43        |

|           |   |           |
|-----------|---|-----------|
| 3.5       | Research limitations  | 43        |
| 3.6       | Research methodology  | 43        |
| 3.6.1     | Design of hybrid cooling-lubricating system   | 44        |
| 3.6.1.1   | Cryogenic cooling system  | 45        |
| 3.6.1.2   | Minimum quantity lubrication MQL system   | 46        |
| 3.6.2     | Hybrid cryogenic/MQL in comparison with individual cooling and lubricating techniques   | 46        |
| 3.6.3     | Data collection and analysis  | 46        |
| <b>4.</b> | <b>Design and manufacture of cryogenic cooling systems</b>  | <b>48</b> |
| 4.1       | Introduction  | 48        |
| 4.2       | Cryogenic cooling systems   | 49        |
| 4.2.1     | Cryogenic storage and delivery system   | 49        |
| 4.2.2     | Cryogenic cooling nozzle/s system   | 50        |
| 4.3       | Design and manufacturing of single- nozzle external cryogenic cooling system  | 51        |
| 4.3.1     | Conceptual design of external nozzle for cryogenic cooling applications   | 51        |
| 4.3.2     | Design requirements and constrains for the cryogenic cooling nozzle   | 51        |
| 4.3.3     | First trial of design of single nozzle for cryogenic cooling applications and CFD modelling   | 52        |
| 4.3.4     | Updating the external cryogenic nozzle design and CFD analyses  | 54        |
| 4.3.5     | Manufacturing of the updated design of cryogenic cooling nozzle and testing with LN2  | 56        |
| 4.4       | Design and manufacturing of flexible cryogenic nozzle holder  | 57        |
| 4.5       | Design and manufacturing of dual-nozzle cryogenic cooling system  | 58        |
| 4.5.1     | Installing the dual- nozzle system onto the machine tool  | 60        |
| 4.5.2     | Thermal insulation of the dual-nozzle system and final spaying test with LN2  | 60        |
| <b>5.</b> | <b>Experimental investigation of machinability of hybrid cryogenic/MQL technique in comparison with individual cooling and lubricating conditions</b> | <b>62</b> |
| 5.1       | Introduction  | 62        |
| 5.2       | Preparations for machining experiments  | 63        |
| 5.2.1     | Measurement of hardness of Ti-6Al-4V and the effect of excessive LN2 cooling on the workpiece properties  | 63        |
| 5.2.2     | Identification of cutting parameters  | 66        |
| 5.2.2.1   | Fixed cutting parameters  | 66        |
| 5.2.2.2   | Variable cutting parameter and criterion of selected level range  | 67        |
| 5.2.3     | Selection of cutting tool   | 68        |

|           |   |           |
|-----------|---|-----------|
| 5.2.4     | Identification of cooling/lubrication conditions (machining environments)           | 68        |
| 5.2.5     | Identification of the machinability metrics to be investigated                      | 69        |
| 5.3       | Design of experiments   | 69        |
| 5.4       | Procedure of machining experiments  | 70        |
| 5.4.1     | Machine tool setup  | 71        |
| 5.4.2     | Machining operation setup   | 71        |
| 5.4.3     | Machining experiments for investigations of machinability                           | 72        |
| 5.4.4     | Operation of machining experiments  | 73        |
| 5.4.4.1   | Minimum quantity lubrication MQL  | 75        |
| 5.4.4.2   | Conventional flood cooling  | 76        |
| 5.4.4.3   | Cryogenic machining   | 76        |
| 5.4.4.4   | Hybrid/cryogenic-MQL cooling/ lubricating   | 77        |
| 5.5       | Evaluating machinability  | 78        |
| 5.5.1     | Measurement of tool wear  | 78        |
| 5.5.2     | Measurement of surface roughness  | 79        |
| 5.5.3     | Microscopic inspection and analyses of chip morphology                              | 80        |
| <b>6.</b> | <b>Results and Analysis</b>   | <b>82</b> |
| 6.1       | Introduction  | 82        |
| 6.2       | Tool wear results and discussion  | 82        |
| 6.2.1     | Flood cooling machining experiments   | 82        |
| 6.2.2     | MQL machining experiments   | 95        |
| 6.2.3     | Cryogenic machining experiments   | 104       |
| 6.2.4     | Hybrid cryogenic/MQL machining experiments  | 112       |
| 6.3       | Results of surface roughness  | 120       |
| 6.4       | Comparative statistical analyses for the results of tool life and surface roughness | 121       |
| 6.4.1     | Testing the normality of tool life and surface roughness data                       | 122       |
| 6.4.2     | Statistical analyses of variance ANOVA for tool wear results                        | 124       |
| 6.4.3     | Comparison tests for tool wear  | 126       |
| 6.4.3.1   | Statistical analysis of variance ANOVA for surface roughness                        | 127       |
| 6.5       | Results of chip morphology  | 131       |



|           |  |            |
|-----------|--|------------|
| <b>7.</b> | <b>Discussion</b>  | <b>138</b> |
| 7.1       | Introduction   | 138        |
| 7.2       | Design of cryogenic cooling system   | 138        |
| 7.3       | Experimental investigation of machining performance of cryogenic, MQL, and hybrid cryogenic/ MQL techniques as compared with conventional flood cooling method | 139        |
| 7.3.1     | Preparation for machining experiments  | 139        |
| 7.3.2     | Machining experimentation  | 140        |
| 7.3.3     | Comparison of experimental results   | 141        |
| 7.3.3.1   | Tool wear  | 141        |
| 7.3.3.2   | Surface roughness  | 144        |
| 7.3.3.3   | Chip morphology  | 145        |
| <b>8.</b> | <b>Conclusions and recommended research work</b>   | <b>146</b> |
| 8.1       | Introduction   | 146        |
| 8.2       | Conclusion   | 146        |
| 8.3       | Contribution to knowledge  | 147        |
| 8.4       | Recommended research area for further investigation  | 148        |

## List of Figures

|             |  |    |
|-------------|--|----|
| Figure 2.1  | Microstructure of Ti6Al4V alloy. A) optical microscopy image, and B) SEM image   | 5  |
| Figure 2.2  | Schematics illustrating sequence of chip segmentation steps under dry machining condition. (a) Localization of strain along the path of shear band. The shear initiates from the tool tip and takes curved path upwards till meeting the free surface, (b) Crack initiation at the tool tip, (c) Crack propagation | 6  |
| Figure 2.3  | Schematic of heat generation zones and chip formation in metal cutting   | 7  |
| Figure 2.4  | Classification of cutting fluids   | 8  |
| Figure 2.5  | Tool lives when machining titanium alloy with polycrystalline diamond inserts at various coolant pressures and with conventional coolant flow  | 12 |
| Figure 2.6  | Schematic layout of oil mist supply  | 16 |
| Figure 2.7  | Dual cryogenic cooling technique   | 23 |
| Figure 2.8  | Main tool wear modes observed in dry and cryogenic turning after 8 min when adopting a cutting speed of 80 m/min and a feed rate 0.2 mm/rev  | 28 |
| Figure 2.9  | Chip morphology resulted from: (a) oil-based coolant and (b) cryogenic Machining   | 30 |
| Figure 2.10 | Orthogonal cutting of Ti-6Al-4V (a) under cryogenic pre-cooled workpiece after an elapsed time of 7 s, (b) SEM of chips obtained from cryogenic machining showing the separation between chip segments, (c) schematic illustrating a typical serrated chip formation during cryogenic machining                    | 32 |
| Figure 2.11 | Microstructure of chip showing the influence different cooling/lubrication conditions on the chip breaking and shear and width, and the microstructure of the resulting chip when machining Ti-6Al-2Sn-4Zr-6Mo; cutting speed = 100 m/min; depth of cut = 1 mm; feed rate = 0.2 mm/rev                             | 36 |
| Figure 2.12 | Schematics cryogenic cooling strategies in turning. a) CO <sub>2</sub> rake. b) CMQL rake, c) CO <sub>2</sub> rake and MQL flank, d) Modified CO <sub>2</sub> delivery   | 38 |
| Figure 3.1  | Input–output schematic illustration of the framework of this research  | 44 |
| Figure 3.2  | Photographic illustration of cryogenic delivery system used in this research   | 45 |
| Figure 3.3  | Flow chart of the planned methodology for this research  | 47 |
| Figure 4.1  | Schematic and graphic illustration of the cryogenic delivery system adopted by Shokrani (2014), used in the present research   | 50 |
| Figure 4.2  | Sources of heat generation during machining process and directions of application cooling nozzle/s   | 50 |
| Figure 4.3  | Schematic illustration of the main concept of external nozzle cryogenic cooling  | 51 |

|             |   |    |
|-------------|---|----|
| Figure 4.4  | Residuals convergence for CFD simulation of first design of external cryogenic nozzle   | 53 |
| Figure 4.5  | Simulation of velocity vectors of interior surface of the initial design of cryogenic nozzle  | 54 |
| Figure 4.6  | Updated design of external cryogenic cooling nozzle with CFD axisymmetric meshing   | 55 |
| Figure 4.7  | CFD simulation of velocity vectors of the updated design of cryogenic nozzle  | 56 |
| Figure 4.8  | Updated design of external cryogenic cooling nozzle. A) Front view, B) Section view   | 56 |
| Figure 4.9  | Successful testing of the updated cryogenic cooling nozzle after installation to the machine tool and spraying NL2  | 57 |
| Figure 4.10 | Cryogenic nozzle holder. A) CAD model B) installed in the machine tool and hold the cryogenic hose  | 58 |
| Figure 4.11 | Nozzle design of the Dual-nozzle cryogenic cooling system. A) Front view, B) section view   | 59 |
| Figure 4.12 | The dual-nozzle cryogenic cooling system used in this research. A) CAD model, and B) manufactured prototype   | 59 |
| Figure 4.13 | Model shows the retrofit of the cryogenic cooling system onto the machine tool frame  | 60 |
| Figure 4.14 | A) Retrofitting the dual- nozzle system after insulation (front view), B) successful spraying of liquid nitrogen (rear view)  | 61 |
| Figure 5.1  | Microstructure of Ti-6Al-4V titanium alloy analysed by Shokrani   | 64 |
| Figure 5.2  | Effect of temperature on hardness of Ti-6Al-4V  | 66 |
| Figure 5.3  | The Three-axis CNC vertical milling centre (Brigdeport VMC 610XP <sup>2</sup> ) with cryogenic nozzle system installed and ready for conducting machining experiments | 71 |
| Figure 5.4  | Schematic showing the experimental set up   | 74 |
| Figure 5.5  | Schematic illustration of machining operation   | 74 |
| Figure 5.6  | Minimum quantity lubrication system used in this study. A) Schematic of dual-nozzle MQL system, B) ACCU-Lube MQL applicator   | 75 |
| Figure 5.7  | Application of MQL during milling of Ti-6Al-4V. A) Schematic of MQL nozzle positions (top view), B) dual- nozzle MQL during machining (front view)                    | 76 |
| Figure 5.8  | Cryogenic machining with dual-nozzle system. A) Schematic top view showing cooling strategy, B) During machining  | 77 |
| Figure 5.9  | Hybrid MQL/cryogenic machining set up. A) Schematic showing cooling/lubrication strategy, B) during machining.  | 78 |
| Figure 5.10 | Cutting tool with its BT-40 holder carried by plastic holder on the stage of microscope for measurement of tool wear.   | 79 |

|             |  |    |
|-------------|--|----|
| Figure 5.11 | Surface roughness measurements. (A) Taylor Hobson® Surtronic S128 surface roughness measuring device used in this research. (B) Zoomed image of diamond stylus profiler  | 80 |
| Figure 5.12 | Inspection of titanium alloy chips. A) Macroscopic, B) microscopic   | 81 |
| Figure 6.1  | Results of tool flank wear for different cutting speeds when flood cooling was applied. Dashed lines indicate the 300µm wear criterion according to ISO 8688   | 83 |
| Figure 6.2  | Results of tool flank wear for different cutting speeds when MQL was applied. Dashed lines indicate the 300µm wear criterion according to ISO 8688   | 83 |
| Figure 6.3  | Results of tool flank wear for different cutting speeds when cryogenic cooling was applied. Dashed lines indicate the 300µm wear criterion according to ISO 8688   | 84 |
| Figure 6.4  | Results of tool flank wear for different cutting speeds when Hybrid cryogenic/MQL was applied. Dashed lines indicate the 300µm wear criterion according to ISO 8688  | 84 |
| Figure 6.5  | Results of tool life in terms of cutting length until reaching wear criterion for different cutting and cooling/lubricating conditions   | 85 |
| Figure 6.6  | Improvement in tool life for various cooling/lubricating methods in comparison to conventional flood cooling   | 86 |
| Figure 6.7  | Images of tool taken with three views at rake face, cutting edge, and flank face at different cutting speeds; 60, 90, 120, 150, 180 m/min under flood cooling, taken after the wear criterion has been reached | 89 |
| Figure 6.8  | Tool images showing flank wear development until wear criterion for the most affected tooth when machining Ti-6Al-4V at 60 m/min under flood cooling   | 90 |
| Figure 6.9  | Tool images showing flank wear development until wear criterion for the most affected tooth when machining Ti-6Al-4V at 90 m/min under flood cooling   | 91 |
| Figure 6.10 | Tool images showing flank wear development until wear criterion for the most affected tooth when machining Ti-6Al-4V at 120 m/min under flood cooling  | 92 |
| Figure 6.11 | Tool images showing flank wear development until wear criterion for the most affected tooth when machining Ti-6Al-4V at 150 m/min under flood cooling  | 93 |
| Figure 6.12 | Tool images showing flank wear development until wear criterion for the most affected tooth when machining Ti-6Al-4V at 180 m/min under flood cooling  | 94 |
| Figure 6.13 | Images of tool taken with three views at rake face, cutting edge, and flank face at different cutting speeds; 60, 90, 120, 150, 180 m/min under MQL, after the wear criterion has been reached                 | 98 |
| Figure 6.14 | Tool images showing flank wear development until wear criterion for the most affected tooth when machining Ti-6Al-4V at 60 m/min under minimum quantity lubrication  | 99 |

|             |   |     |
|-------------|---|-----|
| Figure 6.15 | Tool images showing flank wear development until wear criterion for the most affected tooth when machining Ti-6Al-4V at 90 m/min under minimum quantity lubrication   | 100 |
| Figure 6.16 | Tool images showing flank wear development until wear criterion for the most affected tooth when machining Ti-6Al-4V at 120 m/min under minimum quantity lubrication  | 101 |
| Figure 6.17 | Tool images showing flank wear development till wear criterion for the most affected tooth when machining Ti-6Al-4V at 150 m/min under minimum quantity lubrication   | 102 |
| Figure 6.18 | Tool images showing flank wear development until wear criterion for the most affected tooth when machining Ti-6Al-4V at 180 m/min under minimum quantity lubrication  | 103 |
| Figure 6.19 | Images of tool with three views at rake face, cutting edge, and flank face at different cutting speeds; 60, 90, 120, 150, 180 m/min with cryogenic cooling, taken after the wear criterion has been reached     | 106 |
| Figure 6.20 | Tool images showing flank wear development until wear criterion for the most affected tooth when machining Ti-6Al-4V at 60 m/min under cryogenic cooling  | 107 |
| Figure 6.21 | Tool images showing flank wear development until wear criterion for the most affected tooth when machining Ti-6Al-4V at 90 m/min under cryogenic cooling  | 108 |
| Figure 6.22 | Tool images showing flank wear development until wear criterion for the most affected tooth when machining Ti-6Al-4V at 120 m/min under cryogenic cooling   | 109 |
| Figure 6.23 | Tool images showing flank wear development until wear criterion for the most affected tooth when machining Ti-6Al-4V at 150 m/min under cryogenic cooling   | 110 |
| Figure 6.24 | Tool images showing flank wear development until wear criterion for the most affected tooth when machining Ti-6Al-4V at 180 m/min under cryogenic cooling   | 111 |
| Figure 6.25 | Tool images taken for different machining environments at cutting speed of 60 m/min and after nearly 53m length of cut (tool life for food cooling). A) Flood cooling. B) MQL. C) Hybrid cryogenic/MQL          | 112 |
| Figure 6.26 | Tool images showing flank wear development until wear criterion for the most affected tooth when machining Ti-6Al-4V at 60 m/min under hybrid cryogenic/ MQL  | 113 |
| Figure 6.27 | Images of tool with three views at rake face, cutting edge, and flank face at different cutting speeds; 60, 90, 120, 150, 180 m/min under hybrid cryogenic/MQL, taken after the wear criterion has been reached | 114 |
| Figure 6.28 | Tool images showing flank wear development until wear criterion for the most affected tooth when machining Ti-6Al-4V at 90 m/min under hybrid cryogenic/ MQL  | 115 |
| Figure 6.29 | Tool images showing flank wear development until wear criterion for the most affected tooth when machining Ti-6Al-4V at 120 m/min under hybrid cryogenic/ MQL   | 116 |

|             |   |     |
|-------------|---|-----|
| Figure 6.30 | Tool images showing flank wear development until wear criterion for the most affected tooth when machining Ti-6Al-4V at 150 m/min under hybrid cryogenic/ MQL | 117 |
| Figure 6.31 | Tool images showing flank wear development until wear criterion for the most affected tooth when machining Ti-6Al-4V at 180 m/min under hybrid cryogenic/ MQL | 118 |
| Figure 6.32 | Average surface roughness for different cooling and cutting speed conditions  | 121 |
| Figure 6.33 | Normal probability plot for tool life   | 123 |
| Figure 6.34 | Normal probability plot surface roughness   | 124 |
| Figure 6.35 | Normal probability plot of residuals for tool life statistical model  | 125 |
| Figure 6.36 | Main effect of cooling conditions and cutting speed as generated by Minitab 18  | 125 |
| Figure 6.37 | Interaction plots for tool life. A) Cutting speed, B) cooling condition   | 126 |
| Figure 6.38 | Normal probability plot of residuals for surface roughness statistical model  | 128 |
| Figure 6.39 | Surface roughness plots at different cooling conditions and cutting speeds. a) Main effect, b) Interaction  | 130 |
| Figure 6.40 | Images of chips for machining under flood cooling   | 133 |
| Figure 6.41 | Images of chips when machining under MQL  | 134 |
| Figure 6.42 | Images of chips when machining under cryogenic cooling  | 135 |
| Figure 6.43 | Macro and microscopic images of chips when end milling Ti-6Al-4V at 60m/min. under different cooling/lubricating strategies                                   | 136 |
| Figure 6.43 | Images of chips when machining under hybrid cryogenic/MQL   | 137 |

## List of Tables

|            |   |     |
|------------|---|-----|
| Table 4.1  | Some input parameters for CFD modelling of cryogenic nozzle   | 53  |
| Table 5.1  | Chemical composition of Ti-6Al-4V alloy analysed by Shokrani  | 63  |
| Table 5.2  | Vickers hardness of Ti-6Al-4V blocks used in the present investigation, 24 measurement for each block                               | 65  |
| Table 5.3  | Fixed levels of cutting parameters used in this study   | 67  |
| Table 5.4  | Fixed and variable machining conditions used for each cooling/lubricating condition in this   | 68  |
| Table 5.5  | Full-factorial DoE for cutting speeds and machining environments conditions   | 70  |
| Table 5.6  | Calculated spindle speed and feed rate ready to input to the machining programme  | 73  |
| Table 6.1  | Results of tool life and percentage of improvement compared with flood cooling  | 85  |
| Table 6.2  | Results of tool life and percentage of improvement compared with flood cooling  | 121 |
| Table 6.3  | Surface roughness results and percentage of improvement compared with flood cooling   | 123 |
| Table 6.4  | Tool life and surface roughness data for statistical analyses   | 125 |
| Table 6.5  | Standard analyses of variance for tool life statistical model   | 127 |
| Table 6.6  | Fisher individual comparison tests of tool life means between different groups of cooling conditions                                | 127 |
| Table 6.7  | Fisher individual comparison tests of tool life means between different groups of cutting speeds                                    | 128 |
| Table 6.8  | Standard analyses of variance for surface roughness statistical model   | 128 |
| Table 6.9  | Standard analyses of variance for surface roughness showing the interaction between cutting speed and cooling/lubricating condition | 129 |
| Table 6.10 | Fisher individual comparison tests of surface roughness means between different groups of cooling conditions                        | 130 |

## List of Abbreviations

|                                |                                       |
|--------------------------------|---------------------------------------|
| °C                             | Celsius                               |
| 2D                             | Two Dimensional                       |
| 3D                             | Three Dimensional                     |
| $a_a$                          | Axial Depth of Cut                    |
| Al                             | Aluminum                              |
| Al <sub>2</sub> O <sub>3</sub> | Alumina                               |
| AlCrN                          | Aluminum Chrome Nitride               |
| ANOVA                          | Analysis of Variance                  |
| $a_r$                          | Radial Depth of Cut                   |
| b.b.c                          | Body-Centered Cubic                   |
| BUE                            | Build Up Edge                         |
| C                              | Carbon                                |
| CAD                            | Computer Aided Design                 |
| CCNGOM                         | Compressed Cold Nitrogen Gas Oil Mist |
| CFD                            | Computational fluid dynamics          |
| CNC                            | Computer Numerical Control            |
| Co                             | Cobalt                                |
| CO <sub>2</sub>                | Carbon Dioxide                        |
| c.p.h                          | Closed-Pack Hexagonal                 |
| Cr                             | Chrome                                |
| CrTiAlN                        | Chrome Titanium Aluminum Nitride      |
| Cu                             | Copper                                |
| CVD                            | Chemical Vapor Deposition             |
| d.o.c.                         | Depth of Cut                          |
| DMLS                           | Direct Laser Metal Sintering          |
| DRX                            | Dynamic Recrystallization Mechanism   |
| EDS                            | Energy-dispersive Spectroscopy        |
| $f$                            | Feed rate                             |
| Fe                             | Iron                                  |
| FEA                            | Finite Element Analysis               |
| $f_z$                          | Feed per Tooth                        |
| HP                             | High Pressure                         |
| HRC                            | High Pressure Cooling                 |
| HSS                            | High Speed Steel                      |
| ISO                            | International Standard Organization   |
| LCO <sub>2</sub>               | Liquid Carbon Dioxide                 |
| LN <sub>2</sub>                | Liquid Nitrogen                       |
| MMR                            | Material Removal Rate                 |
| Mn                             | Manganese                             |
| Mo                             | Molybdenum                            |
| MQC                            | Minimum Quantity Cooling              |
| MQCF                           | Minimum Quantity Cutting Fluid        |



|                                |                                     |
|--------------------------------|-------------------------------------|
| MQCL                           | Minimum Quantity Cooled Lubrication |
| MQL                            | Minimum Quantity Lubrication        |
| N                              | Nitrogen                            |
| nc                             | Nano Composite                      |
| Ni                             | Nickel                              |
| O                              | Oxygen                              |
| PCBN                           | Polycrystalline Cubic Boron Nitride |
| PCD                            | Polycrystalline Diamond             |
| PVD                            | Physical Vapor Deposition           |
| Ra                             | Arithmetic Surface Roughness        |
| SEM                            | Scanning Electron Microscopy        |
| Si <sub>3</sub> N <sub>4</sub> | Silicon Nitride                     |
| SiC                            | Silicon Carbide                     |
| Sn                             | Tin                                 |
| Ta                             | Tantalum                            |
| TiAlN                          | Titanium Aluminum Nitride           |
| TiC                            | Titanium Carbide                    |
| TiN                            | Titanium Nitride                    |
| TiSiN                          | Titanium Silicon Nitride            |
| V                              | Vanadium                            |
| V <sub>B</sub>                 | Flank Wear                          |
| V <sub>c</sub>                 | Cutting Speed                       |
| WC                             | Tungsten Carbide                    |
| Zn                             | Zinc                                |
| α                              | Alpha                               |
| β                              | Beta                                |
| ΔT                             | Temperature Difference              |

## Chapter 1 Introduction

Titanium and its alloys continue to provide excellent service in many engineering applications that require improved in-service performance, such as aerospace, biomedical, and nuclear industries. This is owing to their light weight, high hot strength and hardness, superior fracture and corrosion resistance (Ezugwu and Wang 1997; Revuru et al. 2017).

However, the majority of these alloys are still manufactured by conventional machining and well recognised as difficult-to-machine materials. Their high hot strength and hardness cause plastic deformation of the cutting tool owing to high compressive stresses on the cutting edge resulting in premature tool failure (Ezugwu et al. 2003; Pramanik 2014). The extremely low thermal conductivity of titanium alloys (1/6 that for steel) confines the heat generated during machining from being dissipated resulting in high localised temperatures which can easily reach well beyond 1000 °C at the tool-chip interface. The temperature distribution of the cutting tool when machining Ti-6Al-4V, the most widely used titanium alloy, at a cutting speed 75m/min is comparable to that when cutting carbon steel at 240m/min (Grearson 1986; Abdel-Aal et al. 2009). This will accelerate the thermally related wear (diffusion and plastic deformation), mechanical wear (abrasion and attrition) as a result of the weakening in bonding strength of the tool substrate at such elevated temperatures. In addition, short tool-chip contact length results in high thermal gradient at the tool tip. This would result in excessive chipping especially if high cooling capacity coolant such as water-based cutting fluids and liquid nitrogen (Hartung et al. 1982; Venugopal et al. 2007a).

Flood cooling is still the most common cooling method used in industry to remove the heat generated during machining of titanium alloys. Cutting fluids can act as a lubricant by reducing the friction at the tool-chip and tool-workpiece interfaces hence reducing cutting forces and improving surface finish by minimising the tendency to build up edge (BUE) (Adler et al. 2006; Rotella et al. 2014). However, beside their environmental, health and economic consequences, flood cooling have not been found effective in machining difficult-to-cut titanium alloys due to the inability of the coolant to penetrate the cutting zone due to the formation of a vapour blanket (Ezugwu 2005). This high temperature blanket seizes and prevents the coolant accessibility to the cutting zone (Pramanik 2014). From the environmental point of view, the degradation and dissolution of cutting fluids can result in soil and water pollution during the eventual disposal. In addition, cutting fluids can cause many skin and body diseases to the machine operator (Shokrani et al. 2012). Prolonged

physical exposure to mineral oils exacerbates dermal ailments (Priarone et al., 2016). Moreover, biocides, chemical and pressure additives such as chlorinated paraffin and sulphurized additives are considered hazardous to health and the environment on the shop floor due to their toxicity (Yildiz and Nalbant 2008).

From the economic viewpoint, the disposal cost of cutting fluids can be as high as 2-4 times the purchase cost. While the cutting tool only share 4% of the machining cost, the purchase, maintenance, and disposal cost of cutting fluids can account up to 17% of the total machining cost (Feng and Hattori 2000; Ezugwu 2005). Besides their major negative environmental, hygienic, and economic consequences of flood cooling, their machining performance makes them inefficient in machining titanium alloys.

The safety issues of using cutting fluids provide a strong driver to eliminate their use. However, in dry machining the absence of a coolant/lubricant significantly compromises tool life due to the high generated temperature especially when machining titanium alloys even at low cutting speeds (Werda et al. 2016; Thakur and Gangopadhyay 2016). Various cooling/lubricating techniques have been proposed to improve the machinability of titanium alloys such as minimum quantity lubrication (MQL), cryogenic machining, high pressure cooling (HPC), etc. Cryogenic cooling and MQL have been introduced to enable effective cooling and satisfactory lubrication with reduced health and environmental issues (Revuru et al. 2017).

MQL has been regarded as an effective alternative to conventional flood cooling and dry machining. It involves spraying a very small amount (6-200ml/h) of mineral or vegetable oil in a mist form with compressed air stream (normally 5-7bars) through external nozzle/s directly to the tool-workpiece and/or tool-chip interfaces (Sharma et al. 2015). MQL has shown encouraging performance in turning, milling and grinding due to its ability to penetrate the cutting zone providing essential lubrication, thus reducing the cutting forces and friction at the cutting interfaces resulting in less heat generation (Astakhov 2009). In addition, MQL can satisfactorily reduce the cutting zone temperature by the cooling effect of the pressured air stream and the evaporation of lubricant (Ezugwu et al. 2003; Sun et al. 2006). In milling titanium alloys, the application of MQL can drastically reduce the chip pressure welding to the cutting edge which significantly improves tool life and surface finish (Park et al. 2017). Promising machining performance has been shown in precision machining of Ti-6Al-4V with MQL at a high cutting speed and low feed conditions (Sharma et al. 2015).

Cryogenic cooling, that uses liquefied nitrogen as a coolant, is recognized as an effective approach for maintaining the temperature at the cutting zone well below the softening temperature range of the cutting tool materials (Shokrani et al. 2013). Cryogenic machining could provide a significant potential in improving the tool life when machining titanium alloys. Using cryogenic cooling reduces the chemical reactivity between titanium and tool material, and reduce thermally related diffusion wear and plastic deformation caused by thermal softening (Hong and Zhao 1999; Hong and Ding 2001). Furthermore, cryogenic machining has demonstrated a substantial improvement in tool life and significantly contributes to improved functional performance of machined components through the desirable surface integrity characteristics due to altering the properties of the cutting tool and workpiece surfaces and hence, changing the tribological system beneficially resulting in reduced thermally related wear (Shokrani et al. 2013; Kaynak et al. 2014; Schoop et al. 2017).

As the high cutting temperature and friction are the main issues in machining titanium and its alloys, the combined application of cryogenic cooling and MQL could result in potential improvements in the machinability of Ti-6Al-4V, while satisfying environmental friendliness. This research intends to investigate the cooling/lubricating performance of MQL, external-nozzle cryogenic, and the hybrid combination of MQL-cryogenic cooling/lubrication conditions when CNC end milling of Ti-6Al-4V titanium alloy. The machining performance in terms of tool wear, surface finish, and chip morphology are analysed and compared with that for conventional flood cooling after conducting a series of end milling experiments.

The structure of the chapters presented in this thesis begins with this introduction followed by a comprehensive and in-depth literature review on the various applications of cooling and lubrication techniques in chapter 2. The scope of the author's research is presented in chapter 3. In chapter 4, a computational fluid dynamics (CFD) simulation together with a specially designed cryogenic cooling system is provided. In the experimental part of this research, chapter 5 provides an experimental investigation of the machining performance during the application of cryogenic cooling using the designed dual-nozzle cryogenic cooling system. Chapter 6 outlines the results and analysis of the machining experiments, with the results and analysis discussed in chapter 7. Finally, chapter 8 presents conclusions and recommends further areas of research.

## Chapter 2 Literature review

### 2.1 Titanium alloys and their machinability

The demand of titanium and its alloys in aerospace, biomedical and chemical industries has been dramatically increased during the last few decades because of the unique combination of specific strength and excellent corrosion resistance (Ezugwu and Wang 1997; Rahman et al. 2006; Revuru et al. 2017; Kale and Khanna 2017). While pure titanium has no attractive mechanical properties, alloyed titanium exhibits excellent hardness and strength that is maintained at elevated temperatures making titanium alloys attractive in aeroengine applications (Arrazola et al. 2009; Li et al. 2017). Two crystalline structures are commonly experienced in the metallurgy of titanium and its alloys: i) closed pack hexagonal  $\alpha$ -phase at low temperature, and ii) body-centred cubic  $\beta$ -phase at high temperature. Commercially pure CP titanium undergoes allotropic transformation at 822°C (Donachie 2000; Da Rocha et al. 2005).

The addition of Al, O, N, C promote the  $\alpha$  structure, whilst  $\beta$  stabilizer elements which have body-centred cubic crystalline structure can be either isomorphous formers such as V, Mo, Ta, or eutectoid formers Cr, Cu, Mn, Ni, Co, and Fe. Four major classifications of titanium alloys are (Veiga et al. 2012; Da Rocha et al. 2005):

- i.  $\alpha$ -alloys: such as commercially pure CP titanium, containing  $\alpha$  stabilizing elements, having low strength and excellent corrosion resistant properties.
- ii. Near  $\alpha$ -alloys:  $\alpha$  stabilizers and small amount of  $\beta$  stabilizers, with excellent creep resistant.
- iii.  $\alpha$ - $\beta$  alloys: contain both  $\alpha$  and  $\beta$  stabilizing elements, counting for around 70% of titanium used, among which Ti-6Al-4V alloy is the most used in aerospace and nuclear industries and comprises nearly 50% of the total produced titanium. Figure 2.1 shows a microstructure of Ti-6Al-4V alloy.
- iv.  $\beta$ -alloys: contain  $\beta$  stabilizers, possess high hardenability with higher density.

However, titanium alloys are classified as hard-to-machine materials because of their inherent properties such as low thermal conductivity that cause very high temperature localized close to the cutting edge, their high chemical affinity to all available cutting tool materials, their high strain hardening during the cutting operation due to high temperature strength resulting in high compressive stresses developed at the cutting edge owing to the

high mechanical properties, self-induced chatter and springback during machining due to titanium low elastic modulus, and the tendency to form a BUE that could deteriorate the surface quality of the machined component (Pramanik and Littlefair 2015; Pramanik 2014; Pervaiz et al. 2014). Large amount of efforts have been invested to improve the machinability of titanium workpieces by inventing effective cooling techniques and appropriate selection of cutting tool materials and geometries as well as the proper use cutting parameters (Pervaiz et al. 2014; Revuru et al. 2017).

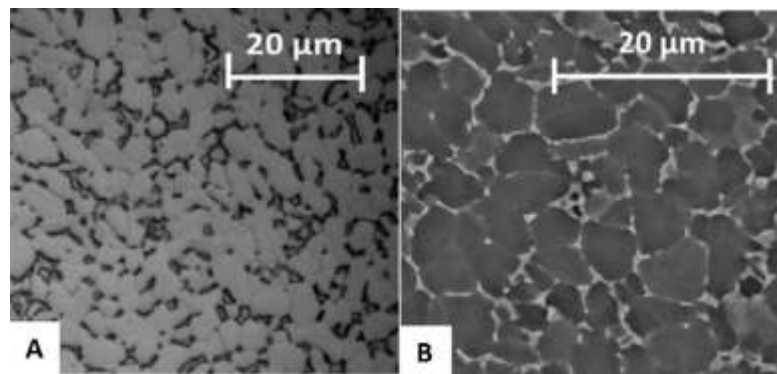


Figure 2.1 Microstructure of Ti-6Al-4V alloy. A) optical microscopy image, and B) SEM image(Sartori et al. 2017b).

## 2.2 Chip formation in machining titanium alloys

In machining titanium alloys, the shear localized chip segmentation characterized by plastically deformed shear bands is the dominant chip formation mechanism (Joshi et al. 2015). The onset of thermoplastic shear for a given chip thickness is determined by the critical cutting speed which is very low in machining titanium alloys (Komanduri and Hou 2002). The mechanics of material removal from a workpiece is attributed to the crack initiation and propagation along the cutting direction. The chip is raised along the rake face of the advancing cutting tool due to the fracture of chip as a consequence of stresses built up by the cutting tool (Krishnamurthy et al. 2017). Figure 2.2 illustrated the sequence of events that lead to shear localized chip segmentation.

Chip segmentation in machining titanium alloys is associated with tool vibration and chatter which is mainly caused by periodic oscillation in components of cutting forces. This instability in machining can increase the tool wear rate and worsen the surface finish as well as limiting the material removal rate (MMR). The segmented chip formation is generally associated with the reduction of shear strength by either localised thermoplastic

shear or growth of periodic microcracks (Shaw and Vyas 1998; Komanduri and Reed 1983).

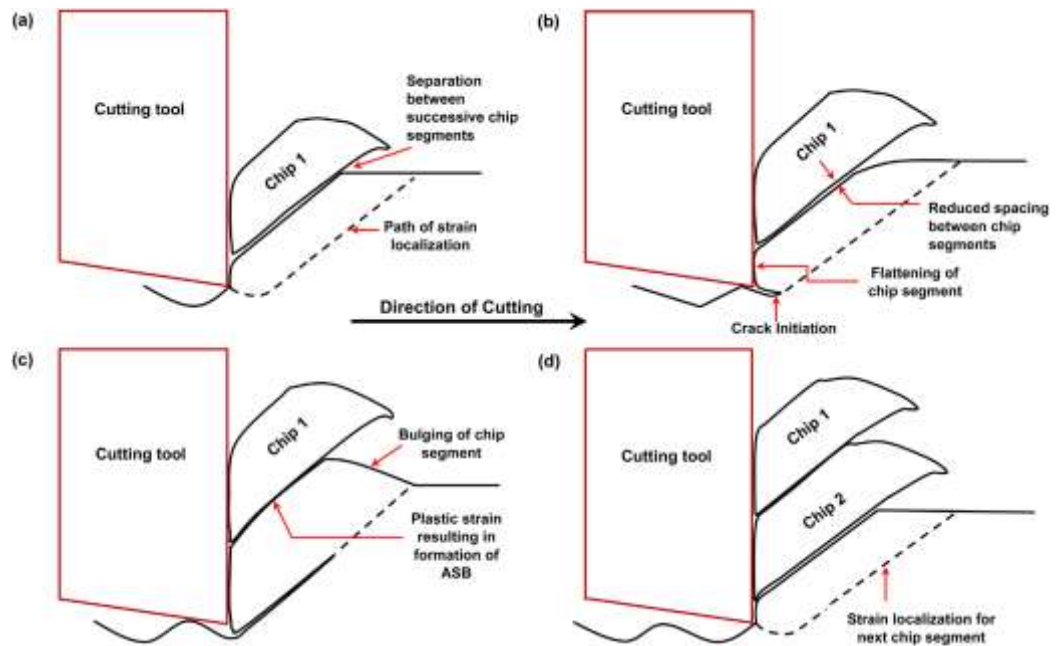


Figure 2.2 Sequence of chip segmentation steps under dry machining condition. (a) Localization of strain along the path of shear band. The shear initiates from the tool tip and takes curved path upwards till meeting the free surface, (b) Crack initiation at the tool tip, (c) Crack propagation (Krishnamurthy et al. 2017)

### 2.3 Enhancing the machinability of titanium alloys using coolants and lubricants

In metal cutting, mechanical energy is used to shear the workpiece material along the cutting direction, plastically deform the chips and overcome friction. The majority of the mechanical energy used for machining is converted into heat (Trent, E.M.&Wright 2000; Revuru et al. 2017; Abukhshim et al. 2006). This generated heat comes from three sources during the chip formation process: i) in the primary shear zone, as a result of work done along the shear plane, ii) in the secondary shear zone, due to the chip deformation and dynamic friction between tool and chip, iii) in the tertiary zone, caused by rubbing contact between the newly machined surface and the tool flank face, as shown in figure 2.3 (Abukhshim et al. 2006; Pervaiz et al. 2014). Therefore, the cooling medium is essential to minimize or even eliminate this principal problem. The cooling fluid tends to lower the cutting temperature well below the softening temperature of the tool material, thus decreasing the thermally related wear caused by adhesion diffusion (Ezugwu et al. 2003; Ayed et al. 2017).

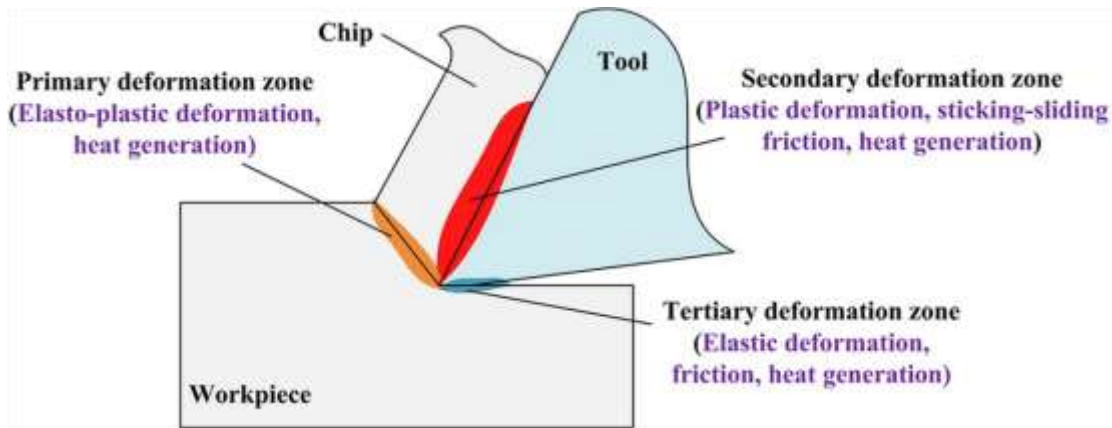


Figure 2.3 Schematic of heat generation zones and chip formation in metal cutting (Abukhshim et al. 2006).

In addition, the cutting fluid can act as a lubricant reducing the friction forces and welding of chips onto the tool rake face. This is commonly encountered in machining titanium which could cause rapid chipping, plastic deformation and catastrophic tool failure (Sun et al. 2006; Hoier et al. 2017). The lubricating characteristics of the cutting fluid can also diminish the abrasion between tool and chip resulting in reduced mechanical wear (Molinari et al. 2002; Islam et al. 2013). Furthermore, the abundant and continuous coolant stream can flush the chips away from the cutting area, moderate thermal shocks of milling tools and inhibit chip ignition (Chandler 1978; Ezugwu and Wang 1997; Tapoglou et al. 2017). However, the excessive cooling of the workpiece could increase its hardness and shear strength resulting in increased cutting forces that leads to reduced tool life (Revuru et al. 2017; Deiab et al. 2014; Park et al. 2017).

The correct choice of cutting fluid can beneficially affect the tool life, power consumption and surface integrity of the machined part. This is largely dependent on the cutting conditions and the dominant tool wear mechanism. (Trent & Wright 2000; Oberg, Jones, Horton and Ryffel 2004; Tapoglou et al. 2017).

#### 2.4 Cutting fluids (coolants and lubricants)

Cutting fluids are generally classified into three main groups depending on their variety in cooling and lubricating characteristics; water-soluble fluids, neat cutting oils and gases, as can be shown in figure 2.4 (Yildiz and Nalbant 2008).



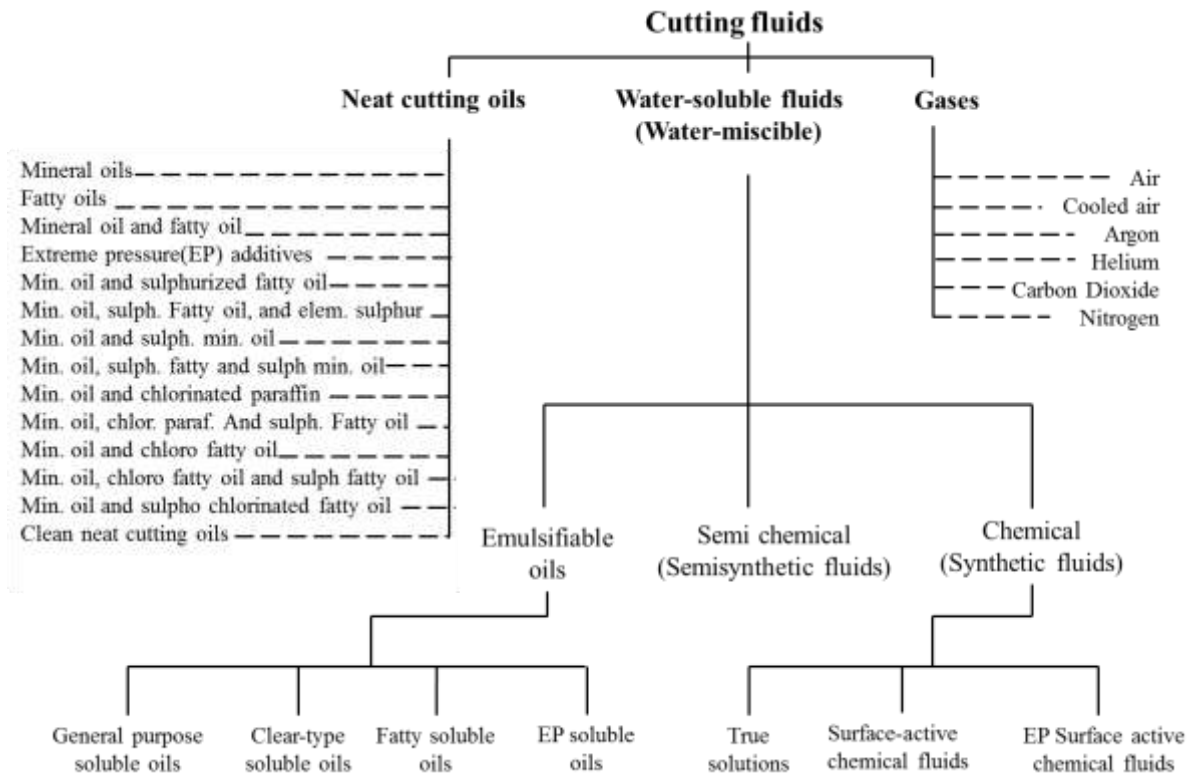


Figure 2.4 Classification of cutting fluids (Yildiz and Nalbant 2008).

### 2.4.1 Water soluble (water miscible) cutting fluids

Water-based cutting fluids have generally been acknowledged to be efficient for high speed machining with low cutting pressure due to their good cooling but have poor lubricating characteristics as compared with oil-based cutting fluids. They are also used to provide adequate cooling to the workpiece to avoid thermal distortion. Water-based coolants are still regarded as the most effective cooling fluids because of the high heat transfer coefficient of water and its high heat of evaporation (Rotella et al. 2014; A. El Baradie 1996; Revuru et al. 2017; Astakhov 2006). Iturbe et al. (2016) studied the feasibility of replacing conventional cooling by hybrid MQL/cryogenic cooling/lubricating when finishing Inconel 718. Results showed that conventional flood cooling outperformed the application of hybrid cooling/lubrication in terms of tool life and surface integrity when machining Inconel 718 alloy (Iturbe et al. 2016).

Different mixing ratios of water soluble cutting fluids are used depending on the particular machining operation, ranging from about 1:25 for chip making processes to nearly 1:45 for grinding (A. El Baradie 1996). According to figure 2.4, water-soluble fluids can be categorised into three types; soluble oils, synthetic (chemical), and semi-synthetic (semi-chemical) fluids. Soluble oils have good lubricating and rust resistance characteristics as well

as the cooling effect of water. Synthetic cutting fluids are mineral oil free or chemical solutions which contain high pressure additives in addition to lubrication and corrosion inhibitor additives (Yildiz and Nalbant 2008; El Baradie 1996). Semi-synthetic cutting fluids contain both mineral oils and chemical additives in order to have effective lubrication and better corrosion prevention. However, water-miscible cutting fluids are susceptible to bacteria and fungi growth which may adversely affect their service life and exacerbate health issues. To reduce these problems, bactericides, germicides and humectants should be added to the water-miscible cutting fluids (Tapoglou et al. 2017; El Baradie 1996).

#### **2.4.2 Neat cutting oils**

Neat oils are oil-based fluids that may be mineral oil based or mineral oils with extreme-pressure additives as shown in figure 2.4. They are generally used for high cutting pressure machining applications where lubrication is the primary consideration (Shaw 1986; Yildiz and Nalbant 2008). There are two main groups of mineral oils that are used as cutting fluids, namely paraffinic and naphthenic mineral oils. The lubricating characteristics of these oils can be enhanced through the addition of extreme pressure additives such as chlorine, sulphate, phosphate, viscosity index modifiers, friction modifiers, fatty lubricants, odorants, thickness modifiers and polar additives (Astakhov 2006). However, straight oils cannot maintain their lubricating characteristics at high temperatures and high pressure conditions. Therefore, they are well-suited for machining easy-to-cut materials such as aluminium, brass, magnesium and carbon steels. Furthermore, some of the additives can react with the machining surface at high cutting speeds causing corrosion (Astakhov 2006; Yildiz and Nalbant 2008; Revuru et al. 2017). As a result, compounded mineral oils are suitable for low temperatures and high pressure cutting applications such as tapping, broaching, gear hobbing, etc. (Donachie 2000).

#### **2.4.3 Gases**

The use of gases as a coolant in many machining applications can be justified due to their capability to penetrate the cutting zone which can be considered under seizure where the conventional cooling fluid fails to access because of high cutting temperatures (Revuru et al. 2017; Su et al. 2007; Ezugwu 2005). Pressurised air is an attractive option due to its abundance and the beneficial effect as a boundary lubricant. However, its poor cooling characteristics make it inefficient if used as a coolant. Compressing and/or chilling and liquefying air usually are taken for granted to increase its cooling capability (Sartori et al. 2017b; Trent & Wright 2000). Gases such as argon, helium and nitrogen can provide an inert

environment in some machining applications where the workpiece material is chemically reactive with the tool material, but the high cost and poor cooling capacity limit their use (Su et al. 2007; El Baradie 1996; Shaw 1986).

## **2.5 Oil/Water-based cooling techniques in machining titanium alloys**

### **2.5.1 Flood cooling**

It has been found that the application of a large quantity of cutting fluid at low pressure is an effective method in removing heat from the cutting zone at low cutting conditions where relatively low temperature is generated (Rotella et al. 2014; Tapoglou et al. 2017). Despite the fact that flood cooling can minimise the built-up-edge (BUE), generally experienced in milling titanium with HSS and carbide tools, it is found that the use of water-based and oil-based cutting fluids can reduce the tool life more than dry machining of titanium alloys (Ezugwu et al. 2003). At higher cutting speed conditions, the coolant fails to access the tool-chip and tool-workpiece interfaces which were mainly under seizure condition (Ezugwu 2005; Revuru et al. 2017). A boiling film is generated from the boiling of the coolant close to the cutting edge causing a high temperature blanket (350 °C for conventional fluids) (Ezugwu et al. 2003). It limits the cooling effect of cutting fluids. Therefore, a high pressure emulsion jet system has been introduced as an effective cooling technique that is capable of delivering the coolant to reach close to the cutting edge (Islam et al. 2013; Hoier et al. 2017).

### **2.5.2 High pressure cooling (HPC)**

The delivery of a convenient fluid at high pressure close to the secondary shear zone can drastically improve the machinability of titanium alloys at high cutting speeds and prolong the tool life (Ezugwu 2005; Hoier et al. 2017; Bermingham et al. 2012). The high speed coolant jet penetrates the tool-chip interface and eliminates the seizure condition thus, significantly minimise the boiling film at the cutting zone (Pramanik and Littlefair 2015). Moreover, the better cooling performance of water based coolants is considered due to the higher conductive and convective heat transfer coefficient compared to conventional cooling methods (Islam et al. 2013; Pramanik 2014). Furthermore, a hydraulic wedge can be developed between the chip and the tool rake face as a result of HPC. This provides an adequate lubrication action with significant reduction in friction. The pressure and high speed coolant can also alter the chip flow condition and offer an effective flushing of the chips away from the cutting area (Ezugwu et al. 2009). Excellent chip breakability was also observed, especially when

machining difficult-to-cut materials such as titanium and nickel based alloys using HPC (Palanisamy et al. 2009).

HPC administered to the tool tip has made great improvement in tool life when machining hard-to-cut materials and its credibility over years has been thoroughly investigated (Ezugwu et al. 2003; Bermingham et al. 2012). The tool life has been enhanced by over 700% compared to conventional flood cooling when machining Inconel 718 with HPC at cutting speeds (up to 50m/min) with coated carbide, while rapid tool failure was reported when the machining was done with ceramic tools. This drop in tool life was attributed to the decrease of the tool-chip contact length/area which can increase the compressive stresses on the cutting edge and accelerate notching of ceramic tools (Kitagawa et al. 1997).

Machado and Walbank (1994) compared the effectiveness of HPC when carbide tools were used to machine Ti-6Al-4V with conventional overhead flood cooling. Results revealed that up to a three-fold improvement in tool life can be achieved. They proved the high efficiency of the HPC as a chip breaker, while no adverse effect on surface finish was observed (Machado and Wallbank 1994). Ezugwu et al. (2007) investigated the use of HPC when machining Ti-6Al-4V with coated carbide, uncoated carbide and polycrystalline diamond (PCD) tools. They showed that high pressure jet cooling can significantly improve the life of the coated and uncoated carbide tools without compromising the surface integrity. They reported that increasing the coolant pressure can prolong the tool life (Ezugwu et al. 2007). Moreover, substantial improvement in tool life was observed when applying HPC in high speed machining of Ti-6Al-4V with PCD that is impossible to achieve with conventional coolant, as shown clearly in figure 2.5 (Ezugwu 2005). Surface integrity analysis showed acceptable surface finish when machining Ti-6Al-4V with PCD tools under HPC. HPC tended to soften the subsurface layer due to the effective cooling of the cutting zone with subsequent tempering action, while hardening to the machined surface was observed when machining with conventional coolant probably because of the irregular quenching caused by flood cooling (Ezugwu et al. 2007). Unlike cemented carbide and PCD tools, cubic boron nitride (CBN) tools were found inefficient for high speed machining of titanium alloys with HPC. This has been attributed to the fact that CBN tools suffer excessive nose wear and severe chipping at the cutting edge (Ezugwu et al. 2005).

Nandy et al. (2009) suggested that HPC demonstrated significant improvement in tool life when machining Ti-6Al-4V alloy. Their results indicated that the application of HPC water-

soluble oil can improve the tool life up to 250% compared with conventional low pressure flood and HPC neat-oil cooling. They attributed this improvement to the efficient cooling of the cutting zone due to the higher thermal conductivity, momentum and convective heat transfer coefficient of HPC water-base coolant. Moreover, significant reduction in cutting forces has been achieved under HPC environment. However, the lowest value of cutting force and power consumption were found under HPC neat oil conditions due to the better lubrication, whereas feed and thrust forces were a minimum when HPC water-soluble oil was applied. This was attributed to the effective lifting of chip away from tool rake face that resulted in significant reduction in the tool-chip contact length (Nandy et al. 2009).

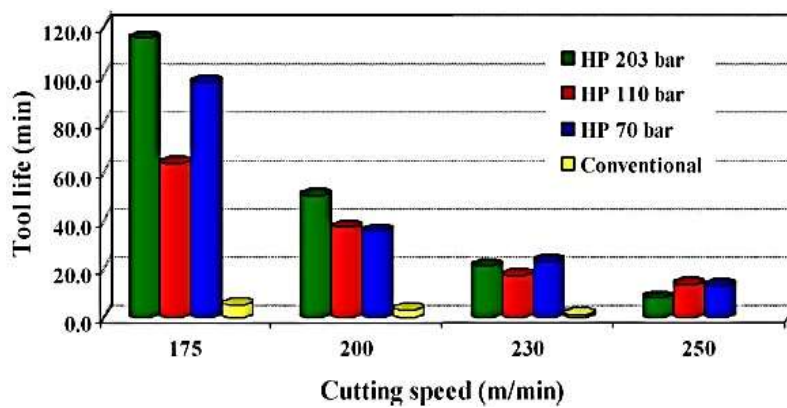


Figure 2.5 Tool lives when machining titanium alloy with polycrystalline diamond inserts at various coolant pressures and with conventional coolant flow(Ezugwu 2005).

According to Da Silva et al. (2013), great improvement in tool life ranging from 9 to 21 fold can be achieved when HPC is used in the machining of Ti-6Al-4V with PCD tools relative to conventional coolant. They proved that tool life is beneficially affected by increasing the coolant pressure and higher cutting speed conditions did not reduce the performance of the PCD tools. They attributed this improvement to the fact that the adhesion tendency experienced in machining titanium alloys is reduced with the increase of coolant pressure. Finally, they observed that segmented C-shaped chips were generated when machining titanium alloys with HPC, whilst long continuous chips were formed under conventional flood cooling (Da Silva et al. 2013).

Ayed et al. (2015) suggested that the tool life can be increased up to 9 times with coolant pressure of 100 bar and cutting speed of 75m/min., when machining Ti-5Al-2Sn-4Mo-2Zn-4Cr) alloy using HPC with uncoated carbide tools. However, water pressure beyond 100 bar could result in scratches and welded chip fragments onto the workpiece which can deteriorate the machined surface quality. It is worth mentioning that the effectiveness of HPC decreases

with increasing the cutting speed (Ayed et al. 2015). Beside the fact that conventional cutting fluids with associated health and safety issues and costs are used in HPC, the high initial cost of the installation of the high pressure jet system in the machine tool which requires additional sealing devices to prevent coolant spilling and leaking can limit its use. Also, the direct exposure of the operator to normal and atomised coolant can cause additional health hazards (Kopac 2009; Priarone et al. 2016).

## **2.6 Sustainable cooling/lubricating techniques in machining titanium alloys**

It is well recognized that the use of conventional cutting fluids has failed to provide an effective cooling, especially at high cutting speeds and when machining difficult to-cut materials such as titanium alloys. Their degradation and ultimate disposal could exacerbate the environmental problem (Hong and Zhao 1999; Priarone et al. 2014; El Baradie 1996). The disposal cost of cutting fluids can be as high as 2-4 times the purchase cost. Chemical dissolution of cutting fluids can cause environmental pollution by soil contamination and water pollution during disposal (El Baradie 1996). It has been reported that the annual disposal of the used cutting fluids into the environment in the United States is around 150 million gallon (Gupta and Laubscher 2017; Deiab et al. 2014). The cutting fluids can also cause severe skin and body ailments to the machine operator, in addition to fumes, smoke, odour, and bacteria. Prolonged physical exposure to mineral oils could exacerbate dermal ailments (Pusavec et al. 2014; Hong and Zhao 1999). Moreover, biocides, chemical additives and extreme pressure additives such as chlorinated paraffin and sulphurized additives can be considered hazardous to health and environment due to their toxicity. This can put additional disposal costs to meet the environmental regulations (Shokrani et al. 2012; Werda et al. 2016; Priarone et al. 2014).

Revuru et al. (2017) provided a comprehensive overview of the recent studies in machining titanium alloys. They concluded that coated carbides outperformed uncoated carbides in terms of tool life and the machinability of titanium alloys was highly affected by the microstructure of the machined material. Moreover, MQL demonstrated an improved machining performance in terms of tool life and surface finish via forming a thin oil film at the tool-chip and tool-workpiece interfaces thus, reducing temperature caused by friction. They noted that cryogenic cooling was effective in reducing the cutting temperature and improving surface integrity and chip breakability. However, the excessive cooling can result in workpiece hardening, and hence higher cutting forces that cause a loss of sharpness of the

tool cutting edge. Finally, they suggested that minimum quantity cooled lubrication MQCL can be regarded as a promising cooling/ lubricating technique if employed properly.

### **2.6.1 Dry machining**

The ecological and economic considerations have encouraged a strong tendency to limit or eliminate the use of conventional coolants (Thakur and Gangopadhyay 2016; Shokrani et al. 2013). Dry machining eliminates the use of hazardous cutting fluids which pollute the environment and prevent the exposure of the shop operator to that harmful substance. It can also be effective in reducing the machining costs. More than 50 billion dollars are spent annually on cutting fluids in the U.S. only (Feng and Hattori 2000).

The best approach to reduce the cost of machining and satisfy environmental regulations is by adopting dry machining (Werda et al. 2016). However, in most machining operations, dry machining can be accepted when the surface quality of the machined part is equal or surpass that achieved in wet machining (Thakur and Gangopadhyay 2016). The absence of cooling and/or lubricating fluid leads to high friction and high temperature generated at the tool-chip and tool-workpiece interfaces. This can result in increased tool wear and reduced tool life, especially when machining aeroengine materials such as titanium and nickel based alloys (Nouari and Ginting 2006).

Numerous studies conducted different approaches to compensate the elimination of cutting fluids in machining titanium alloys. Such approach is using ultrahard cutting tool materials like CBN and PCD tool and adapting the geometry of the tool. Another approach is to introduce various coatings for tools to provide solid lubrication and prevent direct contact between the tool substrate and the workpiece material (Ginting and Nouari 2007).

Dearnly and Grearson (1986) tested several tool materials when dry turning Ti-6Al-4V. They pointed out that the high temperature at the rake face at relatively low cutting speeds is of major problem which is the main cause of crater wear by dissolution-diffusion. The straight (WC-Co) grades were found best in resisting this type of wear and have shown excellent resistance to flank wear caused by attrition. They suggested that CBN tools outperform ceramic and TiB<sub>2</sub> and TiC coated carbide tools in combatting dissolution-diffusion wear (Grearson 1986).

Wang and Rahman (2005) introduced binderless CBN tools for high speed milling of Ti-6Al-4V. Their investigations revealed that longer tool life and high material removal rates can be

achieved with higher cutting speeds and low feed rate and depth of cut. They contrasted what was reported by Nabhani (2001) when they suggested that BCBN tools outperform PCD tools in terms of tool life, and could be the most effective tool material available when machining Ti6-Al-4V at high cutting speeds (Wang et al. 2005).

Ginting and Nouari argued that flank wear localized at the tool leading edge is the major mode of wear when dry milling the titanium alloy Ti-624S with alloyed carbide (P grade) tool. Their experimental investigations showed that a tool life of 11.3min and surface finish Ra as low as  $0.1\mu\text{m}$  can be achieved at cutting speed  $\geq 15\text{m/min.}$ , feed rate of  $0.15\text{mm/tooth}$ , radial depth of cut  $8.8\text{mm}$ , and  $2\text{mm}$  axial depth of cut. They observed that flank wear  $V_B$  is followed by cracking, chipping and flaking which can lead to tool failure. It was suggested that tool wear is highly dependent on the cutting tool geometry and on the cutting direction of up or down milling. They concluded that chip morphology and machining conditions such as cutting temperature, shear angle and contact length can drastically affect the cutting performance of the alloyed carbide tool (Ginting and Nouari 2006). Further study by Ginting and Nouari (2007) has been conducted to investigate the wear mechanism of uncoated and multi-layer coated CVD carbide tools. Results showed that adhesion is the dominant wear mechanism when dry milling Ti-624S with these tools. Delamination in coating was observed initially. A diffusion process occurred between the tool coating, substrate and workpiece due to the high temperature at the tool-chip interface ( $950^\circ\text{C}$  -  $1180^\circ\text{C}$ ). Best results of tool life (613min) and good surface finish ( $0.4\mu\text{m}$ -  $0.5\mu\text{m}$ ) for the both tool materials were found at the cutting speed range from  $100$  to  $110\text{m/min}$ . The experimental and numerical study showed that the optimum cutting condition regarding tool life and material removal rate when uncoated alloyed tool was used for dry milling Ti-624S are (Ginting and Nouari 2007):

- i. Cutting speed  $V_c=88\text{m/min}$ , with feed rate  $f_z=0.2\text{mm/tooth}$
- ii. Cutting speed  $V_c=113.5\text{m/min}$ , with feed rate  $f_z=0.15\text{mm/tooth}$
- iii. Cutting speed  $V_c=163\text{m/min}$ , with feed rate  $f_z=0.1\text{mm/tooth}$

Surface integrity investigations showed that uncoated carbide tools produce better surface finish than CVD coated tools, and the former can carry out dry machining when the cutting conditions are limited for finish or semi-finish machining operations (Ginting and Nouari 2009).



### 2.6.2 Minimum quantity lubrication (MQL)

Minimum quantity lubrication (MQL) or near dry cutting has been regarded as an effective alternative to conventional flood cooling from ecological and economic considerations (Deiab et al. 2014; Sartori et al. 2018; Dhar et al. 2006). It can be considered as a potential to fill the gap between dry machining and flood cooling (Park et al. 2017). This technique involves the application of a very small amount of mineral oil or water based coolant (flow rate range from 6-200ml/h) sprayed with a compressed air stream directly to the cutting interfaces (Rahim et al. 2015; Werda et al. 2016), as shown schematically in figure 2.6 (Kamata and Obikawa 2007). MQL has shown encouraging success in turning (Obikawa et al. 2006; Sharma et al. 2009; Deiab et al. 2014; Werda et al. 2016), milling and grinding (Park et al. 2015; Sales et al. 2009; Park et al. 2017). These improvements in tool life and surface quality could be attributed to the ability of the lubricating oil spray to reach very close to the cutting interfaces, thus reducing the cutting forces and friction generated in machining titanium alloys (Revuru et al. 2017).

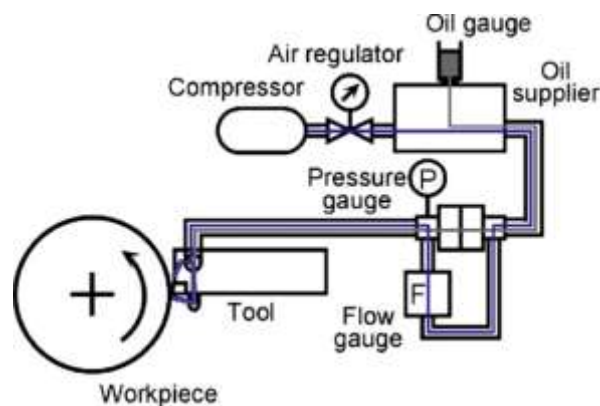


Figure 2.6 Schematic layout of oil mist supply (Kamata and Obikawa 2007)

Moreover, MQL can significantly reduce the cutting zone temperature by the cooling effect of the air stream and the heat absorbed by evaporation of the lubricant (Rahim et al. 2015; Sun et al. 2006). With MQL, the pressure welding of the chips to the cutting edge that is experienced in milling titanium alloys at high cutting speeds can be dramatically reduced which leads to significant enhancement in surface finish and tool life (Ezugwu 2005; Revuru et al. 2017). It has been proved that MQL technology shows promising performance in precision machining of titanium alloys at high cutting speeds and low feed conditions (Sartori et al. 2018; Werda et al. 2016). Recent studies introduced graphite nano-platelets that

are mixed with vegetable oil to enhance the machining performance when milling Ti-6Al-4V. They suggested that there is an optimum value of MQL flow rate for each cutting condition that give the best results in terms of tool life and it occurred at 9ml/h for 100m/min cutting speed, 0.15mm/rev., 2mm depth of cut and 16.7mm width of cut (Park et al. 2017). Sharma et al. (2015) reviewed the various methods of MQL applied for different machining processes for different cutting tool and workpiece materials.

Many studies have investigated the cooling and lubricating effect of MQL technology when machining difficult-to-cut materials such as titanium and nickel based alloys. Kamata and Obikawa (2007) investigated the cutting performance of the MQL technique in terms of tool life and surface integrity when finish-turning Inconel 718, using coated carbide tools with different coatings. It was found that an increase in cutting speed from 60 to 90m/min can drastically reduce the tool life and surface quality. The best cutting performance was obtained with the TiCN/Al<sub>2</sub>O<sub>3</sub>/TiN coated tool at cutting speed as low as 60m/min. The same coating achieved the longest tool life when flood cooling with poor surface finish. They suggested that air pressure plays an important role in the cutting performance and there is an air pressure value that gives an optimum tool life in turning Inconel 718 (Kamata and Obikawa 2007).

Obikawa et al. (2006) suggested that the application of MQL with vegetable oil mist at very small flow rates, of 7 ml/h, outperform soluble cutting fluid in terms of flank and nose wear when high speed grooving Ti-6Al-4V using triple-layer TiC/TiCN/TiN coated carbide tools. They showed that the increase in air stream pressure in MQL can lead to reduced flank and nose wear. They concluded that oil mist direction controlled by the air stream have significant effect in the lubrication between the flank and the machined faces (Obikawa et al. 2006). Sun et al. (2006) studied the cutting performance of MQL in terms of tool life and material removal rate when milling Ti-6Al-4V. They used uncoated carbide tool H1 due to its adequate hot hardness needed in machining titanium alloys (Trent, E.M.&Wright 2000). It was shown that MQL significantly outperforms air and flood cooling in terms of tool life. Significant reduction in cutting forces was observed due to the better lubricating effect of MQL. They suggested that MQL can provide satisfactory cooling and lubrication when machining titanium alloys (Sun et al. 2006).

Liu et al. (2013) investigated the wear rate, wear pattern and wear mechanism when high speed machining Ti-6Al-4V with straight carbide (WC-Co) tools and two types of

nanocomposite (nc-AlTiN)/(a-Si<sub>3</sub>N<sub>4</sub>) and (nc-AlCrN)/(a-Si<sub>3</sub>N<sub>4</sub>) coated tools under dry and MQL conditions. Results confirmed that MQL dramatically prolonged the life of (nc-AlTiN)/(a-Si<sub>3</sub>N<sub>4</sub>) coated tool, which seemed more efficient than (nc-AlCrN)/(a-Si<sub>3</sub>N<sub>4</sub>) coated tool in machining titanium alloys. Using MQL, uncoated carbide tools exhibited improved cutting performance over dry machining. Adhesion was the dominant wear mechanism when machining with (nc-AlTiN)/(a-Si<sub>3</sub>N<sub>4</sub>) coated tool, while for (nc-AlCrN)/(a-Si<sub>3</sub>N<sub>4</sub>) adhesion, diffusion and oxidation were the main wear modes. They suggested that MQL technique does not only provide effective cooling and lubrication to nanocomposite coated tools, but also has a beneficial effect to promote a powerful TiC protective layer (Liu et al. 2013).

Deiab et al. (2014) implemented different sustainable cooling and lubricating strategies, namely; dry, MQL, minimum quantity cooled lubricant MQCL, cooled air and cryogenic cooling during turning of Ti-6Al-4V with uncoated carbide tools. Results showed a promising performance of MQL and MQCL with vegetable rapeseed oil in terms of surface quality, tool life and cutting energy (Deiab et al. 2014). It was shown that dry machining has lower energy consumption than flood cooling and MQL due to the elimination of the energy required for coolant pump. Increasing feed rates can lead to lower energy consumption because of the reduced machining time at a cost of higher surface roughness. It was suggested that the machining environment significantly affected tool wear rate and wear mechanism. Dry machining was characterized by its rapidly increased wear rate with an increased cutting speed. On the other hand, flood cooling showed better performance than MQL at low speed and feed rates, while MQL demonstrated better tool life at higher speed and feed rates. Tool wear analysis showed that adhesion-diffusion and abrasion were dominant when uncoated tools were used due to the high cutting temperature, while coating delamination starts the wear mechanism for coated tools (Pervaiz et al. 2013).

Rahim et al. (2015) investigations showed that the application of minimal quantity coolant/lubricant (MQCL) with synthetic ester enhanced the machining performance compared to dry machining by lowering the cutting temperature by 10% to 30% and reducing the cutting forces by 5% to 30% as a result of lower friction coefficient and better penetration to cutting zone. It was concluded that MQCL was found superior to dry machining and can be considered as a sustainable machining environment (Rahim et al. 2015). Gupta and Sood (2017) suggested that the application of MQL when optimising the cutting conditions and tool geometry can lead to improvement in machinability in terms of reducing tool wear,

cutting forces, and surface roughness in comparison to conventional flood cooling when machining titanium and nickel based alloys (Gupta and Sood 2017)

Werda et al. (2016) suggested that well-chosen oil in MQL can improve the cooling/lubricating performance. Both synthetic and fatty oils show improved machinability in terms of cutting temperature, cutting forces, and surface roughness as compared with dry machining. They suggested that high flash point synthetic ester can provide more lubricity, and hence better results under loads, while low flash point fatty oil can improve the tool life via providing more cooling in MQL (Werda et al. 2016).

Park et al. (2017) introduced graphite nano-platelets that are mixed with vegetable oil to enhance the machining performance when milling Ti-6Al-4V. They suggested that there is an optimum value of MQL flow rate for each cutting condition that give the best results in term of tool life and it occurred at 9ml/h for 100m/min cutting speed, 0.15mm/rev, 2mm depth of cut and 16.7mm width of cut (Park et al. 2017).

Sartori et al. (2018) introduced minimal quantity lubrication and cooling, MQL and MQC strategies to improve the machinability in terms of tool wear and surface integrity (surface roughness, surface defects, and hardened layer) compared with dry, conventional wet and pure MQL when finish turning Ti-6Al-4V alloy. These techniques are based on the addition of solid lubricant to both MQL and MQC, namely; enriching MQL vegetable oil with PTFE particles and the addition of graphite powder at different percentages to an aqueous solution. Findings revealed that MQL with or without PTFE were effective in reducing the tool nose wear and limiting abrasive wear mechanism due to the high dynamic viscosity of the lubricant. However, due to its low cooling capacity, MQL was not efficient in eliminating the tool crater wear. On the other hand, the solid lubricant-assisted MQC demonstrated the lowest tool crater and nose wear with slight improvement when increasing graphite content. Its significantly lower flow rate can be considered an excellent sustainable alternative to conventional flood cooling strategies. They concluded that the machined surface integrity was less influenced by the cooling/lubricating technique (Sartori et al. 2018).

The main drawback of the use of MQL as a cooling system in machining is the generation of oil mist which could be hazardous to the machine tool operator. Effective mist extractors (filters) can be used to minimise this health problem (Ezugwu 2005; A. Shokrani et al. 2012). The use of vegetable oil can improve the performance of MQL technique from health, environmental, safety and economical viewpoints (Sharma et al. 2015; Park et al. 2017). It is

worth noting that the limited cooling effect of MQL depends mainly on the compressed air and partially on the cutting fluid evaporation. This has made MQL inefficient cooling technique, especially when the machining is associated with high generated temperature such as titanium alloys (Kamata and Obikawa 2007; Park et al. 2015).

### **2.6.3 Cryogenic cooling**

Cryogenic machining has shown a growing demand in material cutting operations due to its effectiveness, as a sustainable and viable machining technology as compared to oil/water based conventional machining in improving the machinability of hard to-machine materials (Kaynak et al. 2014; Kale and Khanna 2017). It is also acknowledged as an efficient cooling method that is capable to maintain the temperature of the cutting zone well below the softening temperature of the cutting tools' materials (Sartori et al. 2018; Revuru et al. 2017). It is emerging as one of the most favourable and promising cooling techniques as a consequence of its capability to considerably improve the cutting tool life and surface finish through the desirable control of cutting zone temperature (Yildiz and Nalbant 2008; Sartori et al. 2016). The principle of cryogenic cooling involves the injection of a liquefied gas, such as nitrogen, carbon dioxide and helium, at temperatures lower than -150 °C and supplied under pressure to the cutting zone (Shokrani et al. 2013; Ayed et al. 2017). Liquid nitrogen LN2 is commonly used as a cryogenic coolant, because of its safety, inertness, non-toxicity, low cost and environmental friendliness (A. Shokrani et al. 2012; Yildiz and Nalbant 2008; Jawahir, Attia, et al. 2016). In addition to the significant reduction in cutting temperature due to effective heat removal, cryogenic cooling has demonstrated a substantial improvement in tool life and machinability through altering the properties of the cutting tool and the workpiece materials (Shokrani et al. 2013; Tang et al. 2017; Sun et al. 2016; Jawahir, Puleo, et al. 2016).

It was suggested that the main function from lowering the temperature with applying cryogenic coolant, especially in machining difficult-to-cut materials is altering the frictional characteristics of the tool-chip and tool-workpiece interfaces. Furthermore, cryogenic application can change the chemical, physical and mechanical properties of the contact surfaces of the tool and workpiece materials which can beneficially affect surface integrity of the machined component. Due to the reduced cutting zone temperature, the tool will retain its hardness and strength resulting in significant reduction in temperature dependent wear under all cutting conditions (Wang and Rajurkar 2000; Hong and Zhao 1999).

Major reviews have been undertaken in cryogenic machining and cooling by Yildiz et al. (2008), Shokrani et al. (2013), Kaynak et al. (2014), and Jawahir et al. (2016). Yildiz et al. (2008) presented a detailed review of cryogenic liquid nitrogen cooling techniques in machining and their influence on tool wear/life, properties of the tool and workpiece, surface integrity, cutting temperature and cutting forces (Yildiz and Nalbant 2008). Shokrani et al. (2013) classified their review into two main categories; cryogenic treatment (processing) and cryogenic machining and concluded that cryogenic cooling can provide effective heat treatment to enhance machinability by altering the material properties of the tool and workpiece at the cutting zone (Shokrani et al. 2013). Kaynak et al. (2014) presented an overview to the effect of cryogenic machining on the surface integrity characteristics of the machined component in terms of surface roughness, microhardness, topography, phase transformation, grain refinement and machining induced layer, residual stresses and fatigue life. They compared this effect with other cooling processes such as dry machining, flood cooling and MQL. They concluded that cryogenic machining can dramatically improve the functional performance of the machined part through its superior and desirable surface integrity specifications (Kaynak et al. 2014).

Jawahir et al. (2016) presented an overview or the state-of-the-art of the application cryogenic cooling in manufacturing processes such as machining, grinding, forming and burnishing. For cryogenic processing, material performance and tribological and thermo-mechanical were described. Also, they discussed the influence of cryogenic processing methods on surface integrity characteristics in terms of induced residual stresses, and grain refinements which affect the functional performance of the product such as fatigue life and wear and corrosion resistance. In addition, the performance of the application of LN<sub>2</sub> and LCO<sub>2</sub> were discussed in terms of effectiveness and limitations and compared with conventional flood cooling, HPC and MQL, in terms of tool wear/tool life, surface roughness/surface finish, chip control, power consumption, etc. They briefly described the economic, environmental, health and safety aspect associated with the application of various coolants in manufacturing processes. They concluded that cryogenic processing can be regarded as a novel and sustainable process forward to improving the functional performance of the machined product (Jawahir, Attia, et al. 2016).

### **2.6.3.1 Cryogenic cooling of titanium alloys in turning operations**

Zhao and Hong (1992) indicated that hardness of Ti-6Al-4V increases from 33.5 HRC at room temperature to around 42 HRC at LN2 temperature and can retain its impact strength and ductility at extremely low temperatures. They suggested that directing the LN2 jet to the workpiece and cutting tool can effectively reduce the chemical reactivity, while freezing the cutting tool can improve its hardness, toughness, and transverse rupture strength (TRS), which can beneficially affect the tool wear resistance (Zhao and Hong 1992).

Hong and Zhao (1999) developed an effective and economical cooling strategy that is capable of improving the tool life five folds as compared with conventional emulsion cooling. Their cooling technique involved injecting LN2 to the tool-chip and tool-workpiece interfaces with small amount of LN2 consumption. This significantly improved the machinability and reduce the machining time (Hong and Zhao 1999). Wang and Rajurkar (2001) showed that the value of flank wear when applying conventional flood cooling in machining Ti-6Al-4V with H13A cemented carbide at a cutting speed 132m/min, feed rate 0.2mm/rev and depth of cut 1.0mm, is five times that when LN2 cutting tool cooling is used for the same cutting parameters. They attributed this improvement in tool life when LN2 cooling is used to the large reduction in cutting temperature due to the change of convection condition surrounding the cutting tool (Wang and Rajurkar 2000).

For their approach, Hong and Ding (2001) introduced a cryogenic cooling technique when machining Ti-6Al-4V by directing small amount of LN2 simultaneously to the tool rake and the flank faces via primary nozzle with chip breaker and secondary nozzles, as shown in figure 2.7. With reducing the cutting temperature below 500°C, a significant improvement in tool life has been achieved at a cutting speed as high as 150 m/min. The cutting temperature findings were verified theoretically using finite element analysis (FEA) with the effect of cutting speed analysed. They ranked the effectiveness of the investigated cooling techniques, worst to best, i) dry machining, ii) cryogenic indirect tool cooling, iii) conventional emulsion cooling, iv) cryogenic cooling the tool flank face, v) cryogenic cooling the tool rake face, vi) simultaneous cryogenic cooling the tool flank and rake faces (Hong and Ding 2001). Similar experimental investigation reported five times improvement in tool life when cryogenic cooling the tool rake and flank faces as compared with emulsion cooling (Hong, Markus, et al. 2001).

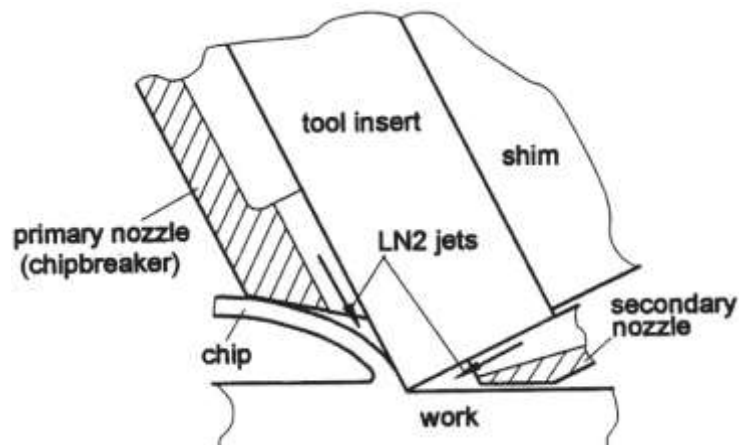


Figure 2.7 Dual cryogenic cooling technique(Hong and Ding 2001; Hong, Markus, et al. 2001).

Venugopal et al. (2007) compared the cutting performance of cryogenic cooling in terms of tool life with dry and wet machining when turning Ti-6Al-4V with a straight WC tool. They reported that the maximum reduction in flank wear can be achieved at a cutting speed as high as 100 m/min. with high crater wear, while effective cryogenic cooling was observed at moderate cutting speed (70 m/min.). They attributed this improvement in tool life to the fact that the desirable control of machining temperature due to cryogenic cooling could reduce the adhesion-dissolution-diffusion tool wear (Venugopal et al. 2007b).

Hong et al. (2001) examined the lubricating influence of application LN2 in machining Ti6-Al-4V. They converted the 3D measured forces in oblique cutting into friction and normal force components via mathematical modelling. Results revealed that considerable reduction in friction between tool and chip has been achieved with cryogenic machining. Microstructure inspection showed decreased secondary thickness deformation (flow zone) and increased shear angle which can support their argument. The lubricating effectiveness can be further enhanced by proper positioning of the chip breaker/primary nozzle (figure 5.6) to provide a lifting movement to the chip allowing LN2 to reach closer to the cutting edge and form a hydrodynamic cushion (Hong, Ding, et al. 2001). Hong (2006) conducted a disc-flat-contact test to verify the lubricating mechanism of LN2 and showed that uncoated WC insert with titanium alloy disc resulted in lower friction under cryogenic cooling, while coated inserts exhibited higher friction. He concluded the lubrication of LN2 is highly dependent to the material pairs and suggested that the reduction in friction forces when injecting LN2 is caused by the formation of hydro dynamic layer between the contact bodies. A more recent study showed that the wear modes in dry sliding of Ti56 against WC insert are adhesion and delamination, while abrasion and delamination were the observed wear



mechanisms in cryogenic sliding (Hong 2006). Yap et al. (2015) proved experimentally that the use of LN<sub>2</sub> as a cryogenic coolant at low pressure in machining Ti56 with K 313 grade carbide can reduce the friction coefficient and surface roughness (Yap et al. 2013).

Venugopal et al. (2003) investigated the cutting performance of TiB<sub>2</sub>-coated tool when machining titanium alloy Ti-5Al-5Mo-2Sn-V under cryogenic cooling and dry machining in terms of tool wear, cutting forces and surface roughness. Though reduced cutting forces in cryogenic cooling was reported, TiB<sub>2</sub> coated tools have shown poor machining performance in terms of tool wear and surface finish, since these tools suffer excessive coating delamination when machining titanium alloys. This deterioration in cutting performance was attributed to the fluctuation in cutting forces cause by chip segmentation. Severe abrasion and adhesion- diffusion at the flank and rake faces were the dominant mechanisms of wear as a consequence of TiB<sub>2</sub> removal during machining (Venugopal et al. 2003). Armacharoen and Chuan (2014) proved that cryogenic cooling showed improved machinability and sustainability compared with dry and conventional oil-based cooling through the reduction of tool wear and friction at the secondary deformation zone. The lower consumption of energy as well as environmental friendliness of cryogenic cooling helped for more sustainability in machining process (Aramcharoen and Chuan 2014).

It is worth mentioning that nitrogen has no recorded health hazards to machine operator and can safely be dispersed into the atmosphere when used as a coolant, since it is lighter than oxygen and forms 78% of the atmosphere. The use of CO<sub>2</sub> as a cryogenic coolant essentially requires a ventilation system over the machine environment as it is heavier than air and can accumulate over the shop floor causing oxygen depletion (Hong 2001). However, CO<sub>2</sub> has been proved as more effective coolant than N<sub>2</sub> and O<sub>2</sub> in machining purposes (Çakir et al. 2004). Machai and Biermann (2011) investigated the effectiveness of CO<sub>2</sub> cooling when machining beta-titanium alloy, Ti10V-2Fe-3Al, which possesses the highest strength among titanium-based alloys, with uncoated and TiAlN-TiN coated cemented carbide tools. Comparative investigations revealed that at cutting speed as high as 100m/min, the tool life has been doubled under CO<sub>2</sub> snow cooling over conventional flood cooling with a uniform spread of flank wear and noticeable suppression of notch wear and burr formation on the workpiece. On the other hand, no effective penetration of CO<sub>2</sub> stream and reduction in chemical reactivity was observed (Machai and Biermann 2011). It was shown that a small quantity usage of CO<sub>2</sub> may not causes asphyxiation risks if it is not in direct contact with the machine operator. Moreover, the low cost of CO<sub>2</sub> as compared to LN<sub>2</sub> can make it promising

in future titanium machining (Machai et al. 2013). Jerold and Kumar (2013) studied the influence of the application of cryogenic coolants namely; LN2 and LCO2 on the machinability of Ti-6Al-4V in terms of cutting forces, cutting temperature, tool wear, service integrity and chip morphology. They reported a reduction in cutting temperature by 47% and 36% with a cryogenic LN2 and CO2, respectively as compared with dry and wet machining. For cryogenic LCO2, the cutting forces and surface roughness were reduced up to 24% and 48%, respectively in comparison to cryogenic liquid LN2 machining. They concluded that better tool life and chip breakability were achieved with LCO2 over dry, wet, and LN2 machining (Jerold and Kumar 2013).

Sadik et al. (2016) studied the influence of coolant flow rate on tool life and wear development when milling Ti-6Al-4V alloy under cryogenic CO2. Tool life was shown to increase with increasing the flow rate of LCO2. Experimental results indicated that notch wear is limiting the tool life irrespective of coolant type and the coolant flow rate has limited effect on flank wear. It has been concluded that cryogenic cooling with CO2 significantly improve the tool life over emulsion cooling due to the reduction of the thermal cracks tendency, and to the delay of chipping of the cutting tool (Sadik et al. 2016).

Birmingham et al. (2011) studied the effect of changing cutting parameter combinations with fixing cutting speed and material removal rate on the tool life when cryogenic turning of Ti-6Al-4V with uncoated tungsten carbide insert. The greatest reduction in tool flank wear was found at high feed rates and low depths of cut, while the longest tool life was achieved at low feed rate and high depth of cut combinations. They proposed that cryogenic influence in reducing the tool-chip contact length is the main reason for limited heat generated at the secondary shear zone which could reduce the heat transfer to the cutting tool. The researchers argued that extending the tool life through preventing the generation of heat during machining Ti-6Al-4V is more advantageous than cryogenically extracting the heat generated at the cutting zone (Birmingham et al. 2011).

Birmingham and et al. (2012) conducted a comparative investigation of HPC and cryogenic cooling techniques using consistent cutting tools, different cooling delivery strategies and various cutting parameters when machining Ti-6Al-4V alloy. Significant effectiveness has been confirmed for LN2 and HPC in terms of tool life as compared with dry machining, with slight superiority in HPC. Cryogenic cooling exhibited more sensitivity to the technique of coolant delivery than HPC. It was concluded that the strategy of cooling delivery is of equal

importance to the type of coolant used. They suggested that tool life can be further maximized with the capability of the coolant delivery system to get precisely into the cutting zone (Birmingham et al. 2012).

Klocke et al. (2013) showed that cryogenic LN<sub>2</sub> machining of gamma titanium aluminide (Ti<sub>45</sub>Al-8Nb-0.2C-0.2B) can significantly reduce the cutting forces and be beneficial in terms of reducing the tool temperature at the cutting zone without compromising the desired material removal rate (Klocke, Lung, et al. 2013). Another investigation into the same material concluded that cryogenic cooling provided extended tool life and improved surface quality due to its effective cooling-lubricating action (Klocke, Settineri, et al. 2013). Sun et al. (2010) compared the chip temperature, cutting forces and chip morphology during machining Ti-6Al-4V under cryogenic compressed air with those measured when dry machining and compressed air cooling. A substantial reduction in chip temperature was shown under cryogenic compressed air cooling. High speed super cooled air could promote higher chip segmentation and reduce the chip thickness resulting in reduced friction and more bending chips away from the cutting zone. However, this beneficial effect tended to diminish when increasing the cutting speed. Moreover, the marginal increase in cutting forces was attributed to the very low chip temperature and the slight increase in the shear plane angle (Sun et al. 2010). Dhananchezian and Kumar (2011) investigated the application of cryogenic LN<sub>2</sub> and conventional flood cooling when turning Ti-6Al-4V. Cryogen was delivered to the cutting edge via holes in the cutting tool insert that enabled LN<sub>2</sub> injection to the rake face and the two flank faces. Results showed that cryogenic cooling achieved nearly 64% and 36% reduction in cutting temperature and surface roughness, respectively over wet machining. A reduction in cutting forces and flank wear of around 40% and 34% respectively was reported in benefit of cryogenic machining. The researchers concluded that tool wear geometry can be significantly reduced through by using cryogenic cooling (Dhananchezian and Kumar 2011).

Rotella et al. (2014) studied the effect of different cooling conditions on surface integrity when turning Ti-6Al-4V with a coated tool at varying cutting parameters. It was shown that cryogenic cooling enabled significant reduction in surface roughness as well as a substantial increase in surface and subsurface hardness. The improvement in the dynamic recrystallization mechanism and phase change due to cryogenic cooling was inferred to the change in surface microstructure. Further improvement in surface integrity can be achieved with cryogenic machining through the generation of smaller surface and subsurface grain size

as a consequence of cryo-processing. It was concluded that the surface characteristics of titanium alloys can be significantly improved with cryogenic cooling. This improvement holds a great impact on enhancing product quality and reliability (Rotella et al. 2014).

Sun et al. (2015a) conducted a quantitative investigation on the effect of cryogenic compressed air on cutting forces and tool wear during turning Ti-6Al-4V alloy at speeds of 150 and 220m/min. Tool wear was compared with dry machining in which tool failure occurred as a result of gradual development of flank wear followed by catastrophic deformation of cutting edge. Results showed that cryogenic compressed air dramatically improved tool life especially at high cutting speeds due to the significant reduction of plastic deformation of the cutting edge when cryogenic compressed air was applied. They attributed this improvement in tool life to the high delivery pressure of cryogenic air jet and the low temperature which resulted in the reduction in the temperature of tool-chip contact area. They suggested that low cutting temperature suppressed thermally related wear, limited BUE and reduced plastic deformation of cutting edge caused by thermal softening ( Sun et al. 2015a). Sun et al. (2015b) introduced cryogenic cooling when machining Ti5553 alloy. Machinability was investigated in terms of tool wear, cutting forces, and surface roughness with those for flood cooling and MQL. Results indicated that MQL provided the best surface finish due to the higher ductility resulted from the material thermal softening. On the other hand, cryogenic cooling demonstrated the lowest tool wear owing to the reduced adhesion of titanium to the cutting tool material. In terms of cutting forces, 30% reduction in thrust forces generated from the application of cryogenic cooling were reported compared to flood cooling and MQL. This was in agreement with the finite element simulation results (Sun et al. 2015b).

Bordin et al. (2015) evaluated the developing tool wear mechanisms when dry and cryogenic machining additive manufactured Ti-6Al-4V using TiAlN coated carbide tools at various cutting speeds and feed of rates. SEM and EDS were used to measure and analyse the tool flank and nose wear, and to measure the adhesion of work material on the tool rake face and cutting edge, respectively. Also, a 3D optical profilometer to evaluate the abrasive and adhesive crater wear. Furthermore, chemical etching analysis was employed to measure the width of the adhered layer via removing the workpiece material from the tool thus enabling the determination of the adhesive relative abrasive wear as shown in figure 2.8. Results demonstrated that tool wear was increased when increasing the cutting speed and feed rates. Cryogenic cooling prevented adhesive crater wear via reducing to tool-chip contact area and

reducing the adhered layer on the tool rake face even with increasing the machining time in all tested cutting conditions. The researchers concluded that cryogenic cooling can improve surface integrity in terms of surface roughness characteristics and microstructural alteration even at severe cutting conditions (Bordin et al. 2015).

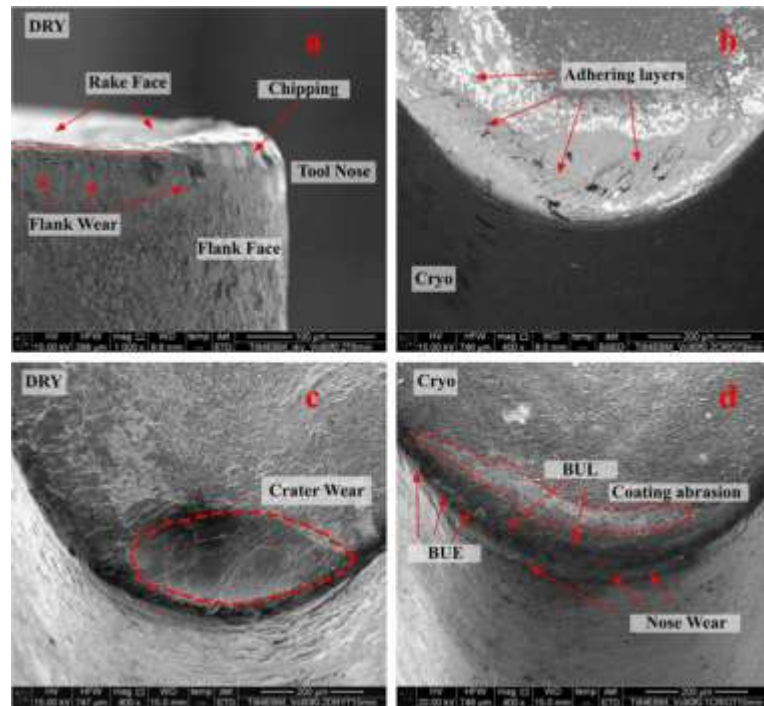


Figure 2.8 Main tool wear modes observed in dry and cryogenic turning after 8 min when adopting a cutting speed of 80 m/min and a feed rate 0.2 mm/rev(Bordin et al. 2015).

Shokrani et al. (2016) conducted a surface integrity investigation in terms of surface roughness, microscopic surface morphology and subsurface microhardness when end milling of Ti-6Al-4V with different cutting conditions under cryogenic cooling environment. The experimental results showed that cryogenic cooling resulted in a reduction in surface roughness of up to 31% and 39% compared to conventional wet and dry machining, respectively. Best results ( $R_a=0.58\mu\text{m}$ ) were found at  $V_c=115\text{m/min}$ ,  $f=0.03\text{mm/tooth}$ , axial depth of cut=5mm, and radial depth of cut=4mm. Analyses of the surface morphology demonstrated a significant reduction in the defects of the machined surface compared to dry and flood cooled machining. They concluded that cryogenic cooling can considerably improve surface integrity when milling titanium alloy. The researchers attributed the improvements in machinability to the reduction in percentage elongation and fracture toughness of titanium as a result of lowering temperature to that of liquid nitrogen (Shokrani et al. 2016b).

Bruschi et al. (2016) suggested that the application of cryogenic cooling during the machining of wrought and additive manufactured AM Ti-6Al-4V can significantly affect the mechanical properties of the machined surface. The wear performance of Ti-6Al-4V surface can be improved via lowering the coefficient of friction and altering the wear mode to adhesive rather than abrasive through the increase of surface microhardness and residual stresses without compromising the surface quality. This reduces the debris formation and hence improves the service life of the machined part (Bruschi et al. 2016). Sartori et al. (2016) investigated the influence of dry and cryogenic machining on the tool wear mechanism during semi-finishing of different produced Ti-6Al-4V alloys namely; wrought, electron beam (EBM) additive manufactured (AM), and direct metal laser sintering (DMLS) Ti-6Al-4V alloys. Results showed that crater wear depth was reduced up to 60% with cryogenic cooling compared to dry machining when machining DMLS titanium alloy. Also, both adhesion of the cutting edge and abrasion-adhesion flank wear were reduced when applying cryogenic cooling to DMLS manufactured Ti-6Al-4V alloy. They concluded that EBM manufactured Ti-6Al-4V alloy demonstrated the best machinability in terms of tool life, and that the thermal and mechanical characteristics of the manufactured alloys affected the tool wear mechanism in both dry and cryogenic machining conditions (Sartori et al. 2016).

Aramchareon (2016) carried out an experimental investigation to the influence of cryogenic rake and flank cooling on tool life and chip formation when turning Ti-6Al-4V with coated carbide tools (CNMG120412 from Mitsubishi) at cutting speeds 70 and 100m/min. His results indicated an improved cutting performance in terms of wear resistance in both rake and flank faces compared to oil-based coolants. Moreover, chip formation analyses when machining under cryogenic cooling showed a cracked morphology of chip segmentation and thinner secondary deformation layer compared to oil-based conventional cooling as shown in figure 2.9 (Aramchareon 2016). Sun et al. (2016) conducted cryogenic machining of the titanium alloy Ti-6Al-7Mo that emerged as an alternative to replace Ti-6Al-4V in biomedical applications. A surface integrity investigation was carried out in terms of surface roughness and surface layer hardness. Results demonstrated a considerable improvement in surface integrity when cryogenic cooling was applied; 7% and 53% improvement in surface roughness, respectively compared with flood cooling and dry machining. The surface layer hardness has been increased by 15% and 34% respectively as compared with wet and dry machining. They attributed the increased hardness of the surface and the subsurface to the

cooling effect of LN2 that mitigated the thermal softening effect of the machining process, which suppress the phase transformation from  $\beta$ -phase to  $\alpha$ -phase (Sun et al. 2016).

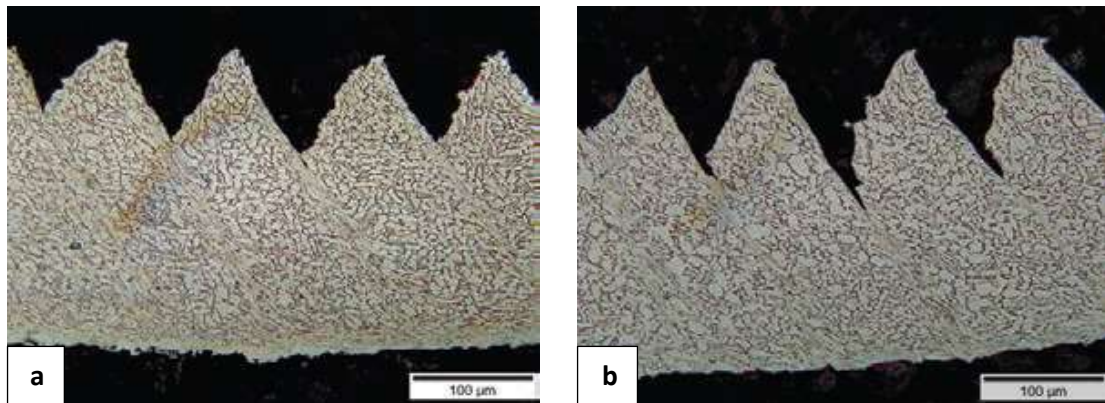


Figure 2.9 Chip morphology resulted from: (a) oil-based coolant and (b) cryogenic Machining (Aramcharoen 2016)

Ahmed and Kumar (2017) investigated the effect of cryogenic cooling on the cutting temperature, surface roughness, surface microhardness, hole quality, thrust forces and applied torque when reaming Ti-6Al-4V with different cutting speeds and feed rates. Results indicated that cryogenic cooling resulted in 15-31% reduction in cutting temperature compared with flood cooling. In addition, reduction in thrust forces and applied torque of 23-57% and 14-64% respectively has been achieved compared to conventional flood cooling. Moreover, an 8-19% increase in microhardness of the surface and subsurface was observed when cryogenic cooling was applied. Furthermore, an improvement in reaming circularity and cylindricity from 9-91% and 33-90% respectively was achieved with cryogenic cooling compared with flood cooling. However, higher surface roughness was observed for all cryogenic cutting conditions. This was attributed to the higher surface damage occurred when cryogenic cooling was applied to reaming Ti-6Al-4V (Ahmed and Kumar 2017).

Sartori et al. (2017b) investigated the machinability when semi-finishing Ti-6Al-4V under different temperatures of nitrogen gas (from 0°C to -150°C). The machining performance in terms of tool wear and surface integrity were compared with those for cryogenic LN2 and flood cooling. The study suggested that the temperature of the cooled gas significantly influenced the machinability, and there is a critical cooling capacity below which no improvement in machinability can be achieved compared to LN2 and wet machining. The lowest value of flank and crater and deformed layer was found at -100°C. At this cooling condition, the deformed layer was reduced 40% and 26%, respectively compared with cryogenic LN2 and conventional wet cooling. Surface roughness and topography analysis for the cooled gas showed comparable results with conventional and cryogenic LN2 cooling.

While, cryogenic LN2 showed the highest cooling capacity (ten times that for N2 cooled gas at  $-100^{\circ}\text{C}$ ). It was concluded that the application of cooled gas at  $-100^{\circ}\text{C}$  was sufficient for optimum improvement in both tool wear resistant and machined surface integrity (Sartori et al. 2017b).

Bordin et al. (2017) investigated the effect of cooling conditions (dry, wet, and cryogenic machining) and cutting conditions at two levels of cutting speed and depth of cut on the machinability of turning AM Ti-6Al-4V evaluated in terms of tool wear, surface integrity, and chip morphology. Findings showed that cryogenic cooling enabled improved tool life, surface finish, less surface defects and better chip breakability compared with dry and wet machining. The researchers concluded that cryogenic machining can be regarded as a sustainable cooling process in machining biomedical products made of AM titanium alloy (Bordin et al. 2017).

Krishnamurthy et al. (2017) suggested the use of cryogenic cooling and the adoption of ethanol blended flood cooling to improve the machinability of Ti-6Al-4V. This was achieved by mitigating the high localized cutting zone temperature in order to reduce the adhesion-diffusion tool wear and reduce the fluctuation of cutting forces caused by serrated chip formation that leads to vibration (chatter) and severe flank wear. Compared to dry machining, cryogenic cooling resulted in 25% reduction in cutting forces. They attributed this reduction in cutting forces to the fact that the high localized deformation during chip formation experienced in dry machining had been decreased via the reduced fracture energy which led to brittle and short segments during cryogenic machining (figure 2.10). On the other hand, the use of ethanol blended flood cooling further achieved 65.5% reduction in cutting forces and eliminated adhesion the tool wear due to absorption of carbon from the cutting tool to the OH groups from ethanol at the tool flank and rake surfaces(Krishnamurthy et al. 2017).

Ayed et al. (2017) investigated the impact of delivering pressure and flow rate of LN2 cooling on the machining performance in terms of tool life and surface integrity when turning Ti-6Al-4V alloy at fixed machining conditions. It was shown that cryogenic cooling demonstrated a significant improvement in tool life compared to a dry and conventional flood cooling (more than 4 times of that for flood cooling). The best results were obtained at the highest tested LN2 pressure and flow rate. SEM and EDS analysis showed that adhesion was the main wear mechanism. Moreover, great enhancement in surface integrity in terms of residual stresses was achieved at higher LN2 pressure and flow rate due to the reduced



thermal loads, while no considerable improvement in surface roughness was achieved with cryogenic cooling (Ayed et al. 2017).

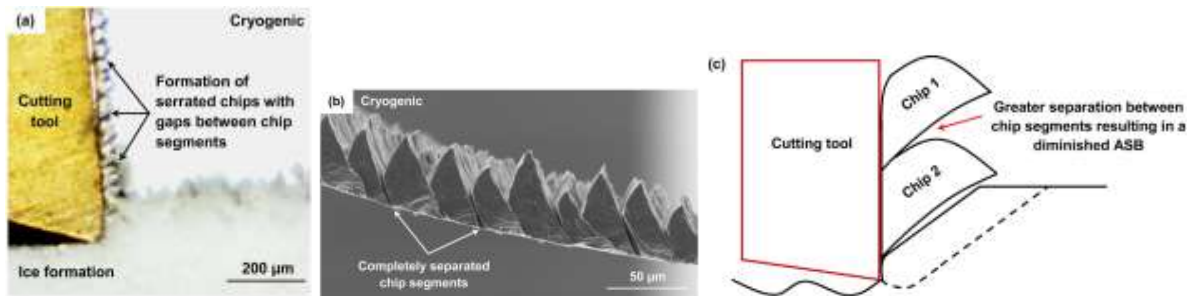


Figure 2.10 Orthogonal cutting of Ti-6Al-4V (a) under cryogenic pre-cooled workpiece after an elapsed time of 7 s, (b) SEM of chips obtained from cryogenic machining showing the separation between chip segments, (c) schematic illustrating a typical serrated chip formation during cryogenic machining (Krishnamurthy et al. 2017).

Lequien et al. (2018) conducted analytical modelling to determine the convective heat transfer coefficient in multi-phase cryogenic LN<sub>2</sub> cooling and to the influence of the jet parameters (nozzle diameter, jet flow and nozzle projection) on the cooling performance. The thermal boundary conditions were measured via a thermocouple to analyse the thermal distribution. It was found that the convective heat coefficient is highly dependent to the measured temperature and can reach as high as 15630W/m<sup>2</sup>°C, and the most effective parameter in a cryogenic cooling was found to be the nozzle diameter. The LN<sub>2</sub> pressure and plate projection angle can influence the thermal distribution on the plate. They concluded that higher pressure and nozzle diameter can increase the cooling performance when machining Ti-6Al-4V (Lequien et al. 2018).

### 2.6.3.2 Cryogenic cooling in milling titanium alloys

It is well known that chatter caused by interrupted cutting is the main problem in milling operations, especially at high speed machining. Haung et al. (2014) proved that milling stability can be enhanced with cryogenic cooling as a consequence of the substantial reduction in cutting forces (Huang et al. 2014). On the other hand, the application of cryogenic cooling in milling can inhibit chip burning at high cutting speeds. Ke et al. (2009) showed that the supply of LN<sub>2</sub> at high speed when milling Ti-6Al-4V has many advantageous functions, such as (KE et al. 2009) :

- i. Preventing chip burning.
- ii. Speeding up chip removing away from the cutting zone.
- iii. Reducing the cutting force.

- iv. Minimizing the BUE formation.
- v. Inhibiting the adhesion at the tool-chip interface.
- vi. Significantly reducing surface roughness and improving surface integrity.

Shokrani et al. (2012) conducted a pioneering investigation into the effect of cryogenic cooling on tool wear, surface integrity, and power consumption when CNC milling Ti-6Al-4V. After a series of machining trials with uncoated carbide end mills and a comparison with dry machining, it was shown that liquid nitrogen LN2 cooling has a significant potential to improve titanium alloy machinability as well as enhancing surface finish and improving tool life. Surface roughness has been improved up to 2.5 times that for dry machining, while no considerable increase in power consumption was observed when cryogenic cooling is used (Shokrani et al. 2012). The researchers reported that the application of LN2 reduced the surface roughness by 59% as compared to flood cooling when milling Ti-6Al-4V with TiAlN coated carbide. They concluded that the improvement in tool life and surface finish is highly related to the ability of the cryogen to penetrate the cutting zone (Shokrani 2014).

Lee et al. (2015) carried out a cryogenic-assisted milling of preheated Ti-6Al-4V workpiece to avoid the material hardening by the application of cryogenic LN2 which is also reported by other researcher (Zhao and Hong 1992; Hong and Zhao 1999; Park et al. 2015). The machining performance in terms of tool wear, cutting forces, tool wear morphology and chip morphology were investigated for three low cutting speeds (25, 37.5, and 50m/min.), three machining environments (dry, cryogenic, and cryogenic preheated workpiece), and two types of coated carbide tools (hard (CrTiAlN) and soft Si coated tools). For Si coated tools, an increase of tool life of 90% and 50% was recorded under cryogenic preheated and cryogenic cooling conditions, respectively, compared with dry machining, whereas 55% and 50% increase in tool life was achieved for the same comparison with CrTiAlN coated tools. The application of cryogenic preheated resulted in reduced forces by 65%. Chipping and abrasion of the primary flank was the main tool wear mechanism for soft Si coated tools while, chipping controlled the mode of wear for hard CrTiAlN coated tools. They concluded that cryogenic cooling and workpiece preheat can improve tool life without increasing the cutting forces and be considered an environmentally friendly alternative for milling Ti-6Al-4V alloy (Lee et al. 2015).

From the above reviewed studies, it can be concluded that cryogenic machining enabled higher productivity without compromising machining quality and performance. Major potential advantages of cryogenic machining can be summarised as:

- i. Sustainable machining (environmentally conscious, safe and clean machining).
- ii. Reduced production cost by reducing chemical and abrasion tool wear which leads to increased tool life and reduced cost of tool changeover, with no decrease in material removal rate (MMR)
- iii. Improved surface quality/integrity without chemical and mechanical degradation of the machined surface.

## **2.7 Hybrid sustainable cooling/lubricating techniques in machining titanium alloys**

It is well recognized that effective cooling and sufficient lubrication along with environmental friendliness can enable improved machining performance, while, addressing machining sustainability in terms of enhancing tool life, surface quality/integrity, power consumption, cutting temperature, chip breakability and increasing productivity (Pusavec et al. 2014; Schoop et al. 2017; Benjamin et al. 2018). The implementation of hybrid cooling/lubrication techniques has been used to lower the cutting temperature and reduce the induced friction at the tool-chip and tool-workpiece interfaces (Benjamin et al. 2018). It was suggested that cryogenic/lubrication conditions enabled further improvements in machining performance and sustainability in terms of tool life, surface integrity, chip breakability, and power consumption (Pusavec et al. 2015). The application of oil or emulsion with compressed air or cryogen can be beneficial in improving the cooling/lubrication effectiveness in machining hard-to-cut materials such as titanium alloys (Sun et al. 2015).

Based on their experimental investigation to the effect of cooling/lubrication conditions on the machining performance, Su et al. (2006) showed that the simultaneous application of cold compressed nitrogen gas and oil mist (CCNGOM) when high speed milling of Ti-6Al-4V with coated cemented carbide tools can significantly improve tool life as well as providing environmental friendliness. Results revealed that tool life can be improved up to 2.69 times that with dry machining and 1.93 times longer than under nitrogen-oil-mist. SEM analysis suggested that diffusion at the tool flank face dominates wear mechanism under dry machining, nitrogen-oil-mist, compressed cold nitrogen gas and CCNGOM, while under flood cooling, excessive chipping caused by severe thermal fatigue at the cutting edge was

the dominant mode of wear. This led to the conclusion of non-suitability of flood cooling for high speed milling (Su et al. 2006). Kopac (2009) suggested that the simultaneous application of cryogenic cooling and MQL (cryo-lubrication) demonstrates the best overall performance in terms of tool wear, cutting forces, surfaces finish and chip breakability compared with other cooling/lubrication conditions; dry, near dry (MQL) and cryogenic cooling. It was concluded that in machining high temperature alloys such as titanium and nickel alloys, the high temperature and lubrication issues are of major concern. To overcome this problem, efficient cooling and sufficient lubrication can be provided through introducing innovative integration of more than one cooling/ lubrication condition, simultaneously (Kopac 2009).

Yuan et al. (2011) examined the influence of cooling air temperature in MQL on the cutting performance in terms of tool wear, cutting forces and surface finish when milling Ti-6Al-4V with uncoated carbide tool. Experimental investigations were done with 20ml/h synthetic based oil sprayed with four different temperatures; 0°C, -15°C, -30°C, and -45°C. Performance was compared with that for MQL at room temperature, dry machining and emulsion flood cooling. Results showed that a significant reduction in tool wear, cutting force and surface roughness has been achieved when milling titanium alloy under MQL with cooled air. The most favourable effect compared to other cooling temperatures was MQL with -15°C air temperature. The reduction in tool wear and cutting force when applying MQL cooling air was attributed to the enhanced cooling and lubricating effect of this approach. Further reduction in cooling air temperature (MQL with -30°C and -45°C) can increase the cutting force because of the increased mechanical properties of the workpiece which increases the plastic deformation at the cutting edge, thus reducing the tool life and surface finish. Poor surface quality was observed when milling Ti-6Al-4V under dry, wet, MQL and MQL at 0°C, due to the severe flaking and notching wear on the tool flank face (Yuan et al. 2011).

Machai et al. (2013) investigated the cooling/lubrication effectiveness of combining cryogenic CO<sub>2</sub> snow cooling and MQL in terms of tool wear, cutting forces, chip morphology and power consumption when machining different heat treated grades of the  $\beta$ -titanium alloy Ti-10-V-2Fe-3Al, with TiN coated tungsten carbide. Results were compared with conventional emulsion cooling, supplying CO<sub>2</sub>-snow jet at the tool rake face, the tool flank face, and the two faces together. Only marginal reduction in tool flank wear was observed in comparison to that when CO<sub>2</sub>-snow jet was applied to the tool flank and rake

faces. This was attributed to the upsurge in work material strength as a consequence of CO<sub>2</sub>-snow pre-cooling (Machai et al. 2013). Bierman et al. (2015) carried out a tool life and chip formation study when cryogenic machining of titanium alloys with CO<sub>2</sub>. Their results showed that cryogenic cooling with LCO<sub>2</sub> demonstrated an improvement in tool life in comparison with conventional emulsion cooling. They suggested that the combined application of LCO<sub>2</sub> and MQL when machining high strength Ti-6Al-2Sn-4Zn-6Mo alloy led to smoother chip breakability and to reduced width of shear band between chip segments as illustrated in figure 2.11. They attributed this to the reduced welding between chip segments which could reduce the force for the separation of segments (Biermann et al. 2015)

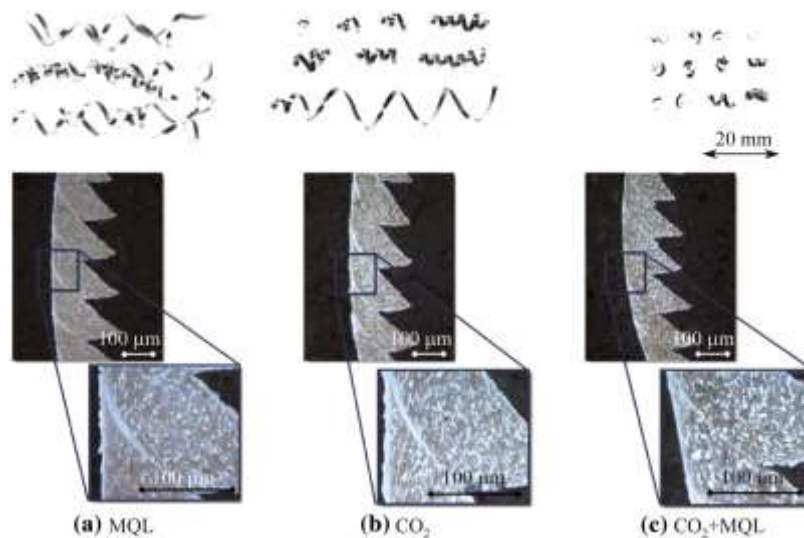


Figure 2.11 Microstructure of chip showing the influence different cooling/lubrication conditions on the chip breaking and shear and width, and the microstructure of the resulting chip when machining Ti-6Al-2Sn-4Zr-6Mo; cutting speed = 100 m/min; depth of cut = 1 mm; feed rate = 0.2 mm/rev. (Biermann et al. 2015).

Park et al. (2015) investigated the machining performance when milling Ti-6Al-4V in terms of tool wear and cutting forces under various cooling and lubrication methods, namely MQL, cryogenic, and hybrid combination of internally tool channelled cryogenic cooling and MQL. Results indicated that hybrid internal cryogenic/MQL provided the best tool life among other machining environment by up to 32% compared to flood cooled methods. Significant reduction in the cutting forces were achieved when the hybrid cooling/lubricating technique were applied (Park et al. 2015).

Sartori et al. (2017a) conducted an experimental study on the effect of various cooling/lubricating conditions on the machinability when semi-finish turning Ti-6Al-4V in terms of tool flank wear, crater wear, surface topography, and deformed layer, while fixing the machining parameters. They introduced three hybrid cooling techniques; namely hybrid

LN2 (rake)+MQL (flank), LN2 (flank)+MQL (rake), and CO<sub>2</sub> (rake)+MQL (flank). They suggested that the application of low temperature hybrid strategies can necessarily eliminate the tool crater wear and preserve the tool geometry with superiority to LN2 in improving the machined surface topography. They also proposed that MQL can reduce the flank wear through the reduction of the cutting forces and the enhancement of chip-flow. However, they observed that the performance of hybrid LN2/MQL was significantly affected by nozzle position and the best strategy in this combination was to direct MQL to the tool flank and LN2 to the rake face. They concluded that hybrid CO<sub>2</sub>/MQL provided the best performance owing to higher pressure and lower temperature of CO<sub>2</sub> compared to LN2 (Sartori et al. 2017a).

Schoop et al. (2017) studied the feasibility of high speed precision turning of Ti-6Al-4V with PCD tools under cryogenic and hybrid MQL/cryogenic cooling/lubricating techniques. Their investigation scored 4-5 times tool wear in flood cooling more than cryogenic and hybrid conditions. Cryogenic machining showed the lowest tool wear among all cooling conditions ( $V_B < 10\mu\text{m}$  after a machining time of 65 min). This sustained machining performance was attributed to the fact that cryogenic cooling has sufficiently changed the tribological system resulted in reduced thermally related tool wear. In addition, significant improvement in surface finish with cryogenic machining was reported (40 nm) at speed as high as 240m/min and low feed rate and depth of cut (0.01mm/rev and 0.1mm, respectively). Moreover, hybrid cooling/lubricating (cryogenic+MQL) demonstrated significant improvement in surface integrity in terms of surface and subsurface properties They suggested that high speed cryogenic-finish machining of Ti-6Al-4V could replace traditional grinding process even for slender components (Schoop et al. 2017).

Park et al. (2017) examined the machinability of Ti-6Al-4V alloy in hybrid cryogenic/MQL cooling/lubrication during end and face milling with different cutting speed using uncoated carbide inserts and compared it with that for dry, wet, MQL and cryogenic cooling. They also investigated the application of exfoliated graphite nano-platelets added to rapeseed vegetable oil in minimum quantity lubrication (MQLN). The results showed that the combined application of MQL and cryogenic cooling marginally outperformed the individual cooling and lubrication conditions in terms of tool wear and cutting forces. For cryogenic machining, the direct exposure to LN2 hardened the workpiece and caused thermal gradient onto the cutting tool resulting in excessive tool wear and increased cutting forces. Furthermore, the application of MQLN showed the least tool wear in all tested cutting speeds

due to the enhanced lubrication caused by the adhered nano-particles of graphite on the cutting tool resulting in reduced friction between the cutting tool and the work material (Park et al. 2017). Tapoglou et al. (2017) investigated the tool life when milling Ti-6Al-4V under various cooling/lubricating conditions, namely; dry, flood cooling, tool-channelled emulsion cooling, MQL, LCO<sub>2</sub>, hybrid LCO<sub>2</sub>+air, and hybridLCO<sub>2</sub>+MQL. Results revealed that the longest tool life was achieved with flood cooling at 100m/min (30 mins), while the best cryogenic CO<sub>2</sub> performance was found in the hybrid combination of cryogenic LCO<sub>2</sub> with MQL (18.5 mins)(Tapoglou et al. 2017).

Bagherzadeh and Budak (2018) investigated the machining performance of various cooling/lubricated strategies in terms of tool wear, component cutting forces, surface roughness and chip morphology when machining Ti-6Al-4V and Inconel 718 at moderate and high cutting speeds (100and 150m/min). The cooling conditions investigated were LCO<sub>2</sub> (rake), hybrid combination of minimum quantity carbon dioxide and oil CMQL (rake), hybrid LCO<sub>2</sub> (rake) + MQL (flank), and modified LCO<sub>2</sub> delivery on the rake and flank faces as schematically shown in figure 2.12. Findings indicated that hybrid CMQL enabled reduced tool wear and improved service quality compared to other strategies. Tool life was improved with CMQL up to 60% and 30% respectively, when machining Ti-6Al-4V and Inconel 718 compared to hybrid (CO<sub>2</sub> rake + MQL flank). They concluded that CMQL can be introduced as an alternative sustainable cooling/lubricating technique in machining hard-to-cut materials (Bagherzadeh and Budak 2018).

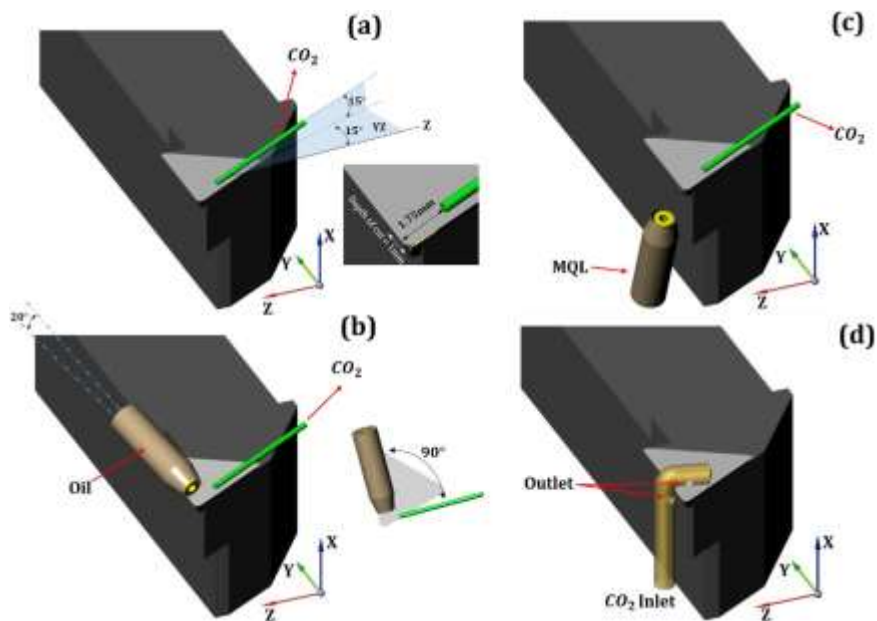


Figure 2.12 Schematics cryogenic cooling strategies in turning. a) CO<sub>2</sub> rake, b) CMQL rake, c) CO<sub>2</sub> rake and MQL flank, d) Modified CO<sub>2</sub> delivery(Bagherzadeh and Budak 2018).

Benjamin et al. (2018) investigated machining performance when applying sub-zero air in MQL or minimum quantity cooled lubrication (MQCL) in terms of cutting temperature, surface roughness, friction coefficients and chip morphology during milling Ti-6Al-4V alloy with different speeds and feed conditions. It was shown that MQCL demonstrated considerable improvement in machining performance over standard MQL. The enhanced lubricity at lower cutting temperature resulted in lower cutting forces and coefficient of friction and easier chip separation from the rake face due to the colder air. In addition, MQCL resulted in lower surface roughness, and thinner chips with less chip segmentation due to adiabatic shear (Mark Benjamin et al. 2018). A study by Sartori et al. (2018) introduced two hybrid minimal cooling/lubrication techniques namely; minimum quantity lubrication MQL with vegetable oil and minimum quantity cooling (MQC) with aqueous solution. These techniques were applied with the addition of solid lubricants; PTFE particles added to MQL, and graphite powder added to MQC at different percentages when finish turning Ti-6Al-4V alloy. Results indicated that the application of solid solid-assisted minimum quantity cooling demonstrated the best performance in terms of tool wear (crater and nose wear), and surface integrity (surface quality and deformed layer), with slight increase as a function of graphite particles content. The surface integrity improvement for solid-assisted MQC was more in the deformed layer; 44%, 36%, and 29% compared to dry, conventional flood cooling, and standard MQL machining. On the other hand, solid-assisted MQL guaranteed the lowest nose wear and abrasion, due to their higher dynamic viscosity. It was concluded that SL-assisted MQC may be considered as an excellent alternative to conventional cooling strategies when machining Ti-6Al-4V alloy (Sartori et al. 2018).

## **2.8 Critique**

Conventional oil and/or water-based coolants have been considered effective in removing the heat generated at the cutting zone at lower cutting conditions. They also act as a lubricant and thus lowering the friction and reducing the cutting forces and consequently improving the tool life. Many additives are added to neat oils and water soluble cutting fluids to improve their lubricating characteristics and reduce the bacterial growth and disposal contamination which could pose more health and environmental problems.

However, the application of the flood cooling technique is not the way forward to successful machining of titanium, since this technique fails to achieve coolant penetration to the cutting zone due to the formation of high temperature blanket that form a seizure zone preventing



coolant to reach the cutting zone. Although, high pressure jet cooling systems are efficient in penetrating the cutting zone, they suffer from coolant misting and excessive leaking as well as the health and environmental issues associated with the use of cutting fluids.

While MQL systems have shown outstanding lubrication and satisfactory cooling in machining titanium alloys, cryogenic cooling of cutting tools has demonstrated significant potential for reducing the cutting temperature, hence improving the machinability in terms of tool life and surface integrity. As the high temperature and lubrication are the main issues in machining titanium alloys, the innovative administering of hybrid friendly cooling/lubrication techniques resulted in a step increase in productivity, hence lower machining cost without compromising the surface quality/integrity, dimensional accuracy of the machined part.

## **Chapter 3 Scope of research and framework**

### **3.1 Introduction**

According to the literature reviewed in chapter 2, titanium and its alloys represent a serious challenge to the cutting tool materials due to the excessive stresses and temperatures generated during machining. The use of abundant quantity of oil-based or water-based cutting fluids are recognised as effective in removing the heat generated from the cutting zone and in providing satisfactory lubrication thus, improving the machinability. However, flood cooling is inefficient in lowering the high cutting zone temperatures generated during machining titanium alloys. HPC has shown effective performance in machining titanium alloys, but environmental issues, system installation, cutting fluid misting and leaking can limit its adoption.

As mentioned in sections 2.6.2 and 2.6.3, spraying a small amount of synthetic or vegetable oil into the cutting zone remarkably reduces the mechanical wear via reducing the heat generated due to friction and the cutting forces. On the other hand, the use of liquefied gases such as LCO<sub>2</sub> or LN<sub>2</sub> as a cooling medium in machining titanium alloys are believed to enhance their machinability via removing the heat generated due to material cutting and plastic deformation of chips, friction between the chip and tool rake face and friction between the workpiece and tool face thus, reducing the thermally related wear. Therefore, it is believed that the application of hybrid combination of both cryogenic cooling and MQL can improve the machining performance when CNC milling of Ti-6AL-4V alloy in terms the tool life, surface finish, and chip morphology that affects chip flow, hence enhance overall productivity.

### **3.2 Research gaps**

Based on the literature reviewed in chapter 2, a number of research gaps have been identified:

- i. The machinability of titanium alloys has neither kept pace with progress in machining other structural materials nor met the developments of cutting tool materials.
- ii. While significant research gaps can be found in the application of the cryogenic cooling technique in milling operations, there is also limited research on the effect of cryogenic cooling in milling titanium alloys as the major concentration is on turning operations.

- iii. While there are initial studies on the effect of integrated cooling strategies in turning titanium alloys, the author found that there is limited research on the effect of the application of hybrid cooling/lubricating techniques in milling titanium alloys.
- iv. Unlike turning operations, the hybrid application of cryogenic cooling and MQL in end milling of Ti-6Al-4V, has not been thoroughly investigated.

### **3.3 Research aims and objectives**

The aim of this research is to investigate the effect of using a novel dual-nozzle hybrid cryogenic/MQL cooling/lubricating technique when CNC milling on machinability of Ti-6Al-4V titanium alloy.

To achieve this aim, the main objectives of this study are:

- i. To provide a comprehensive and in-depth understanding of titanium alloys and their machinability.
- ii. To critically study the effect of various cooling and lubricating techniques used to enhance the machinability of titanium alloys.
- iii. To design and manufacture a viable and flexible and multi-nozzle cryogenic cooling system that can be easily installed and retrofitted to majority of conventional milling machines with full control of nozzle/s orientation to conduct cryogenic and hybrid cryogenic/MQL machining experiments
- iv. To examine the machining performance of the designed cryogenic nozzle system when CNC milling of titanium alloy.
- v. To examine the machining performance of the application dual-nozzle MQL system with environmentally friendly vegetable rapeseed oil when CNC milling of titanium alloy.
- vi. To evaluate and compare the machining performance of hybrid cryogenic/MQL cooling/lubricating technique with the individual application of cryogenic cooling, MQL, and conventional machining environment, namely flood cooling method in terms of tool life, surface finish (roughness), and chip morphology.

### **3.4 Research scope**

Based on the aim and objectives outlined above, the areas of investigation parameters will consist of:

#### **3.4.1 Configuration of hybrid cooling/lubricating technique and strategy**

Based on the findings from the literature review, a cryogenic dual- nozzle cooling system will be designed, manufactured, and integrated with dual-nozzle MQL system to conduct a set of experiments in order to investigate the machining performance of each cooling/lubricating technique, namely; MQL, cryogenic cooling, and hybrid cryogenic/MQL with different cutting speeds when CNC milling of Ti-6Al-4V titanium alloy. The machining performance for each cooling/lubricating strategy will be assessed in terms of tool wear, surface roughness and chip morphology and compared to that for conventional soluble-oil emulsion flood cooling.

### **3.5 Research limitations**

This research will be limited to the investigation of the hybrid application of cryogenic/MQL cooling/lubricating methods when CNC milling of Ti-6Al-4V titanium alloy with PVD coated solid tungsten carbide end mills. For cryogenic cooling, liquid nitrogen will be sprayed through two external nozzles, especially designed and manufactured for this purpose, to the cutting interfaces and/or cutting tool, since the literature has demonstrated a significant potential of cryogenic cooling in lowering the cutting temperature when machining titanium alloys. On the other hand, MQL will spray a small rate of vegetable oil droplets at high pressure through two external nozzles to the cutting zone.

### **3.6 Research methodology**

In order to achieve the aims and objectives, the proposed research methodology can be divided into three major stages, namely (i) design and manufacture of cryogenic cooling system that can be integrated with MQL to improve the machining performance when CNC milling of titanium alloy, (ii) experimental investigation of machinability of hybrid cryogenic/MQL technique in comparison with individual cooling and lubricating conditions (iii) analysing the results of machining performance in terms of tool wear, surface roughness and chip morphology. Figure 3.1 provides an overview of facilities, input, output and parameters as well as the required resources to execute the three planned methodology stages.

According to figure 3.1 the input parameters have been classified into three main groups; (i) theoretical background and preparation, (ii) machining requirements and (iii) experimental requirements.

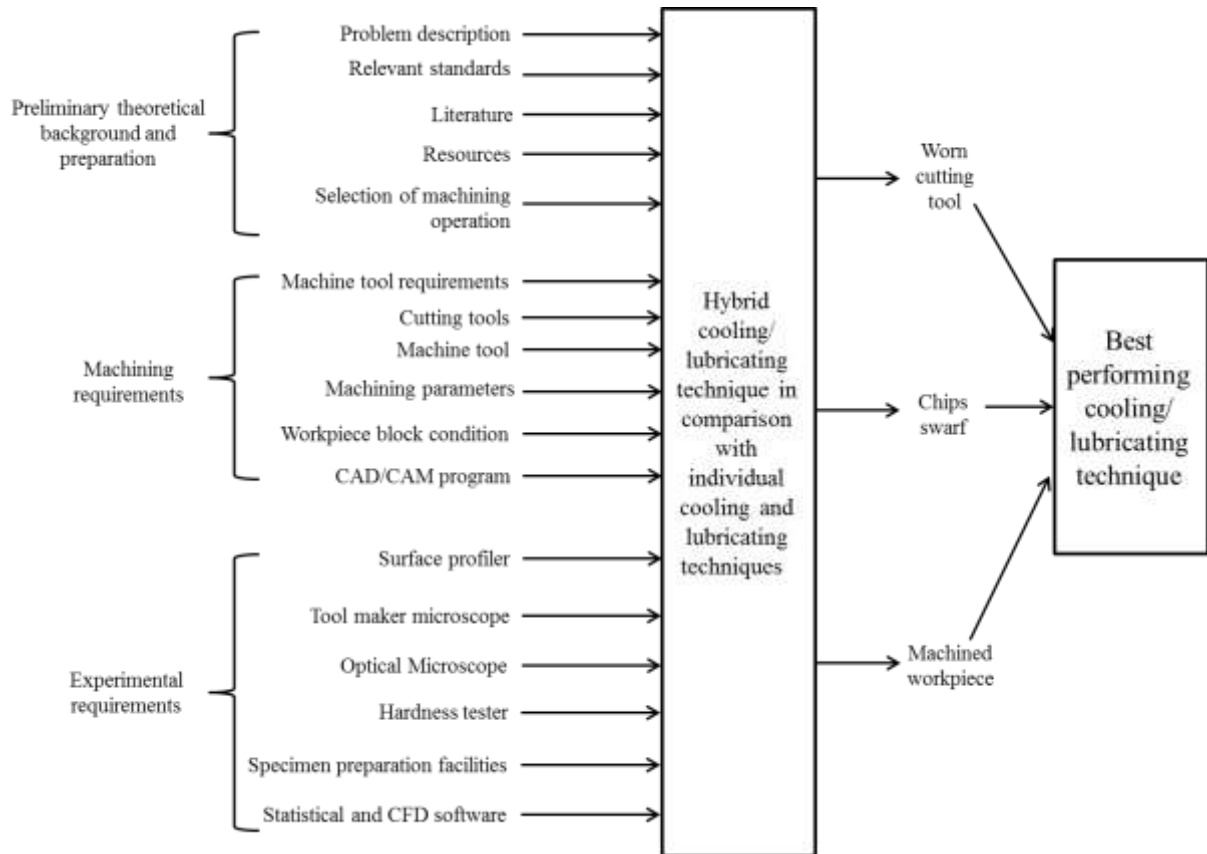


Figure 3.1 Input–output schematic illustration of the framework of this research

### 3.6.1 Design of hybrid cooling-lubricating system

Based on the reviewed cooling techniques used to improve the machinability of titanium alloys, cryogenic machining has been acknowledged as an effective cooling strategy in removing the excessive generated heat at the cutting zone, whilst MQL showed a significantly improved lubricating performance. The two machining strategies namely, cryogenic cooling and MQL will be applied simultaneously via an integrated (hybrid) cooling/lubricating strategy as explained below.

### 3.6.1.1 Cryogenic cooling system

The cryogenic cooling system used in this research is divided into two systems:

- **Cryogenic delivery system:** the cryogenic delivery system developed by Dhokia (2009) and Shokrani (2014) will be used to conduct cryogenic and hybrid machining experiments. It involves a LN2 storage (Dewar), pressure gauge, globe valve, solenoid valve, flow control valve, vacuum insulated hose to deliver LN2 from storage to nozzle system. Figure 3.2 shows the cryogenic delivery system used in this research.



Figure 3.2 Photographic illustration of cryogenic delivery system used in this research (Dhokia 2009; Shokrani 2014)

- **Cryogenic cooling nozzle system:** a dual-nozzle external cryogenic cooling nozzle system will be specially designed and manufactured to spray a small amount of LN2 to the cutting zone and/or to the flank of the rotating cutting tool. This will effectively lower the cutting tool temperature well below the softening temperature of the tool material and to provide sufficient cooling to titanium alloy workpiece to reduce its chemical reactivity with tool material (Hong and Zhao 1999).

### **3.6.1.2 Minimum quantity lubrication MQL system**

Based on the literature findings in section 2.6.2 the proposed delivery system of MQL will be the same as that adopted by Kamata and Obikawa which is schematically shown in figure 2.6 (Kamata and Obikawa 2007). A dual-nozzle MQL system will be used to feed a small amount of oil to the cutting zone at high air stream pressure and at room temperature.

### **3.6.2 Hybrid cryogenic/MQL comparison with individual cooling and lubricating techniques**

In order to understand the effect of hybrid cooling/lubricating technique on the machinability of Ti-6Al-4V it is essential to compare the machining performance of this strategy in terms of tool wear/life, surface roughness (finish) and chip morphology with individual cooling and lubricating techniques, namely conventional emulsion flood cooling, MQL and cryogenic cooling. A design of experiment (DoE) will be employed for better definition of affecting parameters and sequence of machining trials. Moreover, statistical and microscopic analyses will be used to demonstrate the effect of integrated cooling techniques in comparison to conventional dry and wet machining. The data will be collected and documented for each individual experiment for comparative analysis, with selection of the best machining parameters for CNC milling of Ti-6Al-4V under hybrid cryogenic/MQL cooling/lubricating condition.

### **2.6.3 Data collection and analyses**

After implementing the machining experiments for a different combination of cutting and cooling/lubricating conditions, the data for tool wear/life, surface roughness, and chip morphology will be collected and used for microscopic and statistical analyses to select the best performing cooling system. Figure 6.3 provides a useful illustration of the methodology in this research.

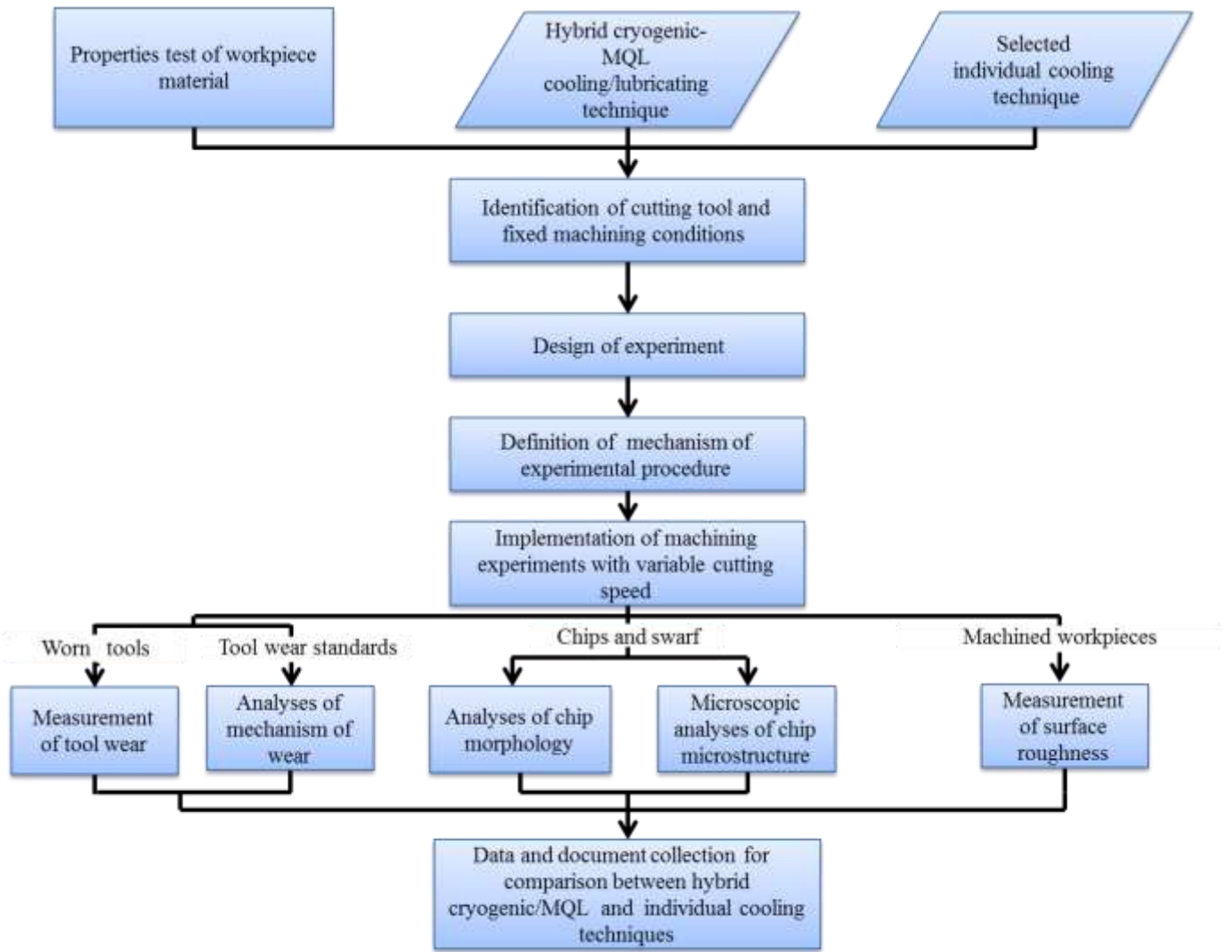


Figure 3.3 Flow chart of the planned methodology for this research



## **Chapter 4 Design and Manufacturing of Cryogenic cooling system**

### **4.1 Introduction**

The effect of cooling the cutting zone during machining of difficult-to-cut materials such as titanium alloys can play an important role in improving the machining performance of these alloys and extending the cutting tool life. This chapter describes the activities of creative design, modelling, simulation and manufacturing of a viable cryogenic cooling system that can effectively reduce the cutting temperature during CNC milling of Ti-6Al-4V. This cooling system has been designed to be retrofitted in majority of vertical milling centres and can be used simultaneously with another cooling/lubricating technique such as MQL to further enhance the machining performance of Ti-6Al-4V.

According Zhao and Hong (1992), the significant decrease of the cutting zone temperature due to application of cryogenic cooling in machining Ti-6Al-4V is essentially associated with a considerable increase of material strength and hardness of the workpiece material (Zhao and Hong 1992). Up to 18% increase in hardness was reported when the temperature of titanium alloy workpiece was reduced to -196 °C (Hong and Zhao 1999; Hong and Ding 2001). In order to overcome the effect of excessive cooling of work material during machining of titanium alloy, a specially designed external cryogenic cooling nozzle system is used to directly spray a limited amount of LN<sub>2</sub> to lower the temperature at the tool-chip and tool-workpiece interfaces. This could dramatically reduce the chemical reactivity of titanium with the cutting tool material and hence extend the cutting tool life.

Based on the specifications of the machining problems identified in section 2.1 and as a consequence of the three sources of heat generation associated in machining operations identified in section 2.3 and following the methodology proposed in section 3.6, and according to the requirements resources and constrains, an initial design of external nozzle has been specially made by the author for cryogenic cooling with LN<sub>2</sub>. The design was then simulated using computational fluid dynamic package CFD Ansys Fluent® (Ansys 2016). The findings of the simulation were used to upgrade the nozzle design. After simulating the updated design, a prototype was manufactured and tested visually by delivering LN<sub>2</sub> into the nozzle. Finally, a nozzle holder that provides 5-axis movement was designed to give full position control to the cryogenic nozzle system. The nozzle orientation control system was used to retrofit the cooling nozzle/s in the CNC milling centre. The detail design is then

conducted and finalised and installed in the machine tool to be ready for cryogenic machining.

## **4.2 Cryogenic cooling system**

The cryogenic cooling system adopted in this research essentially consists of two systems depending on their functional activities; namely (i) cryogenic storage and delivery system and (ii) cryogenic cooling nozzle. The storage and delivery system involves the selection of components that store and supply LN2 to the nozzle system. For the cryogenic storage and delivery, the system design and developed by Dhokia (2009) and Shokrani (2014) was adopted. In this research, the cryogenic cooling nozzle was specially designed and manufactured by the author to spray LN2 directly to the cutting zone during the CNC milling of Ti-6Al-4V.

### **4.2.1 Cryogenic storage and delivery system**

The storage and delivery system adopted in this research was first designed by Dhokia (2009) for machining elastomers and further developed by Shokrani (2014) for machining titanium alloy with cryogenic shower nozzle (Dhokia 2009; Shokrani 2014). The stainless steel storage unit (Dewar) has a nominal capacity of 180 litre with maximum pressure of 3 bars and maximum capacity of 180 litre. This self-pressurised vessel (Dewar) is vacuum insulated and covered with stainless steel enclosure as shown schematically and graphically in figure 4.1. The cryogenic delivery components are; electrical contact pressure gauge, globe valve, two-way shut off solenoid valve, and stainless steel flexible hose for LN2 delivery from the cryogenic Dewar to the cooling nozzle with maximum delivery flow rate of 20 kg/min. This hosing was vacuum insulated to eliminate the heat loss which might cause LN2 evaporation. The cryogenic delivery system (Dewar and hose) is provided with safety relief valves to prevent any increase in the pressure during LN2 delivery and storage.

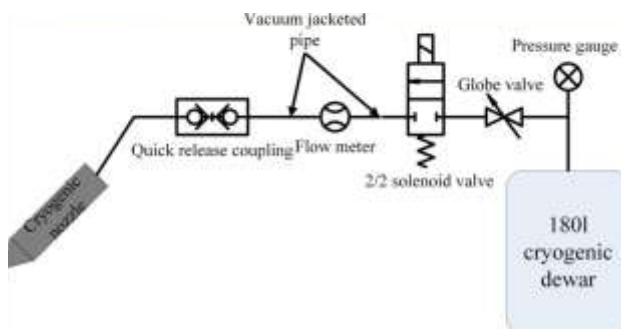


Figure 4.1 Schematic and graphic illustration of the cryogenic delivery system adopted by Shokrani (2014), used in the present research (Shokrani 2014).

#### 4.2.2 Cryogenic cooling nozzle system

As mentioned previously in the literature, the effective machining with cryogenic cooling should involve spraying LN<sub>2</sub> to the cutting zone, specifically the tool-chip and tool-workpiece interfaces. The cooling system should be efficient enough to dissipate the heat generated during the machining operation, namely, heat generated during chip formation (primary), friction between tool rake and chip (secondary), and heat due to friction between tool flank and the newly generated surface of the workpiece (tertiary) as shown schematically in figure 4.2. Furthermore, the cryogenic spraying design should provide effective chip breaking away from the cutting zone and should be designed to retrofit in any CNC machining centre.

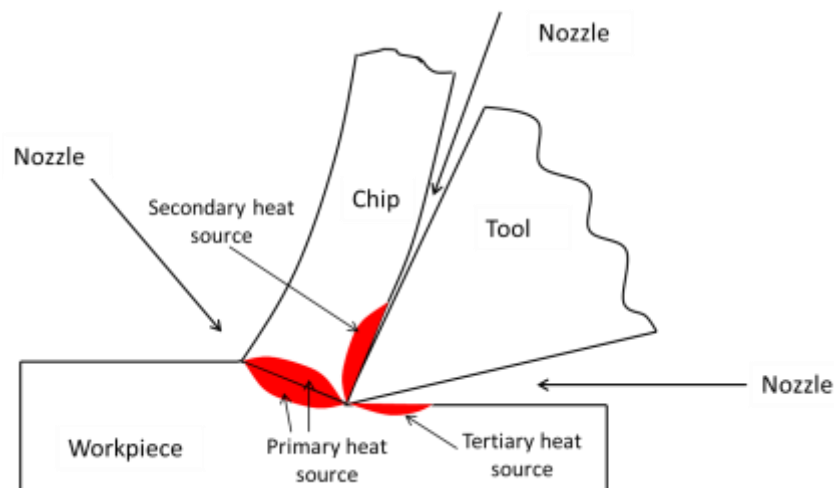


Figure 4.2 Sources of heat generation during machining process and directions of application cooling nozzle/s

### 4.3 Design and manufacturing of single- nozzle external cryogenic cooling system

In the following sub-section the activities regarding the design, modelling, manufacturing and testing of external nozzle for cryogenic cooling when CNC milling of Ti-6Al-4V alloy.

#### 4.3.1 Conceptual design of external nozzle for cryogenic cooling applications

The concept of common cooling nozzles used in flood cooling and MQL applications can be adapted to start designing an external nozzle for cryogenic cooling purposes as shown in figure 4.3.

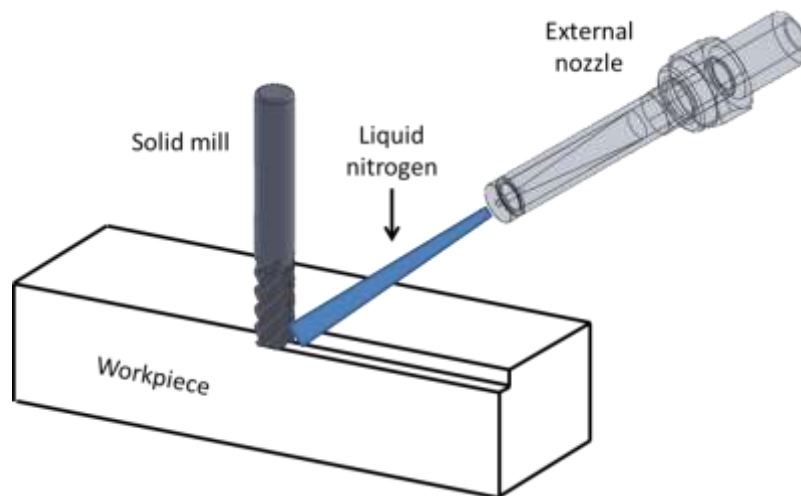


Figure 4.3 Schematic illustration of the main concept of external nozzle cryogenic cooling

#### 4.3.2 Design requirements and constrains for the cryogenic cooling nozzle

Based on the main concept of conventional flood and MQL cooling during machining operation, an external nozzle design can be initiated with some design modifications that ensure the following requirements:

- i. The cryogenic cooling nozzle should keep liquid nitrogen in its liquid phase in order to provide effective cooling.
- ii. The cryogenic cooling nozzle should spray the cryogen at sufficiently high speed to help chip blowing away from the cutting zone. Furthermore, the high speed spraying can improve the heat extraction from the cutting zone due to the increase of the overall heat transfer coefficient.
- iii. The cryogenic cooling nozzle holding system should be designed to have full orientation control to allow the selection of the best nozzle position target the cutting

tool in terms of the distance set and projection angles in order to maximise cooling performance.

- iv. The cryogenic cooling nozzle system should be designed to retrofit in any CNC machining centre.
- v. The cryogenic cooling nozzle system should be able to be used for different cutting tool diameters.
- vi. The cryogenic cooling nozzle should be designed to be used economically and effectively through spraying a limited but concentrated amount of coolant to target the desired area (cutting zone, cutting tool and/or workpiece).
- vii. The design of the cryogenic cooling nozzle system should be flexible, viable, and easy to manufacture with available resources and technical facilities.

#### **4.3.3 First trial of design of single nozzle for cryogenic cooling applications and CFD analysis**

Based on the machining problems identified in section 2.1, heat generation issues disclosed in section 2.3, methodology in section 3.6, and according to the design requirements resources and constrains, an initial external nozzle design has been specially made by the author for cryogenic cooling with LN<sub>2</sub>. This design sprays a small amount of LN<sub>2</sub> to the cutting zone to achieve effective cooling to the tool rake and flank faces and to avoid the excessive hardening of the workpiece (Hong and Zhao 1999; Hong and Ding 2001). The outlet nozzle diameter was selected to be 0.5 mm to ensure minimum amount of LN<sub>2</sub> which can be controlled to target the cutting area. The design was then simulated using computational fluid dynamic package CFD Ansys® Fluent (Ansys R 16.1 Academic 2016). The meshing method provided very fine element size especially at the nozzle outlet (0.025 mm). For solving the continuity equation (Navier-Stokes), the pressure-based solver is selected with the assumption that LN<sub>2</sub> will keep constant density during flow. Furthermore, axisymmetric fluid flow in the nozzle is assumed to simplify the model and reduce computational requirements of the model. In addition, the energy equation is not activated since the cryogenic cooling system is considered thermally insulated with negligible heat transfer to and from nozzle. Table 5.1 showed the input parameters for CFD modelling. The initialization and run of calculation is selected for 500 iterations and the convergence of residuals for continuity equation (Navier-Stokes equation), x-velocity, y-velocity and k-epsilons are less the 0.01 shown in figure 4.4, which indicates that the residuals are converge enough and the net mass

flow rate of LN2 must be closer to zero as suggested by continuity equation, and the values of velocity, pressure and coefficients of friction are accurate.

Table 4.1 Important input parameters for CFD modelling of cryogenic nozzle

|                           |                          |
|---------------------------|--------------------------|
| Input pressure            | 100000 Pascal            |
| Flow rate                 | 33 lit/hour              |
| Input velocity            | 0.1167 m/s               |
| Inlet hydraulic diameter  | 0.01 m                   |
| Outlet hydraulic diameter | 0.0005 m                 |
| Density of N2             | 806.08 kg/m <sup>3</sup> |
| Viscosity of N2           | 0.00016 kg/m.s           |
| Temperature               | 77 K                     |
| Turbulence intensity      | 5%                       |
| Residual error            | 1×10 <sup>-6</sup>       |

K-epsilon model constants are taken as they are from the CFD solver

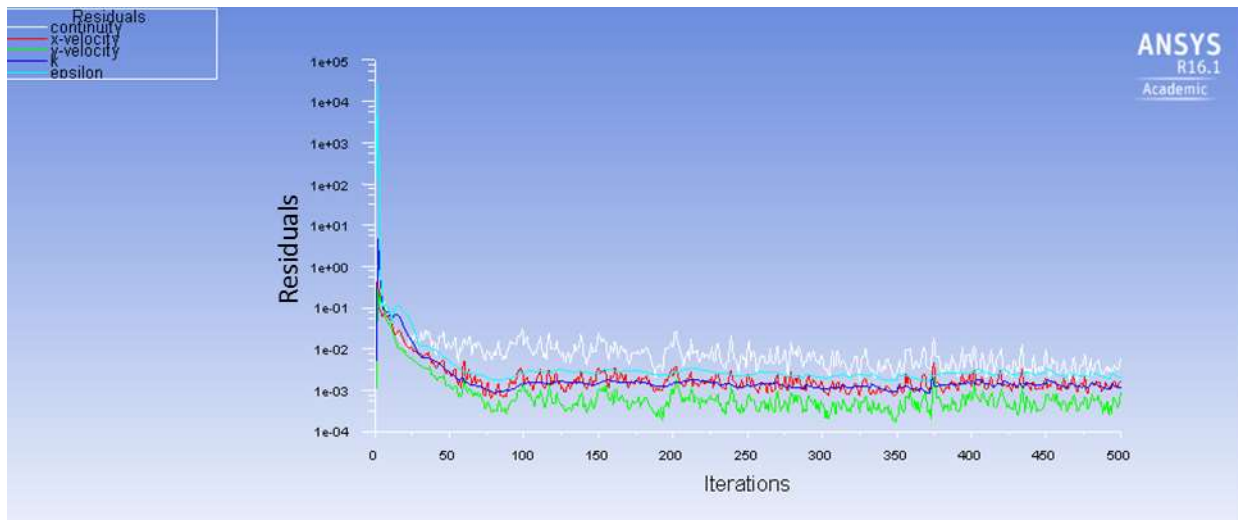


Figure 4.4 Residuals convergence for CFD simulation of first design of external cryogenic nozzle

Figure 4.4 indicated that the residuals of continuity equation, there were severe fluctuations during the convergence in solving the continuity equation, x and y velocities. This could be attributed to the severe turbulence in liquid nitrogen flow especially in the narrow part of the nozzle. Figure 4.5 shows that the velocity vectors of LN2 are moving in multi-direction inside the narrow part of the nozzle and the speed of LN2 stream is extremely high (116 m/s) at the nozzle outlet. The interior surface velocity reveals that the nozzle design is ineffective

in delivering LN2, since the stream near the centreline is only moving while the fluid away from the nozzle centreline is nearly stagnant.

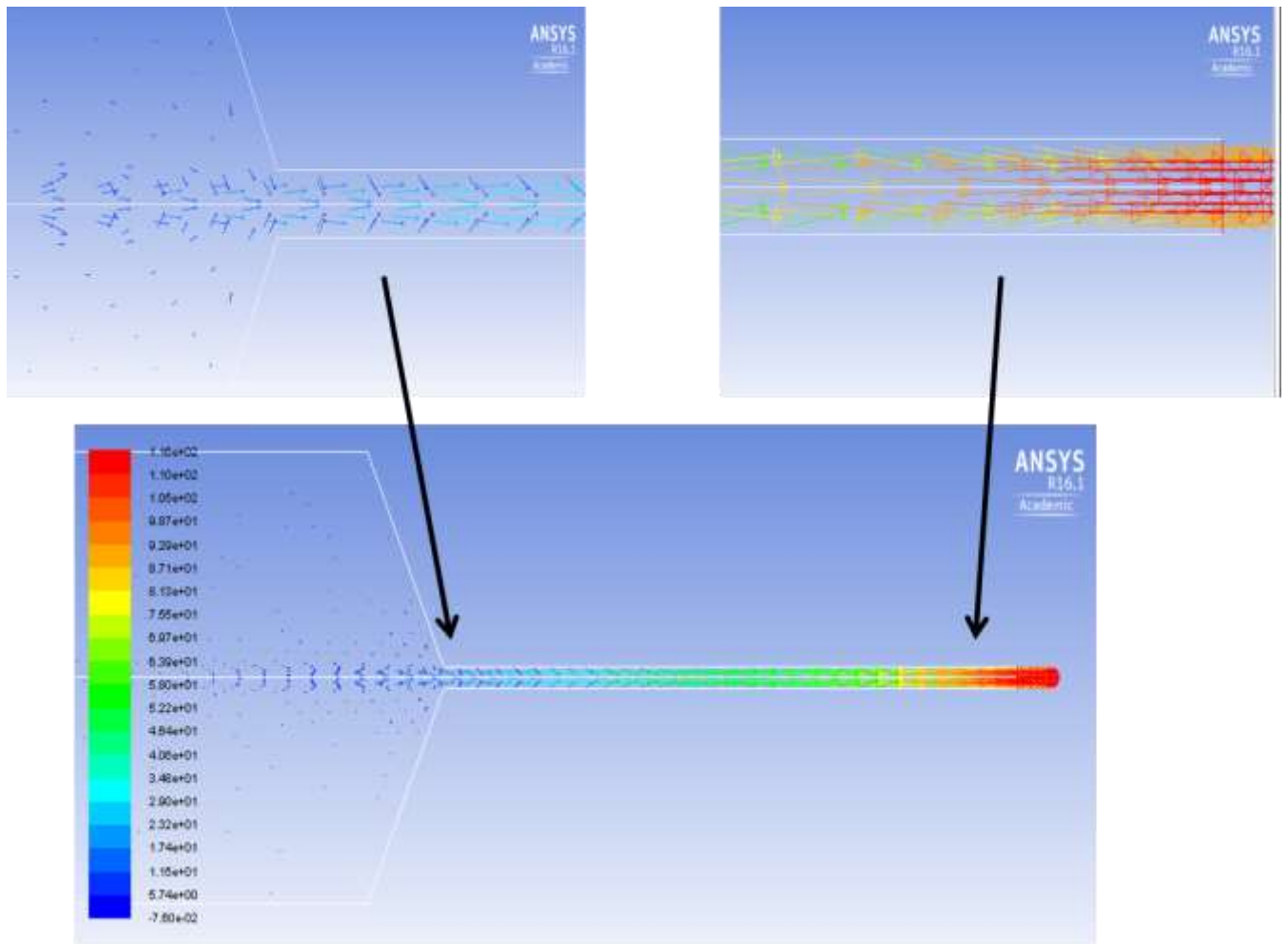


Figure 4.5 Simulation of velocity vectors of interior surface of the initial design of cryogenic nozzle

A prototype of the initial design of cryogenic nozzle has been manufactured and installed to the cryogenic delivery system to test its efficiency in spraying LN2 within the design requirements mentioned above. Testing results showed that according to the given design pressure of cryogenic delivery system (1 bar), the initial design of cryogenic cooling nozzle failed to spray nitrogen in liquid phase to achieve the cooling requirements. This could be attributed the steep contraction of the nozzle from 10 mm to 0.5 mm diameter with 60° countersink drilling angle. In addition, the extremely high wall friction at the narrow part of the nozzle (coefficient of friction as high as 7500) could generate the latent heat required for evaporation and suppress any liquid delivery out of this nozzle.

#### 4.3.4. Updating the external cryogenic nozzle design and CFD analyses

Based on the findings obtained from the first trail design of external cryogenic nozzle and its CFD analysis in section 4.3.3, a significant design update has been made to improve the cooling effectiveness and satisfy the given design conditions of the cryogenic delivery system. With the updated nozzle design, LN2 has been kept in steady and uniform flow till reaching the convergent part of the nozzle as shown in figure 4.6. The nozzle convergence angle was made less steep ( $4.7^\circ$  with flow centreline) with nozzle outlet of 2mm diameter. The cross sectional area of the LN2 manifold has been kept constant to avoid any sudden contraction and expansion in the flow area which could cause friction and turbulence and could change the nitrogen phase from liquid to gas.

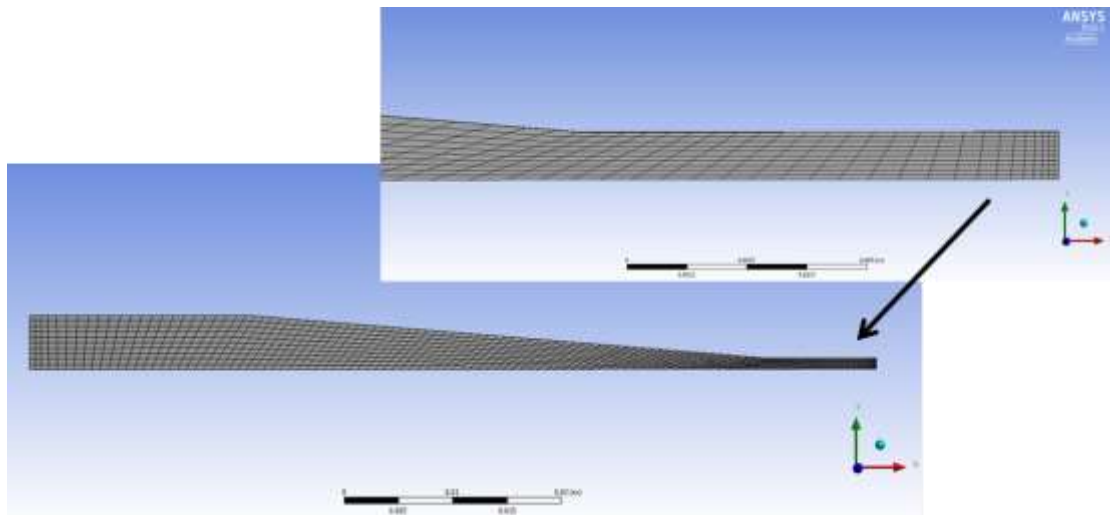


Figure 4.6 Updated design of external cryogenic cooling nozzle with CFD axisymmetric meshing

CFD analysis of the velocity vectors supported this hypothesis and showed less fluctuations in residual convergence of continuity equation, x and y components of velocity, K and epsilon constants. Also, velocity vectors show uniform flow and less turbulent with maximum velocity of LN2 of 4.73 m/s at the nozzle outlet, as shown in figure 4.7. Moreover, analysis of nozzle wall friction indicated significant reduction in frictional coefficient compared with initial design. The coefficient of friction of the wall was computed as less than 1% that for initial nozzle design).



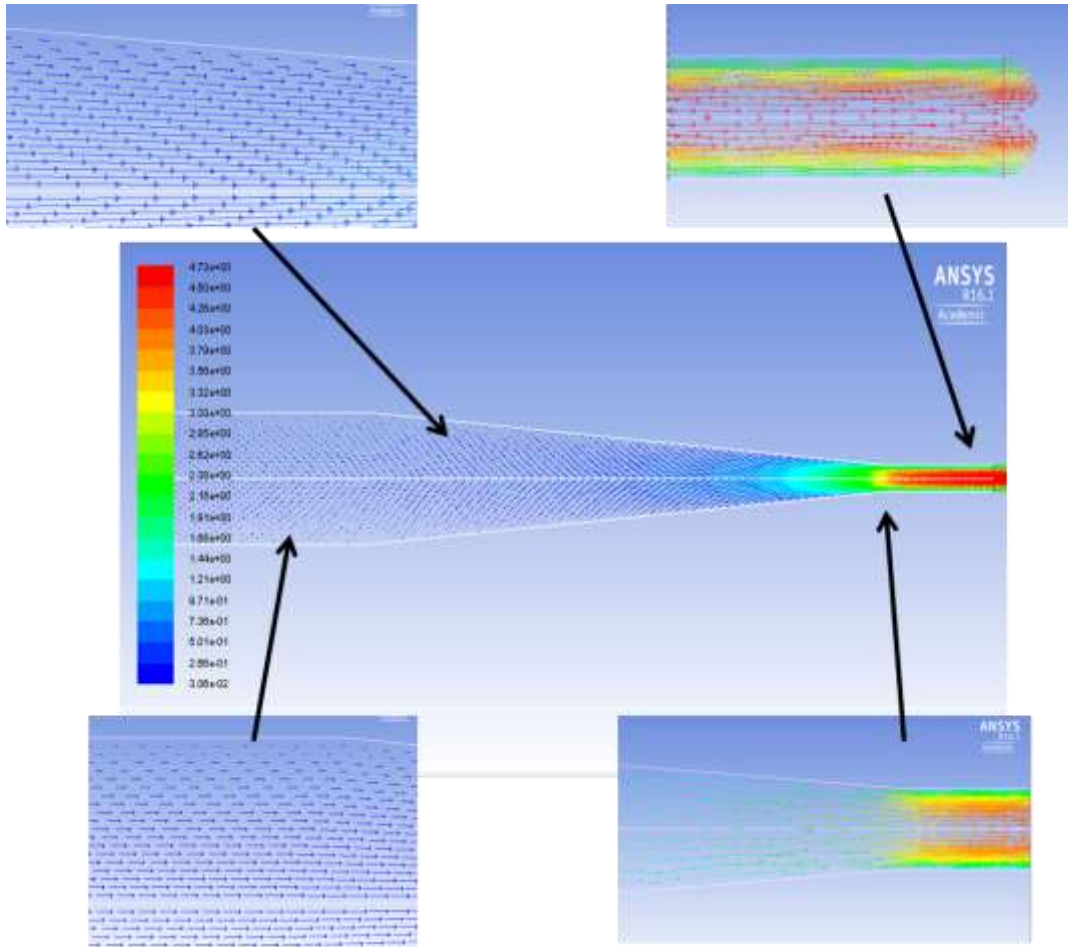


Figure 4.7 CFD simulation of velocity vectors of the updated design of cryogenic nozzle

#### 4.3.5 Manufacturing of the updated design of cryogenic cooling nozzle and testing with LN<sub>2</sub>

Full dimensions and CAD models of the updated design of the cryogenic cooling nozzle were generated as shown in figure 4.8.

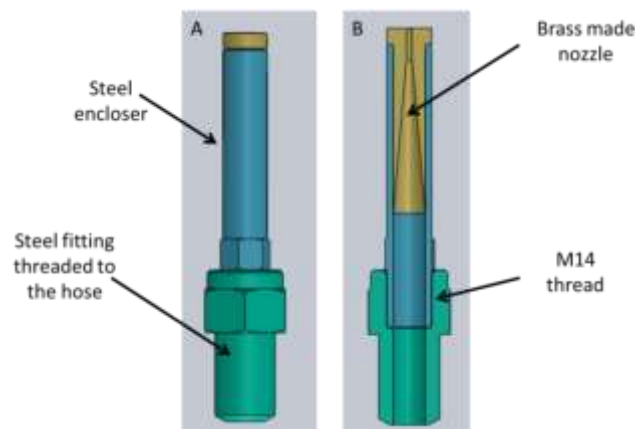


Figure 4.8 Updated design of external cryogenic cooling nozzle. A) Front view, B) Section view

A prototype of the updated single cryogenic cooling nozzle has been manufactured by the author and installed to the cryogenic delivery system to test its affectivity in spraying LN2 to the desired area in the machine tool as shown in figure 4.9. As shown, the updated design of the cryogenic cooling nozzle successfully sprayed nitrogen in liquid phase and delivered it onto the cutting tool. It can be concluded that the designed cryogenic nozzle is now ready to perform cryogenic cooling in CNC milling.

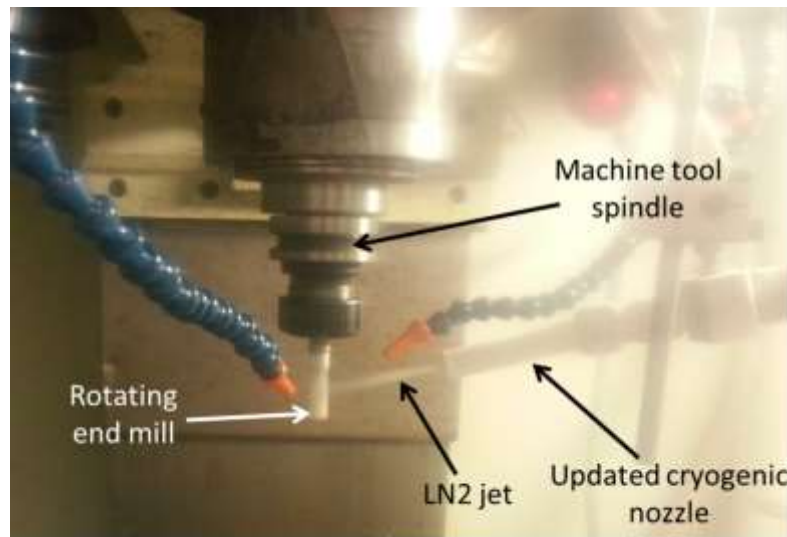


Figure 4.9 Successful testing of the updated cryogenic cooling nozzle after installation to the machine tool and spraying LN2

#### 4.4. Design and manufacturing of flexible cryogenic nozzle holder

In order to install and fix the cryogenic nozzle system in the machine tool and to enable full control of nozzle projection angle and distance with respect to the cutting region, a nozzle holder has been designed and manufactured by the author especially for this purpose. The holder is mounted to the frame of the vertical spindle via a steel rod which is fitted loosely to an aluminium alloy sliding block to provide vertical sliding. For horizontal sliding, another steel rod is also loosely fitted to an aluminium block that can easily slide along the horizontal rod and fixed in position via locking bolts. This horizontally sliding block is mounted to aluminium two-jaw fixture. This fixture is used to climb the cryogenic hose on the holder system as shown in figure 4.10. The horizontal, vertical, and rotational sliding motion provide 5-axis position control to the two-jaw fixture in order to adjust the nozzle orientation to the desired projection angle and distance with respect to the cutting region. After achieving the desired position, the slider system was locked via locking bolts (figure 4.10).

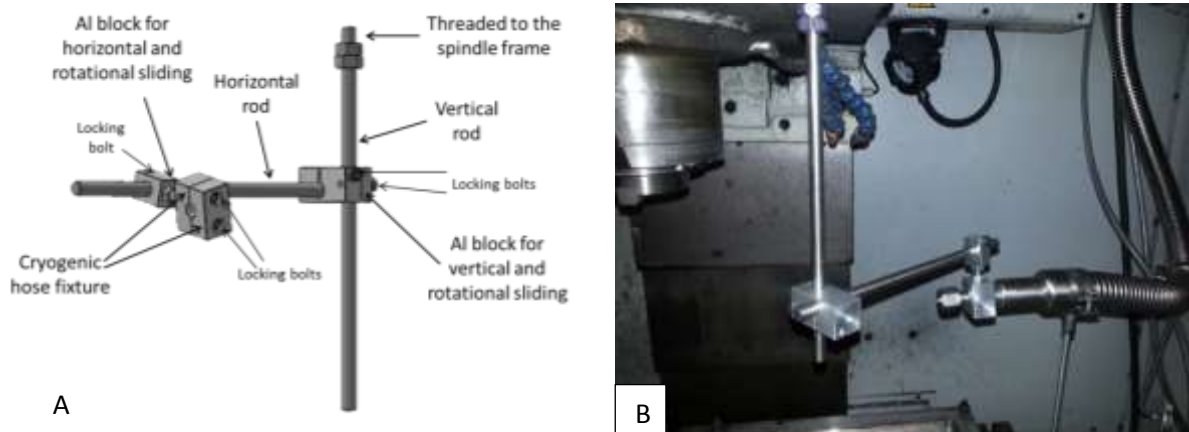


Figure 4.10 Cryogenic nozzle holder. A) CAD model B) installed in the machine tool and hold the cryogenic hose.

#### 4.5 Design and manufacturing of dual-nozzle cryogenic cooling system

Based on the successful design of single-nozzle cryogenic cooling system explained in sections 4.3.4 and 4.3.5, a dual-nozzle is designed and manufactured by the author to increase the cooling performance of the cryogenic cooling nozzle system through improving the effectiveness of the cryogenic nozzle system to effectively target and cool selective regions when CNC machining Ti-6Al-4V. In designing the dual-nozzle system, the same inlet diameter and LN<sub>2</sub> flow rate is considered. In order to maintain uniform flow and constant speed of LN<sub>2</sub> inside the dual-nozzle system manifold, the cross-sectional area before and after the flow division should be the same. This means that the inner diameter of the dual-system manifold after flow division should be 7 mm. Axisymmetric CFD modelling of the single nozzle system (section 4.3.4) indicated that the LN<sub>2</sub> jet velocity at the outlet of each nozzle is 2.37 m/s. The external dual-nozzle cryogenic cooling system consists of the following components:

- i. Two cryogenic nozzles; each one has inlet and outlet diameters of 7mm and 2mm, respectively as shown in figure 4.11.
- ii. An aluminium alloy made flow divider (distributor) to equally divide the LN<sub>2</sub> flow to two streams
- iii. Two copper tubes; to connect each nozzle to the flow distributor and to allow more accurate nozzle positioning via bending each tube to the desired nozzle position.

- iv. Specially designed and manufactured steel fittings to join the ends of the copper tube, one to the flow distributor and the other to the nozzle.

The assembly of the designed and manufactured dual-nozzle cryogenic cooling system is illustrated in figure 4.12.

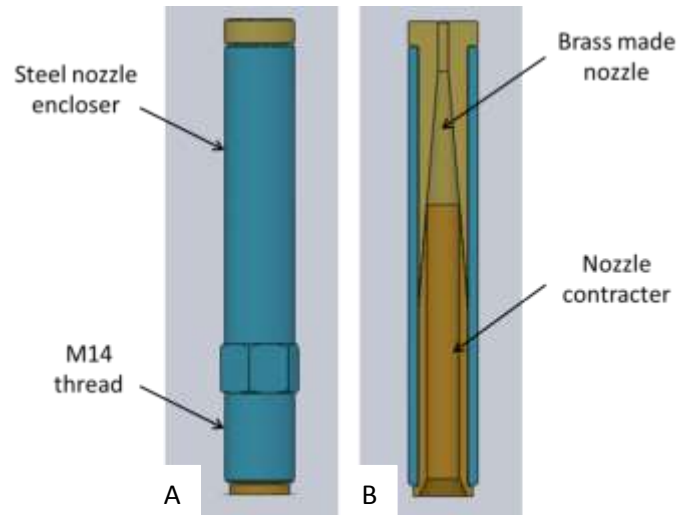


Figure 4.11 Nozzle design of the Dual-nozzle cryogenic cooling system. A) Front view, B) section view

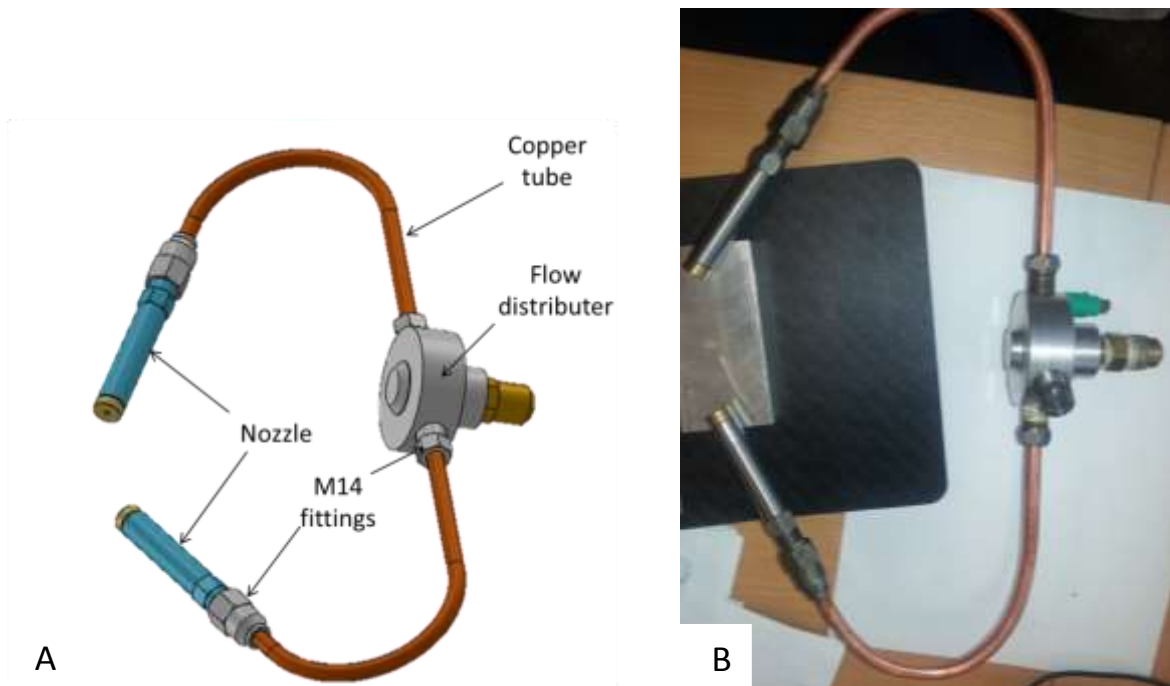


Figure 4.12 The dual-nozzle cryogenic cooling system used in this research. A) CAD model, and B) manufactured prototype

#### 4.5.1 Installing the dual-nozzle system onto the machine tool

The dual-nozzle system is secured in the desired position on to the machine tool via the nozzle holder system described in section 4.4. Figure 4.13 showed a pictorial illustration of retrofitting the dual-nozzle system on the CNC vertical milling centre.

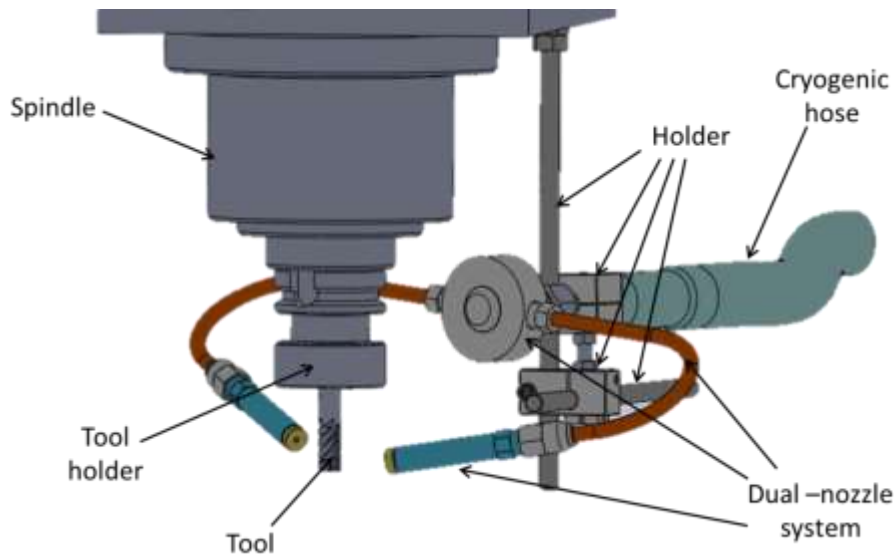


Figure 4.13 CAD model shows the retrofit of the cryogenic cooling system onto the machine tool frame

#### 4.5.2 Thermal insulation of the dual-nozzle system and final spaying test with LN2

A thermal insulation design is made to reduce the heat transfer from the environment to the nozzle system. The high temperature difference ( $\Delta T$  as high as 217 °C), and the high thermal conductivity of the nozzle system components could increase the overall heat transfer coefficient delaying the steady-state liquid phase spraying. The thermal insulation of the dual-nozzle system involves the following materials and activities:

- i. Foam encloser (machined) with 20mm thickness to thermally insulate the aluminium alloy distributor.
- ii. Natural wool band (first layer) wrapped around the copper tubes to give 4 mm wall thickness
- iii. O pipe insulator (second layer) with 19 mm wall thickness to further increase the thermal insulation of the copper pipes
- iv. Pipe insulation tape to protect the insulating materials from damage during machining operations

- v. Plastic straps to prevent any dissembling of the integrated insulators due to the very low temperature working conditions.

Finally, the insulated dual-nozzle system is installed to the machine tool and connected to the cryogenic delivery system to test its efficiency in spraying LN2 as shown in figure 4.14.

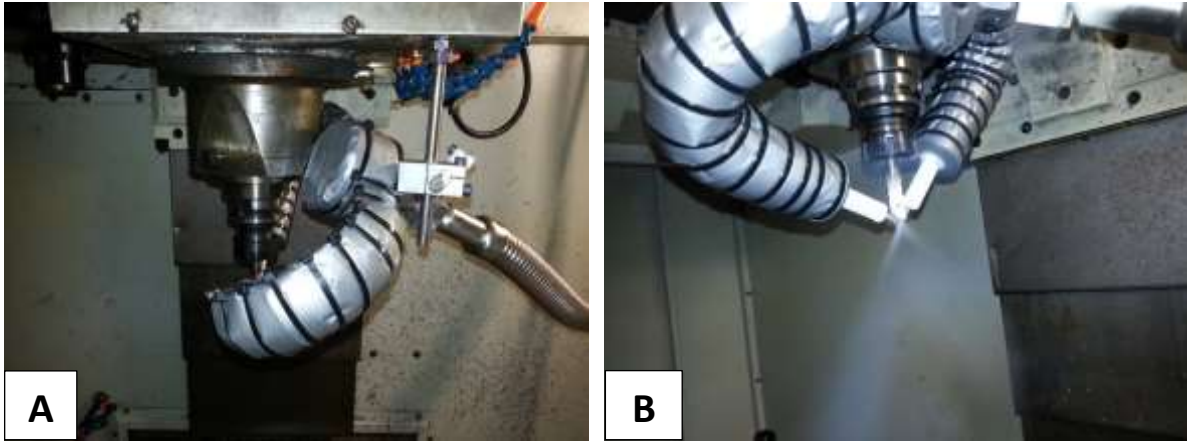


Figure 4.14 A) Retrofitting the dual- nozzle system after insulation (front view), B) successful spraying of liquid nitrogen (rear view)

A visual test demonstrated efficient performance of the dual-nozzle system to spray economical but sufficient amount of LN2. In addition, due to the effective thermal insulation, the time delay of liquid delivery due to LN2 evaporation has been reduced from 20 to only 5 minutes. This gives the cryogenic cooling system more flexibility and capability to conduct cryogenic experiments that require stopping, measuring, and continuing at any setting of period intervals.

From the above design, modelling, manufacturing, and testing activities it can be concluded that the dual-nozzle cooling system is now ready to conduct cryogenic machining experiments.

## **Chapter 5 Experimental investigation of machinability of hybrid cryogenic/MQL technique in comparison with individual cooling and lubricating conditions**

### **5.1 Introduction**

In order to investigate the effectiveness of the designed cryogenic cooling system, it is an essential objective to compare its performance with existing cooling and lubrication systems namely, flood and minimum quantity lubrication (MQL). In this chapter, the machining performance of the designed dual-nozzle external cryogenic cooling system was investigated in terms of tool wear, surface roughness, and chip morphology. Also the cooling /lubrication performance of a hybrid combination of external nozzle cryogenic cooling and minimum quantity lubrication when machining Ti-6Al-4V was compared with conventional flood cooling, MQL, and cryogenic cooling. It is the purpose of this chapter to provide a quantitative investigation that enables comparison of the machining performance of integrate cryogenic-MQL with other cooling/lubrication techniques in terms of tool wear, surface roughness, and chip morphology. The methodology suggested four consequent actions as illustrated in figure 3.3. Three of them are carried out in this chapter, namely, preparation for machining experiment, design and implementation of machining experiments, collection of experimental data of the investigated machining performance. The fourth action is the results and statistical analyses which is covered in the next chapter.

In the preparatory part, the effect of excessive LN2 cooling on the hardness of the Ti-6Al-4V alloy workpiece material were studied after measuring the hardness of the whole patch of workpiece blocks at room temperature to make sure that the average value and the variation of hardness across each block have satisfied the relevant standards. Then and according to the literature in chapter 2, the cutting tool material, coating, and geometry were selected for the machining experiments. After selecting the constant and variable cutting parameters, identifying the investigated cooling/lubricating conditions, a full-factorial design of experiment DoF with a total number of 20 machining experiment was generated. Then experimental machining procedure was conducted on CNC vertical milling machine after generating a G-code program that takes into consideration the instability of the machining operation. The tool wear was measured using an optical calibrated microscope provided with a digital camera. The measurements were performed at various intervals throughout the machining until the wear criterion of the flank wear according to ISO 8688-2 (1989) was reached. The surface roughness of the machined surface is measured for each machining

experiment. The chips are collected for microscopic analyses of chip formation and morphology. It is worth mentioning that the surface roughness measurements and chip collection are made at early stage of each machining experiment to avoid the effect of tool wear on surface roughness and chip segmentation.

## 5.2 Preparation for machining experiments

The preparatory activities in this research involves the measurement of the hardness along the workpiece surface to be machined for the whole patch of the workpiece blocks, and then measuring the effect of reduction of temperature beyond the room temperature till the LN2 temperature on the properties of Ti-6Al-4V alloy. Also fixed and variable cutting parameters are selected according to the literature reviewed in chapters 2 (López De Lacalle et al. 2000; Shokrani et al. 2016b). Furthermore, the selection of the material, coating and geometry of the cutting tool used in the machining experiments is explained. Finally, the cooling/lubricating conditions (machining environments) to be investigated and the machining performance metrics or the area of investigation are identified.

### 5.2.1 Measuring the effect of excessive liquid nitrogen cooling on the properties of Ti-6Al-4V

The workpiece material used in this research was milled annealed Ti-6Al-4V  $\alpha$ - $\beta$  alloy (ASTM B265 grade 5 titanium). The dimension of the workpiece blocks were 150×52×52mm. The chemical composition of the workpiece material is listed in Table5.1, while the microstructure shown in figure 5.1. The microstructure of the annealed Ti-6Al-4V consists of coarse grain plate-like primary alpha phase (dark areas) with beta inter-granular (light areas) at the boundary of  $\alpha$  grains (Hong and Zhao 1999; Sun et al. 2010).

Table 5.1 Chemical composition of Ti-6Al-4V alloy (wt. %)analysed by Shokrani (Shokrani 2014).

| Spectrum            | Al   | Ti    | V    | Fe   | Total (wt. %) |
|---------------------|------|-------|------|------|---------------|
| Mean of 9 specimens | 6.75 | 89.37 | 3.46 | 0.12 | 100.00        |
| Std. deviation      | 0.33 | 0.5   | 0.68 | 0.13 |               |



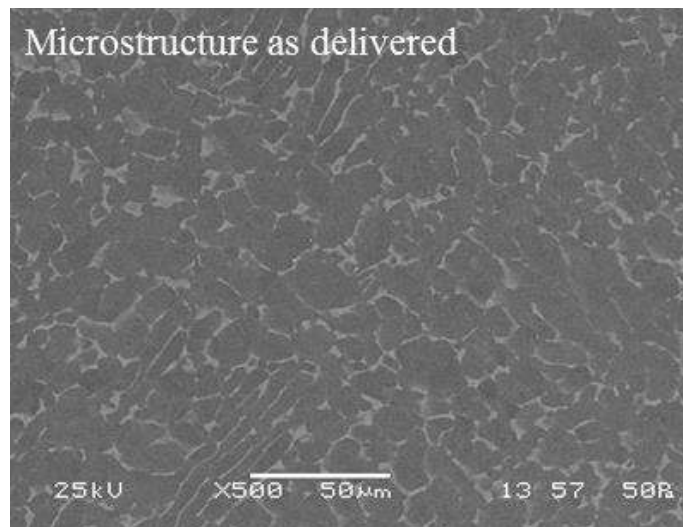


Figure 5.1 Microstructure of Ti-6Al-4V titanium alloy analysed by Shokrani (Shokrani 2014).

For hardness testing purposes, the Vickers hardness tester with 30 kg indentation load was employed. After measuring the average length of diagonal resulting from the indentation, the Vickers hardness was calculated according to the following equation:

$$HV = \frac{F}{A} \approx \frac{1.8544 F}{d^2} \text{ [kgf/mm}^2\text{]}$$

Where  $F$  is the applied load in kg (30kg),  $A$  is the surface area of resulting indentation in square mm and  $d$  is the average diagonal lift by the indentation.

The hardness test was carried out on the workpiece surface to be machined of 150×52mm. In total, 24 sample points (6×4) equally distributed across the length and width of the machined area were generated. Table 5.2 indicates the Vickers hardness measurements for each workpiece block of the batch with the calculated mean and variance. The overall average measured Vickers hardness and the overall standard deviation for the whole Ti-6Al-4V workpiece blocks were 348±11.8 HRV.

Figure 5.2 indicates the change of Ti-6Al-4V hardness due to the cryogenic cooling. According to figure 5.3 the hardness of Ti-6Al-4V increased at cryogenic temperature nearly 16% more than that of room temperature. This significant increase in hardness with the ductility and toughness maintained their value even at LN2 temperature could lead to an increase in strength of Ti-6Al-4V and affect the machining performance accordingly (Hong and Zhao 1999; Park et al. 2017; Shokrani et al. 2013)

Table 5.2 Vickers hardness of Ti-6Al-4V blocks used in the present investigation, 24 measurements for each block

| Vickers hardness (kgf/mm <sup>2</sup> ) |                        |     |     |     |     |      |     |     |     |     |     |
|---|------------------------|-----|-----|-----|-----|------|-----|-----|-----|-----|-----|
| Measurement                             | Ti-6Al-4V Block number |     |     |     |     |      |     |     |     |     |     |
| Number                                  | 1                      | 2   | 3   | 4   | 5   | 6    | 7   | 8   | 9   | 10  | 11  |
| 1                                       | 346                    | 348 | 387 | 341 | 357 | 331  | 336 | 336 | 346 | 357 | 343 |
| 2                                       | 339                    | 337 | 366 | 331 | 357 | 339  | 341 | 351 | 343 | 351 | 351 |
| 3                                       | 355                    | 337 | 377 | 344 | 357 | 344  | 341 | 346 | 349 | 351 | 349 |
| 4                                       | 344                    | 344 | 373 | 348 | 381 | 333  | 348 | 348 | 341 | 349 | 337 |
| 5                                       | 334                    | 343 | 362 | 344 | 366 | 333  | 351 | 346 | 348 | 349 | 349 |
| 6                                       | 351                    | 358 | 353 | 355 | 364 | 337  | 339 | 331 | 343 | 353 | 349 |
| 7                                       | 348                    | 349 | 371 | 349 | 360 | 336  | 325 | 333 | 336 | 358 | 358 |
| 8                                       | 343                    | 351 | 349 | 341 | 364 | 339  | 346 | 343 | 348 | 375 | 346 |
| 9                                       | 343                    | 348 | 349 | 358 | 364 | 337  | 346 | 353 | 349 | 351 | 355 |
| 10                                      | 343                    | 353 | 381 | 346 | 360 | 336  | 343 | 355 | 349 | 339 | 346 |
| 11                                      | 344                    | 346 | 373 | 355 | 379 | 331  | 348 | 350 | 339 | 349 | 353 |
| 12                                      | 343                    | 346 | 366 | 337 | 366 | 337  | 434 | 339 | 339 | 343 | 346 |
| 13                                      | 343                    | 343 | 368 | 349 | 360 | 339  | 333 | 341 | 339 | 346 | 351 |
| 14                                      | 337                    | 348 | 371 | 339 | 360 | 348  | 346 | 346 | 337 | 348 | 351 |
| 15                                      | 343                    | 344 | 353 | 344 | 351 | 333  | 344 | 343 | 343 | 348 | 349 |
| 16                                      | 344                    | 346 | 357 | 341 | 368 | 329  | 331 | 341 | 343 | 351 | 346 |
| 17                                      | 346                    | 343 | 364 | 343 | 371 | 333  | 343 | 337 | 346 | 348 | 348 |
| 18                                      | 339                    | 355 | 357 | 343 | 360 | 328  | 344 | 341 | 346 | 346 | 355 |
| 19                                      | 343                    | 344 | 368 | 339 | 366 | 346  | 336 | 355 | 346 | 349 | 366 |
| 20                                      | 343                    | 337 | 353 | 337 | 349 | 337  | 337 | 348 | 348 | 343 | 370 |
| 21                                      | 343                    | 341 | 357 | 339 | 348 | 320  | 339 | 357 | 341 | 346 | 362 |
| 22                                      | 355                    | 343 | 368 | 337 | 351 | 341  | 331 | 357 | 343 | 343 | 355 |
| 23                                      | 334                    | 351 | 368 | 339 | 358 | 329  | 344 | 334 | 341 | 348 | 358 |
| 24                                      | 325                    | 344 | 368 | 336 | 360 | 329  | 348 | 343 | 346 | 339 | 349 |
| Overall mean                            |                        |     |     |     |     | 348  |     |     |     |     |     |
| Overall standard deviation              |                        |     |     |     |     | 11.8 |     |     |     |     |     |

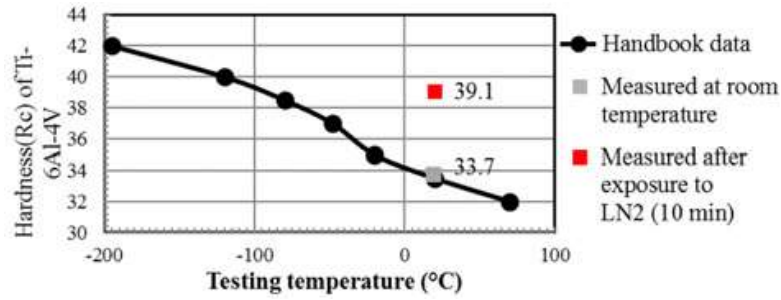


Figure 5.2 Effect of temperature on hardness of Ti-6Al-4V (Park et al. 2017)

## 5.2.2 Identification of cutting parameters

As the conducted machining operation in this study is end milling, four cutting parameters of cutting speed  $V_c$ , feed rate  $f$ , axial depth of cut  $a_a$ , and radial depth of cut  $a_r$  were defined. Since the difference in cutting speed could, to a large extent, affect the machinability of titanium alloys (Bermingham et al. 2011; Shokrani et al. 2016a), the investigation of the machining performance was conducted for various cutting speeds, while the other cutting parameters, namely, feed per tooth, axial depth of cut, and radial depth of cut were kept constant.

### 5.2.2.1 Fixed cutting parameters

As mentioned above, the feed rate  $f$ , axial depth of cut  $a_a$ , and radial depth of cut  $a_r$  were set constant through the whole machining experiments in this research. The selection of the lower level of these cutting parameters was based on literature, manufacturer recommendations for machining titanium alloys that can ensure relatively long tool life with flood cooling. According to ISO 8688-2 (1989), the axial depth of cut was selected so that the end teeth are used predominantly. According to the same standard, when  $a_a < a_r$ , the radial depth of cut should be much higher than the axial depth of cut. It is worth noting that setting of these parameters at such a low level was to reduce their effect on the machinability and give the opportunity to explore the effect of the most important cutting parameter on the machinability which is the cutting speed. Also, this will enable a limited but effective number of experiments. Table 5.3 shows the three fixed cutting parameters adopted in the present research.

Table 5.3 Fixed levels of cutting parameters used in this study

|                            |               |
|----------------------------|---------------|
| Feed per tooth, $f_z$      | 0.03 mm/tooth |
| Axial depth of cut, $a_a$  | 1 mm          |
| Radial depth of cut, $a_r$ | 4 mm          |

### 5.2.2.2 Variable cutting parameter and criterion of selected level range

As mentioned above, the only variable cutting parameter was the cutting speed. Based to the reviewed literature in chapter 2, the most effective parameter on the machinability of Ti-6Al-4V is the cutting speed, since it is highly affects the cutting temperature and hence the tool life (Grearson 1986; Abdel-Aal et al. 2009). According to many researchers and industrial practices, the recommended cutting speed for machining titanium ranges 50 to 60 m/min using flood cooling when machining with tungsten carbide tools (Hong and Ding 2001; Wang and Ezugwu 1997; López De Lacalle et al. 2000). Based on these recommendations, 60m/min was selected as the minimum value of cutting speed in the machining experiment. On the other hand, a maximum value of 180m/min was selected since the tool life is expected to be very short at that sufficiently high cutting speed even if copious amount of conventional flood cooling is used. At high cutting speeds due to the exceptionally high cutting temperature, the cutting tool suffers from dissolution, diffusion and adhesion tool wear mechanisms (Grearson 1986; Hong and Ding 2001). In order to allow for a comparison for a wide range of cutting speeds that could enable a sensible comparable change in machining performance, 30 m/min interval of cutting speed variation was set. That means 5 cutting speed levels were selected for a particular investigated cooling/lubricating condition. Table 5.4 shows the cutting parameters for each machining experiment in a particular given cooling condition or machining environment. According to table 5.4 five machining experiments for five levels of cutting speeds were conducted. These experiments are repeated for each investigated cooling and/or lubricating condition.

Table 5.4 fixed and variable machining conditions used for each cooling/lubricating condition in this study

| Cutting speed<br>(m/min) $V_c$ | Feed<br>$f_z$ (mm/tooth) | Axial depth of<br>cut $a_a$ (mm) | Radial depth<br>of cut $a_r$ (mm) |
|--------------------------------|--------------------------|----------------------------------|-----------------------------------|
| 60                             | 0.03                     | 1                                | 4                                 |
| 90                             | 0.03                     | 1                                | 4                                 |
| 120                            | 0.03                     | 1                                | 4                                 |
| 150                            | 0.03                     | 1                                | 4                                 |
| 180                            | 0.03                     | 1                                | 4                                 |

### 5.2.3 Selection of cutting tool

The cutting tool used in this study is 12 mm diameter solid carbide PVD TiSiN coated end mill (YL 10.2), specially designed and manufactured by Scorpion Tooling UK Limited. The end mill cutter has five flutes, 12° rake angle, and 40 ° helix angles and it is selected as the cutting tool throughout the machining experiments in this research.

### 5.2.4 Identification of cooling/lubrication conditions (machining environment)

Based on the cooling and lubricating techniques used to improve the machinability of Ti-6Al-4V alloy reviewed in chapter 2, and the cryogenic cooling system described in chapter 4, a series of machining experiments have been defined to investigate its cooling performance when CNC milling of Ti-6Al-4V. Moreover, according to the reviewed literature in section (2.7) a simultaneous application hybrid combination of the designed cryogenic cooling system and MQL system is investigated and compared with conventional flood cooling and other individual cooling and lubricating techniques. The cooling/lubricating conditions involved in the investigations are listed as follows:

- i. Dual-nozzle MQL
- ii. Water-based conventional emulsion flood cooling
- iii. External dual-nozzle cryogenic liquid nitrogen cooling
- iv. Hybrid combination of external dual- nozzle cryogenic cooling and dual-nozzle MQL (hybrid cryogenic-MQL)

Full details of the test rig for each cooling/lubricating condition and strategy of application during the machining experiments are explained later in this chapter.

### **5.2.5 Identification of the investigated machinability indices**

As mentioned in the literature, the machinability or the machining performance can be assessed through the measurement of several indices such as tool life (tool wear), surface finish (surface roughness) and/or surface integrity, power consumption, chip morphology, cutting forces, cutting temperature, etc. (Pervaiz et al. 2014; Pramanik and Littlefair 2015). In this research, the machining performance is investigated in terms of tool wear, surface roughness, and chip morphology. Due to the limited resources, the investigations of the other indices of machining performance are out of the scope of this research.

### **5.3 Design of experiment**

The basic principle of design of experiment refer to the activities of planning, designing and analysing of experiments in which meaningful data can be collected and analysed using effective and powerful statistical analyses so that efficient and objective conclusions can be suggested (Montgomery 2009). The appropriate choice of design based on sound planning and proper selection of effective statistical methods that yield powerful analysis of data and skilful work teams could lead to successful industrially designed experiments (Antony 2003). It is worth noting that the selection of input parameters is of major importance in the DoE, since this could affect the quality and number of conducted experiments. Accordingly, the most effective input parameters should be included in the DoE, while the less significant parameters on the output can be neglected or set as fixed or constant parameter/s at a prescribed level/s (Antony 2003; Ghani et al. 2004). It is well known that the reduction of the number of design parameters (or factors) by introducing the most effective factor on the process performance could allow more focus, in terms of process improvement, on using few important factors, i.e. vital few (Antony 2003). For instance, in the case of the present research only two input parameters (or factors), namely; cutting speed and cooling condition or machining environment will be considered in the DoE. Based on the above explanation of DoE, 5 levels of cutting speed  $5^1$  are selected and 4 levels of cooling conditions  $4^1$  are investigated. The other cutting parameters; feed rate, axial and radial depths of cut are kept constant.

It is well accepted that the full factorial designed experiment is the most comprehensive DoE since; it involves all possible combinations of the various levels for the all design parameters (factors). Based on the above, a full factorial design of experiment at 5 levels of cutting

speed and 4 levels of cooling conditions will generate  $5^1 \times 4^1$  or twenty experimental runs as shown in table 5.5

Table 5.5 Full-factorial DoE for cutting speeds and machining environments conditions

| Cooling condition      | Experiment Number | Experiment ID | Cutting speed |
|------------------------|-------------------|---------------|---------------|
| Flood                  | 1                 | F5            | 180           |
| Flood                  | 2                 | F4            | 150           |
| Flood                  | 3                 | F3            | 120           |
| Flood                  | 4                 | F2            | 90            |
| Flood                  | 5                 | F1            | 60            |
| MQL                    | 6                 | M5            | 180           |
| MQL                    | 7                 | M4            | 150           |
| MQL                    | 8                 | M3            | 120           |
| MQL                    | 9                 | M2            | 90            |
| MQL                    | 10                | M1            | 60            |
| Cryogenic              | 11                | C5            | 180           |
| Cryogenic              | 12                | C4            | 150           |
| Cryogenic              | 13                | C3            | 120           |
| Cryogenic              | 14                | C2            | 90            |
| Cryogenic              | 15                | C1            | 60            |
| Hybrid (cryogenic+MQL) | 16                | H5            | 180           |
| Hybrid (cryogenic+MQL) | 17                | H4            | 150           |
| Hybrid (cryogenic+MQL) | 18                | H3            | 120           |
| Hybrid (cryogenic+MQL) | 19                | H2            | 90            |
| Hybrid (cryogenic+MQL) | 20                | H1            | 60            |

#### 5.4 Procedure of machining experiments

In this section, a detailed plan of machining experiments is explained. Firstly, preparation of machining operation is setup in terms of workpiece and fixtures in the machine table, the machining referencing, mounting the cutting tool and designing the strategy of machining operation. Then the details of conducting the experimental machining operation were programmed using the G-code program for the machining operation on the machine tool. Finally, the machining experiments were conducted for each combination of cutting speed and cooling condition according to the design of experiment.

### 5.4.1 Machine tool setup

A Bridgeport VMC 610XP<sup>2</sup> CNC vertical milling centre was employed to conduct 20 machining experiments as shown in figure 5.3. The machine tool is provided with a touch trigger probe to measure and define the machining reference point. The cutting tool diameter and length was defined and measured using a laser tool setting equipment enclosed in the machine tool prior to each machining experiment. A G-code programme was manually generated on the machine tool controller to perform machining of slots individually, one-by-one, along the Ti-6Al-4V block. The machining programme was updated at the end of the machining of each slot to perform the machining of the next slot.



Figure 5.3 The Three-axis CNC vertical milling centre (Bridgeport VMC 610XP<sup>2</sup>) with cryogenic nozzle system installed and ready for conducting machining experiments.

### 5.4.2 Machining operation setup

As described in section 5.2.1, the annealed Ti-6Al-4V alloy blocks of dimensions 150×52×52mm were prepared for the machining operations. These blocks are purchased in one batch so that they all, at large extent, have consistent chemical composition and they have no significant variation in mechanical properties. In order to reduce the vibration in machining due to the low Young modulus of Ti-6Al-4V and the slenderness of the workpiece



developed by progressive machining, the block was fixed securely on the table of the machine tool via four Microlock® fixtures, one on each side as will be shown during machining experiments. Furthermore, sufficient distances were set between the tool centreline and the workpiece's edges (before the start and after the end of machining each slot) to reduce the effect of feed acceleration and deceleration of tool during the machining operation. For the purpose of mounting the cutting tool in the machine tool, a high precision BT-40 tool holder provided with a 12mm collet with 2µm radial and 1µm axial run out, were employed. To help eliminate the effect of tool deflection on the measurement of the output performance parameters during machining operation, 50mm tool overhang was kept constant for each machining experiment.

### 5.4.3 Machining experiments for investigations of machinability

The only parameter data needed to be input to the machine controller were the spindle speed, and the feed rate. These two machining parameters can be simply calculated according to the following equations:

$$Spindle\ speed = \frac{Cutting\ speed}{\pi \times D} \times 1000$$

$$Feed\ rate = Spindle\ speed \times feed\ per\ tooth \times number\ of\ teeth$$

Where, D is the cutting tool diameter in mm. The unit of the parameters in above equations are listed as follows:

- Spindle speed in rpm
- Cutting speed in m/min.
- Feed rate in mm/min.
- feed per tooth in mm/tooth

Table 5.6 listed the machining parameters input in the machine tool controller for each machining experiment.

Table 5.6 Calculated spindle speed and feed rate ready to input to the machining programme

| Experiment number | Experiment ID | Spindle speed | Feed rate |
|-------------------|---------------|---------------|-----------|
| 1                 | F5            | 4775          | 716       |
| 2                 | F4            | 3979          | 597       |
| 3                 | F3            | 3183          | 477       |
| 4                 | F2            | 2387          | 358       |
| 5                 | F1            | 1591          | 239       |
| 6                 | M5            | 4775          | 716       |
| 7                 | M4            | 3979          | 597       |
| 8                 | M3            | 3183          | 477       |
| 9                 | M2            | 2387          | 358       |
| 10                | M1            | 1591          | 239       |
| 11                | C5            | 4775          | 716       |
| 12                | C4            | 3979          | 597       |
| 13                | C3            | 3183          | 477       |
| 14                | C2            | 2387          | 358       |
| 15                | C1            | 1591          | 239       |
| 16                | H5            | 4775          | 716       |
| 17                | H4            | 3979          | 597       |
| 18                | H3            | 3183          | 477       |
| 19                | H2            | 2387          | 358       |
| 20                | H1            | 1591          | 239       |

#### 5.4.4 Operation of machining experiments

In order to evaluate the machining performance of various cooling/lubricating conditions, namely; MQL, cryogenic cooling, and hybrid MQL/cryogenic and compare them with conventional water-based emulsion cooling when end milling Ti-6Al-4V alloy, a series of machining experiments were carried out for each cooling /lubricating condition as shown schematically in figure 5.4.

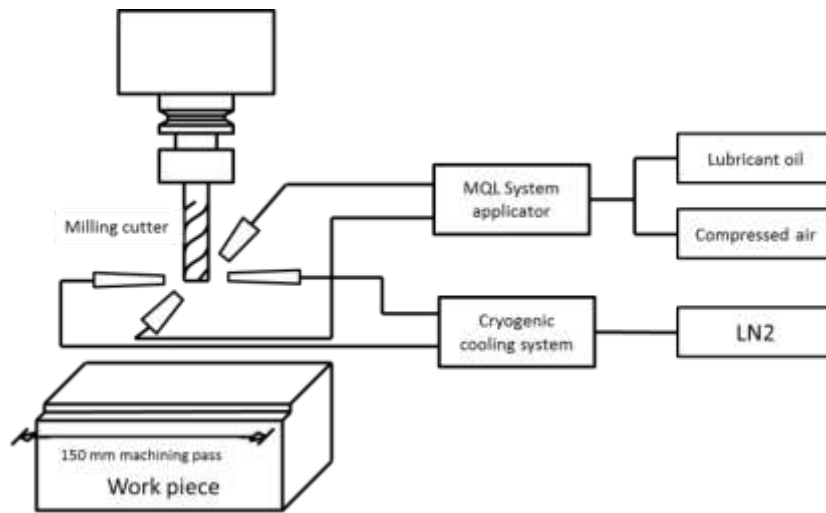


Figure 5.4 Schematic showing the experimental set up

The machining experiments in this research were started by making slots along the Ti-6Al-4V workpiece block. The machining direction is from right to left (down or climb machining) as shown schematically in figure 5.5. The axial and radial depths of cut are 1mm and 4mm, respectively. As a result, each machining pass or slot is 4×150mm and 1mm thick.

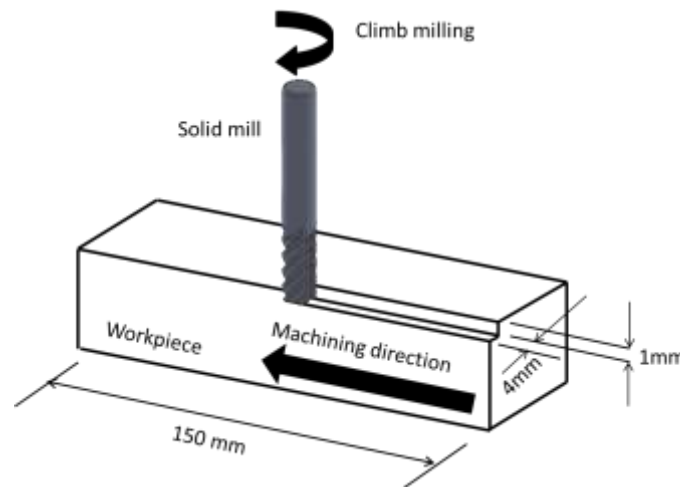


Figure 5.5 Schematic illustration of machining operation

The mechanism of the machining experiments in this investigation is dependent to the evolution of tool wear. The tool wear was measured throughout the machining operation at periodic intervals. Each machining experiment involves the following steps:

- i. Stopping the machining operation at a planned periodic interval.
- ii. Removing the cutting tool with its holder from the machine tool.

- iii. Measuring the tool wear using optical calibrated microscope equipped with digital camera via taking images to the tool and analyse them with measuring package
- iv. Returning the tool to the machine and resuming the machining operation till the next measurement of the tool wear.
- v. Ending the machining experiment when the measured tool wear reached the criterion of tool wear in milling operation according to ISO 8688.
- vi. Another machining experiment involves new combination of cutting speed and machining environment is conducted with new cutting tool.

#### 5.4.4.1 Minimum quantity lubrication MQL

For MQL machining experiments, the dual-nozzle MQL applicator (Accu-Lube Manufacturing GmbH) sprays vegetable rapeseed oil with 9 ml/h flow rate and 6 bar air pressure via two nozzles as shown in figure 5.6. Each MQL nozzle has 2.5 mm outlet diameter and positioned 5-7mm distance from the cutting tool. The first nozzle is directed to the cutting zone with  $110^\circ$  to the feed direction and  $60^\circ$  to the horizontal (machine XY plane). This nozzle orientation insures full coverage of MQL to the cutting zone. On the other hand, the second nozzle was directed to the cutting tool from the opposite side to the first nozzle with  $90^\circ$  to the feed direction and  $20^\circ$  to the horizontal plane. Figure 5.6 illustrates the MQL system used in this study, whilst figure 5.7 shows the positions of the MQL nozzles during machining.

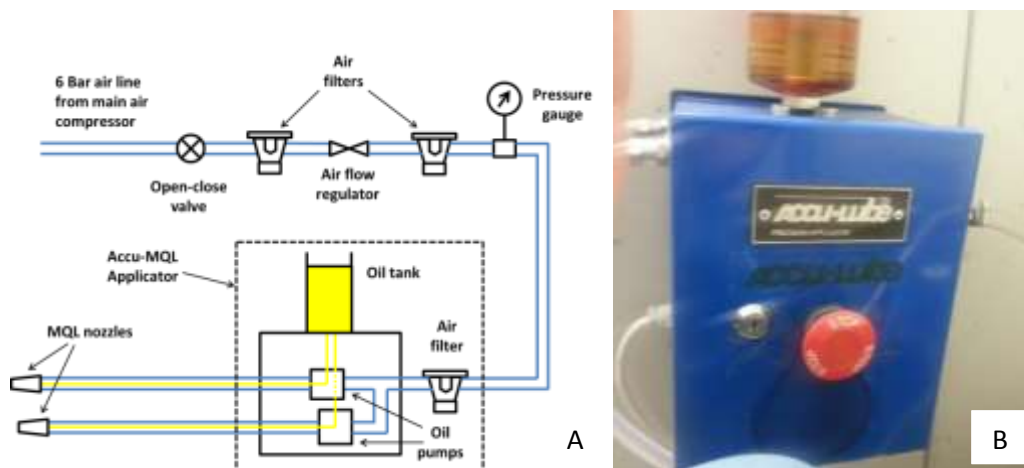


Figure 5.6 Minimum quantity lubrication system used in this study. A) Schematic of dual-nozzle MQL system, B) ACCU-Lube MQL applicator

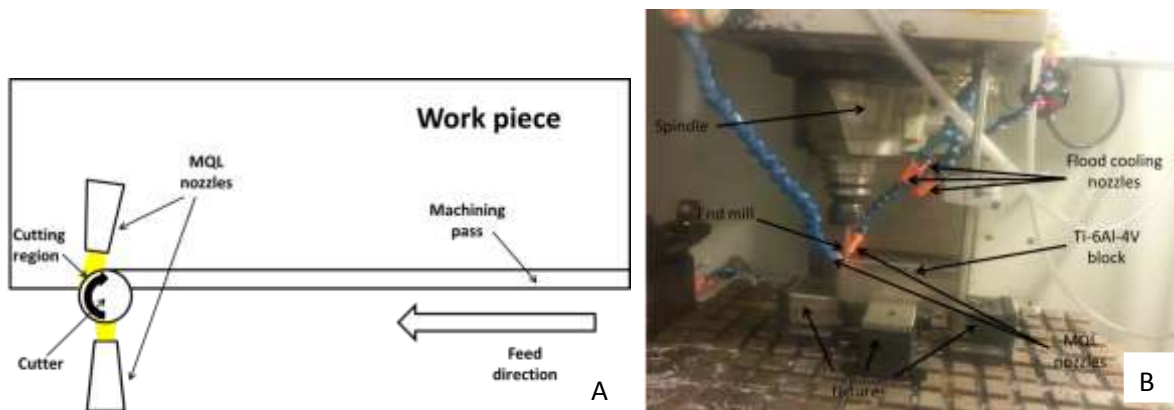


Figure 5.7 Application of MQL during milling of Ti-6Al-4V. A) Schematic of MQL nozzle positions (top view), B) dual- nozzle MQL during machining (front view)

#### 5.4.4.2 Conventional flood cooling

A water-based conventional emulsion flood cooling was used for comparison purposes to evaluate the environmentally friendly alternative environments with current best practice. The coolant is a water-soluble synthetic fluid with mixing ratio of 4% sprayed via three built-in nozzles with total flow rate of 30L/min and pumping pressure of 6 bar. Each coolant nozzle is 5mm outlet diameter and distanced 200mm from the cutting region as shown in figure 5.7b.

#### 5.4.4.3 Cryogenic machining

Cryogenic machining experiments with LN2 were performed via the dual- nozzle external cryogenic cooling system described in chapter 4. The cryogenic delivery system delivered LN2 to the dual- nozzle system at flow rate of 33 litre/h and pressure of 1 bar. The cryogenic delivery system consists of an insulated stainless steel cryogenic tank (Dewar) with nominal capacity of 180 litre, globe valve to manually adjust and control the flow of LN2, a 2/2 initially closed solenoid valve for safely turning the flow on and off, and a vacuum insulated flexible hoses to deliver LN2 from the storage tank (Dewar) to the nozzle system, maintaining nitrogen in liquid phase. Each cryogenic nozzle has a 2mm outlet diameter with a distance as close as 20mm from the cutting tool periphery. This ensured a straight-line non-spreadable coolant steam to reduce the effect of discontinuous spraying of LN2 resulting from the unstable state of liquid-vapour phase. The nozzles were set at exactly the same orientation of MQL nozzles (Section 5.4.4.1) to minimise the effect of nozzle position for different cooling/lubricating conditions. This implied that the first nozzle sprayed LN2

directly to the cutting zone, whilst the second nozzle provided further cooling to the cutting tool and the workpiece as shown in figure 5.8.

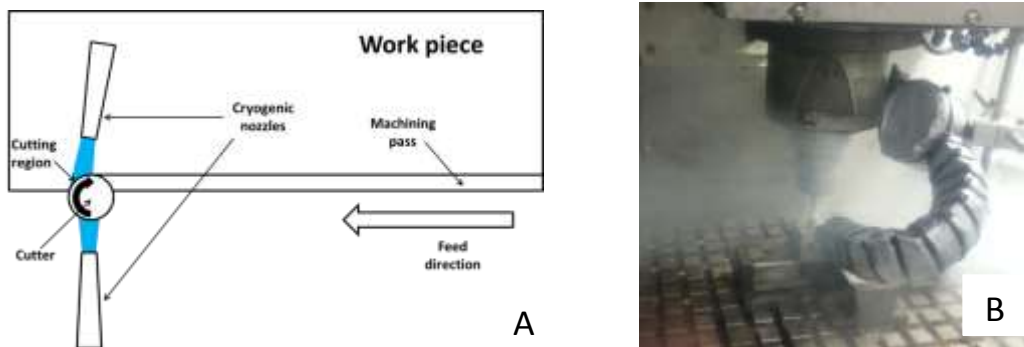


Figure 5.8 Cryogenic machining with dual-nozzle system. A) Schematic top view showing cryogenic cooling strategy, B) During machining

#### 5.4.4.4 Hybrid/cryogenic-MQL cooling/ lubricating

With hybrid combination of MQL and cryogenic cooling, the cooling/lubricating strategy was built on the fact that MQL nozzle system sprays oil directly to the cutting interfaces to provide the lubrication. This was essential to reduce the friction between the tool rake and the machined chip (secondary shear zone), and the friction between the tool flank and the workpiece (tertiary zone). On the other hand the cooling strategy suggested directing the cryogenic nozzles mainly to the cutting tool to reduce the tool temperature well below the softening temperature of the tool material. Also, the cryogenic nozzles orientation provided sufficient cooling to the workpiece to reduce the chemical reactivity of titanium. For this purpose, a combination of MQL and cryogenic cooling was applied during a set of hybrid machining experiments to compare their performance with the individual application of MQL, cryogenic cooling and conventional flood cooling. In hybrid MQL/cryogenic, the original MQL nozzle positions were kept unchanged, while the cryogenic nozzle system is rotated 90° to the original position or to the MQL position, while keeping the projection angles (to the x-y plane) unchanged. Figure 5.9 shows the positions of MQL and cryogenic nozzles when hybrid MQL/cryogenic machining is performed.

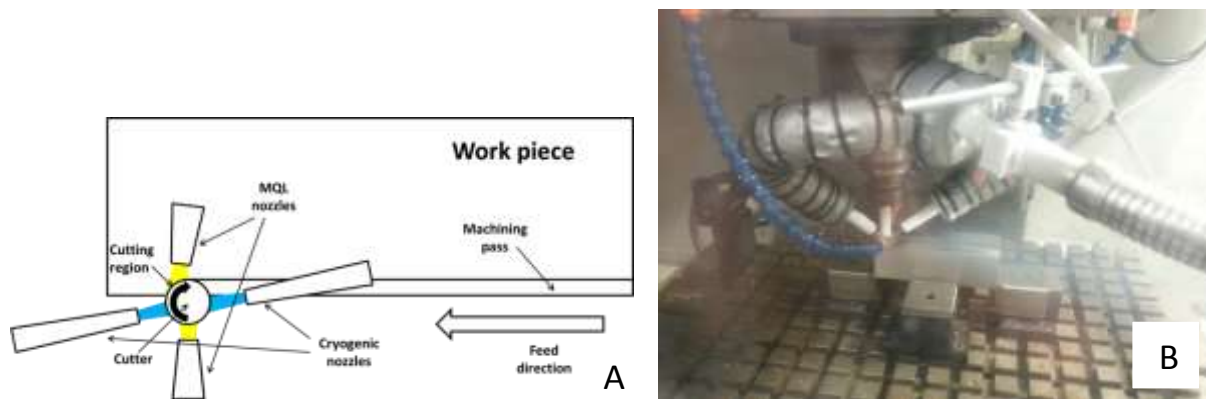


Figure 5.9 Hybrid MQL/cryogenic machining set up. A) Schematic showing hybrid cryogenic/MQL strategy, B) during machining.

## 5.5 Evaluating machinability

As described in section 5.2.5 the machining performance was investigated in terms of tool wear, surface roughness, and chip morphology.

### 5.5.1 Measurement of tool wear

To help determine the tool life and compare the influence of different test cutting and cooling/lubricating conditions on wear rate and modes of tool failure, it is necessary to select one defined type of wear of the cutting tool as a criterion. According to ISO8688-2 (1989) a certain width of flank wear land  $V_B$  is the most commonly used criterion. In order to illustrate the mechanism of tool wear when end milling titanium alloy under different cutting and cooling/lubricating conditions, it was helpful to divide the tool flank clearance face into three locations; nose flank, main flank and depth of cut flank. The nose flank represents the part of flank area in the vicinity of the tool nose, while the depth of cut flank is the tool flank part distanced the depth of cut length value from the tool nose. The main flank located between nose and depth of cut and represents the major or primary flank area. For tool life testing in end milling, ISO 8688-2(1989) suggests that the end of tool life is reached once the average flank wear exceeds  $300\mu\text{m}$  over all tool teeth (Anon 1989). During the measurement of tool wear, all tool deterioration phenomena other than uniform and localised flank wear such as chipping/flaking and plastic deformation of cutting edge was treated as flank wear.

In this research, the tool wear was measured at various periodic intervals throughout the machining operation according to ISO3685 (2003) with some modifications. For every tool wear measurement the machine tool was stopped and the tool was removed with its BT-40

tool holder from the machine tool. Then tool images were analysed and the flank wear was measured according to ISO8688-2 (1989) using a Nikon Tool Maker optical microscope with 60X magnification power as shown in figure 5.10. The microscope is equipped with a digital calibrated Moticom® 3.0 mega pixel camera. The tool wear was measured and images of the worn areas analysed via image analysis software (Motic Images Plus® 2.0). Then the tool returned to its position in the machine tool to resume machining till the next measurement.

In order not to prolong the experiment time, the tool was kept mounted in the BT-40 tool holder during tool image analysis. For this purpose, a plastic made BT-40 carrier was specially designed and manufactured by the author to hold the cutting tool with its BT-40 holder on the stage of the microscope (figure 5.10). This carrier allowed a free rotation of the tool to facilitate the measurement of wear and the inspection for each tooth of the cutting tool without further adjustment and refocus of the successive tool images.



Figure 5.10 Cutting tool with its BT-40 holder carried by plastic holder on the stage of microscope for measurement of tool wear.

### 5.5.2 Measurement of surface roughness

A high precision diamond stylus surface profiler with a nose diameter of  $70 \times 10^{-9}$ m was employed for surface roughness measurement. The digital screen of the Taylor Hobson® Surtronic S128 contact surface roughness measuring device shown in figure 5.11, which can display the graph of the surface profile over a set sampling length. Three roughness parameters are indicated on device screen as a measure of roughness of the machined surface. They are, namely, the arithmetic mean( average) roughness,  $R_a$ , the root-mean squared ( the



arithmetic mean of the squares of a set of number of measurements over a sampling length),  $R_q$ , and  $R_z$  which based on the difference five highest peaks and lowest valleys over the entire sampling length. The last two roughness parameters are not included in the analysis of surface roughness in this research.

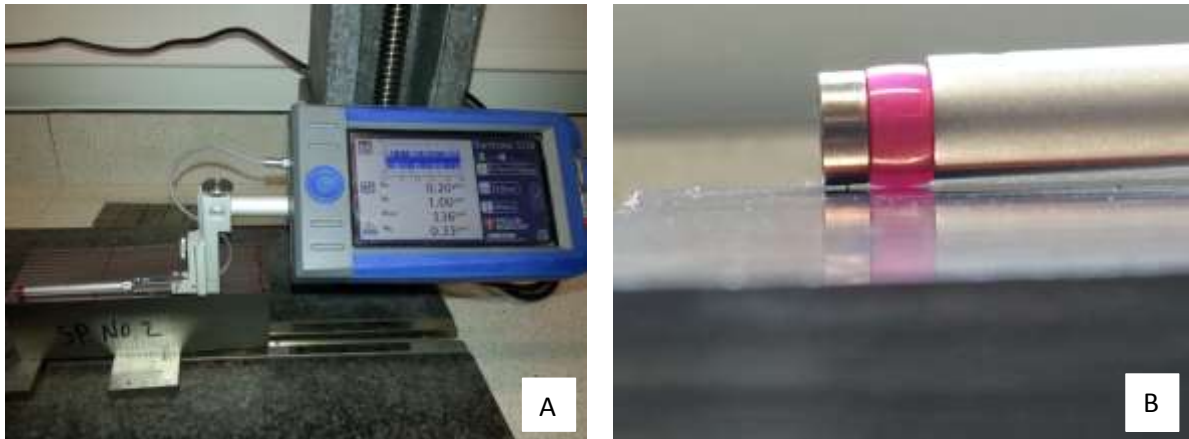


Figure 5.11 Surface roughness measurements. (A) Taylor Hobson® Surtronic S128 surface roughness measuring device used in this research. (B) Zoomed image of diamond stylus profiler

For surface roughness measurement, the nose diameter stylus moves over a 20mm sampling length with a 0.8mm cut off. The measurement was repeated 2 times on each machining pass within the machined surface, i.e. 26 measurements repetitions are performed for each machining experiment. The average value of the arithmetic (average roughness  $R_a$ ) for each machining experiment was calculated with its standard deviation. In order to minimise the effect of tool wear on the roughness of the machined surface the measurements of surface roughness were taken at early stages for all machining experiments.

### 5.5.3 Microscopic inspection and analyses of chip morphology

In order to investigate the effect of cutting speed on chip morphology for different cooling conditions, a chip specimen was prepared for microscopic inspection and analysis. Two type of chip inspection are proposed; macroscopic and microscopic inspection. For this purpose, two optical microscopes equipped with digital cameras were used as illustrated in figure 5.12. Macroscopic inspection was performed using Leica microscope with magnification power  $\times 80$  with putting the chips directly on the microscopic platform (figure 5.12A). For microscopic inspection, samples of chips collected from each machining experiment are mounted with epoxy and sectioned perpendicular to the chip width. After polishing the cross-

sectioned chips along the direction of serration the chip specimen was analyzed using Zeiss optical microscope with 10×50 magnification as shown in figure 5.12B.

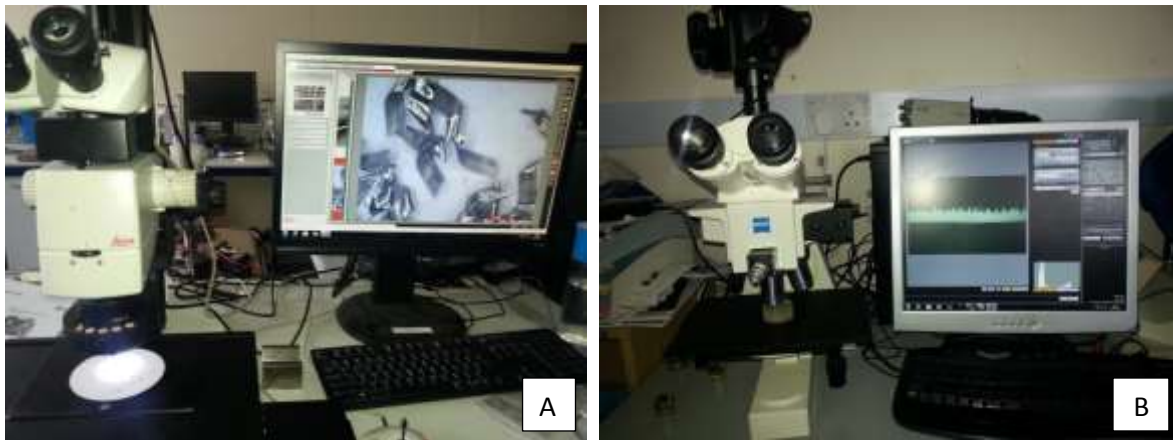


Figure 5.12 Morphology inspection of titanium alloy chips. A) Macroscopic, B) microscopic

## **Chapter 6 Results and analyses**

### **6.1 Introduction**

In order to identify the influence of hybrid cooling/lubricating on the machinability of Ti-6Al-4V, it is essential to compare the performance of the new machining environments with that of conventional flood cooling. Following the methodology illustrated in chapter 5, this chapter demonstrates the results and analysis from the machining experiments. In specific, the machining performance of MQL, cryogenic machining, and hybrid cryogenic/MQL cooling lubricating technique in terms of tool wear, surface roughness and chip morphology are provided and compared with those for conventional flood cooling. For tool wear results, a detailed understanding and analyses of the tool wear mechanism progress during the application, and the dominated tool wear mechanism is presented for each cooling and lubricating condition. In addition, tool life analysis is conducted with the effect and interactions for each machining environment in comparison with flood cooling.

### **6.2 Tool wear**

For tool life testing in end milling, ISO 8688-2(1989) suggests that the end of tool life is reached once the average flank wear exceeds 300 $\mu$ m over all tool teeth (Anon 1989). During the measurement of tool wear, all tool deterioration phenomena other than uniform and localised flank wear such as chipping/flaking and plastic deformation of the cutting edge were treated as flank wear. Figures 6.1, 6.2, 6.3, and 6.4 showed the results of tool flank wear progress for each cooling/lubricating condition. In each particular figure, five curves show the progress of tool wear for different cutting speeds. The intersection of each curve with the horizontal 300 $\mu$ m tool life criterion indicates the tool life for that machining experiment. On the other hand, table 6.1 and figure 6.5 indicate tool life for each machining experiment that involved different combination of cutting speed and machining environment. As flood cooling is considered the basis of comparison for machining performance in this research, the improvement in machining performance for various machining environments is provided based on flood cooling as shown in figure 6.6.

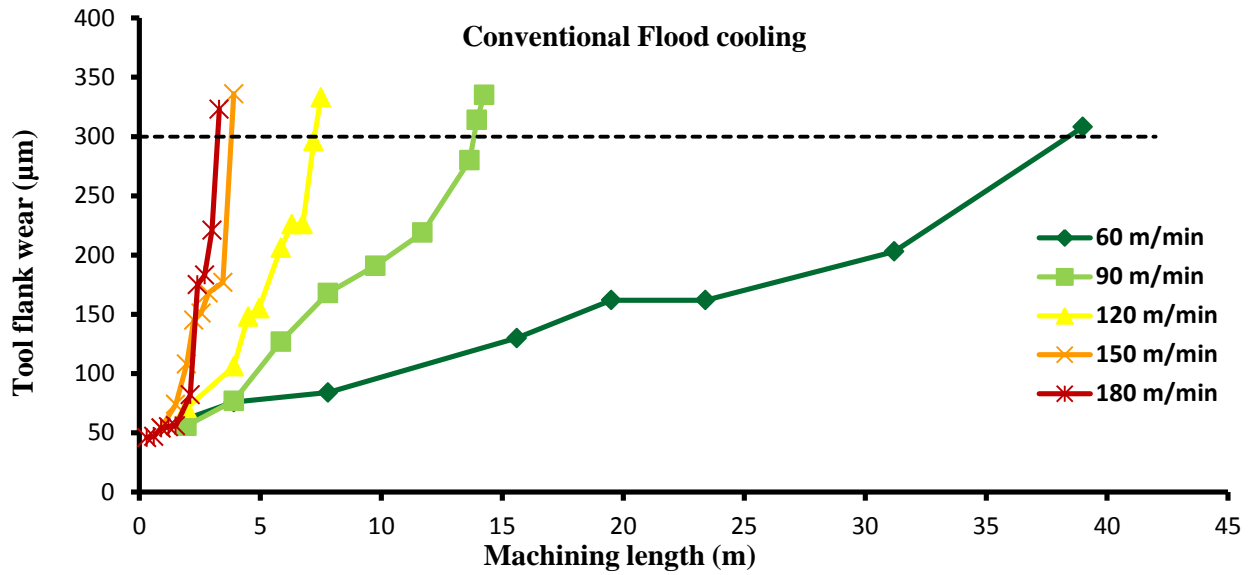


Figure 6.1 Results of tool flank wear for different cutting speeds when flood cooling was applied. Dashed lines indicate the 300µm wear criterion according to ISO 8688.

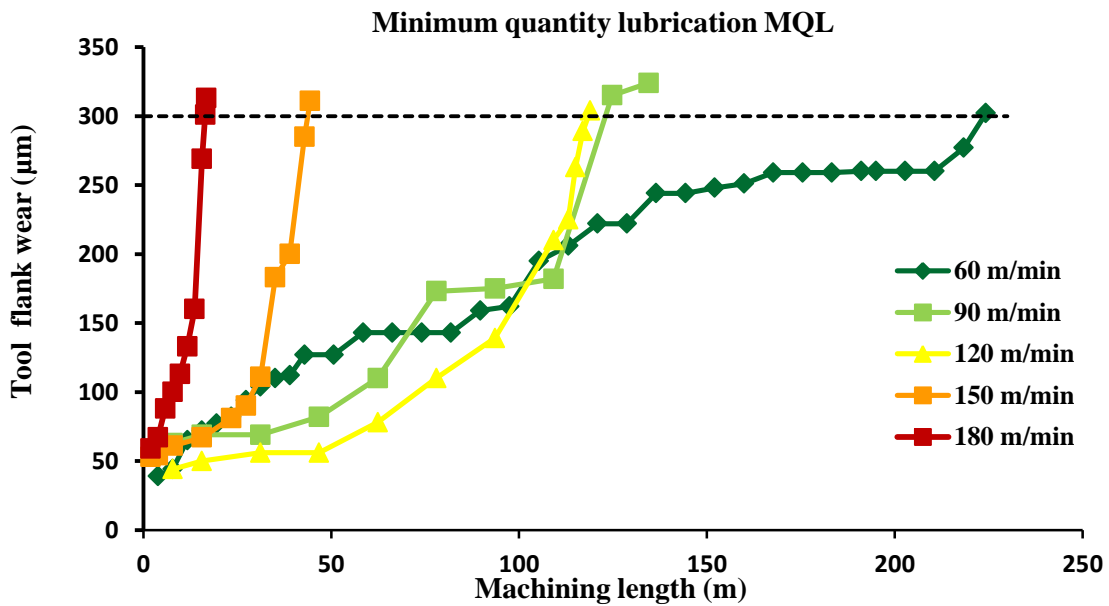


Figure 6.2 Results of tool flank wear for different cutting speeds when MQL was applied. Dashed lines indicate the 300µm wear criterion according to ISO 8688

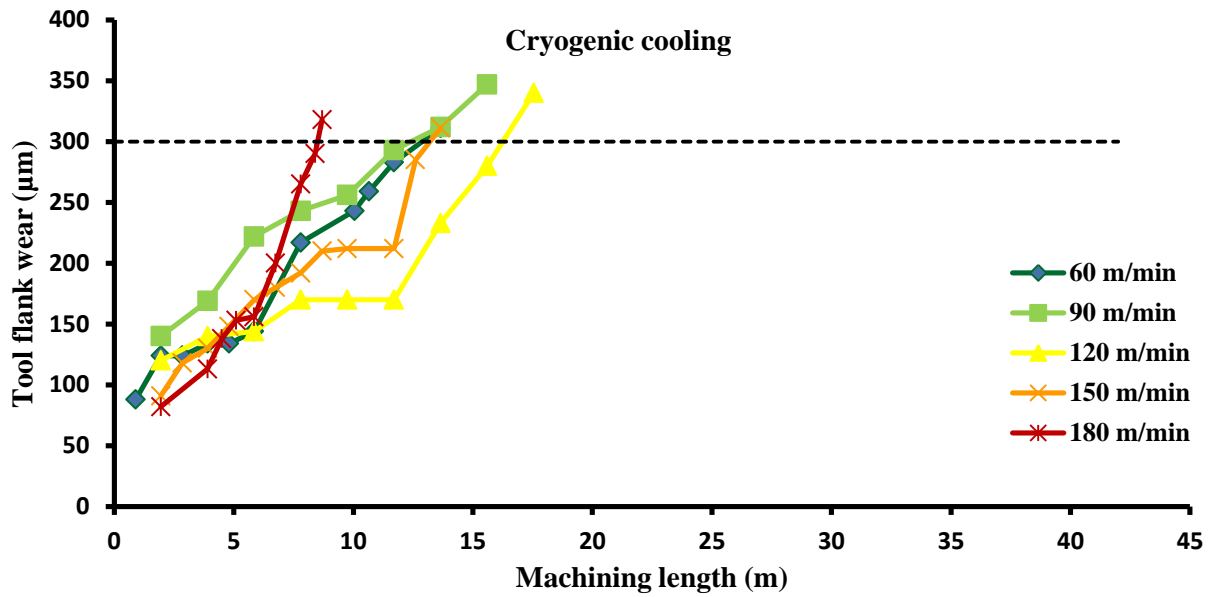


Figure 6.3 Results of tool flank wear for different cutting speeds when cryogenic cooling was applied. Dashed lines indicate the 300µm wear criterion according to ISO 8688

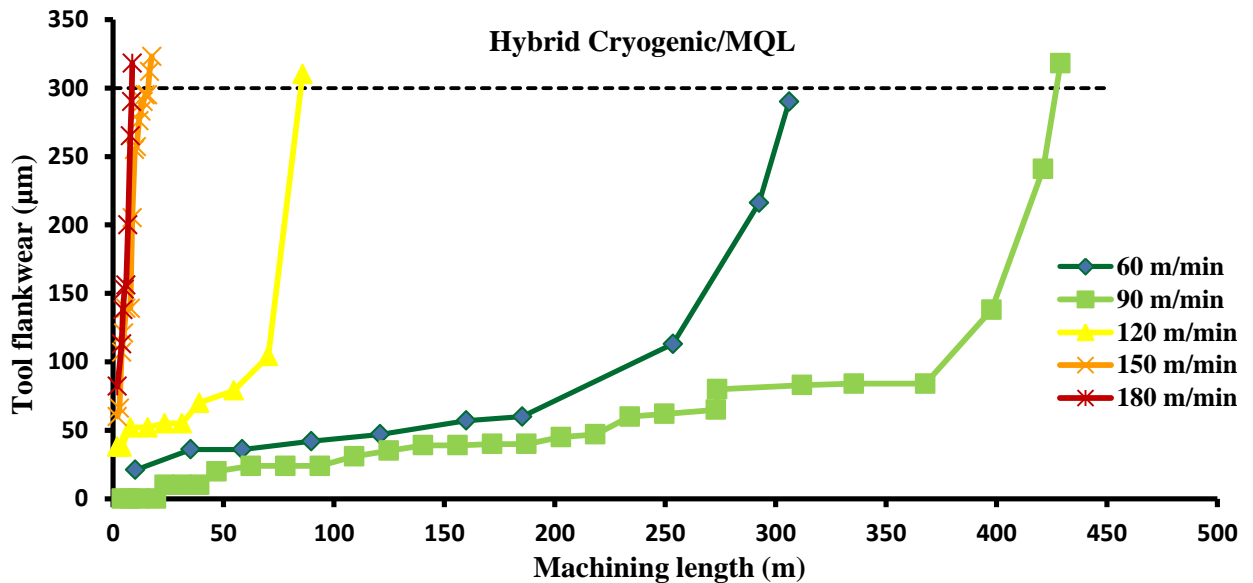


Figure 6.4 Results of tool flank wear for different cutting speeds when Hybrid cryogenic/MQL was applied. Dashed lines indicate the 300µm wear criterion according to ISO 8688.

It is generally agreed that the generation of high temperature at the secondary shear zone (at the rake face) promotes rapid rake face crater wear by dissolution-diffusion when machining Ti-6Al-4V at moderate/high cutting speeds with straight grade (WC-Co) cutting tools. The bonding of titanium chips and/or workpiece to the tool at such high temperatures (beyond 900°C when turning at 75m/min) provides an ideal environment for the diffusion of the tool material constituents across the tool/chip and tool/workpiece interfaces (Grearson 1986;

Birmingham et al. 2012). Furthermore, these adhered pieces of tool material can be removed or torn away by the flowing chips and/or moving workpiece could be the main contributor of flank and/or crater wear by attrition (Venugopal et al. 2007a).

Table 6.1 Results of tool life and percentage of improvement compared with flood cooling

| Experiment ID | Tool life (m) | % Improvement in tool life |
|---------------|---------------|----------------------------|
| F1            | 53.1          | -                          |
| F2            | 13.95         | -                          |
| F3            | 7.34          | -                          |
| F4            | 3.9           | -                          |
| F5            | 3.3           | -                          |
| M1            | 224.25        | 322.3                      |
| M2            | 124.8         | 794.6                      |
| M3            | 93.6          | 1173.5                     |
| M4            | 44.4          | 1038.5                     |
| M5            | 16.8          | 409.1                      |
| C1            | 13.65         | -74.3                      |
| C2            | 15.6          | 11.8                       |
| C3            | 17.55         | 138.8                      |
| C4            | 13.65         | 250.0                      |
| C5            | 8.7           | 163.6                      |
| H1            | 306.15        | 476.6                      |
| H2            | 429           | 2975.3                     |
| H3            | 85.8          | 1067.3                     |
| H4            | 17.6          | 351.3                      |
| H5            | 12.6          | 281.8                      |

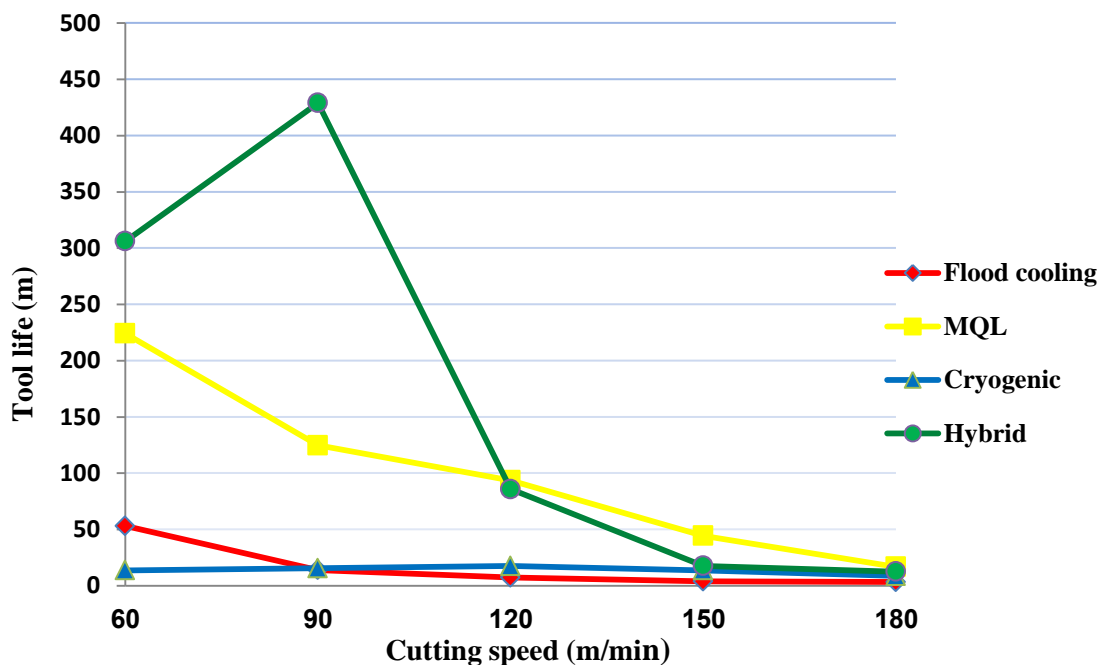


Figure 6.5 Results of tool life in terms of cutting length till reaching wear criterion for different cutting and cooling/lubricating conditions

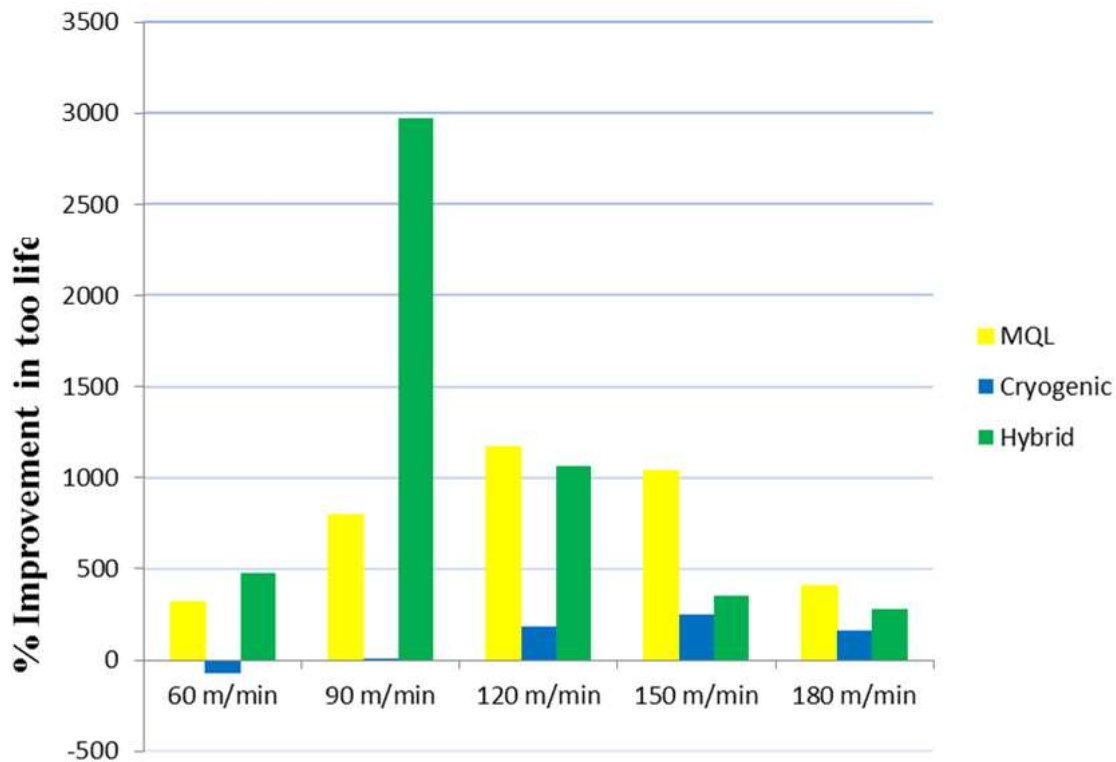


Figure 6.6 Improvement in tool life for various cooling/lubricating methods in comparison to conventional flood cooling

### 6.2.1 Flood cooling machining experiments

In the case of all water-based emulsion flood cooling tests, there was clear evidence that both attrition-abrasion on flank face and chipping/flaking on the rake face have occurred as shown in figure 6.7. Figure 6.7 presented three different views of worn teeth for the five-tooth end milling cutter after tool wear has been reached according to ISO 8688. At the low cutting speed of 60m/min, uniform attrition wear was developed thinly along the whole flank length. Then a localised flank wear developed in the vicinity of the tool nose (nose flank) after 15.6m machining length with formation of BUE on the rake face as shown in figure 6.5. This might be attributed to the increase in tool tip temperature that causes adhesion of chips to the tool rake. The high cutting temperature causes loss of tool nose sharpness due to thermal softening which could promote plastic deformation of the tool nose. This thermally related wear at the nose flank was generally followed by crater chipping in vicinity to tool nose, after 31.2 m machining length, mainly due to the high levels of thermal gradient/thermal shocks resulted from the formation of seizure zone formed the by coolant vapour shield. This seizure zone prevents the low pressure coolant from penetrating the cutting interfaces, while cooling all tool areas around the cutting zone (Ezugwu et al. 2003; Dudzinski et al. 2004; Sartori et al.

2017b). With the continuing of the machining experiment, attrition wear was re-developed again along the irregularly formed cutting edge as a result of the crater chipping until the end of tool life after 39m of machining. Plastic deformation of the cutting edge was only noticeable at the vicinity of depth of cut where no chipping was occurred. It is worth noting that crater chipping which caused loss of the tool flank has been identified as the main tool wear mechanism. In addition, non-uniform flank attrition wear was observed when machining titanium alloy at 60m/min under conventional flood cooling as shown in figure 6.7F1 and 6.8.

At the cutting speed of 90 m/min, the tool wear mechanism was identical as that described above for 60 m/min, with faster rate of wear that is highly localised at nose flank is observed after only 6 m length of cut (figure 6.7F2). This loss of tool nose sharpness is then followed by severe crater chipping at the vicinity of the tool nose after nearly 10m of machining, which could be attributed to the increased level of thermal gradient/shock. With continued machining experiments, the crater chipping is propagated at a wider area over the main and axial rake with maximum chipping at the tool nose (figure 4.9). Similar to 60 m/min experiment (F1), flank wear due to attrition, and adhesion of titanium was observed at the worn flank along the irregularly worn cutting edge, with slight localisation of attrition-adhesion at the nose flank until reaching the wear criterion after nearly 14m of machining, as shown in figures 6.7F2 and 6.9. Crater chipping mainly dominated the tool wear mechanism, while flank attrition wear had a limited contribution to the end of the tool life.

For flood machining experiments at moderate cutting speed of 120m/min, crater chipping was highly localised at the tool nose and BUE formed along the newly formed cutting edge due to the increased temperature at the tool nose resulted in increased thermal gradient/stresses caused by the seizure zone. The elevated tool nose temperature also resulted in loss of sharpness of tool nose, hence promoted abrasion-attrition which was observed at the nose flank as shown in figure 6.10. Both crater chipping and flank attrition control the tool wear mechanism until tool failure after 7.5m machining length as shown in figure 6.7F3.

At the higher cutting speed of 150m/min, flood cooling experiment showed uniform flank wear was initiated and propagated along the main (primary) flank, followed by crater chipping spread along the whole cutting edge becoming smaller in size as shown in figure 6.11. This could be attributed to the spread of thermal gradient along the whole cutting edge



due to the high cutting speed that caused high cutting temperature at small heat affected zone. The high heat generation at the cutting edge promoted thermal-mechanical attrition flank wear along the flank face which dominated the tool wear mechanism (figure 6.7F4).

At the cutting speed of 180m/min in the flood cooling experiment, excessive plastic deformation of the cutting edge at nose and depth of cut flank regions was initiated after only 2m length (figure 6.11) of cut owing to excessive heat generation at high cutting speeds. The failure of coolant to access the cutting zone caused initiation and propagation of crater chipping and flank attrition as illustrated in figures 6.7F5 and 6.12. In all flood machining experiments, there was clear evidence of adhesion of the workpiece material onto the tool flank and rake faces and cutting edge resulting in BUE formation.

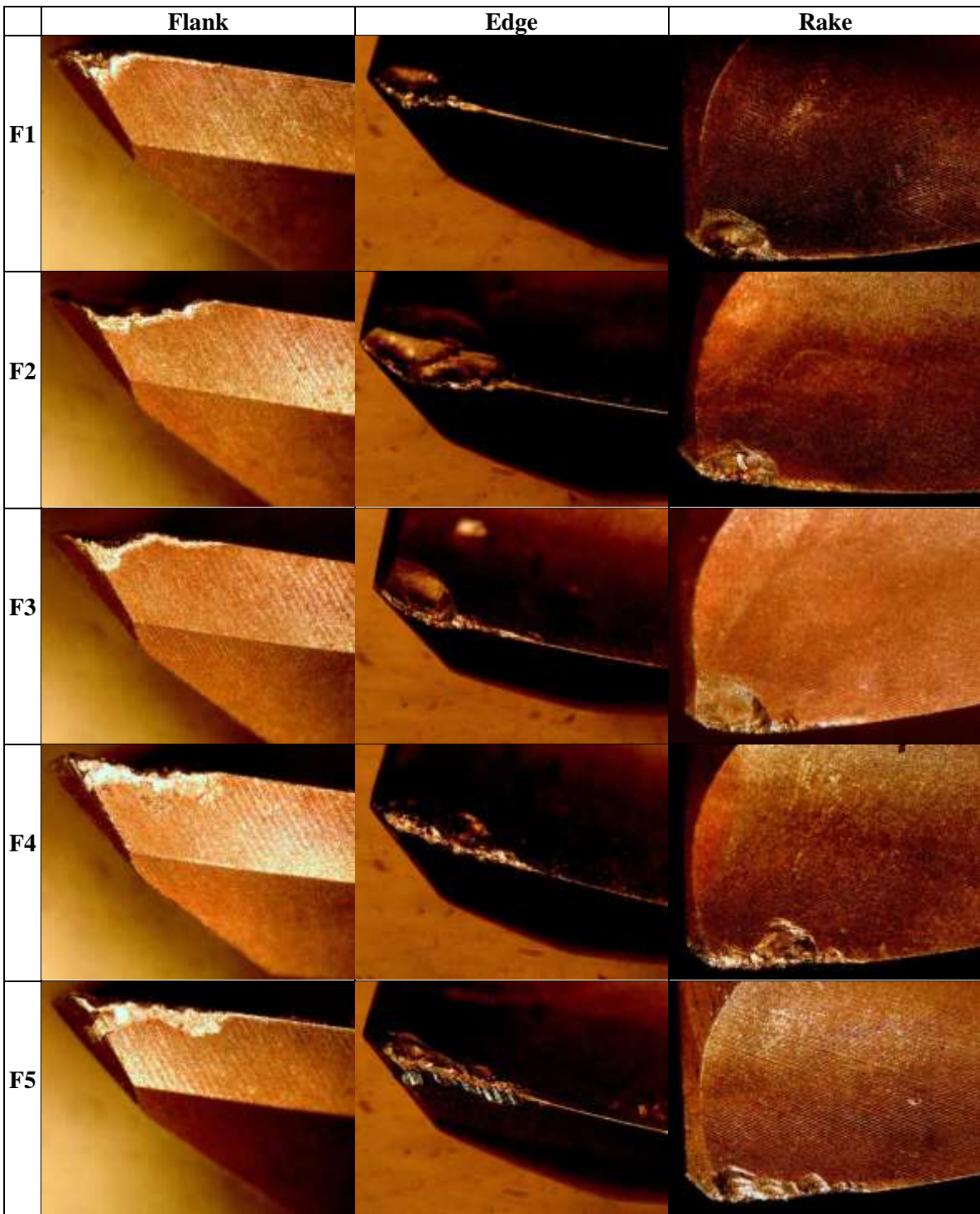


Figure 6.7 Images of tool taken with three views at rake face, cutting edge, and flank face at different cutting speeds; 60, 90, 120, 150, 180 m/min under flood cooling, taken after the wear criterion has been reached

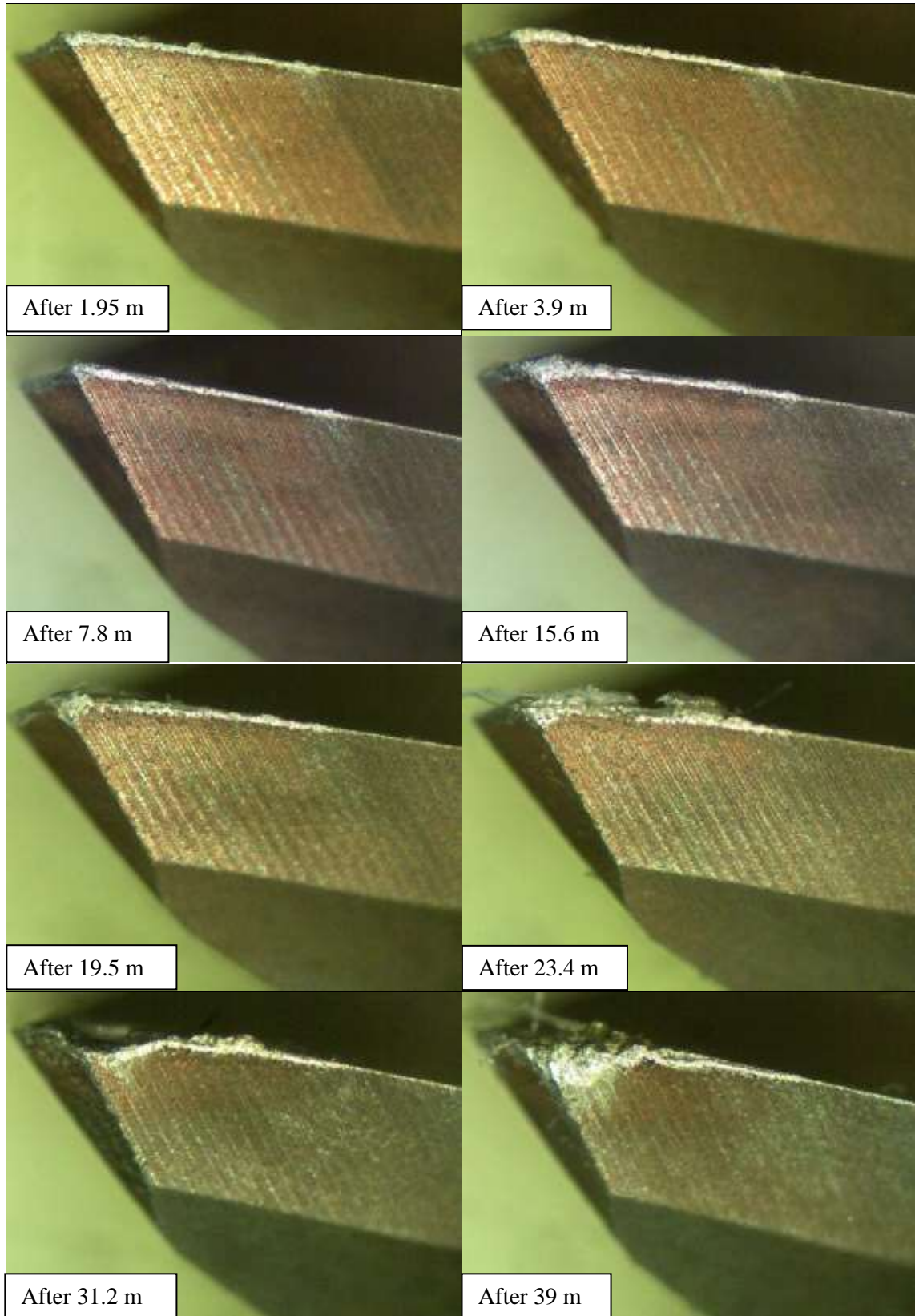


Figure 6.8 Tool images showing flank wear development until wear criterion for the most affected tooth when machining Ti-6Al-4V at 60 m/min under flood cooling

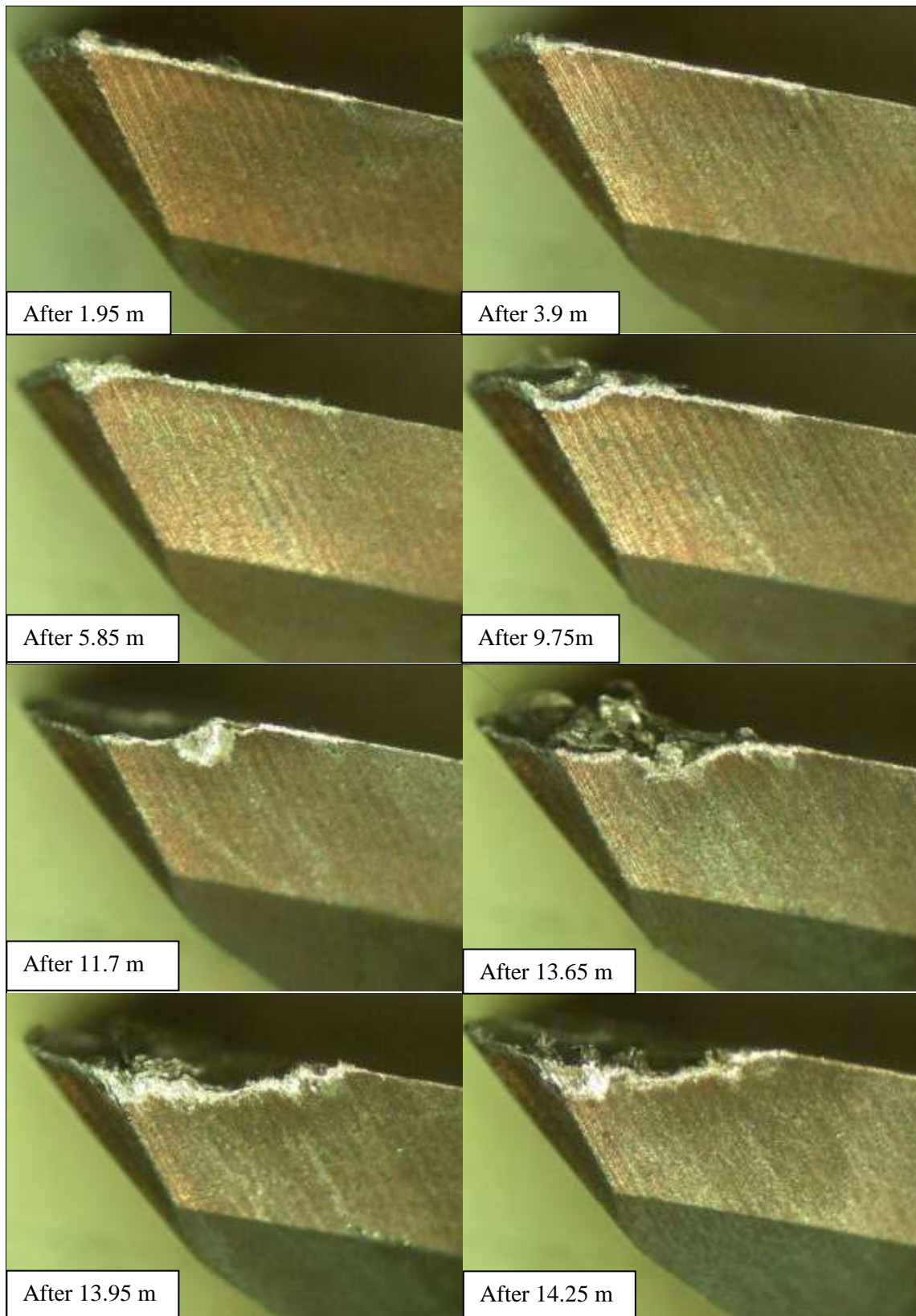


Figure 6.9 Tool images showing flank wear development until wear criterion for the most affected tooth when machining Ti-6Al-4V at 90 m/min under flood cooling

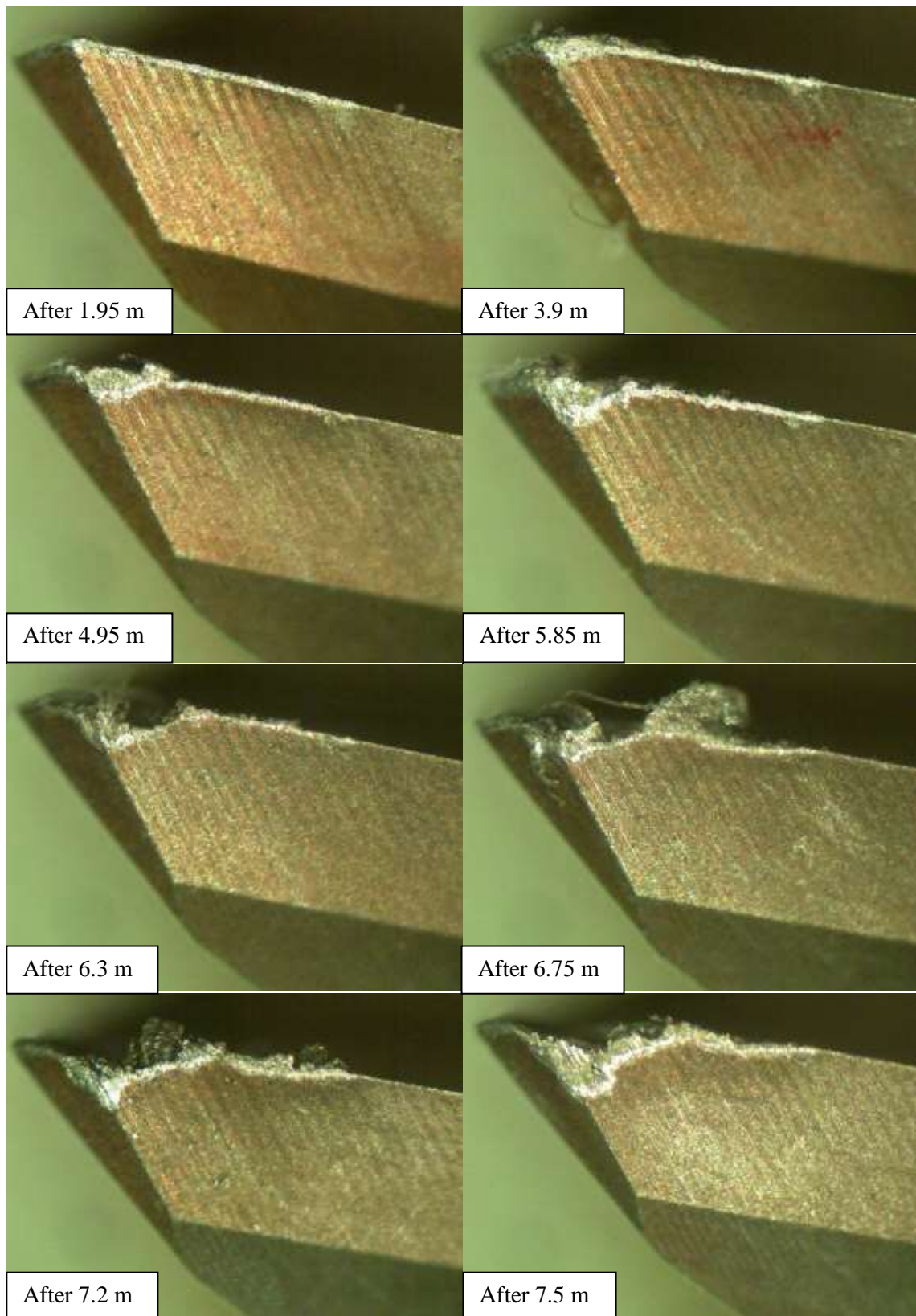


Figure 6.10 Tool images showing flank wear development until wear criterion for the most affected tooth when machining Ti-6Al-4V at 120 m/min under flood cooling

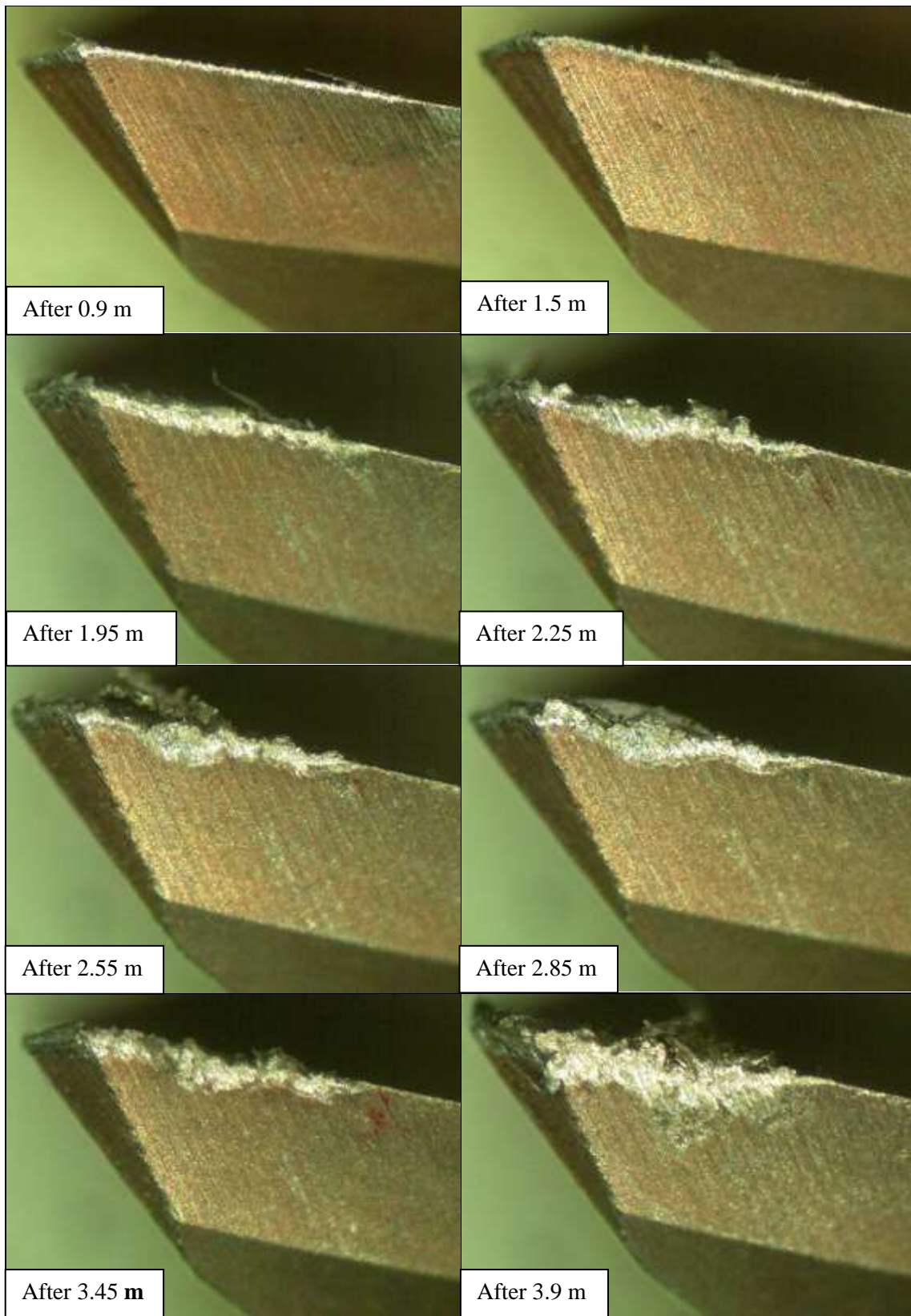


Figure 6.11 Tool images showing flank wear development until wear criterion for the most affected tooth when machining Ti-6Al-4V at 150 m/min under flood cooling

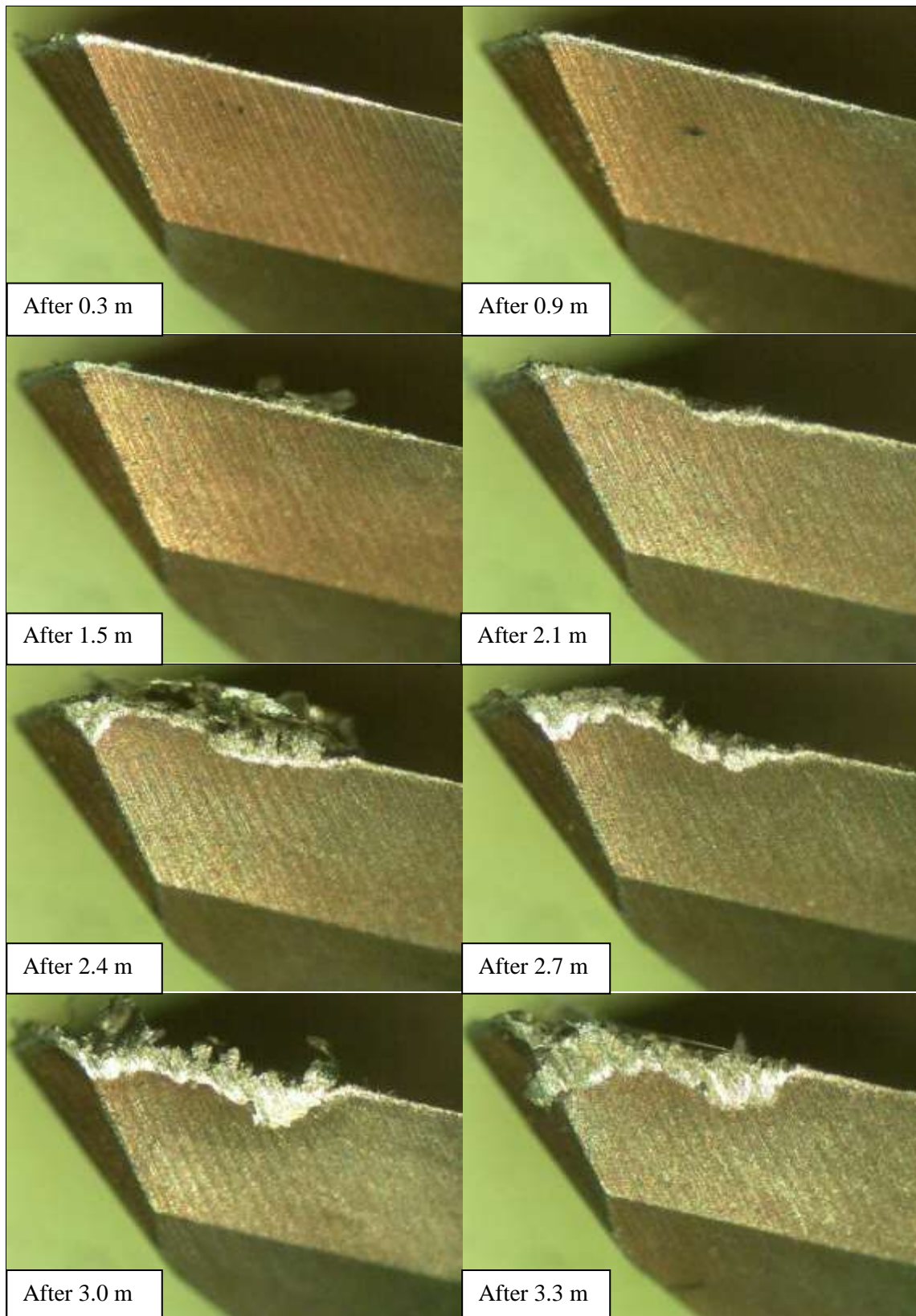


Figure 6.12 Tool images showing flank wear development until wear criterion for the most affected tooth when machining Ti-6Al-4V at 180 m/min under flood cooling

### 6.2.2 MQL machining experiments

For MQL, a dual- nozzle system sprayed rapeseed vegetable oil, one nozzle to the cutting zone and the other to the cutting tool as shown in figure 5.8. It is essential that MQL provides lubricity to the tool-chip and tool-workpiece interfaces leading to reduced cutting/friction forces and surface roughness (Park et al. 2017). At the cutting speed of 60m/min, significant improvement in tool life was achieved as shown in figure 1b. More than a three fold improvement in tool life over flood cooling was recorded (figures 6.5 and 6.6). This improvement is attributed to the reduction in friction resulting in reduced tool wear rate, as shown in figure 6.13 M1, due to effective lubrication of the cutting zone using rapeseed oil.

At early stages of machining, a smooth crater wear was developed uniformly along the rake face due to dissolution-diffusion. This is due to the elevated temperature at the tool-chip interface which promotes chemical reactivity of titanium to tool material (Hartung et al. 1982; Gearson 1986). This smooth crater wear alters the shape of the cutting edge but still keeps it considerably sharp enough to efficiently resume the cutting process as shown in figure 6.13. The progressive removal of tool rake material by dissolution-diffusion also reduces the development of attrition flank wear through the removal of the instantly worn flank and hence prolongs the tool life. It is clearly observed that the tool wear is maximum at the nose flank and linearly reduced till reaching minimum value at the depth of cut flank. This is attributed to the fact that the chemical affinity is proportional to the temperature which is highest at the tool nose (Abdel-Aal et al. 2009; Abukhshim et al. 2006), and to the difficulty of oil mist to provide sufficient lubricity to the tool nose, since the cutting tool can prevent the coolant from targeting the tool nose and cutting edge during the milling operation. By continuing the machining experiment, a slow rate of smooth dissolution-diffusion wear was generated on the tool rake associated with uniform and thin attrition flank wear uniformly distributed along the whole flank up to 195m of machining length. Then relatively rapid progress of flank wear is developed to the end of tool life at nearly 225m (figure 6.14). This rapid increase in flank wear was due to the change of the tool geometry due to the progressive loss of tool material on the rake face resulting in change of the effective rake angle. Also, the loss of sharpness of the effective cutting edge which is continuously varying due to diffusion wear could increase the cutting forces and promote thermally and mechanically related wear (plastic deformation of cutting edge). Dissolution-diffusion of the rake face and attrition of the nose flank dominated tool wear mechanism as



clearly shown in figures 6.13M1, and 6.14. It is worth noting that adhesion wear and the formation of BUE has been significantly reduced when machining Ti-6Al-4V with MQL due to the effective lubrication of the sprayed oil.

By increasing the cutting speed to 90m/min, the dissolution-diffusion crater wear characterized by its low rate is limited by the increased rate of flank attrition wear. At the early stages of machining, uniform and nearly equal in magnitude flank and crater wear are developed till nearly 63m length was cut (figure 6.15). Then loss of nose sharpness due to dissolution-diffusion occurred resulting in attrition wear at the nose flank after 78m of machining. Attrition wear was then propagated and dominated the tool wear mechanism after 125m, with a lower proportion of crater dissolution diffusion wear than that with low cutting speed experiment as shown in figures 6.13M2 and 6.15.

At 120m/min with MQL machining, it is clearly observed that dissolution-diffusion wear was even more limited, with evidence of plastic deformation of cutting edge located at the depth of cut region and attrition-abrasion flank wear at the vicinity of the tool nose after 93m length of cut as shown in figure 6.16. The increased cutting speed resulted in loss of sharpness of the tool nose even faster than at 60 and 90 m/min machining. This is due to the increased friction between to tool flank and the machined surface, especially without the corresponding increase of oil mist flow rate and/or air pressure, and limited cooling capacity of MQL resulting in insufficient lubrication and high generated friction.

With continued machining, flank wear is propagated after 109m of machining near the tool nose and the depth of cut due to loss of sharpness of cutting edge at those regions until reaching the wear criterion after 119m of machining (figure 6.16). Strong adhesion and BUE formation was observed at the later stages of machining. Flank attrition-abrasion dominated the tool wear mechanism as shown in figure 6.13M2.

When MQL milling of at 150m/min, the evolution of dissolution-diffusion wear along the rake face tended to reduce the sharpness of the cutting edge via decreasing the effective rake angle uniformly along the cutting edge resulting in uniform attrition wear along the whole flank up to 31m of machining. Then localized nose wear was observed after 35m and spread along the whole flank ending the tool life after nearly 45m (figure 6.17). BUE formation can be clearly observed at the later stages of machining owing to the limited cooling capacity of MQL to extract the generated heat. Moreover, the inadequate lubricity at high cutting speeds

could cause excessive friction and promote mechanically related wear which is characterised by its high wear rate (figure 6.2). Flank abrasion dominated the tool wear mechanism as shown in figure 6.13M4.

At higher cutting speed of 180m/min, flank attrition followed by abrasion dominated the tool wear mode with clear evidence of plastic deformation of the cutting edge which resulted from the increased cutting forces at high tool speed (figures 6.13)(Park et al. 2015; Huang et al. 2014). At 180m/min cutting speed, attrition wear was initiated at both the nose and the depth of cut flank regions at the early stages of machining due to the loss of cutting edge sharpness at those two regions and kept at a steady rate until nearly 12m (figure 6.18). It is worth noting that no evidence of dissolution-diffusion wear was observed. After exceeding 12m of machining, rapid abrasion flank wear was developed in the vicinity the tool nose and depth of cut, dominating the tool wear mechanism, and ending the tool life at 12.8 m length of cut as indicated in figures 6.13M5 and 6.18.

In all MQL machining tests, significant improvements of tool life have been achieved with a range of improvement as high as 3-12 fold compared with corresponding flood cooling experiments. The maximum improvement in tool life has been attained at the cutting speed of 120m/min, while the maximum cutting length of 224m was recorded at 60m/min as indicated in figures 6.5 and 6.7. Using MQL, the machined length at cutting speed of 150m/min, is comparable to that for flood cooling at 60m/min with more than 50% higher productivity. Moreover, no evidence of adhesion on the tool flank was observed. BUE on the rake face was eliminated at low and moderate cutting speeds MQL experiments (60 and 90m/min). This can be attributed to the effective penetration of oil mist to the cutting interfaces at low cutting speeds demonstrating effective lubrication. The carbon formation around the tool flank wear area gives evidence that evaporation and burning of oil occurred in all MQL machining experiments. This indicates that MQL can significantly improve the machining performance by reducing the generated temperature through reduction in friction at the tool-chip and tool-workpiece interfaces. However, MQL might not be effective to provide the adequate cooling to reduce or extract the heat generated at the primary shear zone.

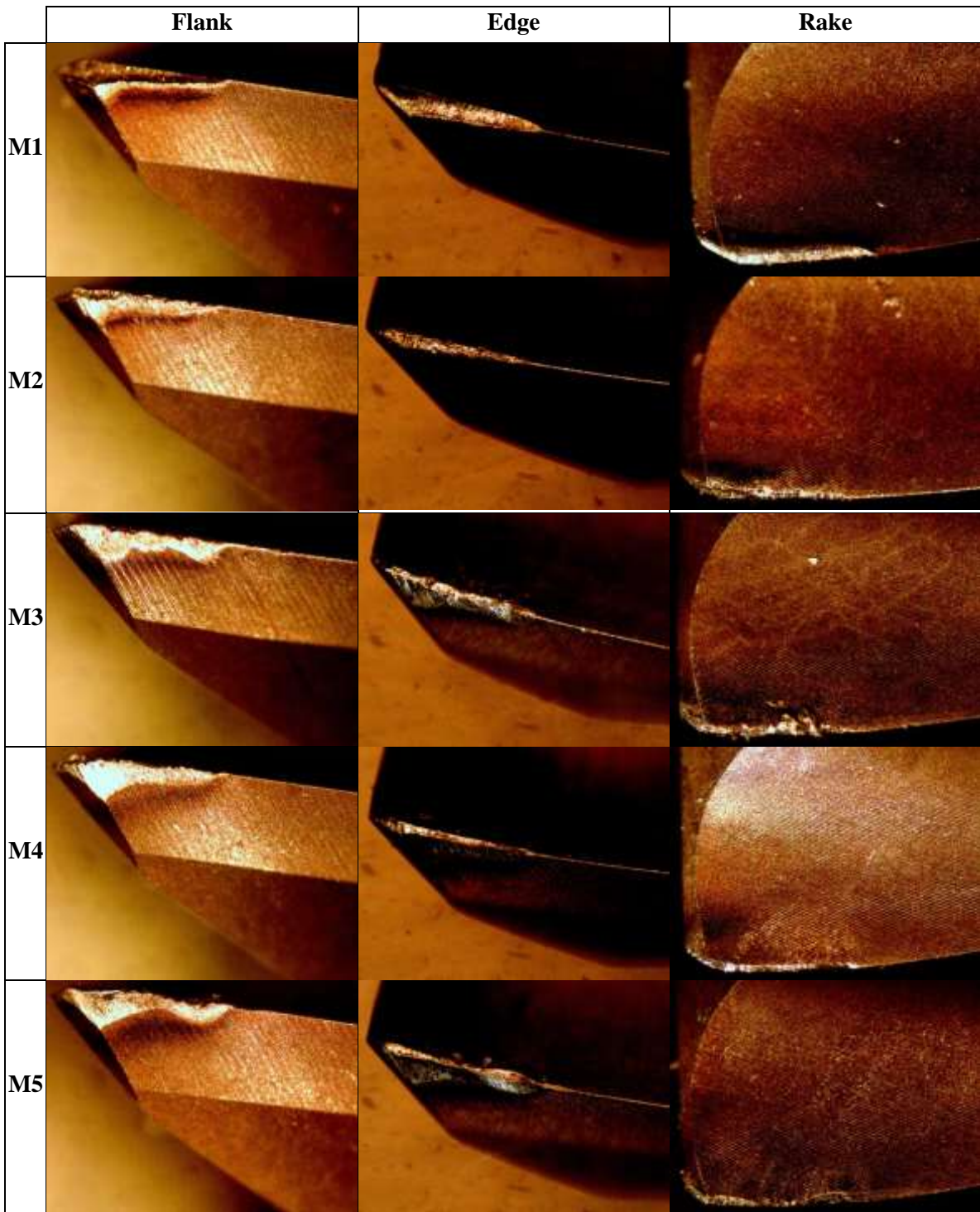


Figure 6.13 Images of tool taken with three views at rake face, cutting edge, and flank face at different cutting speeds; 60, 90, 120, 150, 180 m/min under MQL, after the wear criterion has been reached

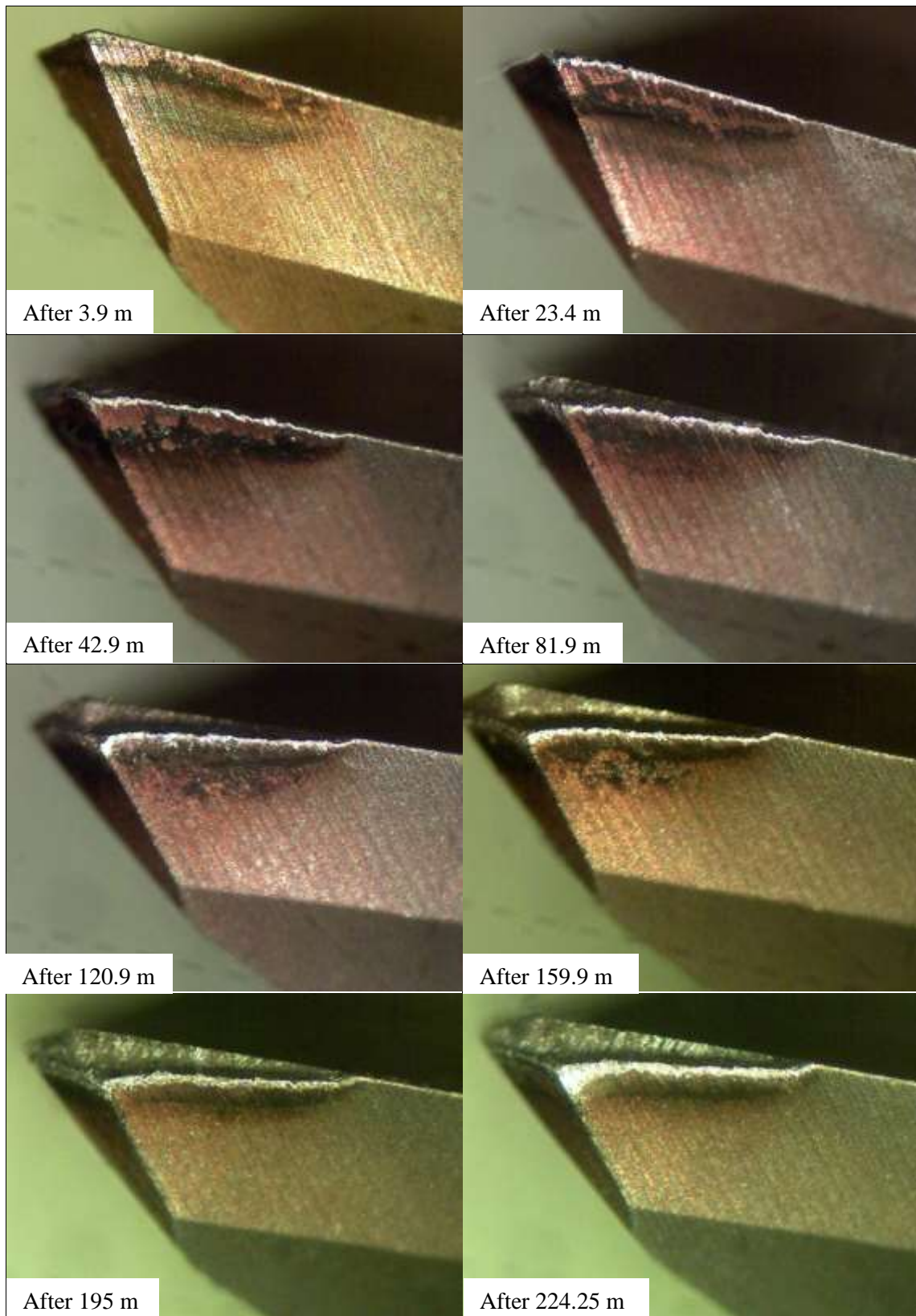


Figure 6.14 Tool images showing flank wear development until wear criterion for the most affected tooth when machining Ti-6Al-4V at 60 m/min under minimum quantity lubrication.

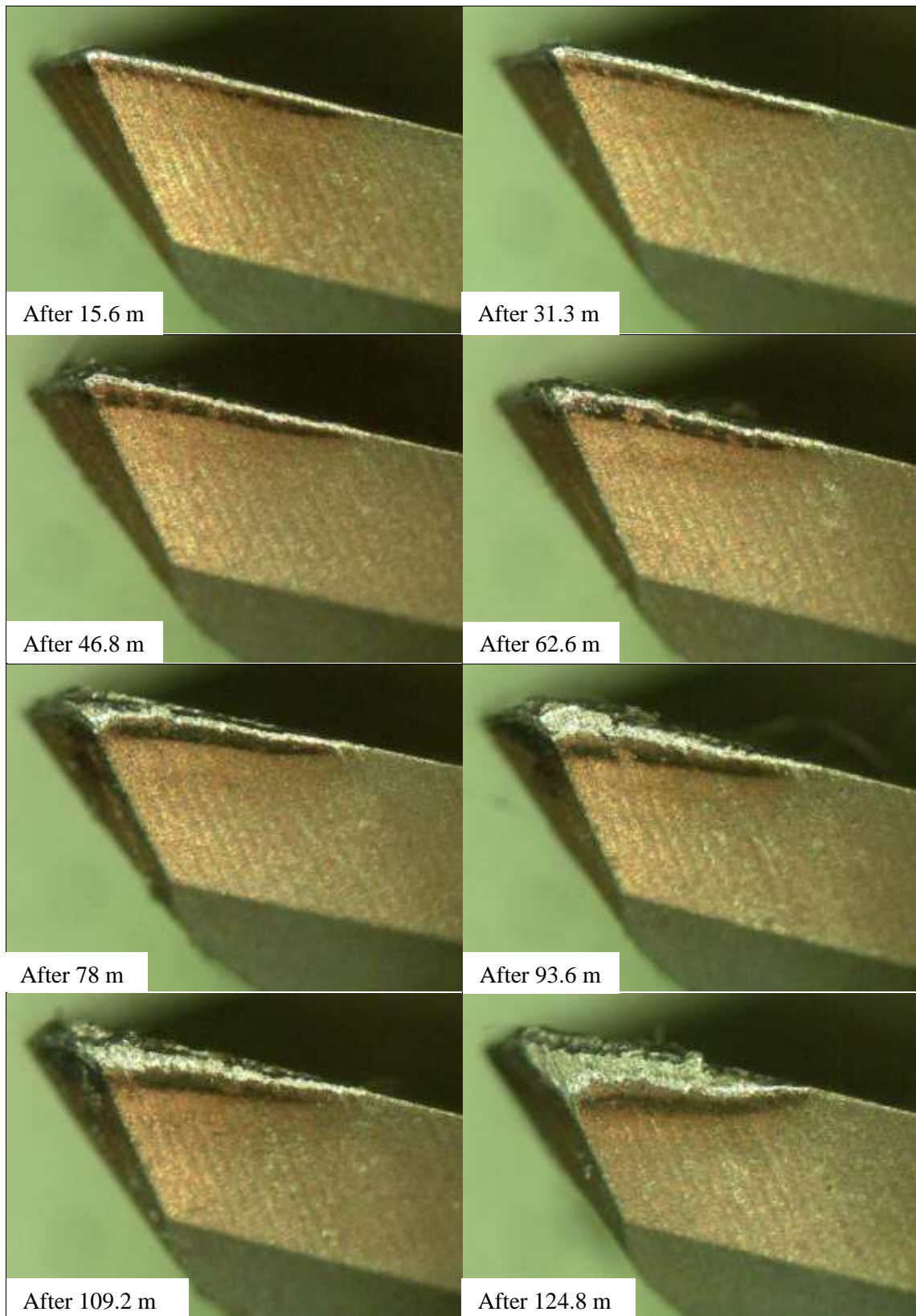


Figure 6.15 Tool images showing flank wear development until wear criterion for the most affected tooth when machining Ti-6Al-4V at 90 m/min under minimum quantity lubrication.

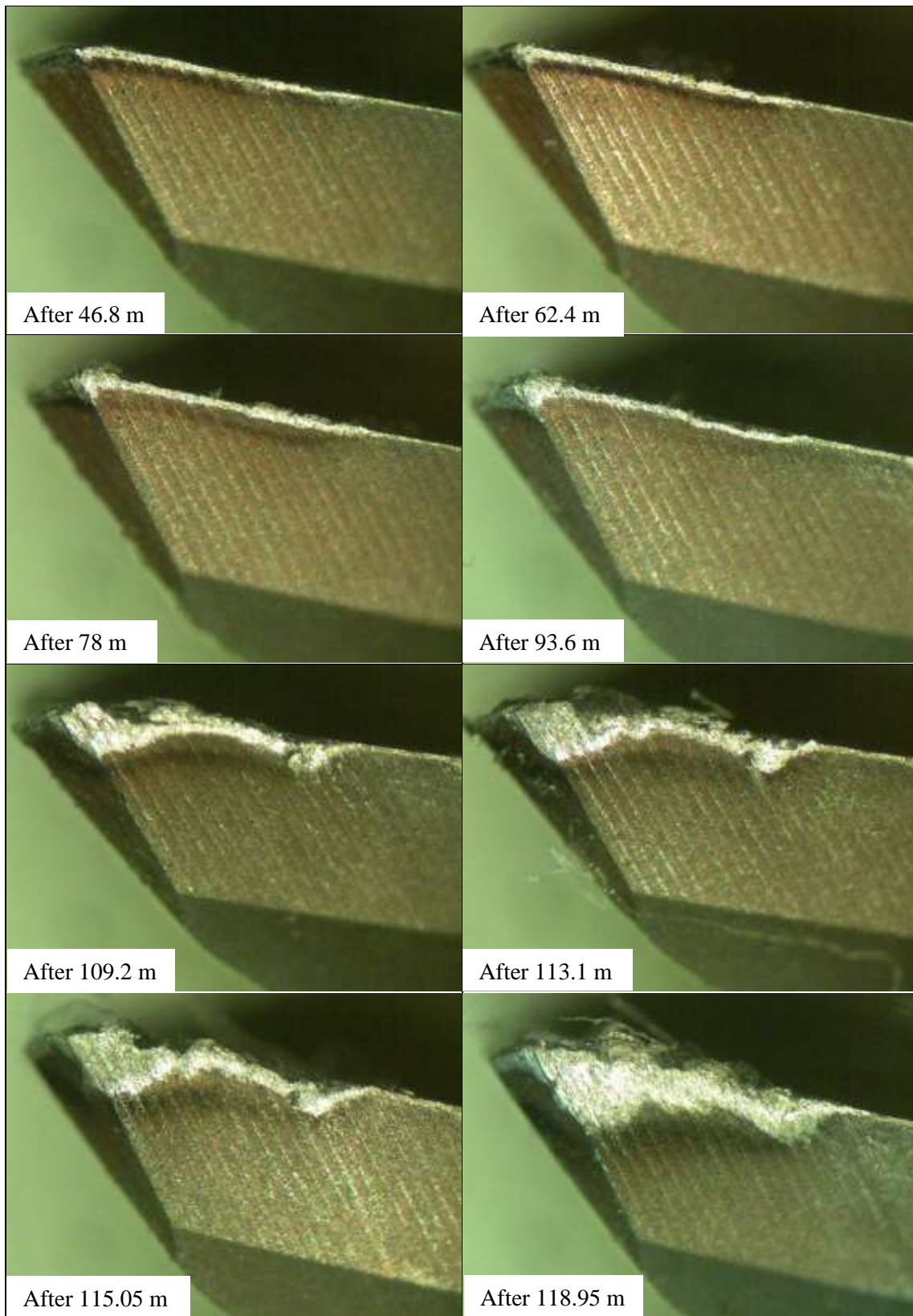


Figure 6.16 Tool images showing flank wear development until wear criterion for the most affected tooth when machining Ti-6Al-4V at 120 m/min under minimum quantity lubrication.

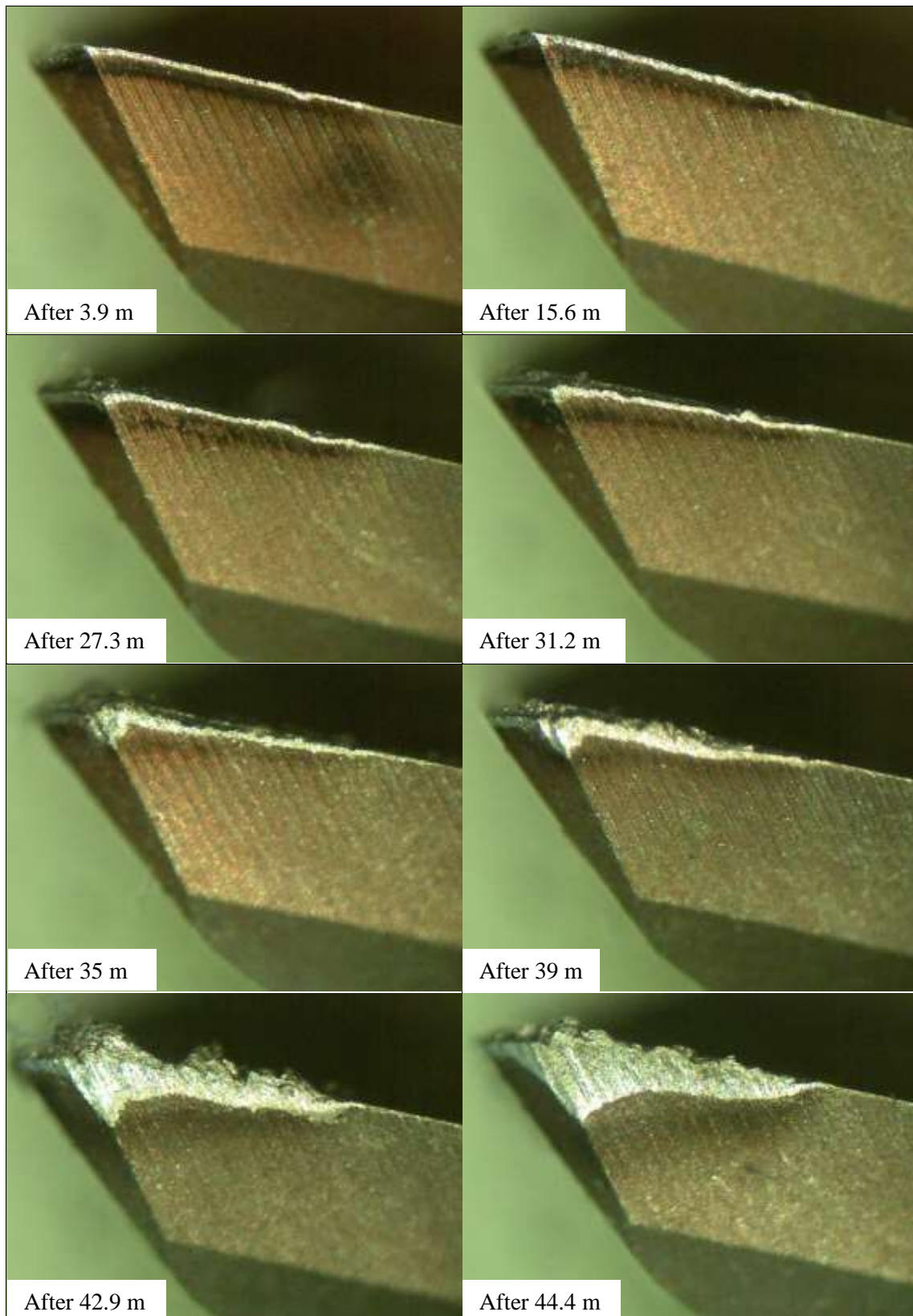


Figure 6.17 Tool images showing flank wear development until wear criterion for the most affected tooth when machining Ti-6Al-4V at 150 m/min under minimum quantity lubrication.

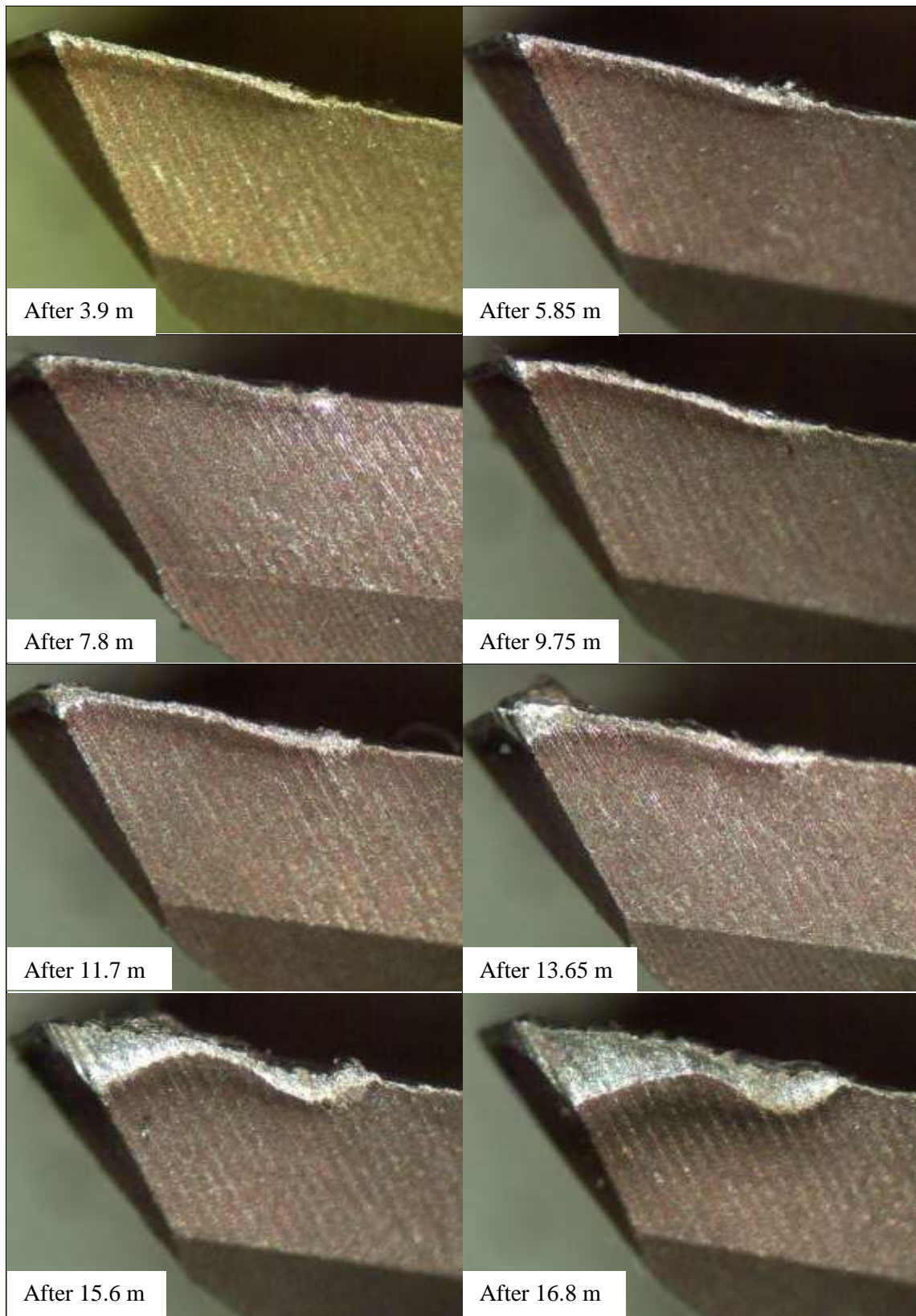


Figure 6.18 Tool images showing flank wear development until wear criterion for the most affected tooth when machining Ti-6Al-4V at 180 m/min under minimum quantity lubrication.



### 6.2.3 Cryogenic machining experiments

For cryogenic machining, two nozzles sprayed LN2 one directly to cutting zone and the other to the cutting tool in a similar orientation to that of MQL as illustrated in figure 5.9. The excessive cooling of the cutting zone caused an increase in tool wear rate resulting in premature tool failure (figures 6.19C1 and 6.3). At the beginning of the cryogenic machining experiment at low cutting speed, namely 60 m/min, and after only less than 1m machining length, there was evidence of initiation of fragmentation and plastic deformation of the cutting edge at the depth of cut region, while the tool nose remained intact as shown in figure 6.20. This could be explained by excessive local hardening of Ti-6Al-4V workpiece especially at the peripheral surface at the vicinity of the tool cut depth due to the direct spraying of LN2 to the cutting zone. After nearly 6m of machining, nose deformation and initiation of nose flank wear was observed (figure 6.20). This rapid development of mechanical wear (abrasion) at the nose and depth of cut flank regions resulted in a tool life of 13.65m shorter than that of flood cooling. Plastic deformation and fracture/chipping of cutting edge and abrasion of tool flank dominate of the tool wear mechanism at low cryogenic machining of 60m/min as shown in figure 6.19C1. It is well observed that tool coating at the flank, rake and the areas around have been adversely affected by the direct spraying of LN2 to the cutting tool which, weakens the bonding between the coating and the tool substrate due to the differential coefficient of thermal contraction which causes coating delamination as shown in figures 6.19 – 6.24.

An increase in flank wear due to attrition-abrasion was observed at moderate to the high cutting speed range of 90-150m/min, with initiation and propagation of micro and macro fracture of the cutting edge at the vicinity to the depth of cut as shown in figures 6.19, 6.21, 6.22, and 6.23. This mechanically related wear mode is even accelerated at the high cutting speed of 180m/min, as indicated in figures 6.19C5, and 6.24.

Cryogenic machining enabled a significant reduction in the cutting temperature, and hence chemically related tool wear due to crater dissolution-diffusion. Outstanding enhancement in terms of tool life at high cutting speeds was achieved over flood cooling with maximum improvement of 250% at 150 m/min as indicated in figures 6.5 and 6.6. However, the direct spraying of the LN2 to cutting area caused excessive hardening of Ti-6Al-4V, which resulted in plastic deformation at the cutting edge and chipping in the vicinity of the depth cut where

maximum hardening occurred. On the other hand, coating delamination was observed in all cryogenic machining experiments at the flank and rake faces. At the flank face, coating delamination progressed with increasing the machining time. It is worth noting that the tool coating was adversely affected by the direct spraying of LN2 to the cutting tool which could weaken the bonding between the coating and the tool substrate (figures 6.19 -6.24).

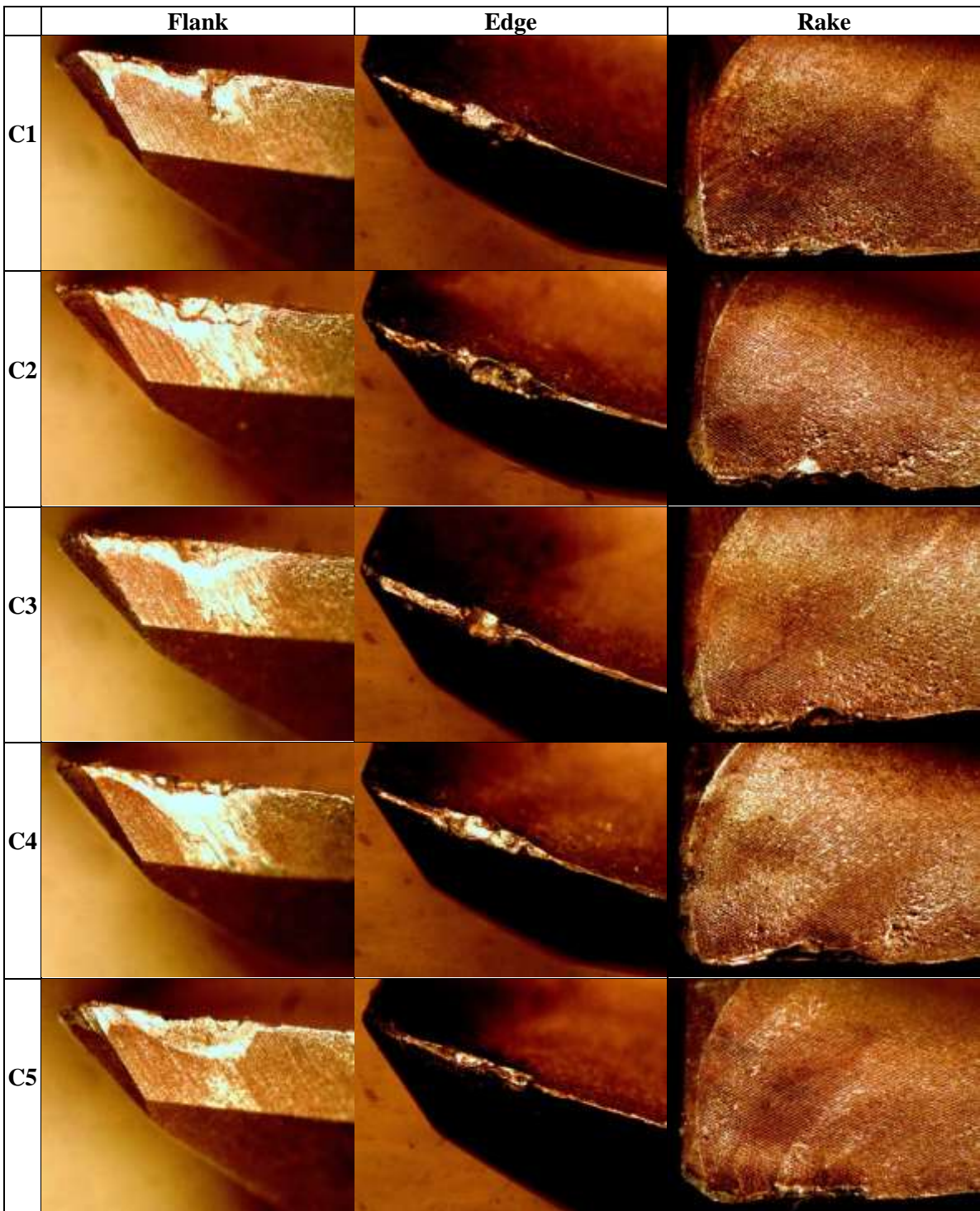


Figure 6.19 Images of tool with three views at rake face, cutting edge, and flank face at different cutting speeds; 60, 90, 120, 150, 180 m/min with cryogenic cooling, taken after the wear criterion has been reached

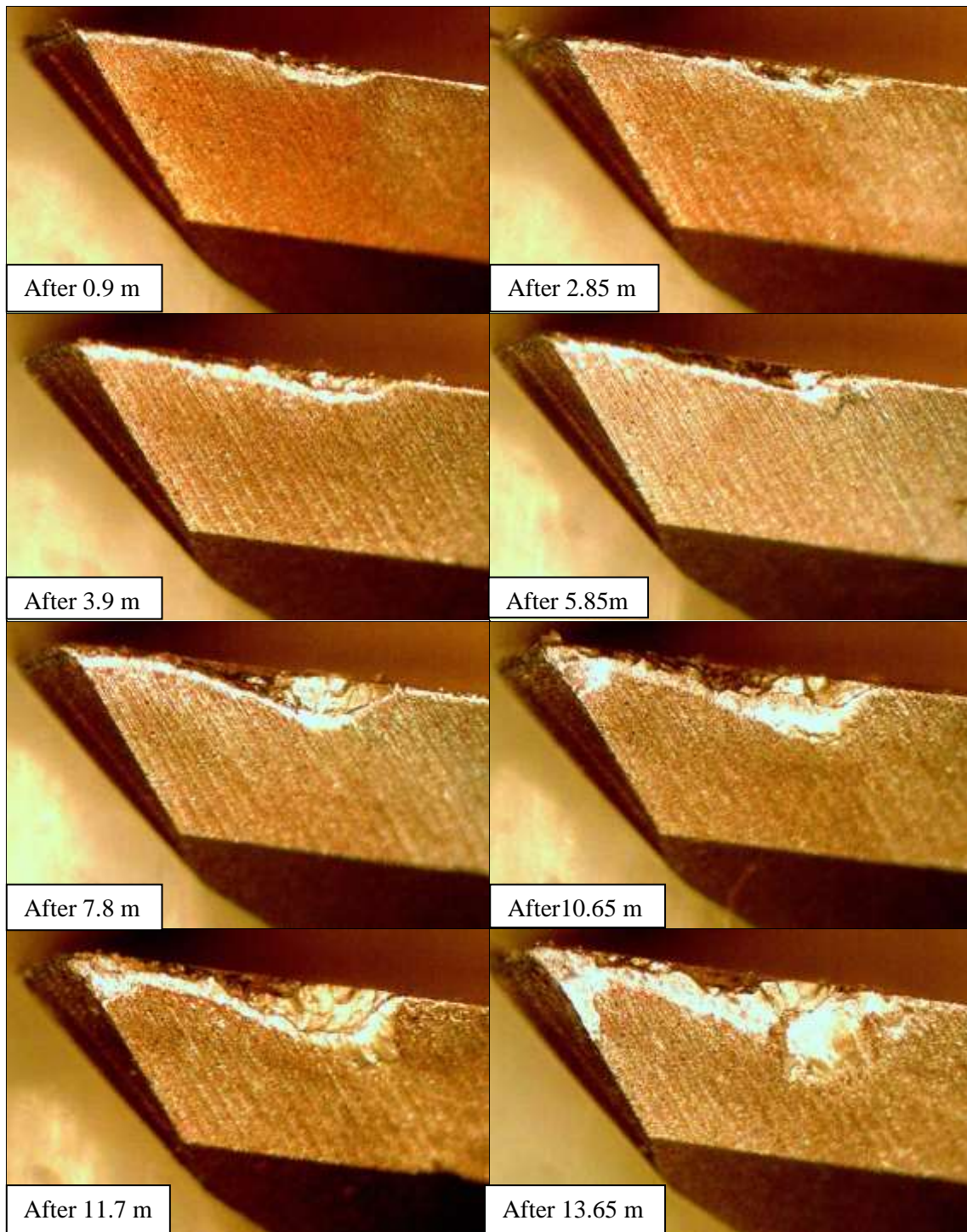


Figure 6.20 Tool images showing flank wear development until wear criterion for the most affected tooth when machining Ti-6Al-4V at 60 m/min under cryogenic cooling.

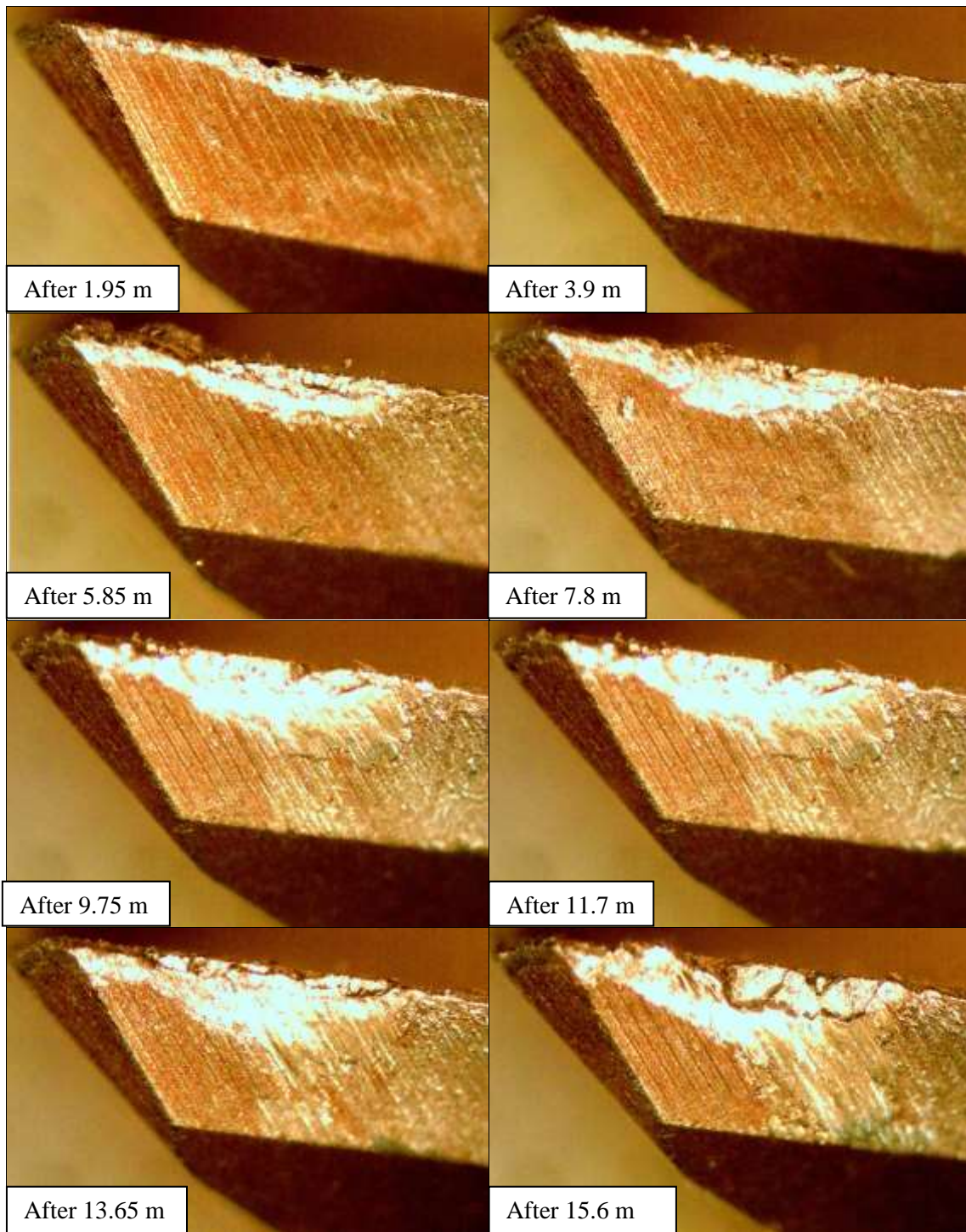


Figure 6.21 Tool images showing flank wear development until wear criterion for the most affected tooth when machining Ti-6Al-4V at 90 m/min under cryogenic cooling.

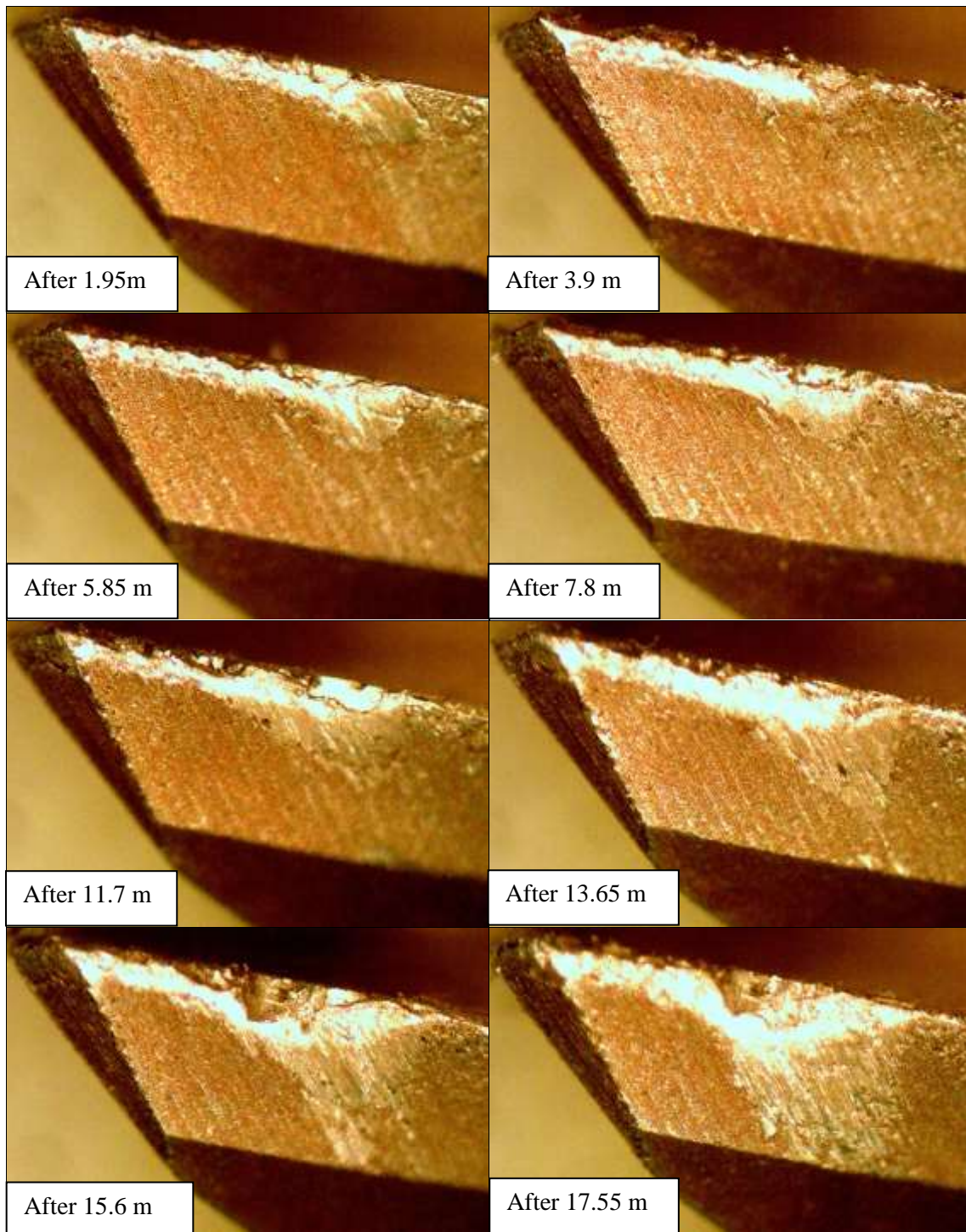


Figure 6.22 Tool images showing flank wear development until wear criterion for the most affected tooth when machining Ti-6Al-4V at 120 m/min under cryogenic cooling.

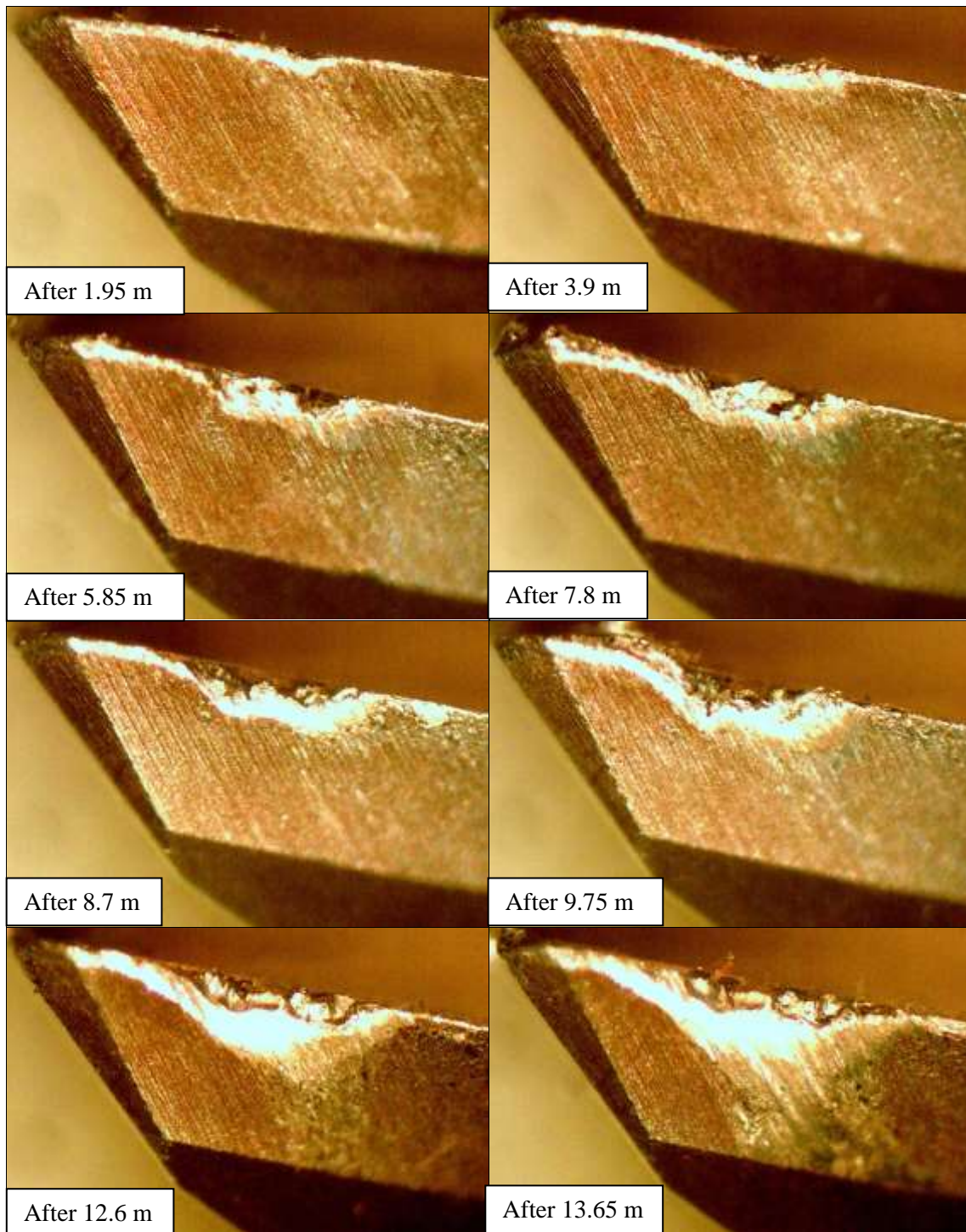


Figure 6.23 Tool images showing flank wear development until wear criterion for the most affected tooth when machining Ti-6Al-4V at 150 m/min under cryogenic cooling.

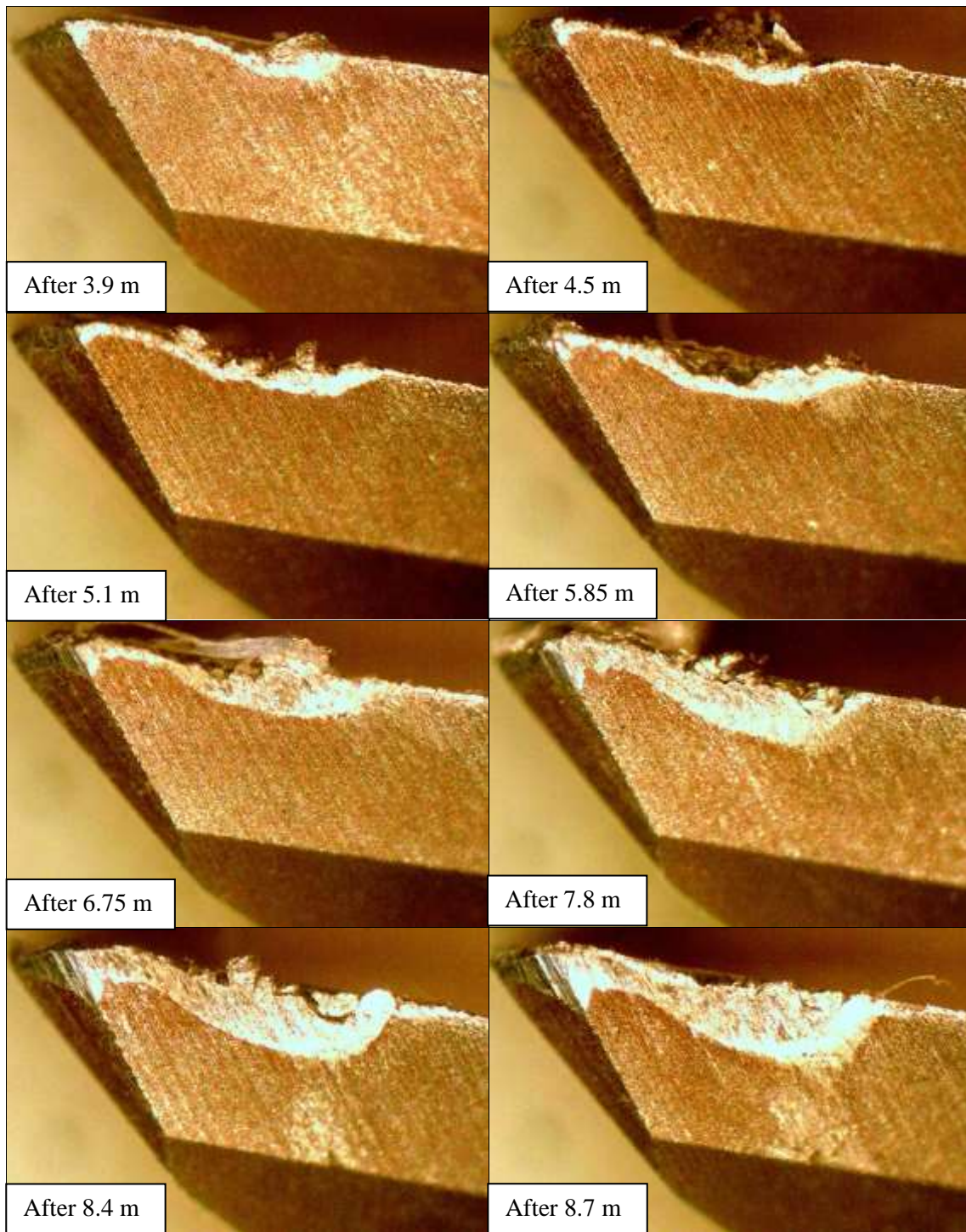


Figure 6.24 Tool images showing flank wear development until wear criterion for the most affected tooth when machining Ti-6Al-4V at 180 m/min under cryogenic cooling.



#### 6.2.4 Hybrid cryogenic/MQL machining experiments

Hybrid cooling/lubricating strategy with combined application of a dual-nozzle MQL and cryogenic cooling systems shown in figure 5.10, demonstrated a significant improvement in tool life in comparison to conventional flood cooling. It showed the best machining performance among all investigated cooling/lubricating conditions and surpassed that for MQL at 60 and 90 m/min. Figure 6.25 showed the outstanding improvement in machining performance in terms of tool wear when hybrid cryogenic/MQL is applied in comparison with MQL and flood cooling. It recorded nearly a 30 fold improvement in tool life over flood cooling; cutting length of 430m, and cutting time of 1200 min at 90m/min, while nearly 5 fold compared with conventional flood cooling; with 307m cutting length, 1280 min cutting time at 60m/min (figures 6.5 and 6.6). This outstanding improvement in tool life was due the efficient cooling and lubrication that suppressed the thermally related wear and delayed the mechanically related wear.

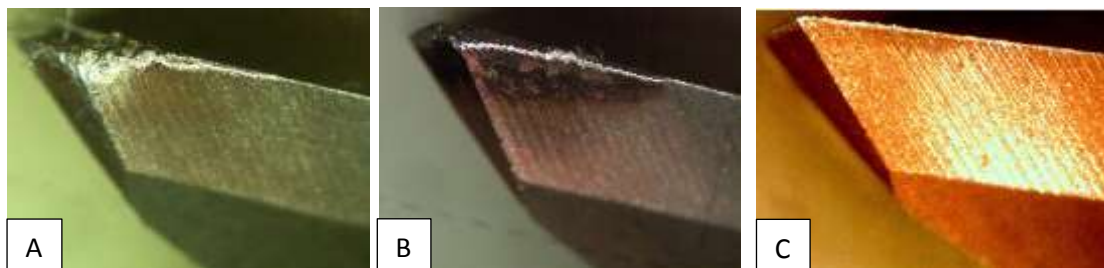


Figure 6.25 Tool images taken for different machining environments at cutting speed of 60 m/min and after nearly 53m length of cut (tool life for food cooling). A) Flood cooling. B) MQL. C) Hybrid cryogenic/MQL.

For low speed hybrid MQL/cryogenic machining at 60m/min, a significant improvement in machining performance in terms of tool life compared to all other cooling/lubricating conditions was achieved in comparison with flood cooling as indicated in figures 6.5 and 6.6. The cutting tool retained its sharpness until 200m cutting length with a cutting time of 840min as clearly shown in figure 6.26. after this, small tip chipping/flaking evolved causing loss of nose sharpness, resulting in localised attrition wear at the nose flank which then propagated and dominated the wear mode until the end of tool life (figures 6.26 and 6.27H1). However, clear evidence of oil burning around the tool flank wear was attributed to the fact that LN2 flow rate was not sufficient enough to reduce the cutting tool temperature to the optimum value that yielded the longest tool life.

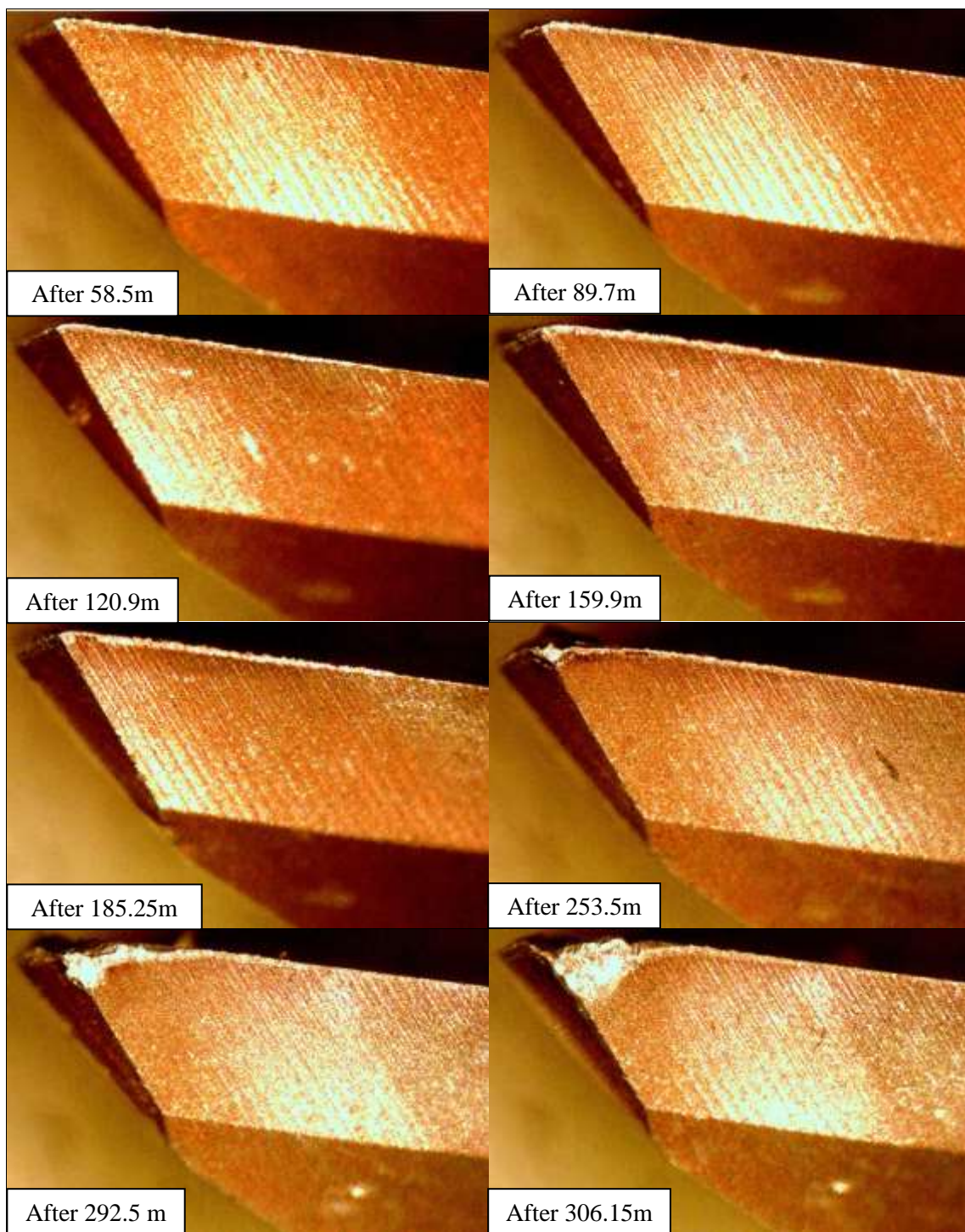


Figure 6.26 Tool images showing flank wear development until wear criterion for the most affected tooth when machining Ti-6Al-4V at 60 m/min under hybrid cryogenic/ MQL

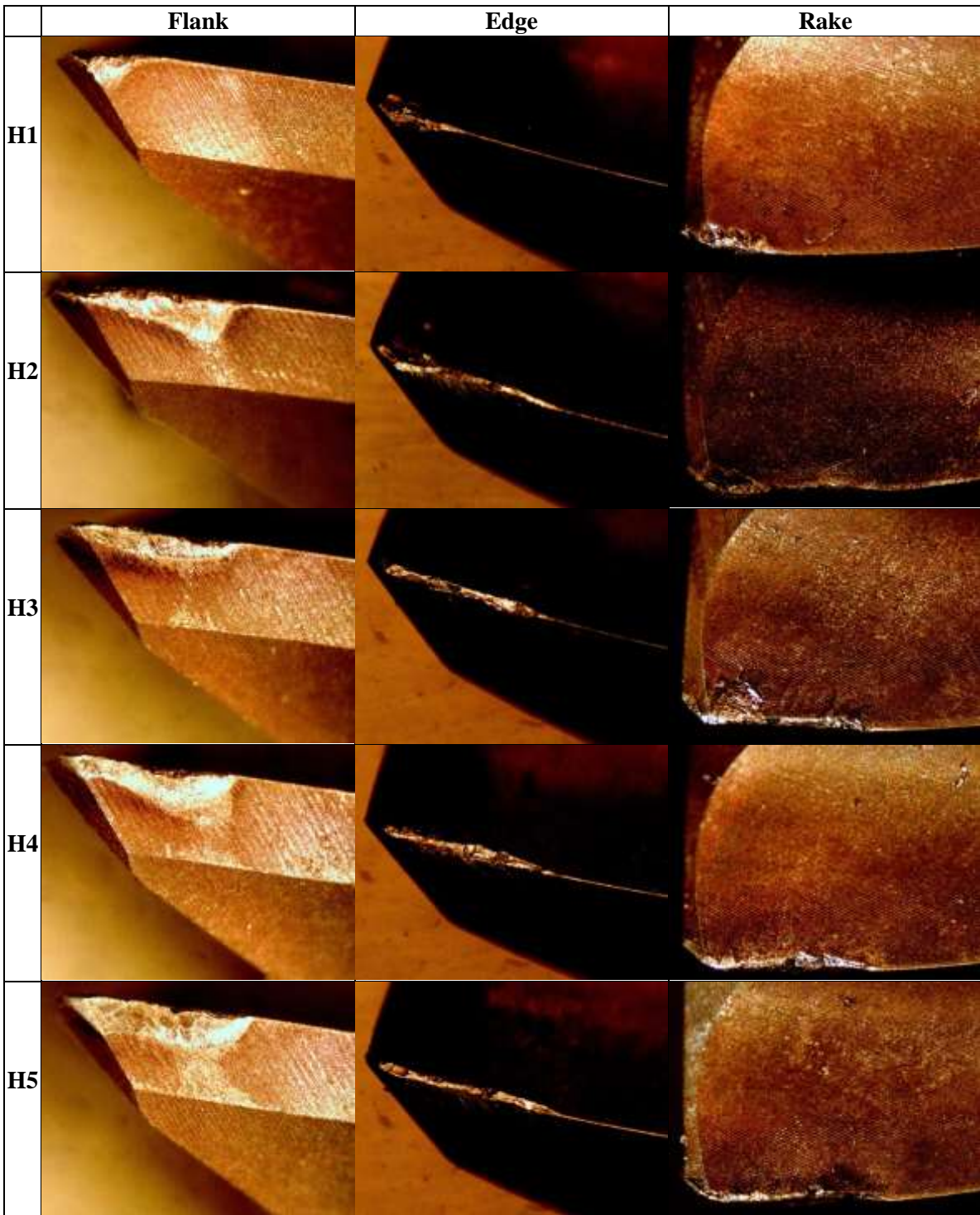


Figure 6.27 Images of tool with three views at rake face, cutting edge, and flank face at different cutting speeds; 60, 90, 120, 150, 180 m/min under hybrid cryogenic/MQL, taken after the wear criterion has been reached

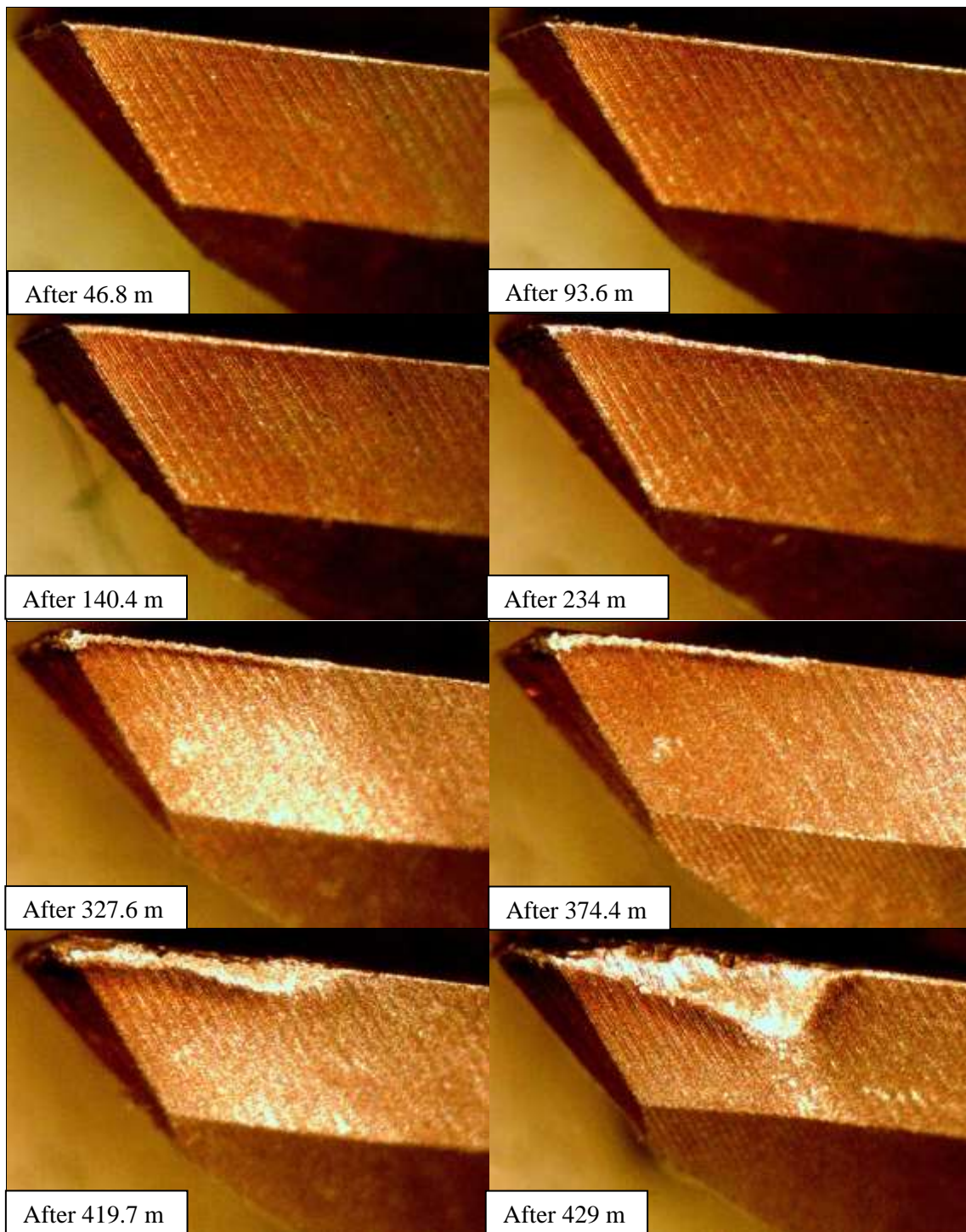


Figure 6.28 Tool images showing flank wear development until wear criterion for the most affected tooth when machining Ti-6Al-4V at 90 m/min under hybrid cryogenic/ MQL

At 90m/min hybrid cooling/lubrication, the best machining performance and the longest tool life was observed among all machining experiments as shown in figures 6.5 and 6.6. Uniform attrition wear at the whole of the flank initiated after 234m machining due to uniform loss of sharpness along the whole length of cutting edge as shown in figure 6.28. Then attrition wear developed uniformly along the whole flank and propagated at the depth of cut flank, ending the tool life after 429m, and was the dominant tool wear mechanism (figure 6.27H2).

For the hybrid machining experiment at 120 m/min, the cutting tool remained sharp until nearly 40m of machining. Then, a very small and uniform flank wear developed along the whole cutting edge with slightly localised wear at the nose flank. At 70m machining, evidence of loss of sharpness of the cutting edge was observed along the whole depth of cut causing rapid flank wear growth resulting in reaching the wear criterion at 86m machining length (figure 6.29). Uniform attrition-abrasion at the whole flank dominated the tool wear mechanism as shown in figures 6.27H3. Despite the fact that MQL slightly outperformed hybrid cryogenic/MQL experiment at 120 m/min., it is still many folds better than conventional flood cooling (more than 10 fold of improvement in tool life) as shown in figure 6.5 and 6.6. Moreover, results indicated that tool life with hybrid cryogenic/MQL at 120 m/min is even higher than that when flood cooling at the recommended cutting speed of 60m/min (figures 6.6, and 6.29).

At high cutting speeds, 150 and 180 m/min, hybrid cooling failed to outperform MQL in spite of its superiority over flood cooling (figures 6.30 and 6.31, and table 6.1). This can be attributed to the fact that the application of LN2 adversely affects the lubricity of MQL when they are simultaneously applied. Also, increasing the cutting speed impedes the frozen oil droplet from being adhered to the tool surface, tool/chip, and tool/workpiece interfaces which could promote flank abrasion that causes chip burning as observed when machining at these speed levels. Attrition-abrasion wear along the whole flank dominated the tool wear mechanism at moderate and high cutting speeds (figures 6.27, 6.30, and 6.31).

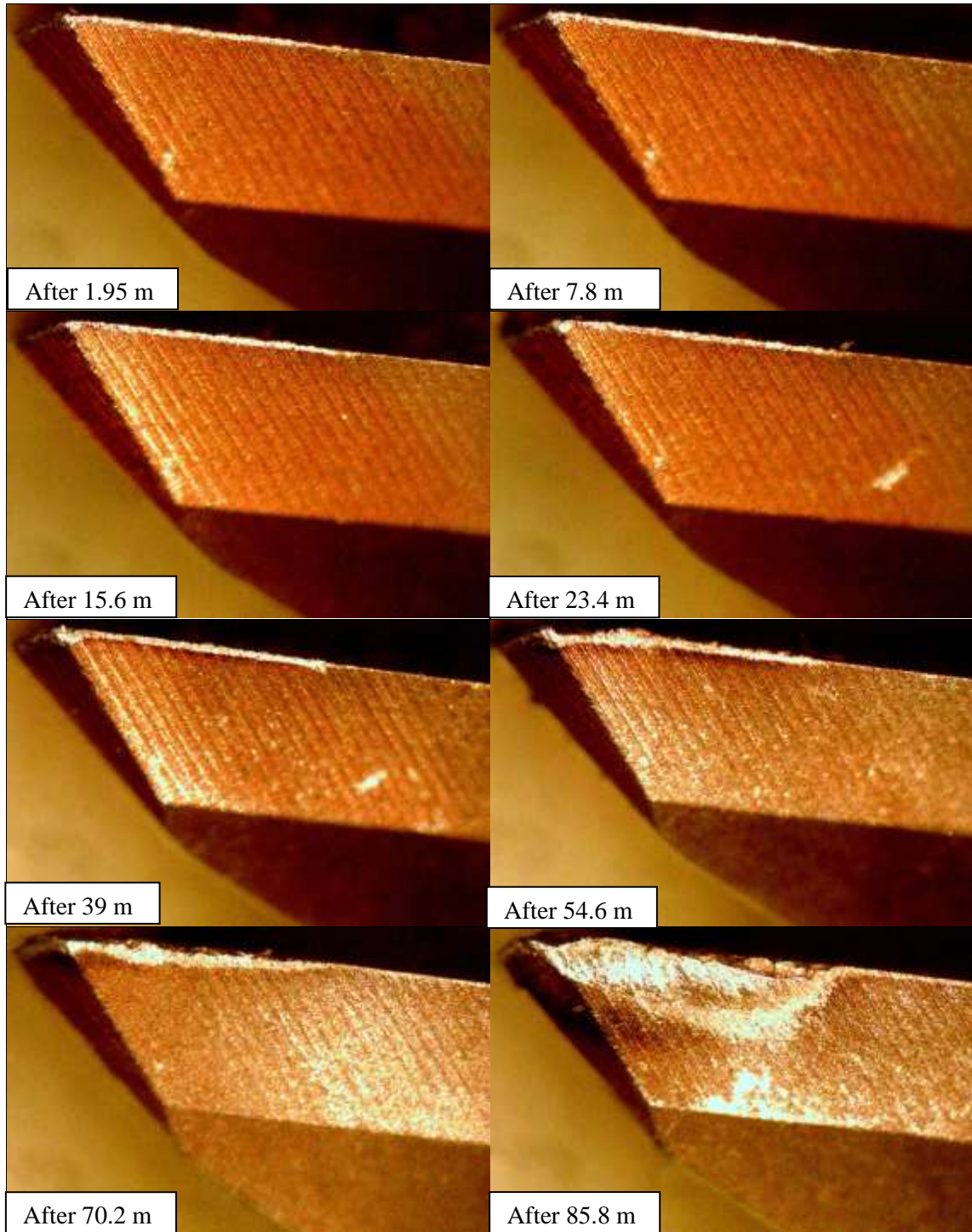


Figure 6.29 Tool images showing flank wear development until wear criterion for the most affected tooth when machining Ti-6Al-4V at 120 m/min under hybrid cryogenic/ MQL

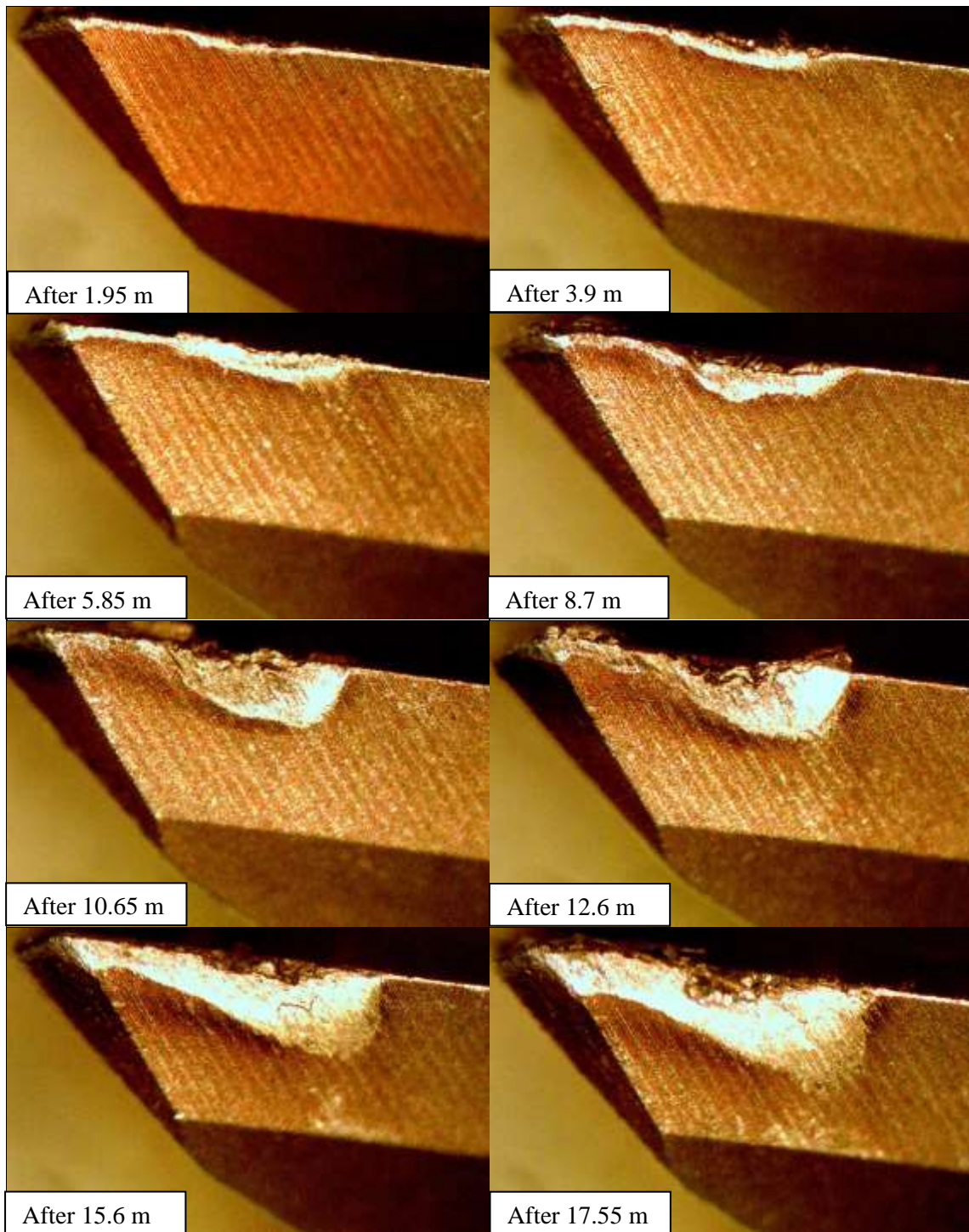


Figure 6.30 Tool images showing flank wear development until wear criterion for the most affected tooth when machining Ti-6Al-4V at 150 m/min under hybrid cryogenic/ MQL

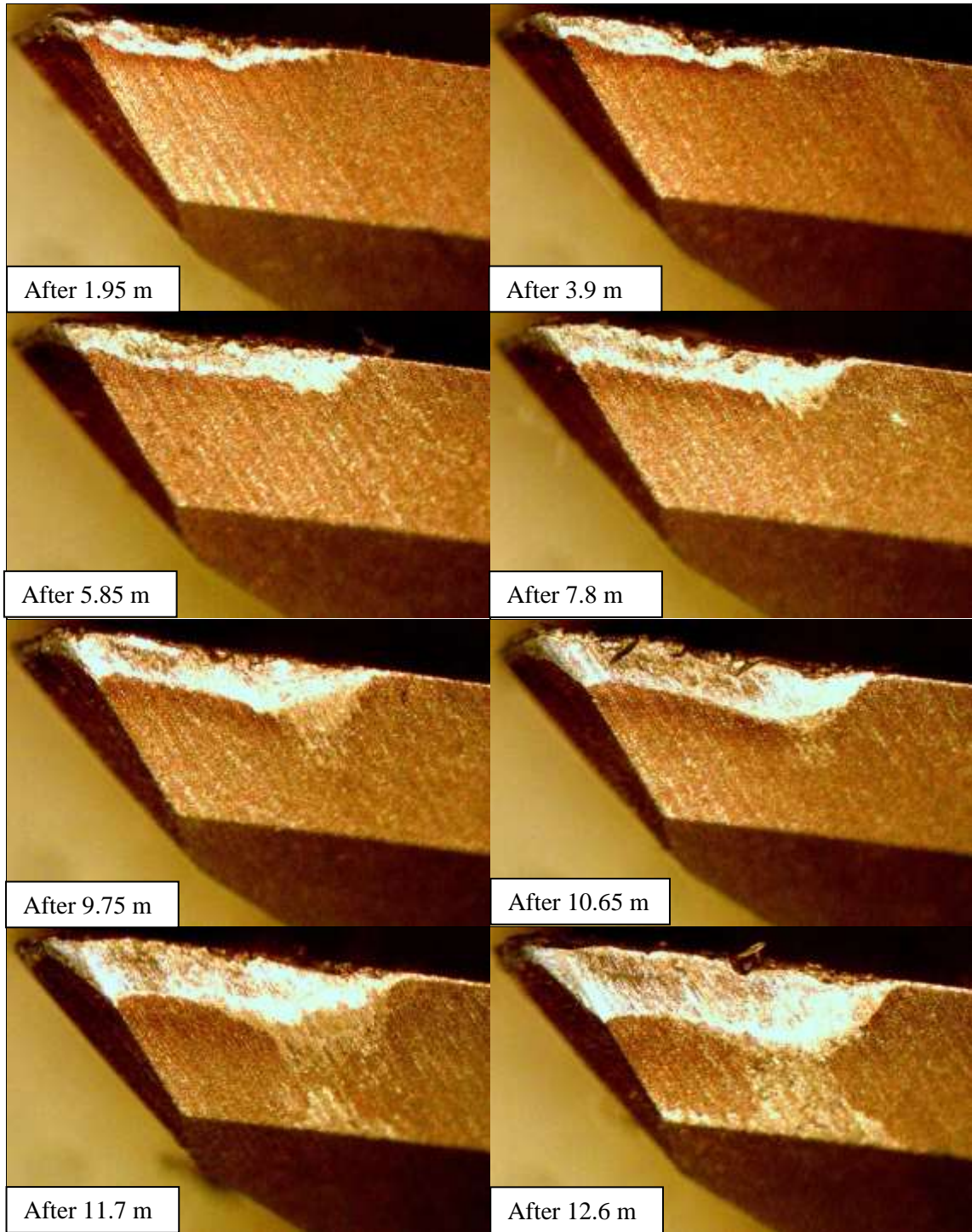


Figure 6.31 Tool images showing flank wear development until wear criterion for the most affected tooth when machining Ti-6Al-4V at 180 m/min under hybrid cryogenic/ MQL



In all hybrid cooling/lubricating experiments crater dissolution-diffusion wear has been dramatically reduced due to the effective cryogenic cooling to the cutting tool zone. The phenomena of lack of bonding of the tool coating experienced in cryogenic machining has been completely eliminated in all hybrid experiments due to the effect of oil mist that adhered to the tool surface and protected the tool coating from direct spraying of LN<sub>2</sub>. Also, to avoid excessive local hardening of the workpiece due to direct spraying of LN<sub>2</sub> to the cutting region, the two cryogenic nozzles were directed only to the cutting tool (figure 5.10). This cooling strategy has kept the tool temperature well below the softening temperature of the tool material and prevented the super cooled tool from being heated to the dissolution temperature with titanium. Furthermore, the inclination of the two cryogenic nozzles to the machining surface allowed for adequate cooling of the workpiece through the reflected LN<sub>2</sub> jets from the tool to the machined surface. This reduced the chemical affinity of the titanium alloy to the tool material without considerable increase of the hardness of the alloy. On the other hand, the MQL nozzles provided the necessary lubrication and hence, significantly reduced the flank attrition wear rate and eliminated the adhesion of titanium chips and workpiece to the rake and flank faces, results in reduced BUE.

### **6.3 Results of surface roughness**

For surface roughness, table 6.2 and figure 6.32 depicts the results of surface roughness for all machining and cooling/lubricating conditions. It can be clearly seen that for, all cutting speeds, that MQL outperformed all other cooling/lubricating conditions with an average value of  $R_a$  of nearly 0.2  $\mu\text{m}$  and improvement up to 50% compared with conventional flood cooling, owing to effective lubricating strategy with dual-nozzle MQL that enabled a significant reduction in adhesion and hence reduced BUE. Hybrid cooling was shown to be comparable to flood cooling at low and moderate cutting speeds, whilst outperforming flood cooling at higher cutting speeds. However, cryogenic machining showed the worst performance in terms of surface finish which was even exacerbated with increasing the cutting speed due to the poor lubricity of LN<sub>2</sub> which promoted adhesion, hence the formation of BUE.

Table 6.2 Surface roughness results and percentage of improvement compared with flood cooling

| Experiment ID | Average surface roughness $R_a$ ( $\mu\text{m}$ ) | % Improvement in surface roughness |
|---------------|---|------------------------------------|
| F1            | 0.1974  | -                                  |
| F2            | 0.2675  | -                                  |
| F3            | 0.2974  | -                                  |
| F4            | 0.4286  | -                                  |
| F5            | 0.2878  | -                                  |
| M1            | 0.1616  | 18.1                               |
| M2            | 0.2025  | 24.3                               |
| M3            | 0.2025  | 31.9                               |
| M4            | 0.2103  | 50.9                               |
| M5            | 0.2342  | 18.6                               |
| C1            | 0.2933  | -48.6                              |
| C2            | 0.3184  | -19.0                              |
| C3            | 0.3806  | -28.0                              |
| C4            | 0.4375  | -2.1                               |
| C5            | 0.5759  | -100                               |
| H1            | 0.2184  | -10.6                              |
| H2            | 0.2582  | 3.5                                |
| H3            | 0.3139  | -5.5                               |
| H4            | 0.3083  | 28.0                               |
| H5            | 0.2407  | 16.4                               |

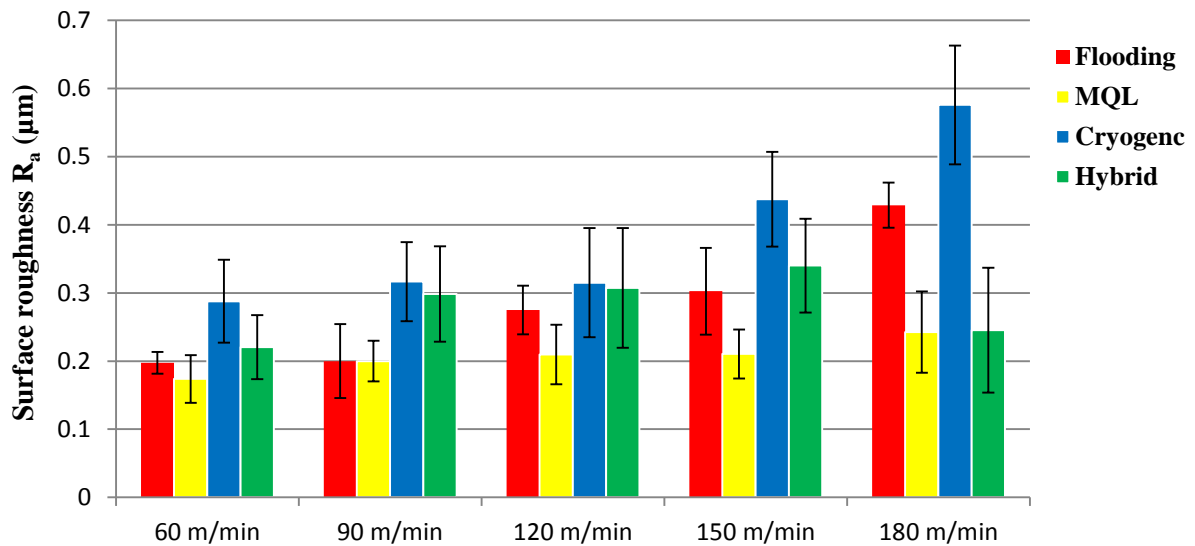


Figure 6.32 Average surface roughness for different cooling and cutting speed conditions

## **6.4 Comparative statistical analysis for the results of tool life and surface roughness**

In order to identify the effect of different cooling conditions it was essential to compare the results of the machinability metrics for the tested cooling conditions, namely; MQL, cryogenic cooling and hybrid cryogenic/MQL with those for conventional flood cooling techniques. For this purpose, statistical analysis of variance ANOVA was used to generate statistical models for machining performance indices in terms of tool life and surface finish. With ANOVA, the variation between groups was used to analyse the difference of group means. For a particular factor (input variable), the observed variance was partitioned into components attributed to different sources of variations. Analysis of variance provides statistical test to identify whether or not the mean values of different groups of variables are equal and therefore, compare for statistical significance of the difference between groups. In this study, the response variables of machining length to wear criterion and arithmetic mean surface roughness (Ra) were referred to as tool life and surface roughness, respectively.

### **6.4.1 Testing the normality of tool life and surface roughness data**

The normal distribution of data is one of the assumptions to run statistical analysis such as analysis of variance (ANOVA). To ensure that the data for tool life and surface roughness were normally distributed, the data was tested for normality. The analysis indicated that the collected data for surface roughness and tool life are not normally distributed. In order to normalise the data for ANOVA, logarithmic transformation was used. For this purpose, the data of tool wear and surface roughness shown in table 6.3 were transformed to logarithmic format and a normal distribution test was run as depicted in figures 6.33 and 6.34. The normality test indicated that logarithm transformation was successful for normalising the data and therefore further analysis could be performed.

Table 6.3 Tool life and surface roughness data for statistical analyses

| Experiment ID | Tool life (m) | Surface roughness Ra ( $\mu\text{m}$ ) |
|---------------|---------------|--|
| F1            | 53.1          | 0.197                                  |
| F2            | 13.95         | 0.267                                  |
| F3            | 7.34          | 0.297                                  |
| F4            | 3.9           | 0.428                                  |
| F5            | 3.3           | 0.287                                  |
| M1            | 224.25        | 0.161                                  |
| M2            | 124.8         | 0.202                                  |
| M3            | 93.6          | 0.202                                  |
| M4            | 44.4          | 0.210                                  |
| M5            | 16.8          | 0.234                                  |
| C1            | 13.65         | 0.293                                  |
| C2            | 15.6          | 0.318                                  |
| C3            | 17.55         | 0.380                                  |
| C4            | 13.65         | 0.437                                  |
| C5            | 8.7           | 0.575                                  |
| H1            | 306.15        | 0.218                                  |
| H2            | 429           | 0.258                                  |
| H3            | 85.8          | 0.313                                  |
| H4            | 17.6          | 0.308                                  |
| H5            | 12.6          | 0.240                                  |

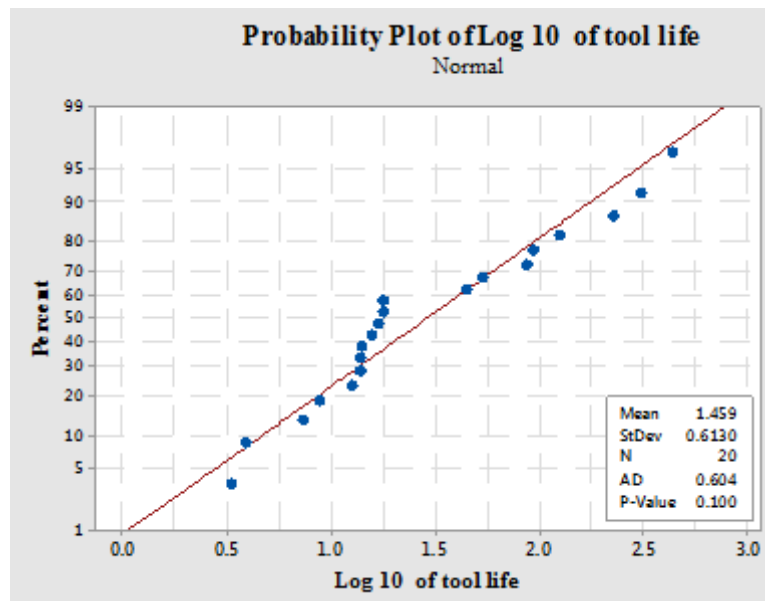


Figure 6.33 Normal probability plot for tool life

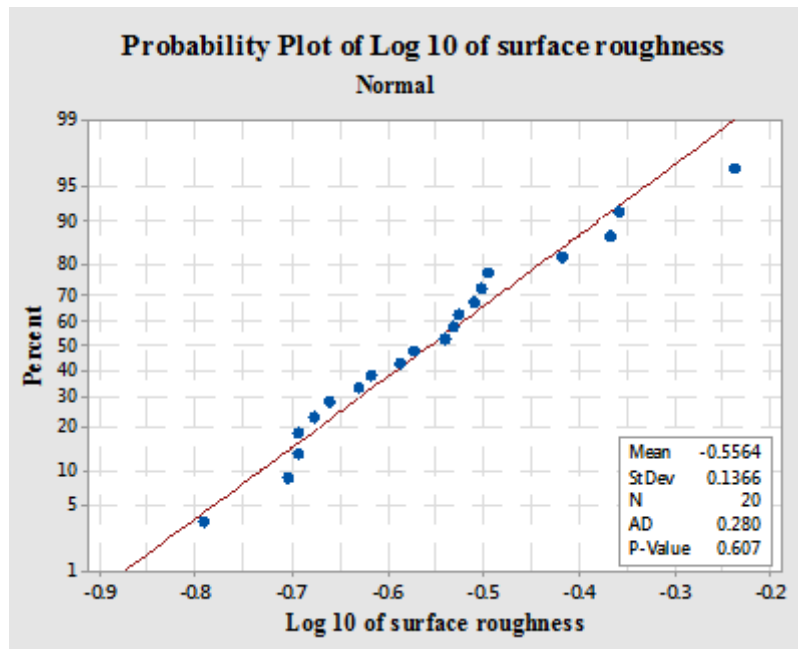


Figure 6.34 Normal probability plot surface roughness

#### 6.4.2 Statistical analysis of variance ANOVA for tool wear results

In order to analyse for the effect of cooling conditions and cutting speed on tool life, ANOVA was used. For ANOVA, the tool life was defined as a response variable with 5 different cutting speeds; 60, 90, 120, 150 and 180 m/min, under 4 different machining environments namely; flood cooling, MQL, cryogenic, and hybrid cooling and/or lubricating strategies as variables. With 5 cutting speeds and 4 machining environments, there are 20 possible different measurements conditions, with one measurement for each machining experiment. For this purpose, the Minitab software package (Minitab 18) was employed. A general linear statistical model was fitted with tool life as a response and both cutting speed and cooling condition as factors in one-way ANOVA. The results of the ANOVA are presented in table 6.4. It shows that the P-value (probability for null-hypothesis) is less than 0.05 for cooling condition and cutting speed, which confirmed that the cooling condition and cutting speed have significant effect on tool life. Figure 6.35 indicated that the residuals for the tool life statistical model are normally distributed. It is worth mentioning that replicate measurements of tool life provides more effective and reliable investigation and results in more sound statistical analysis.

Table 6.4 Standard analysis of variance for tool life statistical model

| Source                        | DF | SS    | MS      | F-Value | P-Value |
|-------------------------------|----|-------|---------|---------|---------|
| Cooling/lubricating condition | 3  | 3.424 | 1.14136 | 13.16   | 0.000   |
| Cutting speed                 | 4  | 2.675 | 0.66885 | 7.71    | 0.003   |
| Error                         | 12 | 1.040 | 0.08670 |         |         |
| Total                         | 19 | 7.140 |         |         |         |

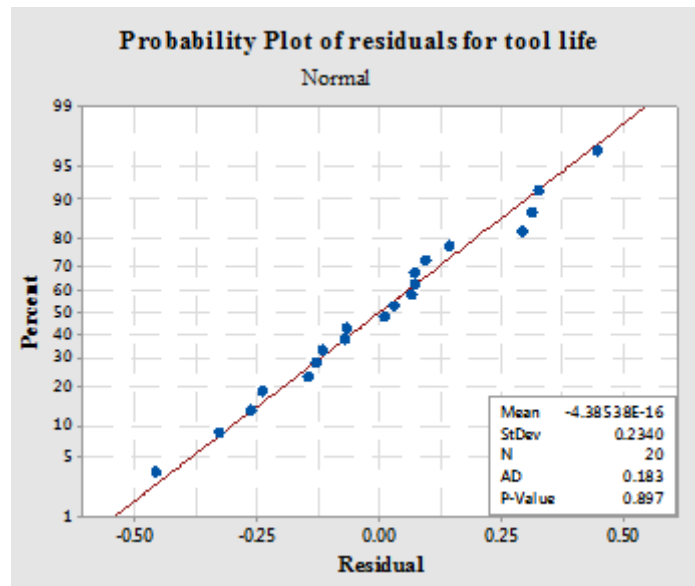


Figure 6.35 Normal probability plot of residuals for tool life statistical model

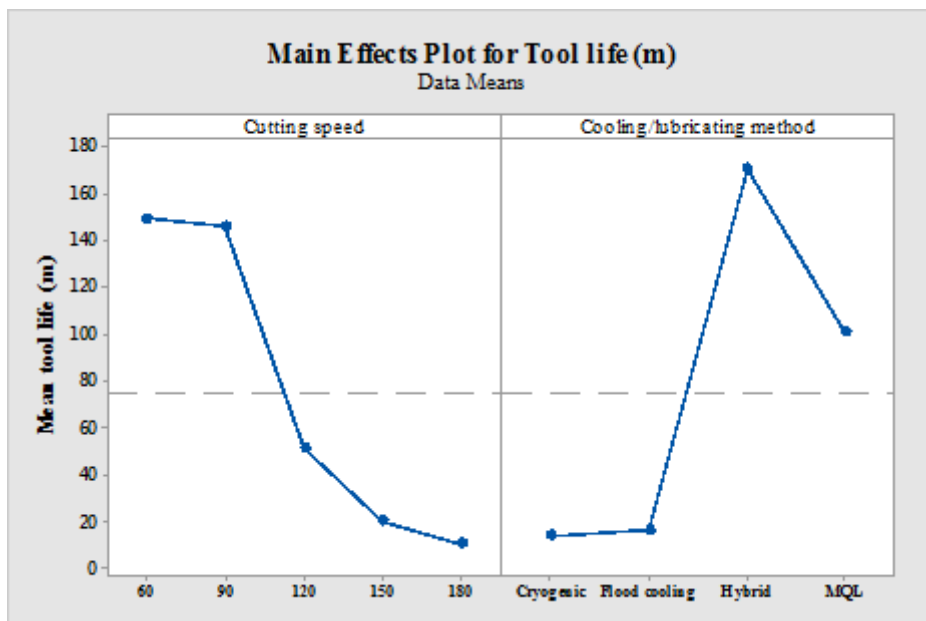


Figure 6.36 Main effect of cooling conditions and cutting speed as generated by Minitab 18.

The main effect in ANOVA was the effect of a variable averaged over levels of all other variables. Figures 6.36 and 6.37 showed the main effect of cooling condition and cutting force on tool life. Visual inspection of main effect plot, shown in figure 6.36, confirmed that both cooling condition and cutting speed have an effect on tool life. Interaction plots presented in figure 6.37 indicated that there is a decrease in tool life with the increase of the cutting speed and hybrid cooling appearing to have a significantly difference from flood and cryogenic cooling which confirm the results of table 6.3. Also, visual inspection of the interaction plots indicated that there is a very small interaction between cutting speeds 150 and 180m/min and between flood and cryogenic cooling (figures 6.37A and B).

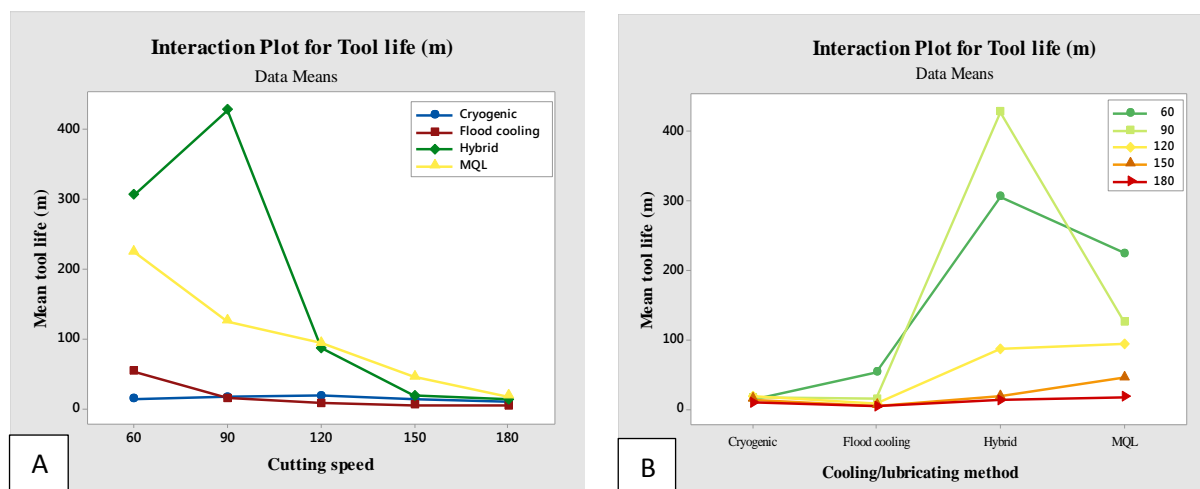


Figure 6.37 Interaction plots for tool life. A) Cutting speed, B) cooling condition

### 6.4.3 Comparison tests for tool wear

In order to identify the effect of each cooling condition (MQL, cryogenic, and hybrid) on tool life at different cutting speeds, and to compare these results with those for flood cooling, it is essential to run ANOVA comparison for these groups. Using Minitab the different groups were generated with comparison tests as shown in tables 6.5 and 6.6. Table 6.5 indicated the individual test for the difference of means between particular groups of cooling conditions. It can be clearly confirmed from table 6.5 that tool life under MQL and hybrid cooling condition is significantly different from that with application of flood cooling and cryogenic cooling conditions. However, the comparison between flood cooling and cryogenic showed a very high P-value, which confirmed that the difference is very small. For the effect of individual groups of cutting speeds on the tool life, a comparison test was run and shown in table 6.6.

Table 6.5 Fisher individual comparison tests of tool life means between different groups of cooling conditions

| Difference of Cooling/lubricating condition Levels | Difference of Means | SE of Difference | Individual 95% CI | T-Value | P-Value |
|--|---------------------|------------------|-------------------|---------|---------|
| Flood cooling - Cryogenic                          | -0.160              | 0.186            | (-0.566, 0.245)   | -0.86   | 0.406   |
| Hybrid - Cryogenic                                 | 0.750               | 0.186            | (0.344, 1.156)    | 4.03    | 0.002   |
| MQL - Cryogenic                                    | 0.729               | 0.186            | (0.323, 1.135)    | 3.91    | 0.002   |
| Hybrid - Flood cooling                             | 0.910               | 0.186            | (0.505, 1.316)    | 4.89    | 0.000   |
| MQL - Flood cooling                                | 0.889               | 0.186            | (0.483, 1.295)    | 4.77    | 0.000   |
| MQL - Hybrid                                       | -0.021              | 0.186            | (-0.427, 0.384)   | -0.11   | 0.911   |

Table 6.6 Fisher individual comparison tests of tool life means between different groups of cutting speeds

| Difference of Cutting speed Levels | Difference of Means | SE of Difference | Individual 95% CI | T-Value | P-Value |
|------------------------------------|---------------------|------------------|-------------------|---------|---------|
| 150m/min - 120m/min                | -0.349              | 0.208            | (-0.803, 0.105)   | -1.68   | 0.119   |
| 180m/min - 120m/min                | -0.558              | 0.208            | (-1.012, -0.104)  | -2.68   | 0.020   |
| 60m/min - 120m/min                 | 0.420               | 0.208            | (-0.033, 0.874)   | 2.02    | 0.066   |
| 90m/min - 120m/min                 | 0.263               | 0.208            | (-0.191, 0.716)   | 1.26    | 0.231   |
| 180m/min - 150m/min                | -0.209              | 0.208            | (-0.662, 0.245)   | -1.00   | 0.336   |
| 60m/min - 150m/min                 | 0.769               | 0.208            | (0.316, 1.223)    | 3.70    | 0.003   |
| 90m/min - 150m/min                 | 0.612               | 0.208            | (0.158, 1.065)    | 2.94    | 0.012   |
| 60m/min - 180m/min                 | 0.978               | 0.208            | (0.525, 1.432)    | 4.70    | 0.001   |
| 90m/min - 180m/min                 | 0.821               | 0.208            | (0.367, 1.274)    | 3.94    | 0.002   |
| 90m/min - 60m/min                  | -0.158              | 0.208            | (-0.611, 0.296)   | -0.76   | 0.464   |

#### 6.4.4 Statistical analyses of variance ANOVA for surface roughness Ra ( $\mu\text{m}$ )

In this section, the surface roughness of the machined workpiece is a response variable as a result of machining experiments with 5 different cutting speed levels under 4 different machining environments which represent the same factors and levels analysed for tool life illustrated in section 6.3.3. As a result, there were 20 different possible measurement conditions. ANOVA was used to analyse for the effect of both cooling condition and cutting speed on surface roughness as shown in table 6.7. Also, it is very useful to run ANOVA to statistically analyse the effect of the interaction of cooling condition and cutting speed on tool life. Tables 6.7 and 6.8 indicated that the P-values for cooling condition, cutting speed, and



the interaction between them (Cutting speed\*Cooling method) are less than 0.05, which confirmed that the cooling condition, cutting speed, and the interaction between cooling condition and cutting speed have a significant effect on surface roughness. For residual analysis, the normal probability plot of residuals was generated for surface roughness as shown in figure 6.38. It is shown the residuals of surface roughness analysis are normally distributed.

Table 6.7 Standard analyses of variance for surface roughness statistical model

| Source                     | DF | Adj SS  | Adj MS   | F-Value | P-Value |
|----------------------------|----|---------|----------|---------|---------|
| Cutting speed              | 4  | 0.09320 | 0.023300 | 5.43    | 0.010   |
| Cooling/lubricating method | 3  | 0.20998 | 0.069994 | 16.30   | 0.000   |
| Error                      | 12 | 0.05152 | 0.004293 |         |         |
| Total                      | 19 | 0.35470 |          |         |         |

Table 6.8. Standard analyses of variance for surface roughness showing the interaction between cutting speed and cooling/lubricating condition

| Source                       | DF | SS    | MS      | F-Value | P-Value |
|------------------------------|----|-------|---------|---------|---------|
| Cutting speed*Cooling method | 12 | 1.107 | 0.09227 | 37.52   | 0.000   |

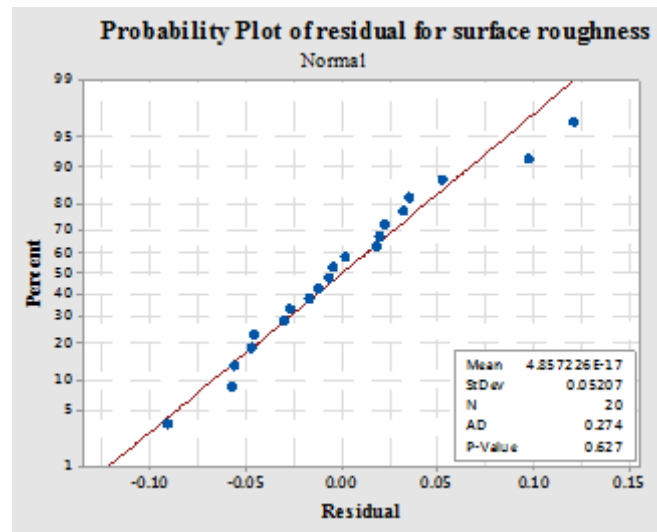


Figure 6.38 Normal probability plot of residuals for surface roughness statistical model

For more detail of the effect of each individual group of cooling condition and cutting speed and their interaction, a comparative statistical analysis was made with conventional flood cooling results as depicted in table 6.9. Table 6.9 indicated that there was a significant difference in surface roughness between different groups of cooling conditions, since the P-value for all comparison tests was less than 0.05. Figure 6.39 showed plots for the main effect of cooling condition and cutting speed on surface roughness and interaction between those factors on surface roughness. Figure 6.39a indicated that MQL recorded the lowest mean of surface roughness over the tested levels of cutting speeds, whilst hybrid and flood cooling showed comparable surface roughness results. However, cryogenic cooling indicated the highest surface roughness among the tested cooling conditions. Therefore, the performance of cooling conditions in term of surface roughness can be ranked from best to worst as; MQL, hybrid, flood cooling, and cryogenic cooling.

Table 6.9 Fisher individual comparison tests of surface roughness means between different groups of cooling conditions

| Difference of Cooling/lubricating method Levels | Difference of Means | SE of Difference | Individual 95% CI  | T-Value | P-Value |
|---|---------------------|------------------|--------------------|---------|---------|
| Flood cooling - Cryogenic                       | -0.1330             | 0.0414           | (-0.2233, -0.0427) | -3.21   | 0.008   |
| Hybrid - Cryogenic                              | -0.1667             | 0.0414           | (-0.2570, -0.0764) | -4.02   | 0.002   |
| MQL - Cryogenic                                 | -0.2877             | 0.0414           | (-0.3780, -0.1974) | -6.94   | 0.000   |
| Hybrid - Flood cooling                          | -0.0337             | 0.0414           | (-0.1240, 0.0566)  | -0.81   | 0.431   |
| MQL - Flood cooling                             | -0.1547             | 0.0414           | (-0.2450, -0.0644) | -3.73   | 0.003   |
| MQL - Hybrid                                    | -0.1210             | 0.0414           | (-0.2113, -0.0307) | -2.92   | 0.013   |

On the other hand, figure 6.39a showed that surface roughness is directly proportional to cutting speed till reaching 150m/min, since the main relation flipped to adverse proportion when moving from 150 to 180m/min. The main ranking of cutting speed performance from best to worst was; 60, 90, 120, 180, and 150m/min. For interaction analyses, figure 6.37b and table 6.10 showed the simultaneous effect of cooling condition and cutting speed on tool life. Surface roughness under the application of MQL demonstrated the best performance at all cutting speeds as shown in figure 6.37b. Among all tested cooling conditions, it was observed, as shown in table 6.3 and figure 6.37, that cryogenic cooling recorded the highest surface roughness at all cutting speeds. Hybrid cooling showed comparable surface roughness results to those for flood cooling at low and moderate speeds (from 60 to 120m/min). With

increasing the cutting speed more than 120m/min, a decrease in surface roughness was observed.

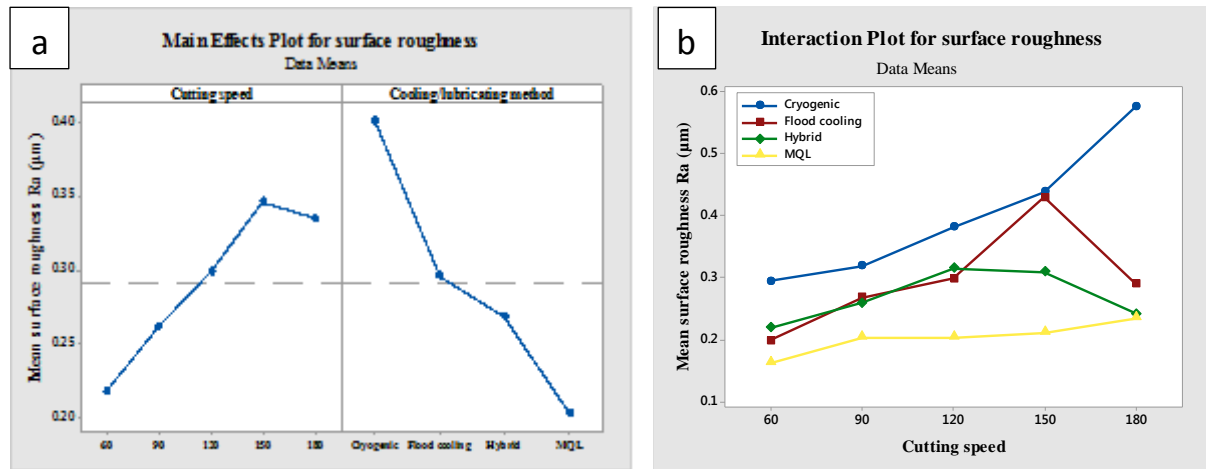


Figure 6.39 Surface roughness plots at different cooling conditions and cutting speeds. a) Main effect, b) Interaction.

Table 6.10 Fisher individual comparison tests of surface roughness means between different interacted groups of cooling conditions and cutting speeds

| Difference of Cutting speed*Cooling method Levels | Difference of Means | SE of Difference | Individual 95% CI  | T-Value | P-Value |
|---|---------------------|------------------|--------------------|---------|---------|
| (60 Flood cooling) - (60 Cryogenic)               | -0.1000             | 0.0135           | (-0.1265, -0.0735) | -7.41   | 0.000   |
| (60 Hybrid) - (60 Flood cooling)                  | 0.0222              | 0.0135           | (-0.0043, 0.0487)  | 1.65    | 0.100   |
| (60 MQL) - (60 Flood cooling)                     | -0.0341             | 0.0135           | (-0.0606, -0.0076) | -2.52   | 0.012   |
| (90 Flood cooling) - (90 Cryogenic)               | -0.0407             | 0.0135           | (-0.0673, -0.0142) | -3.02   | 0.003   |
| (90 Hybrid) - (90 Flood cooling)                  | -0.0148             | 0.0135           | (-0.0413, 0.0117)  | -1.10   | 0.273   |
| (90 MQL) - (90 Flood cooling)                     | -0.0667             | 0.0135           | (-0.0932, -0.0402) | -4.94   | 0.000   |
| (120 Flood cooling)-(120 Cryogenic)               | -0.0815             | 0.0135           | (-0.1080, 0.0550)  | -6.04   | 0.000   |
| (120 Hybrid) - (120 Flood cooling)                | 0.0185              | 0.0135           | (-0.0080, 0.0450)  | 1.37    | 0.171   |
| (120 MQL) - (120 Flood cooling)                   | -0.0963             | 0.0135           | (-0.1228, -0.0698) | -7.14   | 0.000   |
| (150 Flood cooling) - (150 Cryogenic)             | -0.1000             | 0.0135           | (-0.1265, -0.0735) | -7.41   | 0.000   |
| (150 MQL) - (150 Flood cooling)                   | -0.1963             | 0.0135           | (-0.2228, 0.1698)  | -14.54  | 0.000   |
| (150 Hybrid) - (150 Flood cooling)                | -0.1111             | 0.0135           | (-0.1376, -0.0846) | -8.23   | 0.000   |
| (180 Flood cooling) - (180 Cryogenic)             | -0.2815             | 0.0135           | (-0.3080, -0.2550) | -20.86  | 0.000   |
| (180 Hybrid) - (180 Flood cooling)                | -0.0407             | 0.0135           | (-0.0673, -0.0142) | -3.02   | 0.003   |
| (180 MQL) - (180 Flood cooling)                   | -0.0519             | 0.0135           | (-0.0784, -0.0253) | -3.84   | 0.000   |

## 6.5 Results of chip morphology

It is well known that chip formation and breakability play an important role in assessing the machinability through their effect on tool life, surface finish and chips blowing away, and can affect the overall machining performance (Yuan et al. 2011). Many factors can influence the chip formation and morphology such as the machining environment, cutting parameters, tool geometry (Calamaz et al. 2008; Dhar et al. 2006). In the machining experiments of this research, with a 4mm radial depth of cut and 0.03mm/tooth feed rate, the generated chip was 7.3 mm in length and with a thickness varying from 0.03mm to zero. Nearly in all the machining experiments, the chip was broken into two segments; thick and thin segments. It is worth noting that with varying chip thickness the comparative analysis of chip parameters was not useful. Figures 6.40-6.43 illustrates the chip morphology for different cooling/lubricating conditions and different cutting speeds.

For low cutting speed at 60m/min flood cooling, nearly straight thin segment chips together with single-turn twisted thick segment chips were observed as shown in figure 6.40 F1. This could be attributed to the satisfactory cooling of the chips during the machining process which provided uniform cooling for thin chips, whilst curvature was increased with the increase of chip thickness. The segmented teeth at the free chip surface act as fins that dissipate more heat than the chip machined surface, which causes differential thermal contraction in the chip, resulting in twisted or spiral chip formation. Spiral-thick and curved thin chip segments were observed when increasing the cutting speed to 90 m/min (figure 6.40F2). Further increases in cutting speed resulted in evolution of curled and wavy chips as well as straight thin and spiral thick chips. At higher cutting speeds, 150 and 180m/min., thin segment chips observed to be shredded and become more curved, whilst the thick segment chips remained spiral in shape with evidence serration at the chip edge (figures 6.40 F4 and F5).

For MQL, smooth chip formation was observed as shown in figure 6.41. Combination of tubular and spiral morphology for the thick segment chips and straight thin segment chips was observed. With increasing the cutting speed the thick segment chips tended to have two distinct regions, flat and spiral regions, whilst the thin segment became more flat. Similar chip morphology was observed at 120m/min and became more curled and wavy at 150 m/min. With higher cutting speeds the thin segment chips became more curled, wavy and

shredded, whilst thick segment chips had two regions namely; flat and spiral as shown in figure 6.41.

In cryogenic cooling, the chip breaks into two segments which were irregular in shape with two segment ends which were shredded as shown in figure 6.42. At low cutting speeds, flat and shredded (cracked) thin-segment chips, and twisted and rough edge thick-segment chips were observed. This could be explained by cooling of titanium chips due to the application of LN<sub>2</sub> jets which enhance chip cracking and reduce the chip curvature due to uniform cooling from both sides (free and machined surfaces). With increasing the cutting speed, the thin chips became more wrinkle (wavy), curved, and cracked. At higher cutting speeds, the thin chips became highly straight, wavy and cracked, whilst thick chips became less spirally with more cracked edges (figure 6.42).

In similar manner to MQL, hybrid cryogenic/MQL resulted in smooth chip formation, smooth machines surface of chip, smooth edges and spiral and/or tubular chip as compared with chip formation during cryogenic and flood cooling as shown in figure 6.43

For hybrid cooling/lubrication at low cutting speeds, chip morphology showed smooth tubular and spiral multi-turn chips with no chip divisions observed, which indicated smooth cutting and laminar chip formation, as shown in figure 6.44. Also, this could be regarded as an index for high machining performance. The same chip morphology was observed for 90m/min, which recorded the longest tool life.

By increasing the cutting speed to 120m/min, a dramatic change in chip morphology was observed. The chip division into thick and thin segments was again observed with shredding and waviness of thin chips, whilst still having spiral and wavy shape thick chip morphology. At higher cutting speeds, 150 and 180m/min, the thin chip become more flat, wavy and cracked, whilst thick chips were observed to be less spiral in shape and had longer straight region (figure 6.44). From the above results of chip morphology, it can be concluded that the smooth chip formation with tubular and/or spiral shape indicated improved machinability, whilst poor machining performance resulted in curled, rough and/or cracked edge, shredded, and wavy chips (figure 6.43).

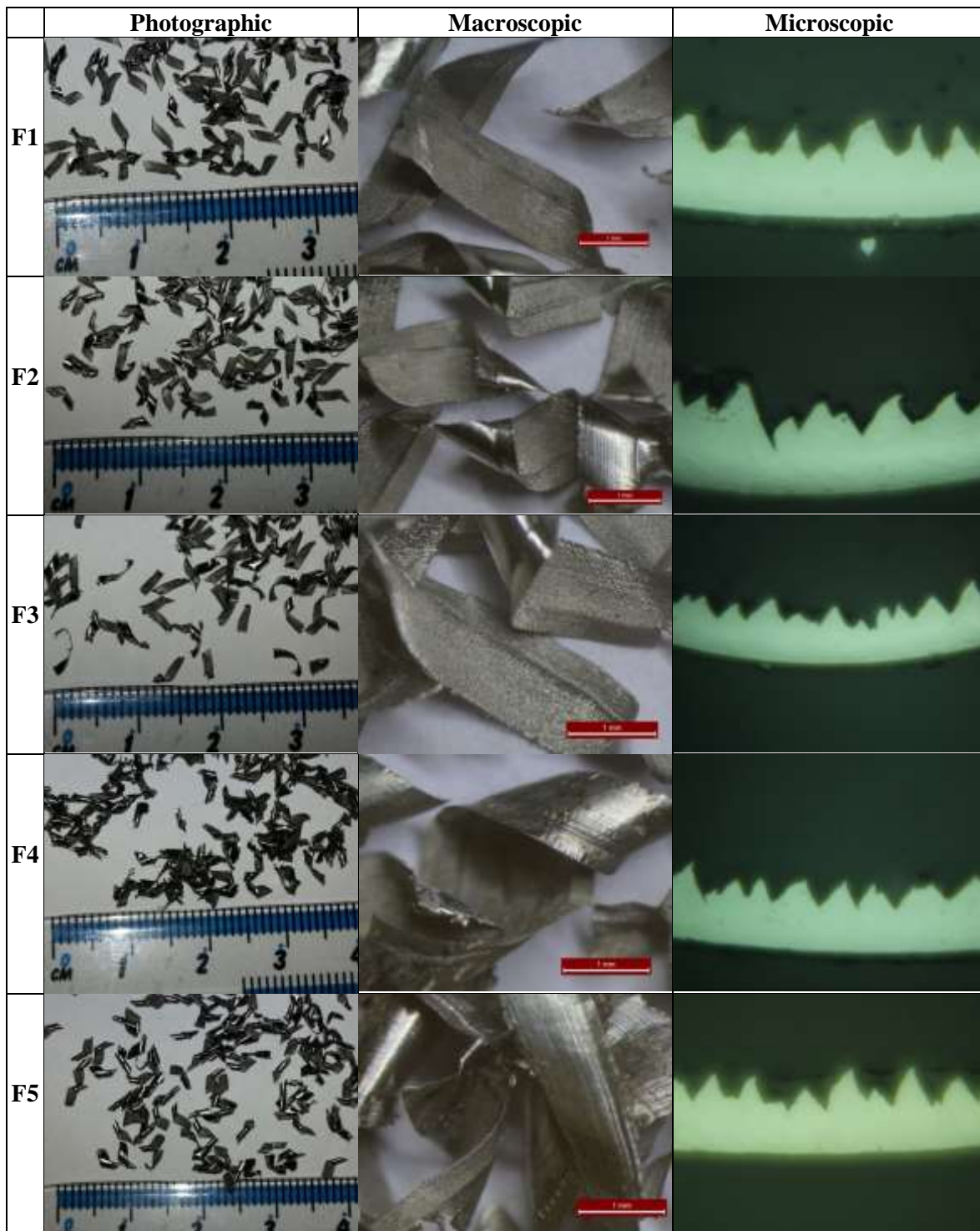


Figure 6.40 Images of chips for machining under flood cooling

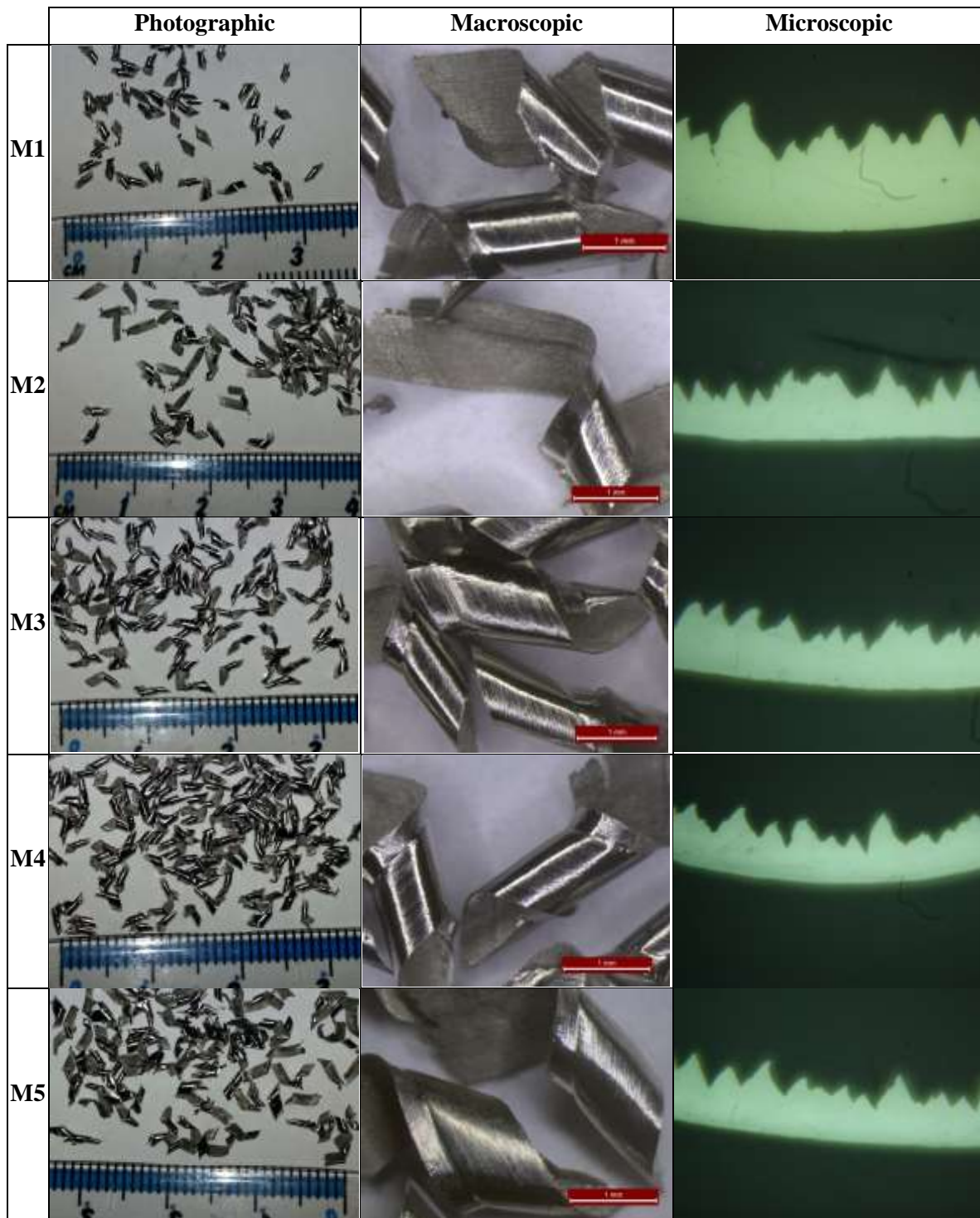


Figure 6.41 Images of chips when machining under MQL

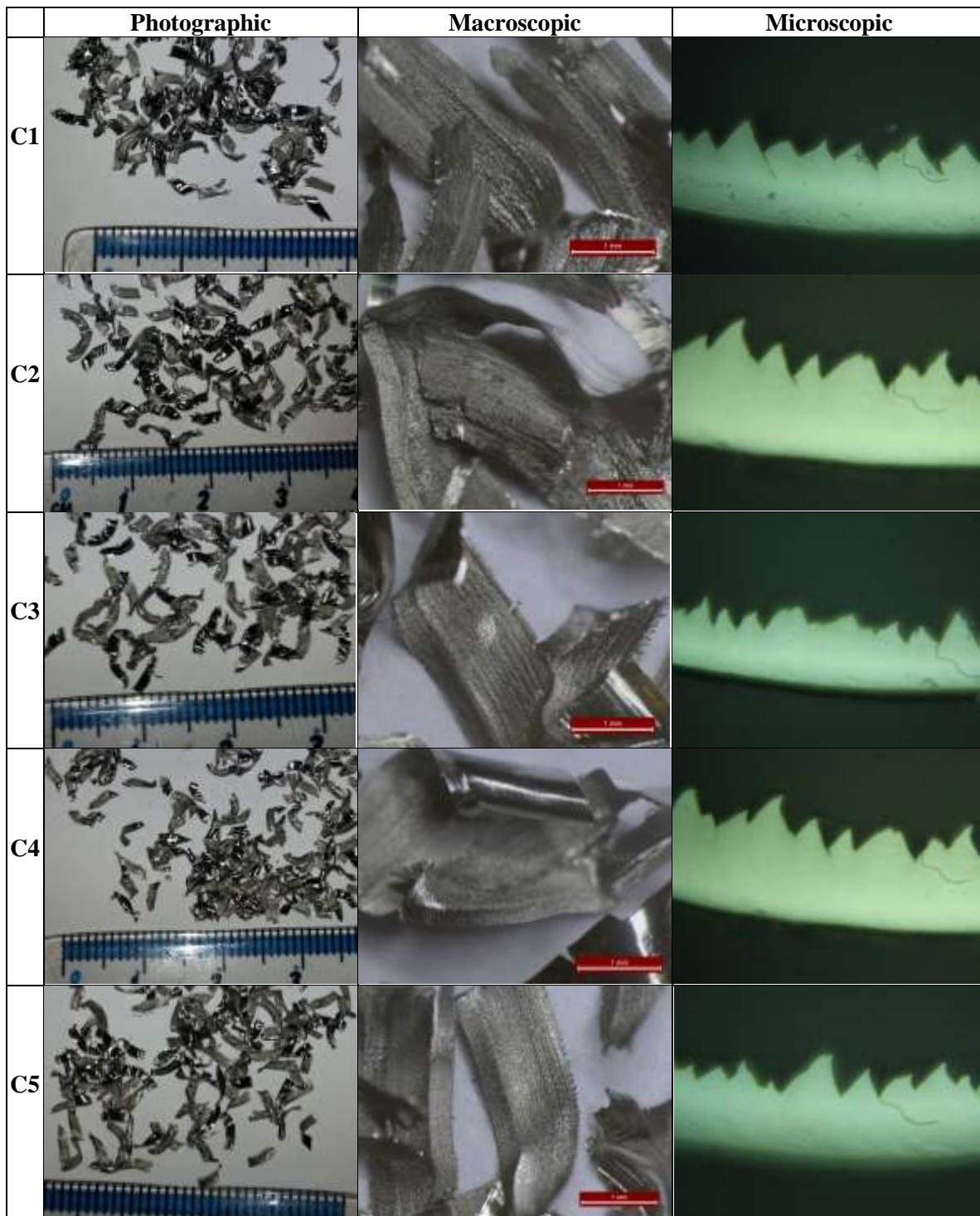


Figure 6.42 Images of chips when machining under cryogenic cooling




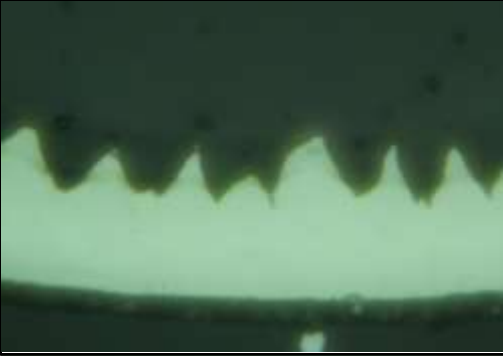





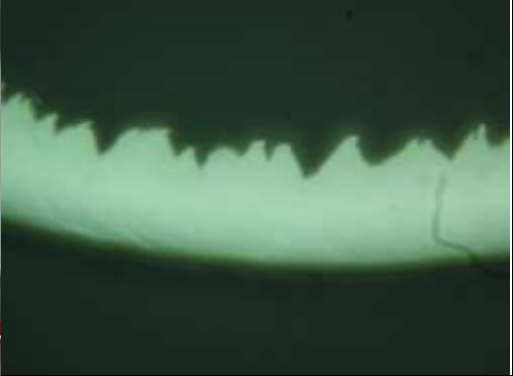
|                      | Macroscopic images  | Microscopic images   |
|----------------------|---|--|
| <b>Flood cooling</b> |    |    |
| <b>MQL</b>           |    |    |
| <b>Cryogenic</b>     |   |   |
| <b>Hybrid</b>        |  |  |

Figure 6.43 Macro and microscopic images of chips when end milling Ti-6Al-4V at 60m/min. under different cooling/lubricating strategies

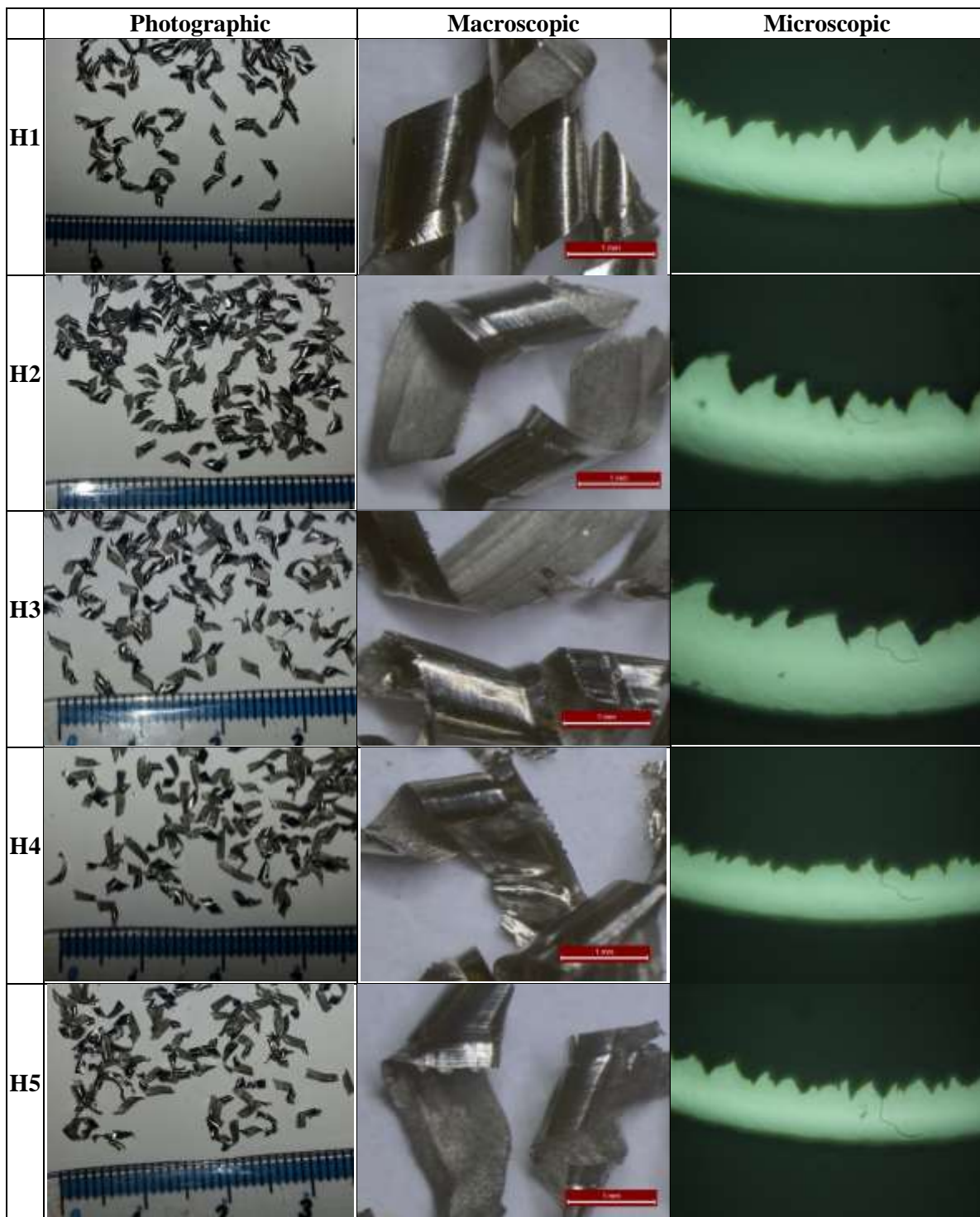


Figure 6.44 Images of chips when machining under hybrid cryogenic/MQL

## **Chapter 7 Discussion**

### **7.1 Introduction**

This chapter provides a critical discussion to activities of design of the cryogenic nozzle that was used to conduct different cryogenic and hybrid machining experiments. Also, the machining experimentation, the results and their statistical analysis were critically discussed so that sound, reliable and valid conclusions can be drawn.

### **7.2 Design of cryogenic cooling system**

A viable and effective dual-nozzle cryogenic cooling system was specially designed to conduct cryogenic and hybrid cooling machining experiments. This system can be easily retrofitted into the majority of milling machine tools. The holder of the cryogenic nozzle system enables full control of nozzle position. This allows precise targeting of the desired regions to be cooled with LN<sub>2</sub>. In addition, the compacted design of dual-nozzle system can give many options to select the regions needed to be cooled with LN<sub>2</sub> and those require MQL. The compact design of the cooling nozzle system enabled the use of a multi-nozzle to further enhance the cooling performance. This provided more flexibility and variety to examine various cooling/lubricating strategies with different orientations of cryogenic and MQL nozzles. Moreover, the designed external nozzle system can be applied during the end milling of different tool diameters. Different machining operations such as turning and face milling can be conducted under the application of LN<sub>2</sub> using this nozzle system. The robust, light weight and stiff design of the system enables CNC machining without putting additional static and dynamic load onto the machine tool spindle during feed and rapid traverse movements. Furthermore, the nozzle system can be used for conducting machining experiments that require interrupting the machining operation. Therefore, the cutting tool can be removed easily for tool wear measurement during the machining experiments without the need to remove the nozzle. This significantly eliminates the time elapsed and the effort of the operator.

From the economic viewpoint, the system enables spraying of a small but effective amount of LN<sub>2</sub> to the desired region (cutting tool and/or cutting interfaces) with full control of coolant flow rate. With a minimum LN<sub>2</sub> flow rate of 0.5l/min, an economic delivery of coolant is achieved with the ability to avoid the abundant and excessive cooling which could result in

increasing machining cost and undesired increase in workpiece hardness. The improvement in tool life with the hybrid combination of multi-nozzle cryogenic cooling and MQL validates the effectiveness of the design of the nozzle system.

On the other hand, and in spite of the capability of the designed nozzle cooling system to deliver coolant to different diameters and different machining operations, it shows limits in the tool changing routine. To implement a tool changing cycle, the nozzle system should be removed from the machine tool spindle to prevent collision with the nozzle and tool changing arm. In addition, control of the relative orientation between the two nozzles was limited to plastic bending of the two copper pipes that deliver LN<sub>2</sub> from the flow distributor to the cooling nozzles (chapter 4). This formability was reduced when the pipes are exposed to LN<sub>2</sub> during cryogenic machining. Furthermore, due to the design constraints of the nozzles' geometry and insulation requirements, positioning the nozzles in a horizontal or low angle of projection was not possible.

### **7.3 Experimental investigation of machining performance of cryogenic, MQL, and hybrid cryogenic/MQL techniques as compared with conventional flood cooling**

Based on the methodology shown in figure 3.1 and section 3.6, this section involves a critical discussion of comparative results of the machinability indices of the application of various machining environments

#### **7.3.1 Preparation for machining experiments**

Previous studies suggested that that the hardness and strength of Ti-6Al-4V titanium alloy is increased because of application of cryogenic LN<sub>2</sub> due to the hardening of workpiece at extremely low temperatures (Hong and Zhao 1999). The literature also suggested that the application of cryogenic LN<sub>2</sub> to the cutting interfaces could significantly improve the machining performance in turning operations, via lowering the tool temperature well below the softening temperature of the tool material. However, the lack of knowledge of the effect of the application of LN<sub>2</sub> in milling operations has led to the design, manufacturing, and implementation of machining experiments with milling operations. The absence of knowledge of the optimum cutting speed (that results in optimum machining performance) for each cooling and/or lubricating condition has led to the investigation of different machining experiments with different combinations of cutting speed and cooling/lubrication

environments. The machining experiments were conducted with different cutting speeds, starting from the lowest level (60m/min) which recommended by literature and manufacturers for conventional cooling, and ending with high cutting speed of 180m/min at which tool life is expected to be very short under conventional cooling. In addition, different cooling and lubrication conditions have different optimum cutting speeds that give the highest machining performance. In particular, the cooling strategy within the same machining environment can affect the machining performance and alter the optimum cutting speed and other cutting parameters. Nozzle orientation, nozzle diameter, number of cooling/lubricating nozzles, coolant flow rate, delivery pressure and speed, distance between nozzle and cutting tool/cutting interfaces can also affect the machining performance and the optimum cutting speed and other cutting parameters.

Based on previous research and in order to focus this research, the investigation on the machining performance was limited to 1mm axial depth of cut, 4mm radial depth of cut and 0.03mm/tooth feed rate. The selection of the cutting tool was also based on previous research in Bath on cryogenic machining (Shokrani, 2014).

### **7.3.2 Machining experimentation**

By fixing the feed rate and axial and radial depth of cut, the number of experiments for this study can be minimized. It is well known that cutting speed is the main parameter affecting cutting temperature. Therefore, cutting speed and cooling/lubricating environment were selected as the main variable parameters for the DoE. In addition, by limiting the variable parameters, the number of experiments required was limited with the author research focusing on cutting speed and the machining environment at multiple levels. This has led to the option to use the full-factorial DoF which represents the best approach for identifying the effect of key input variables (factors) on the output performance, since it involves all possible combinations of input variables. In this research, the machining performance has been evaluated in terms of tool life, surface roughness and chip morphology defined as output variables and tested at 5 levels of cutting speeds, and with 4 levels of cooling/lubrication. Full-factorial DoE implies  $5^1 \times 4^1$ , and the output parameters were tested using 20 different combinations of cutting speed and cooling/lubrication. This has resulted in identification of the best combination of cooling/lubrication method and cutting speed.

In conducting the machining experiments, the uncertainty and variation due to uncontrolled parameters during the collection of data were kept to minimum. The same operator, machining tool, and workpiece batch were used. Also, the elapsed time for stopping the machining experiment, and resuming the experiment was unified and kept to minimum and the measurements were taken with the same calibration of measuring devices. However, during the machining experiments that require LN2 as a coolant (cryogenic and hybrid), the variation of coolant flow rate due to phase change from liquid to vapor and vice versa, the pressure drop in the Dewar during the machining experiments, and the uncertainty to maintain the exact flow rate after each stopping of experiment for tool wear measurement can impose variations in result. In addition, the nozzles orientations are changed during the flow of LN2 through the nozzle system manifolds due to the thermal contraction resulted from the significant reduction in temperature ( $\Delta T$  nearly  $-210^{\circ}\text{C}$ ). This contraction of the nozzle system require further adjustment of nozzle orientation to ensure the targeting of the same desired region to be cooled. For machining experiments where MQL nozzles are involved (MQL and hybrid), the positions of the MQL nozzle should be manually set after each measurement to ensure repeatability of the results. This requires a skilled operator to ensure minimal uncertainty in the measured data.

### **7.3.3 Comparison of experimental results**

In this section, the results of machinability in terms of tool wear/life, surface roughness, and chip morphology are critically discussed and compared with the related literature.

#### **7.3.3.1 Tool wear**

In order to measure and identify the tool wear and the tool wear mechanism, a systematic method was developed to illustrate tool wear progression as a function of machining length. It is very important to understand, identify and follow the progress of tool wear mechanism during the machining operation as presented in figures 6.8-6.12, 6.14-6.18, 6.20-6.24, 6.26 and 6.28-6.31. In addition, different views for worn tool for each machining experiment was taken to identify the most dominant tool wear mechanism as illustrated in figures 6.7, 6.13, 6.19, 6.27. However, the absence of knowledge of the approximate tool life and the total machining time required for each machining experiment made it difficult to decide about the

number of measurements and time interval between measurements. This has resulted in unnecessary extra measurements taken for each machining experiments

In all flood machining experiments in this research, there is a clear evidence that crater chipping/flaking due to thermal and non-uniform flank adhesion-abrasion (attrition) are the most influential tool wear mechanisms as explained in details in subsection 6.2.1. This fairly agreed related studies of tool wear mechanism of flood cooling during turning and milling of Ti-6Al-4V (Grearson 1986; Bermingham et al. 2012; Sun et al. 2006; Shokrani 2014; Park et al. 2017). For MQL machining experiments, remarkable and reliable improvement in tool life has been recorded with the use of rapeseed oil and the application of dual- nozzle lubrication. This improvement can be explained by the effective lubricity that reduced the cutting and friction forces through the control of heat generation from the secondary and tertiary heat zones during the machining operation (Sun et al. 2006; Deiab et al. 2014; Park et al. 2017). Tool life improvement up to 322% to 1173% in comparison with conventional emulsion flood cooling at similar cutting conditions was recorded. The maximum tool life was recorded at 60m/min, which is in agreement with the results by Obikawa et al. (2007). The maximum improvement in tool life was found at 120m/min. this seems not consistent with similar studies in turning conducted by Sun et al. (2006), and Deiab et al. (2014), who suggested that the maximum improvement in tool life was found at the lower cutting speeds. Related work other than Sun et al. (2006), suggested less significant improvement in tool life when MQL with vegetable oil is applied in machining Ti-6Al-4V (Deiab et al. 2014; Park et al. 2017; Garcia and Ribeiro 2016). Sartori et al. (2018) stated that the tool nose wear when MQL was applied to turning of Ti-6Al-4V at 80m/min has been reduced by 17% in comparison with flood cooling.

For cryogenic machining experiments, the dual-nozzle system was set at the same position to MQL nozzles; one nozzle directed to the cutting area, and the other nozzle oriented to the cutting tool as described in subsection 5.4.4.3. The direct spraying of LN2 to the cutting zone has led to excessive local hardening of the workpiece, resulted in micro fracture, fragmentation and plastic deformation of the cutting edge as illustrated in details in subsection 6.2.3. Similar behavior was observed by Park et al. (2017). The rapid loss of cutting edge sharpness resulted in premature development of flank attrition-abrasion due to the excessive rubbing (instead of cutting) between tool flank and workpiece, which can shorten the tool life.

Apart from cryogenic machining experiment at 60m/min, the application of dual-nozzle cryogenic cooling has resulted in an improvement in tool life by 12%-250% compared to flood cooling. The maximum improvement was observed at 150m/min, whilst the maximum tool life was recorded at 120m/min. This seemed consistent with results obtained from similar studies in turning of Ti-6Al-4V conducted by Hong et al. (2001), Wang and Rajurkar (2001) and Venugpal et al. (2007). The tool life results at 90m/min cutting speed agreed with similar investigation conducted by Bordin et al. (2017). Shokrani et al. (2016) reported a reduction in tool wear of 31% when cryogenic cooling was applied in milling. According to Venugpal et al. (2007), the tool life under cryogenic cooling is improved by 40%-70% over flood cooling.

The tool life results in this research suggested that MQL outperforms cryogenic at low and moderate cutting speeds. Related studies conducted by Park et al. (2017) and Deiab et al. (2014) agreed with the results of the present research. However, the relatively short tool life at low cutting speed when cryogenic machining was applied (1/3 that for flood cooling at 60m/min) could limit its feasibility in industrial adoption. Park et al. (2017) proposed the spraying of LN2 to the cutting tool only, since the direct exposure of cutting region to LN2 could result in excessive hardening of Ti-6Al-4V alloy, which resulted in short life even at low cutting speeds.

For hybrid cooling/lubrication condition, analysis indicated that significant improvement tool life can be achieved. Tool life improvement of up to 282%-2975% was recorded. Hybrid application of dual-nozzle cryogenic cooling and dual-nozzle MQL when end milling of Ti-6Al-4V demonstrated the best machining performance in terms of tool life among all cooling and lubrication conditions, and recorded nearly 30 fold increase over flood cooling. This improvement is attributed to the reduction in cutting temperature and friction due to effective cooling and lubrication as described in subsection 6.2.4. This outstanding improvement in tool life with the application of hybrid cryogenic/MQL demonstrated a significant potential of this cooling /lubricating strategies for industrial adoption. Machine tool designers should give provisions to install or build-in cryogenic and MQL systems to be applied simultaneously when end milling Ti-6Al-4V.

The cryogenic cooling tends to control the thermally induced tool wear by diffusion and adhesion, whilst MQL significantly reduced mechanical wear rate by attrition and abrasion. The simultaneous effect of cooling and lubrication can reduce the plastic deformation of the



cutting edge and hence prolong tool life. The maximum tool life and maximum improvement in tool life was record at 90m/min. Schoop et al. (2017) scored 4-5 times reduction in tool flank wear when hybrid cryogenic/MQL was applied compared to flood cooling in high speed turning of Ti-6Al-4V.

However, other related studies showed much less improvement in tool life when hybrid cryogenic/MQL was applied. Park et al. (2015) suggested that hybrid combination of internal cryogenic cooling and MQL resulted in an improvement in tool life of 32% compared with flood cooling. Sartori et al. (2017) reported that hybrid cryogenic/MQL strategies resulted in nearly 10% reduction in tool wear in comparison to conventional flood cooling techniques.

### **7.3.3.2 Surface roughness**

Results and analysis in this research suggested that the application dual-nozzle MQL with vegetable rapeseed oil, and the application of multi-nozzle hybrid cryogenic/MQL when end milling of Ti-6Al-4V demonstrated significant improvement in surface roughness with maximum improvement of up to 50% and 28% for MQL and hybrid cryogenic/MQL, respectively compared to that of conventional flood cooling. For MQL, the improvement in surface roughness agreed with similar investigation conducted by Garcia and Ribeiro (2016) for milling of Ti-6Al-4V and Sartori et al. (2017). In hybrid cooling/lubrication, the significant improvement in surface roughness confirmed in this research agreed with investigations by Schoop et al. (2017). The improvement in surface roughness at higher cutting speeds over flood cooling is in agreement with results obtained by Raza et al. (2014) in turning of Ti-6Al-4V. However, dual-external nozzle cryogenic cooling when end milling of Ti-6Al-4V showed the worst surface roughness performance among all tested cooling and lubricating conditions. The worst performance (100% higher than flood cooling) was recorded at higher cutting speeds. This seemed not consistent with the reviewed literature (Dhananchezian and Pradeep Kumar 2011; Rotella et al. 2014; Bordin et al. 2015; Shokrani et al. 2016b). This deterioration in surface roughness when cryogenic cooling was applied can be due to the rapid progress in tool wear during the machining of the surface at which the measurements were made. The poor lubricating characteristics of the applied LN2 and the excessive BUE formation could result in further deterioration in surface roughness.

### 7.3.3.3 Chip morphology

It is well known that chip breakability could indicate the machining performance of titanium alloys. Improved machinability can be achieved by altering the chip morphology from continuous snarled or tubular form to C-shaped or spiral discontinuous chips (Ezugwu 2005; Jerold and Kumar 2013). However, in end milling, the chip length is limited to the radial depth of cut and tool diameter. In this research, the nominal chip length did not exceed 7.3mm with chip thickness varying from feed per tooth (0.03mm/tooth) to 0. As a result, chip breakability is ineffective in indicating the machinability in end milling titanium alloys. For most conducted machining experiments in this research, the chips were broken into two segments; thin and thick segments. Chip morphology analysis showed smooth edge, smooth machined surface and spiral shapes when MQL and hybrid cooling was applied in end milling of Ti-6Al-4V. This indicated a smooth and laminar flow of chips during machining, whilst, rough, cracked edge, ripped, snarled and straight chip morphology was observed when cryogenic machining was applied. This agreed with the similar investigation conducted by Park et al. (2017) in milling of Ti-6Al-4V and by Bierman et al. (2015) in turning of Ti-6Al-4V with LCO<sub>2</sub>. Microscopic inspection of chips collected during all machining experiments showed that shear localization or adiabatic shear band was the dominant mechanism of chip segmentation. Attached chip segments in the form saw-teeth serration are clearly observed for chips generated in flood cooling, MQL, and hybrid cryogenic/MQL, whilst a combination of attached and cracked chip segmentation was observed when cryogenic cooling was applied. A similar chip morphology was reported by Bierman et al. (2015), Aramcharoen (2016), and Krishnamurthy et al. (2017) in turning Ti-6Al-4V.

## **Chapter 8 Conclusions and Recommended Further Work**

### **8.1 Introduction**

This chapter presented conclusions drawn from the findings of the research together with recommendations for further areas of investigation.

### **8.2 Conclusions**

- A specially designed dual-nozzle external cryogenic cooling system has been designed and manufactured by the author which can be used to conduct both cryogenic and hybrid Cryogenic/MQL machining experiments. The cooling system is retrofitable on any milling and turning machine, and can spray LN<sub>2</sub> from different projection angles with full control of nozzle position. The experimental analysis indicated that the dual-nozzle external cryogenic system can improve the machinability of titanium at moderate cutting speed (150m/min) in terms of tool life when compared to flood cooling. However, its effectiveness is limited at other cutting speeds or for improving the surface roughness of the machined components.
- Both MQL and hybrid MQL/cryogenic environments are highly effective cooling and/or lubricating technologies in extending the tool life (up to 11 fold for MQL and 30 fold for hybrid cryogenic/MQL) over flood cooling. This is due to the effective cooling and lubrication of the cutting tool and the cutting zone that enables a significant reduction of thermally and mechanically related tool wear.
- The application of hybrid cryogenic/MQL environments during end milling of Ti-6Al-4V significantly reduced crater dissolution-diffusion and controlled the rate of tool attrition-adhesion due to the effective cooling and lubricity. It recorded the best performance in tool life with improvements up to 30 fold over flood cooling.
- The application of dual-nozzle MQL system using rapeseed oil demonstrated outstanding improvement in tool life. More than an 11 fold increase in tool life was recorded over flood cooling. MQL generated the best surface roughness among all cooling/lubricating conditions and recorded an improvement of up to 50% compared with flood cooling.
- Cryogenic machining enabled a substantial reduction in dissolution-diffusion wear through the control of the machining temperature at all cutting speeds, and reported an improvement of tool life up to 250% in comparison with flood cooling at a high

cutting speed of 150m/min. However, the increased hardness of workpiece due to direct spraying of LN2 jet to the cutting zone resulted in increased fracture and plastic deformation of tool cutting edge. The poor lubricating characteristics of LN2 resulted in increased friction and promoted adhesion-attrition causing reduction in tool life at low cutting speed of 60m/min.

- Statistical analysis indicated that the cooling condition/lubricating has a significant effect on tool life, whilst both cooling/lubricating condition and cutting speed significantly affect surface roughness when CNC milling of Ti-6Al-4V. In addition, the interaction between cooling/lubricating condition and cutting speed has a significant influence on part surface roughness.
- ANOVA showed that hybrid cryogenic/MQL environment significantly improved the tool life and surface roughness compared with conventional flood cooling. MQL can significantly reduce surface roughness compared with flood cooling.
- For MQL and hybrid cryogenic/MQL environments, chip morphology showed smooth edge, tubular and spiral multi-turn and non-broken chip formations, which indicated both smooth cutting and laminar chip flow, whilst cracked edge, shredded and fattened chip formation was observed in cryogenic machining. It can be concluded that smooth chip formation with tubular and/or spiral shape indicated improved machinability, whilst poor machinability performance resulted in rough and cracked edge, shredded and wavy chips.

### **8.3 Contribution to knowledge**

The main contribution of this research is the provision of new comprehensive and in-depth knowledge on the machining of Ti-6Al-4V using various cooling and lubricating methods. The findings significantly add to the limited research knowledge on the effect of hybrid cooling/lubricating strategies on the machinability of Ti-6Al-4V in CNC milling. The design of the cooling system and the cooling strategy used in this research can be regarded as an effective and sustainable solution in enhancing the machinability of Ti-6Al-4V and can be the basis for its adoption in industry.

## **8.4 Recommended areas for further investigation**

A number of research areas are recommended for further work and are summarised as follows:

### **I. Extending the investigation to different machining processes**

The present design of cryogenic cooling nozzle system can be easily and reliably applied to different machining process such as face milling, ball nose cutter milling, end milling with inserted cutters with different types of tool insert materials and tool coatings. Solid end mills with different diameters, materials and coatings can be used for further investigations. Whilst the cooling system can be applied for turning operations, with further research work to investigate the machinability of turning Ti-6Al-4V with hybrid cooling/lubrication strategies.

### **II. Extending the investigation to different cooling/lubrication strategies**

The cooling nozzle adopted in this research with the MQL applicator can be used to investigate the machinability of Ti-6Al-4V with different cooling/ lubricating strategies. The effect of various nozzle positions and angles, nozzle diameters and number of nozzles can be investigated. In addition, the influence of cryogen coolant delivery pressure, velocity and flow rate together with lubricating oil and air can also be studied.

### **III. Expanding the vision of this research to other materials and coolants**

The present research work can be extended to involve the investigation of the machinability of other materials. In addition, various types of coolants can be used in the investigations such LCO<sub>2</sub> in cryogenic cooling, different vegetable and synthetic oils in MQL. Moreover, the state-of-art of minimum quantity cooling/ lubrication MQLC can be extended to include various types of minimal coolants and lubricants.

### **IV. Optimising the design of cryogenic cooling system**

Further design work is required to improve the functional performance and to minimise the limitations and constraints of the present design of cryogenic cooling system. Controlling the position of each nozzle independently to the others via using a delivery hose to each nozzle could be one of the solutions to provide positional control of cooling nozzle/s. Also, design

modification should be done to enable tool changes to be performed without removing the cooling nozzle system from the spindle.

#### **V. CFD and chip formation modelling**

Comprehensive modelling investigations are required of cutting and CFD with the application of hybrid cryogenic/MQL environments, taking into consideration the heat generation during the machining process. This would then need to be verified with machining experiments. This would enable a unique opportunity to analytically explore the effect of different cooling variables such as nozzle/s diameter, nozzle positions, cooling flow rate, and a number of cooling nozzles. Modelling of the workpiece material, fracture criterion and friction at tool-chip interface in cutting process, using FE techniques such as Johnson-Cook model is particularly required to predict the cutting temperature and chip morphology.

#### **VI. SEM and EDS analysis for tool wear mechanism and chip morphology**

Further research work is required to identify the progress in tool wear and the tool wear mechanism and chip morphology, using SEM imaging and EDS analysis. In end milling of titanium alloys the conventional preparation of chip specimens for optical microscopic inspection is not efficient because of the change in chip thickness due to the milling process. It is suggested that SEM imaging for free chip specimens could provide more information in terms of chip parameters and geometry in order to identify the effect of different cutting and cooling conditions on chip morphology.

#### **VII. Extending the investigation of machinability of Ti-6Al-4V to other machinability metrics**

The machining performance in this research was investigated in terms of tool wear, surface roughness, and chip morphology. Further investigations are required to evaluate the machining performance of the application of hybrid cooling/lubrication strategies when end milling of Ti-6Al-4V for other machinability indices such as cutting forces, cutting temperature, part surface integrity, dimensional accuracy, deformed layers and sub-surface micro characteristics.

## References

- A. El Baradie, M., 1996. Cutting fluids: Part I. Characterisation. *Journal of Materials Processing Technology*, 56, pp.786–797.
- Abdel-Aal, H.A., Nouari, M., and El Mansori, M., 2009. Influence of thermal conductivity on wear when machining titanium alloys. *Tribology International*, 42(2), pp.359–372.
- Abukhshim, N.A., Mativenga, P.T., and Sheikh, M.A., 2006. Heat generation and temperature prediction in metal cutting: A review and implications for high speed machining. *International Journal of Machine Tools and Manufacture*, 46(7–8), pp.782–800.
- Adler, A., Yaniv, I., Solter, E., Freud, E., Samra, Z., Stein, J., Fisher, S., and Levy, I., 2006. Catheter-associated bloodstream infections in pediatric hematology-oncology patients: Factors associated with catheter removal and recurrence. *Journal of Pediatric Hematology/Oncology*, 28(1), pp.23–28.
- Ahmed, L.S. and Pradeep Kumar, M., 2017. Investigation of cryogenic cooling effect in reaming Ti-6AL-4V alloy [Online]. *Materials and Manufacturing Processes*, 32(9), pp.970–978. Available from: <http://dx.doi.org/10.1080/10426914.2016.1221088>.
- Anon, 1989. *ISO 8688-2 Tool life testing in milling Part 2: End milling*.
- Antony, J., 2003. *Design of Experiments for Engineers and Scientists*. Oxford : Butterworth-Heinemann: Elseviere science.
- Aramcharoen, A., 2016. Influence of Cryogenic Cooling on Tool Wear and Chip Formation in Turning of Titanium Alloy. *Procedia CIRP*, 46, pp.83–86.
- Aramcharoen, A. and Chuan, S.K., 2014. An experimental investigation on cryogenic milling of inconel 718 and its sustainability assessment [Online]. *Procedia CIRP*, 14, pp.529–534. Available from: <http://dx.doi.org/10.1016/j.procir.2014.03.076>.
- Arrazola, P.J., Garay, A., Iriarte, L.M., Armendia, M., Marya, S., and Le Maître, F., 2009. Machinability of titanium alloys (Ti6Al4V and Ti555.3). *Journal of Materials Processing Technology*, 209(5), pp.2223–2230.

- Astakhov, V.P., 2006. Tribology of Metal cutting. In: Elseviere science.
- Astakhov, V.P., 2009. Metal cutting theory found ations of near-dry (MQL) machining. *Int. J. Machining and Machinability of Materials*, 7(1/2), pp.1–16.
- Ayed, Y., Germain, G., Ammar, A., and Furet, B., 2015. Tool wear analysis and improvement of cutting conditions using the high-pressure water-jet assistance when machining the Ti17 titanium alloy [Online]. *Precision Engineering*, 42, pp.294–301. Available from: <http://linkinghub.elsevier.com/retrieve/pii/S0141635915001063>.
- Ayed, Y., Germain, G., Melsio, A.P., Kowalewski, P., and Locufier, D., 2017. Impact of supply conditions of liquid nitrogen on tool wear and surface integrity when machining the Ti-6Al-4V titanium alloy. *International Journal of Advanced Manufacturing Technology*, 93(1–4), pp.1199–1206.
- Bagherzadeh, A. and Budak, E., 2018. Investigation of machinability in turning of difficult-to-cut materials using a new cryogenic cooling approach [Online]. *Tribology International*, 119(November 2017), pp.510–520. Available from: <https://doi.org/10.1016/j.triboint.2017.11.033>.
- El Baradie, M. a., 1996. Cutting fluids: Part II. Recycling and clean machining. *Journal of Materials Processing Technology*, 56(1–4), pp.798–806.
- Bermingham, M.J., Kirsch, J., Sun, S., Palanisamy, S., and Dargusch, M.S., 2011. New observations on tool life, cutting forces and chip morphology in cryogenic machining Ti-6Al-4V [Online]. *International Journal of Machine Tools and Manufacture*, 51(6), pp.500–511. Available from: <http://dx.doi.org/10.1016/j.ijmachtools.2011.02.009>.
- Bermingham, M.J., Palanisamy, S., Kent, D., and Dargusch, M.S., 2012. A comparison of cryogenic and high pressure emulsion cooling technologies on tool life and chip morphology in Ti-6Al-4V cutting [Online]. *Journal of Materials Processing Technology*, 212(4), pp.752–765. Available from: <http://dx.doi.org/10.1016/j.jmatprotec.2011.10.027>.
- Biermann, D., Abrahams, H., and Metzger, M., 2015. Experimental investigation of tool wear and chip formation in cryogenic machining of titanium alloys. *Advances in Manufacturing*, 3(4), pp.292–299.



- Bordin, A., Bruschi, S., Ghiotti, A., and Bariani, P.F., 2015. Analysis of tool wear in cryogenic machining of additive manufactured Ti6Al4V alloy. *Wear*, 328–329, pp.89–99.
- Bordin, A., Sartori, S., Bruschi, S., and Ghiotti, A., 2017. Experimental investigation on the feasibility of dry and cryogenic machining as sustainable strategies when turning Ti6Al4V produced by Additive Manufacturing [Online]. *Journal of Cleaner Production*, 142, pp.4142–4151. Available from: <http://dx.doi.org/10.1016/j.jclepro.2016.09.209>.
- Bruschi, S., Bertolini, R., Bordin, A., Medea, F., and Ghiotti, A., 2016. Influence of the machining parameters and cooling strategies on the wear behavior of wrought and additive manufactured Ti6Al4V for biomedical applications [Online]. *Tribology International*, 102, pp.133–142. Available from: <http://dx.doi.org/10.1016/j.triboint.2016.05.036>.
- Çakir, O., Kiyak, M., and Altan, E., 2004. Comparison of gases applications to wet and dry cuttings in turning. *Journal of Materials Processing Technology*, 153–154(1–3), pp.35–41.
- Calamaz, M., Coupard, D., and Girot, F., 2008. A new material model for 2D numerical simulation of serrated chip formation when machining titanium alloy Ti-6Al-4V. *International Journal of Machine Tools and Manufacture*, 48(3–4), pp.275–288.
- Chandler, H.E., 1978. *Metal handbook*.
- Deiab, I., Raza, S.W., and Pervaiz, S., 2014. Analysis of lubrication strategies for sustainable machining during turning of titanium ti-6al-4v alloy [Online]. *Procedia CIRP*, 17, pp.766–771. Available from: <http://dx.doi.org/10.1016/j.procir.2014.01.112>.
- Dhananchezian, M. and Pradeep Kumar, M., 2011. Cryogenic turning of the Ti-6Al-4V alloy with modified cutting tool inserts [Online]. *Cryogenics*, 51(1), pp.34–40. Available from: <http://dx.doi.org/10.1016/j.cryogenics.2010.10.011>.
- Dhar, N.R., Islam, M.W., Islam, S., and Mithu, M.A.H., 2006. The influence of minimum quantity of lubrication (MQL) on cutting temperature, chip and dimensional accuracy in turning AISI-1040 steel. *Journal of Materials Processing Technology*, 171(1), pp.93–99.

- Dhokia, V., 2009. *The cryogenic sculpture surface machining of elastomers*. University of Bath.
- Donachie, J.M.J., 2000. *Titanium-A Technical Guide*. 2nd Editio. ASM International.
- Dudzinski, D., Devillez, A., Moufki, A., Larrouquère, D., Zerrouki, V., and Vigneau, J., 2004. A review of developments towards dry and high speed machining of Inconel 718 alloy. *International Journal of Machine Tools and Manufacture*, 44(4), pp.439–456.
- Ezugwu, E.O., 2005. Key improvements in the machining of difficult-to-cut aerospace superalloys. *International Journal of Machine Tools and Manufacture*, 45(12–13), pp.1353–1367.
- Ezugwu, E.O., Bonney, J., Da Silva, R.B., and Çakir, O., 2007. Surface integrity of finished turned Ti-6Al-4V alloy with PCD tools using conventional and high pressure coolant supplies. *International Journal of Machine Tools and Manufacture*, 47(6), pp.884–891.
- Ezugwu, E.O., Bonney, J., DA SILVA, R.B., Machado, A.R., and Ugwoha, E., 2009. High productivity rough turning of ti-6al-4v alloy, with flood and high-pressure cooling. *Tribology Transactions*, 52(3), pp.395–400.
- Ezugwu, E.O., Bonney, J., and Yamane, Y., 2003. An overview of the machinability of aeroengine alloys. *Journal of Materials Processing Technology*, 134(2), pp.233–253.
- Ezugwu, E.O., Da Silva, R.B., Bonney, J., and MacHado, Á.R., 2005. Evaluation of the performance of CBN tools when turning Ti-6Al-4V alloy with high pressure coolant supplies. *International Journal of Machine Tools and Manufacture*, 45(9), pp.1009–1014.
- Ezugwu, E.O. and Wang, Z.M., 1997. Titanium alloys and their machinability [Online]. *Journal of Materials Processing Technology*, 68(3), pp.262–274. Available from: <http://www.sciencedirect.com/science/article/pii/S0924013696000301>.
- Feng, S. and Hattori, M., 2000. Cost and Process Information Modeling for Dry Machining [Online]. *In Proc. of the International Workshop for Environment Conscious Manufacturing-ICEM-2000*, pp.1–8. Available from: [http://www.mel.nist.gov/div826/library/doc/cost\\_process.pdf](http://www.mel.nist.gov/div826/library/doc/cost_process.pdf).

- Garcia, U. and Ribeiro, M. V., 2016. Ti6Al4V Titanium Alloy End Milling with Minimum Quantity of Fluid Technique Use. *Materials and Manufacturing Processes*, 31(7), pp.905–918.
- Ghani, J.A., Choudhury, I.A., and Hassan, H.H., 2004. Application of Taguchi method in the optimization of end milling parameters. *Journal of Materials Processing Technology*, 145(1), pp.84–92.
- Ginting, A. and Nouari, M., 2006. Experimental and numerical studies on the performance of alloyed carbide tool in dry milling of aerospace material. *International Journal of Machine Tools and Manufacture*, 46(7–8), pp.758–768.
- Ginting, A. and Nouari, M., 2007. Optimal cutting conditions when dry end milling the aeroengine material Ti-6242S. *Journal of Materials Processing Technology*, 184(1–3), pp.319–324.
- Ginting, A. and Nouari, M., 2009. Surface integrity of dry machined titanium alloys. *International Journal of Machine Tools and Manufacture*, 49(3–4), pp.325–332.
- Grearson, A.N., 1986. Evaluation of principal wear mechanisms of carbides and ceramics used for machining. *Materials Science and Technology*, 2(January), pp.47–58.
- Gupta, M.K. and Sood, P.K., 2017. Machining comparison of aerospace materials considering minimum quantity cutting fluid: A clean and green approach [Online]. *Proceedings of the Institution of Mechanical Engineers, Part C: Journal of Mechanical Engineering Science*, 231(8), pp.1445–1464. Available from: <https://doi.org/10.1177/0954406216684158>.
- Hartung, P.D., Kramer, B.M., and von Turkovich, B.F., 1982. Tool Wear in Titanium Machining. *CIRP Annals - Manufacturing Technology*, 31(1), pp.75–80.
- Hoier, P., Klement, U., Tamil Alagan, N., Beno, T., and Wretland, A., 2017. Flank wear characteristics of WC-Co tools when turning Alloy 718 with high-pressure coolant supply [Online]. *Journal of Manufacturing Processes*, 30, pp.116–123. Available from: <https://doi.org/10.1016/j.jmapro.2017.09.017>.
- Hong, S., 2006. Lubrication mechanisms of LN2 in ecological cryogenic machining.

*Machining Science and Technology*, 10(1), pp.133–155.

Hong, S.Y., 2001. Economical and Ecological Cryogenic Machining [Online]. *Journal of Manufacturing Science and Engineering*, 123(2), p.331. Available from:  
<http://manufacturingscience.asmedigitalcollection.asme.org/article.aspx?articleid=1439305>.

Hong, S.Y. and Ding, Y., 2001. Cooling approaches and cutting temperatures in cryogenic machining of Ti-6Al-4V. *International Journal of Machine Tools and Manufacture*, 41(10), pp.1417–1437.

Hong, S.Y., Ding, Y., and Jeong, W. cheol, 2001. Friction and cutting forces in cryogenic machining of Ti-6Al-4V. *International Journal of Machine Tools and Manufacture*, 41(15), pp.2271–2285.

Hong, S.Y., Markus, I., and Jeong, W. cheol, 2001. New cooling approach and tool life improvement in cryogenic machining of titanium alloy Ti-6Al-4V. *International Journal of Machine Tools and Manufacture*, 41(15), pp.2245–2260.

Hong, S.Y. and Zhao, Z., 1999. Thermal aspects, material considerations and cooling strategies in cryogenic machining [Online]. *Clean Technologies and Environmental Policy*, 1(2), pp.107–116. Available from:  
<http://link.springer.com/10.1007/s100980050016>.

Huang, X., Zhang, X., Mou, H., Zhang, X., and Ding, H., 2014. The influence of cryogenic cooling on milling stability [Online]. *Journal of Materials Processing Technology*, 214(12), pp.3169–3178. Available from:  
<http://dx.doi.org/10.1016/j.jmatprotec.2014.07.023>.

Islam, M.N., Anggono, J.M., Pramanik, A., and Boswell, B., 2013. Effect of cooling methods on dimensional accuracy and surface finish of a turned titanium part. *International Journal of Advanced Manufacturing Technology*, 69(9–12), pp.2711–2722.

Iturbe, A., Hormaetxe, E., Garay, A., and Arrazola, P.J., 2016. Surface Integrity Analysis when Machining Inconel 718 with Conventional and Cryogenic Cooling [Online]. *Procedia CIRP*, 45(Table 1), pp.67–70. Available from:  
<http://dx.doi.org/10.1016/j.procir.2016.02.095>.

- Jawahir, I.S., Attia, H., Biermann, D., Duflou, J., Klocke, F., Meyer, D., Newman, S.T., Pusavec, F., Putz, M., Rech, J., Schulze, V., and Umbrello, D., 2016. Cryogenic manufacturing processes [Online]. *CIRP Annals - Manufacturing Technology*, 65(2), pp.713–736. Available from: <http://dx.doi.org/10.1016/j.cirp.2016.06.007>.
- Jawahir, I.S., Puleo, D.A., and Schoop, J., 2016. Cryogenic Machining of Biomedical Implant Materials for Improved Functional Performance, Life and Sustainability [Online]. *Procedia CIRP*, 46, pp.7–14. Available from: <http://dx.doi.org/10.1016/j.procir.2016.04.133>.
- Jerold, B.D. and Kumar, M.P., 2013. The Influence of Cryogenic Coolants in Machining of Ti–6Al–4V [Online]. *Journal of Manufacturing Science and Engineering*, 135(3), p.31005. Available from: <http://manufacturingscience.asmedigitalcollection.asme.org/article.aspx?doi=10.1115/1.4024058>.
- Joshi, S., Tewari, A., and Joshi, S.S., 2015. Microstructural Characterization of Chip Segmentation Under Different Machining Environments in Orthogonal Machining of Ti6Al4V [Online]. *Journal of Engineering Materials and Technology*, 137(1), p.11005. Available from: <http://materialstechnology.asmedigitalcollection.asme.org/article.aspx?doi=10.1115/1.4028841>.
- Kale, A. and Khanna, N., 2017. A Review on Cryogenic Machining of Super Alloys Used in Aerospace Industry. *Procedia Manufacturing*, 7, pp.191–197.
- Kamata, Y. and Obikawa, T., 2007. High speed MQL finish-turning of Inconel 718 with different coated tools. *Journal of Materials Processing Technology*, 192–193, pp.281–286.
- Kaynak, Y., Lu, T., and Jawahir, I.S., 2014. Cryogenic machining-induced surface integrity: A review and comparison with dry, mql, and flood-cooled machining. *Machining Science and Technology*, 18(2), pp.149–198.
- KE, Y. lin, DONG, H. yue, LIU, G., and ZHANG, M., 2009. Use of nitrogen gas in high-speed milling of Ti-6Al-4V [Online]. *Transactions of Nonferrous Metals Society of*

- China (English Edition)*, 19(3), pp.530–534. Available from:  
[http://dx.doi.org/10.1016/S1003-6326\(08\)60307-6](http://dx.doi.org/10.1016/S1003-6326(08)60307-6).
- Kitagawa, T., Kubo, a, and Maekawa, K., 1997. Temperature and wear of cutting tools in high-speed machining of Incone1718 and Ti-6Al-6V-2Sn [Online]. *Wear*, 202(2), pp.142–148. Available from:  
<http://www.sciencedirect.com/science/article/pii/S0043164896072559>.
- Klocke, F., Lung, D., Arft, M., Priarone, P.C., and Settineri, L., 2013. On high-speed turning of a third-generation gamma titanium aluminide. *International Journal of Advanced Manufacturing Technology*, 65(1–4), pp.155–163.
- Klocke, F., Settineri, L., Lung, D., Claudio Priarone, P., and Arft, M., 2013. High performance cutting of gamma titanium aluminides: Influence of lubricoolant strategy on tool wear and surface integrity [Online]. *Wear*, 302(1–2), pp.1136–1144. Available from: <http://dx.doi.org/10.1016/j.wear.2012.12.035>.
- Komanduri, R. and Hou, Z.B., 2002. On thermoplastic shear instability in the machining of a titanium alloy (Ti-6Al-4V). *Metallurgical and Materials Transactions A*, 33(9), pp.2995–3010.
- Komanduri, R. and Reed, W.R., 1983. Evaluation of carbide grades and a new cutting geometry for machining titanium alloys. *Wear*, 92(1), pp.113–123.
- Kopac, J., 2009. Achievements of sustainable manufacturing by machining. *Journal of Achievements in Materials and Manufacturing Engineering*, 34(2), pp.180–187.
- Krishnamurthy, G., Bhowmick, S., Altenhof, W., and Alpas, A.T., 2017. Increasing efficiency of Ti-alloy machining by cryogenic cooling and using ethanol in MRF [Online]. *CIRP Journal of Manufacturing Science and Technology*, 18, pp.159–172. Available from: <http://dx.doi.org/10.1016/j.cirpj.2017.01.001>.
- Lee, I., Bajpai, V., Moon, S., Byun, J., Lee, Y., and Park, H.W., 2015. Tool life improvement in cryogenic cooled milling of the preheated Ti-6Al-4V. *International Journal of Advanced Manufacturing Technology*, 79(1–4), pp.665–673.
- Lequien, P., Poulachon, G., Outeiro, J.C., and Rech, J., 2018. Hybrid experimental/modelling

- methodology for identifying the convective heat transfer coefficient in cryogenic assisted machining [Online]. *Applied Thermal Engineering*, 128, pp.500–507. Available from: <https://doi.org/10.1016/j.applthermaleng.2017.09.054>.
- Li, G., Yi, S., Sun, S., and Ding, S., 2017. Wear mechanisms and performance of abrasively ground polycrystalline diamond tools of different diamond grains in machining titanium alloy [Online]. *Journal of Manufacturing Processes*, 29, pp.320–331. Available from: <http://dx.doi.org/10.1016/j.jmapro.2017.08.010>.
- Liu, Z., An, Q., Xu, J., Chen, M., and Han, S., 2013. Wear performance of (nc-ALTiN)/(a-Si<sub>3</sub>N<sub>4</sub>) coating and (nc-AlCrN)/(a-Si<sub>3</sub>N<sub>4</sub>) coating in high-speed machining of titanium alloys under dry and minimum quantity lubrication (MQL) conditions [Online]. *Wear*, 305(1–2), pp.249–259. Available from: <http://dx.doi.org/10.1016/j.wear.2013.02.001>.
- López De Lacalle, L.N., Pérez, J., Llorente, J.I., and Sánchez, J.A., 2000. Advanced cutting conditions for the milling of aeronautical alloys. *Journal of Materials Processing Technology*, 100(1), pp.1–11.
- Machado, A.R. and Wallbank, J., 1994. The effects of a high pressure coolant jet on machining [Online]. *Proceedings of the Institution of Mechanical Engineers, Part B: Journal of Engineering Manufacture*, 208(12), pp.29–38. Available from: [http://archive.pepublishing.com/openurl.asp?genre=article&id=doi:10.1243/PIME\\_PRO C\\_1994\\_208\\_057\\_02](http://archive.pepublishing.com/openurl.asp?genre=article&id=doi:10.1243/PIME_PRO C_1994_208_057_02).
- Machai, C. and Biermann, D., 2011. Machining of ??-titanium-alloy Ti-10V-2Fe-3Al under cryogenic conditions: Cooling with carbon dioxide snow [Online]. *Journal of Materials Processing Technology*, 211(6), pp.1175–1183. Available from: <http://dx.doi.org/10.1016/j.jmatprotec.2011.01.022>.
- Machai, C., Iqbal, A., Biermann, D., Upmeier, T., and Schumann, S., 2013. On the effects of cutting speed and cooling methodologies in grooving operation of various tempers of  $\beta$ -titanium alloy [Online]. *Journal of Materials Processing Technology*, 213(7), pp.1027–1037. Available from: <http://dx.doi.org/10.1016/j.jmatprotec.2013.01.021>.
- Mark Benjamin, D., Sabarish, V.N., Hariharan, M. V., and Samuel Raj, D., 2018. On the benefits of sub-zero air supplemented minimum quantity lubrication systems: An

- experimental and mechanistic investigation on end milling of Ti-6-Al-4-V alloy [Online]. *Tribology International*, 119(September 2017), pp.464–473. Available from: <https://doi.org/10.1016/j.triboint.2017.11.021>.
- Molinari, A., Musquar, C., and Sutter, G., 2002. Adiabatic shear banding in high speed machining of Ti-6Al-4V: Experiments and modeling. *International Journal of Plasticity*, 18(4), pp.443–459.
- Montgomery, D.C., 2009. *Design and analysis of experiments*. Hoboken, N.J. : Wiley.
- Nandy, A.K., Gowrishankar, M.C., and Paul, S., 2009. Some studies on high-pressure cooling in turning of Ti-6Al-4V. *International Journal of Machine Tools and Manufacture*, 49(2), pp.182–198.
- Nouari, M. and Ginting, A., 2006. Wear characteristics and performance of multi-layer CVD-coated alloyed carbide tool in dry end milling of titanium alloy. *Surface and Coatings Technology*, 200(18–19), pp.5663–5676.
- Oberg, E., Jones, F.D., Horton, H.L., Ryffel, H.H., 2004. *Machinery's Handbook*. 27th ed. Industrial Press.
- Obikawa, T., Kamata, Y., and Shinozuka, J., 2006. High-speed grooving with applying MQL. *International Journal of Machine Tools and Manufacture*, 46(14), pp.1854–1861.
- Palanisamy, S., McDonald, S.D., and Dargusch, M.S., 2009. Effects of coolant pressure on chip formation while turning Ti6Al4V alloy. *International Journal of Machine Tools and Manufacture*, 49(9), pp.739–743.
- Park, K.H., Suhaimi, M.A., Yang, G.D., Lee, D.Y., Lee, S.W., and Kwon, P., 2017. Milling of titanium alloy with cryogenic cooling and minimum quantity lubrication (MQL). *International Journal of Precision Engineering and Manufacturing*, 18(1), pp.5–14.
- Park, K.H., Yang, G.D., Suhaimi, M.A., Lee, D.Y., Kim, T.G., Kim, D.W., and Lee, S.W., 2015. The effect of cryogenic cooling and minimum quantity lubrication on end milling of titanium alloy Ti-6Al-4V. *Journal of Mechanical Science and Technology*, 29(12), pp.5121–5126.
- Pervaiz, S., Deiab, I., and Darras, B., 2013. Power consumption and tool wear assessment



- when machining titanium alloys. *International Journal of Precision Engineering and Manufacturing*, 14(6), pp.925–936.
- Pervaiz, S., Rashid, A., Deiab, I., and Nicolescu, M., 2014. Influence of tool materials on machinability of titanium- and nickel-based alloys: A review. *Materials and Manufacturing Processes*, 29(3), pp.219–252.
- Pramanik, A., 2014. Problems and solutions in machining of titanium alloys. *International Journal of Advanced Manufacturing Technology*, 70(5–8), pp.919–928.
- Pramanik, A. and Littlefair, G., 2015. Machining of titanium alloy (Ti-6Al-4V)-theory to application. *Machining Science and Technology*, 19(1), pp.1–49.
- Priarone, P.C., Klocke, F., Faga, M.G., Lung, D., and Settineri, L., 2016. Tool life and surface integrity when turning titanium aluminides with PCD tools under conventional wet cutting and cryogenic cooling. *International Journal of Advanced Manufacturing Technology*, 85(1–4), pp.807–816.
- Priarone, P.C., Robiglio, M., Settineri, L., and Tebaldo, V., 2014. Milling and Turning of Titanium Aluminides by Using Minimum Quantity Lubrication [Online]. *Procedia CIRP*, 24(Mic), pp.62–67. Available from: <http://linkinghub.elsevier.com/retrieve/pii/S2212827114009640>.
- Pusavec, F., Deshpande, A., Yang, S., M'Saoubi, R., Kopac, J., Dillon, O.W., and Jawahir, I.S., 2014. Sustainable machining of high temperature Nickel alloy - Inconel 718: Part 1 - Predictive performance models. *Journal of Cleaner Production*, 81, pp.255–269.
- Pusavec, F., Deshpande, A., Yang, S., M'Saoubi, R., Kopac, J., Dillon, O.W., and Jawahir, I.S., 2015. Sustainable machining of high temperature Nickel alloy - Inconel 718: Part 2 - Chip breakability and optimization. *Journal of Cleaner Production*, 87(1), pp.941–952.
- Rahim, E.A., Ibrahim, M.R., Rahim, A.A., Aziz, S., and Mohid, Z., 2015. Experimental investigation of minimum quantity lubrication (MQL) as a sustainable cooling technique [Online]. *Procedia CIRP*, 26, pp.351–354. Available from: <http://dx.doi.org/10.1016/j.procir.2014.07.029>.
- Rahman, M., Wang, Z.-G., and Wong, Y.-S., 2006. A Review on Machining of Titanium

Alloys. *JSME International Journal Series C*, 49(1), pp.11–20.

Revuru, R.S., Posinasetti, N.R., Vsn, V.R., and Amrita, M., 2017. Application of cutting fluids in machining of titanium alloys—a review. *International Journal of Advanced Manufacturing Technology*, 91(5–8), pp.2477–2498.

Da Rocha, S.S., Adabo, G.L., Vaz, L.G., and Henriques, G.E.P., 2005. Effect of thermal treatments on tensile strength of commercially cast pure titanium and Ti-6Al-4V alloys. *Journal of Materials Science: Materials in Medicine*, 16(8), pp.759–766.

Rotella, G., Dillon, O.W., Umbrello, D., Settineri, L., and Jawahir, I.S., 2014. The effects of cooling conditions on surface integrity in machining of Ti6Al4V alloy. *International Journal of Advanced Manufacturing Technology*, 71(1–4), pp.47–55.

Sadik, M.I., Isakson, S., Malakizadi, A., and Nyborg, L., 2016. Influence of Coolant Flow Rate on Tool Life and Wear Development in Cryogenic and Wet Milling of Ti-6Al-4V. *Procedia CIRP*, 46, pp.91–94.

Sales, W., Becker, M., Barcellos, C.S., Landre, J., Bonney, J., and Ezugwu, E.O., 2009. Tribological behaviour when face milling AISI 4140 steel with minimum quantity fluid application [Online]. *Industrial Lubrication and Tribology*, 61(2), pp.84–90. Available from: <http://www.emeraldinsight.com/doi/10.1108/00368790910940400>.

Sartori, S., Ghiotti, A., and Bruschi, S., 2017a. Hybrid lubricating/cooling strategies to reduce the tool wear in finishing turning of difficult-to-cut alloys [Online]. *Wear*, 376–377, pp.107–114. Available from: <http://dx.doi.org/10.1016/j.wear.2016.12.047>.

Sartori, S., Ghiotti, A., and Bruschi, S., 2017b. Temperature effects on the Ti6Al4V machinability using cooled gaseous nitrogen in semi-finishing turning [Online]. *Journal of Manufacturing Processes*, 30, pp.187–194. Available from: <https://doi.org/10.1016/j.jmapro.2017.09.025>.

Sartori, S., Ghiotti, A., and Bruschi, S., 2018. Solid Lubricant-assisted Minimum Quantity Lubrication and Cooling strategies to improve Ti6Al4V machinability in finishing turning [Online]. *Tribology International*, 118(October 2017), pp.287–294. Available from: <https://doi.org/10.1016/j.triboint.2017.10.010>.

- Sartori, S., Moro, L., Ghiotti, A., and Bruschi, S., 2016. On the tool wear mechanisms in dry and cryogenic turning Additive Manufactured titanium alloys [Online]. *Tribology International*, 105(June 2016), pp.264–273. Available from: <http://dx.doi.org/10.1016/j.triboint.2016.09.034>.
- Schoop, J., Sales, W.F., and Jawahir, I.S., 2017. High speed cryogenic finish machining of Ti-6Al4V with polycrystalline diamond tools [Online]. *Journal of Materials Processing Technology*, 250(July), pp.1–8. Available from: <http://dx.doi.org/10.1016/j.jmatprotec.2017.07.002>.
- Sharma, V.S., Dogra, M., and Suri, N.M., 2009. Cooling techniques for improved productivity in turning. *International Journal of Machine Tools and Manufacture*, 49(6), pp.435–453.
- Sharma, V.S., Singh, G., and Sørby, K., 2015. A Review on Minimum Quantity Lubrication for Machining Processes [Online]. *Materials and Manufacturing Processes*, 30(8), pp.935–953. Available from: <http://www.tandfonline.com/doi/full/10.1080/10426914.2014.994759>.
- Shaw, M.C., 1986. Metal cutting principles. *Oxford University Press*.
- Shaw, M.C. and Vyas, A., 1998. The Mechanism of Chip Formation with Hard Turning Steel [Online]. *CIRP Annals*, 47(1), pp.77–82. Available from: <http://linkinghub.elsevier.com/retrieve/pii/S0007850607627899>.
- Shokrani, A., 2014. Cryogenic machining of titanium alloy. , p.48.
- Shokrani, A., Dhokia, V., Muñoz-Escalona, P., and Newman, S.T., 2013. State-of-the-art cryogenic machining and processing. *International Journal of Computer Integrated Manufacturing*, 26(7), pp.616–648.
- Shokrani, A., Dhokia, V., and Newman, S.T., 2012. Environmentally conscious machining of difficult-to-machine materials with regard to cutting fluids [Online]. *International Journal of Machine Tools and Manufacture*, 57, pp.83–101. Available from: <http://dx.doi.org/10.1016/j.ijmachtools.2012.02.002>.
- Shokrani, A., Dhokia, V., and Newman, S.T., 2012. Evaluation of cryogenic CNC milling of

Ti-6Al-4V titanium alloy. *22nd International conference on flexible automation and intelligent manufacturing, Helsinki-Stockholm*, pp.1–4.

Shokrani, A., Dhokia, V., and Newman, S.T., 2016a. Comparative investigation on using cryogenic machining in CNC milling of Ti-6Al-4V titanium alloy [Online]. *Machining Science and Technology*, 20(3), pp.475–494. Available from: <http://dx.doi.org/10.1080/10910344.2016.1191953>.

Shokrani, A., Dhokia, V., and Newman, S.T., 2016b. Investigation of the effects of cryogenic machining on surface integrity in CNC end milling of Ti-6Al-4V titanium alloy [Online]. *Journal of Manufacturing Processes*, 21, pp.172–179. Available from: <http://dx.doi.org/10.1016/j.jmapro.2015.12.002>.

Da Silva, R.B., MacHado, Á.R., Ezugwu, E.O., Bonney, J., and Sales, W.F., 2013. Tool life and wear mechanisms in high speed machining of Ti-6Al-4V alloy with PCD tools under various coolant pressures [Online]. *Journal of Materials Processing Technology*, 213(8), pp.1459–1464. Available from: <http://dx.doi.org/10.1016/j.jmatprotec.2013.03.008>.

Su, Y., He, N., Li, L., Iqbal, A., Xiao, M.H., Xu, S., and Qiu, B.G., 2007. Refrigerated cooling air cutting of difficult-to-cut materials. *International Journal of Machine Tools and Manufacture*, 47(6), pp.927–933.

Su, Y., He, N., Li, L., and Li, X.L., 2006. An experimental investigation of effects of cooling/lubrication conditions on tool wear in high-speed end milling of Ti-6Al-4V. *Wear*, 261(7–8), pp.760–766.

Sun, J., Wong, Y.S., Rahman, M., Wang, Z.G., Neo, K.S., Tan, C.H., and Onozuka, H., 2006. Effects of coolant supply methods and cutting conditions on tool life in end milling titanium alloy. *Machining Science and Technology*, 10(3), pp.355–370.

Sun, S., Brandt, M., and Dargusch, M.S., 2010. Machining Ti-6Al-4V alloy with cryogenic compressed air cooling. *International Journal of Machine Tools and Manufacture*, 50(11), pp.933–942.

Sun, S., Brandt, M., Palanisamy, S., and Dargusch, M.S., 2015. Effect of cryogenic compressed air on the evolution of cutting force and tool wear during machining of Ti-

- 6Al-4V alloy [Online]. *Journal of Materials Processing Technology*, 221, pp.243–254. Available from: <http://dx.doi.org/10.1016/j.jmatprotec.2015.02.017>.
- Sun, Y., Huang, B., Puleo, D.A., and Jawahir, I.S., 2015. Enhanced machinability of Ti-5553 alloy from cryogenic machining: Comparison with MQL and flood-cooled machining and modeling. *Procedia CIRP*, 31, pp.477–482.
- Sun, Y., Huang, B., Puleo, D.A., Schoop, J., and Jawahir, I.S., 2016. Improved Surface Integrity from Cryogenic Machining of Ti-6Al-7Nb Alloy for Biomedical Applications [Online]. *Procedia CIRP*, 45, pp.63–66. Available from: <http://dx.doi.org/10.1016/j.procir.2016.02.362>.
- Tang, J., Luo, H.Y., and Zhang, Y.B., 2017. Enhancing the surface integrity and corrosion resistance of Ti-6Al-4V titanium alloy through cryogenic burnishing. *International Journal of Advanced Manufacturing Technology*, 88(9–12), pp.2785–2793.
- Tapoglou, N., Lopez, M.I.A., Cook, I., and Taylor, C.M., 2017. Investigation of the Influence of CO<sub>2</sub> Cryogenic Coolant Application on Tool Wear [Online]. *Procedia CIRP*, 63, pp.745–749. Available from: <http://dx.doi.org/10.1016/j.procir.2017.03.351>.
- Thakur, A. and Gangopadhyay, S., 2016. Dry machining of nickel-based super alloy as a sustainable alternative using TiN/TiAlN coated tool [Online]. *Journal of Cleaner Production*, 129, pp.256–268. Available from: <http://dx.doi.org/10.1016/j.jclepro.2016.04.074>.
- Trent, E.M.&Wright, P.K., 2000. *Metal cutting*. Oxford: Butterworth-Heinemann.
- Veiga, C., Devim, J.P., and Loureiro, A.J.R., 2012. Properties and applications of titanium alloys: a brief review. *Reviews on Advanced Materials Science*, 32(2), pp.133–148.
- Venugopal, K.A., Paul, S., and Chattopadhyay, A.B., 2007a. Growth of tool wear in turning of Ti-6Al-4V alloy under cryogenic cooling. *Wear*, 262(9–10), pp.1071–1078.
- Venugopal, K.A., Paul, S., and Chattopadhyay, A.B., 2007b. Tool wear in cryogenic turning of Ti-6Al-4V alloy. *Cryogenics*, 47(1), pp.12–18.
- Venugopal, K.A., Tawade, R., and Chattopadhyay, A.B., 2003. Turning of Titanium Alloy with Ti-B<sub>2</sub> Coated Carbides Under Cryogenic Cooling. *Journal of Engineering*

*Manufacture*, 217(12), pp.1697–1707.

Wang, Z.G., Wong, Y.S., and Rahman, M., 2005. High-speed milling of titanium alloys using binderless CBN tools. *International Journal of Machine Tools and Manufacture*, 45(1), pp.105–114.

Wang, Z.M. and Ezugwu, E.O., 1997. Performance of pvd-coated carbide tools when machining ti-6al-4v©. *Tribology Transactions*, 40(1), pp.81–86.

Wang, Z.Y. and Rajurkar, K.P., 2000. Cryogenic machining of hard-to-cut materials. *Wear*, 239(2), pp.168–175.

Werda, S., Duchosal, A., Le Quilliec, G., Morandea, A., and Leroy, R., 2016. Minimum Quantity Lubrication: Influence of the Oil Nature on Surface Integrity [Online]. *Procedia CIRP*, 45, pp.287–290. Available from: <http://dx.doi.org/10.1016/j.procir.2016.02.330>.

Yap, T.C., El-Tayeb, N.S.M., and Von Brevern, P., 2013. Cutting forces, friction coefficient and surface roughness in machining Ti-5Al-4V-0.6Mo-0.4Fe using carbide tool K313 under low pressure liquid nitrogen. *Journal of the Brazilian Society of Mechanical Sciences and Engineering*, 35(1), pp.11–15.

Yildiz, Y. and Nalbant, M., 2008. A review of cryogenic cooling in machining processes. *International Journal of Machine Tools and Manufacture*, 48(9), pp.947–964.

Yuan, S.M., Yan, L.T., Liu, W.D., and Liu, Q., 2011. Effects of cooling air temperature on cryogenic machining of Ti-6Al-4V alloy [Online]. *Journal of Materials Processing Technology*, 211(3), pp.356–362. Available from: <http://dx.doi.org/10.1016/j.jmatprotec.2010.10.009>.

Zhao, Z. and Hong, S.Y., 1992. Cooling strategies for cryogenic machining from a materials viewpoint. *Journal of Materials Engineering and Performance*, 1(5), pp.669–678.

